ISSN: 2408-2384 (Online)
ISSN: 1686-5456 (Print)

Environment and Natural Resources Journal

Volume 20, Number 3, May - June 2022

Environment and Natural Resources Journal (EnNRJ)
Volume 20, Number 3, May - June 2022 ISSN: 1686-5456 (Print)
ISSN: 2408-2384 (Online)

AIMS AND SCOPE

The Environment and Natural Resources Journal is a peer-reviewed journal, which provides insight scientific knowledge into the diverse dimensions of integrated environmental and natural resource management. The journal aims to provide a platform for exchange and distribution of the knowledge and cutting-edge research in the fields of environmental science and natural resource management to academicians, scientists and researchers. The journal accepts a varied array of manuscripts on all aspects of environmental science and natural resource management. The journal scope covers the integration of multidisciplinary sciences for prevention, control, treatment, environmental clean-up and restoration. The study of the existing or emerging problems of environment and natural resources in the region of Southeast Asia and the creation of novel knowledge and/or recommendations of mitigation measures for sustainable development policies are emphasized.

The subject areas are diverse, but specific topics of interest include:

- Biodiversity
- Climate change
- Detection and monitoring of polluted sources e.g., industry, mining
- Disaster e.g., forest fire, flooding, earthquake, tsunami, or tidal wave
- Ecological/Environmental modelling
- Emerging contaminants/hazardous wastes investigation and remediation
- Environmental dynamics e.g., coastal erosion, sea level rise
- Environmental assessment tools, policy and management e.g., GIS, remote sensing, Environmental Management System (EMS)
- Environmental pollution and other novel solutions to pollution
- Remediation technology of contaminated environments
- Transboundary pollution
- Waste and wastewater treatments and disposal technology

Schedule
Environment and Natural Resources Journal (EnNRJ) is published 6 issues per year in January-February, March-April, May-June, July-August, September-October, and November-December.

Publication Fees
There is no cost of the article-processing and publication.

Ethics in publishing
EnNRJ follows closely a set of guidelines and recommendations published by Committee on Publication Ethics (COPE).

Environment and Natural Resources Journal (EnNRJ)

Volume 20, Number 3, May - June 2022 ISSN: 1686-5456 (Print)
ISSN: 2408-2384 (Online)

Editorial Office Address
Research Management and Administration Section,
Faculty of Environment and Resource Studies, Mahidol University
999, Phutthamonthon Sai 4 Road, Salaya, Phutthamonthon, Nakhon Pathom, Thailand, 73170
Phone +662 441 5000 ext. 2108 Fax. +662 441 9509-10
Website: https://ph02.tci-thaijo.org/index.php/ennrj/index
E-mail: ennrjournal@gmail.com

Environment and Natural Resources Journal (EnNRJ)

Volume 20, Number 3, May - June 2022 ISSN: 1686-5456 (Print)
ISSN: 2408-2384 (Online)

CONTENT

Mycoremediation Potential of Synthetic Textile Dyes by *Aspergillus niger* via Biosorption and Enzymatic Degradation

Manavi Sulakkana Ekanayake[1,2] and Pathmalal Manage[1,2*]

[1]*Centre for Water Quality and Algae Research, Department of Zoology, University of Sri Jayewardenepura, Nugegoda 10250, Sri Lanka*
[2]*Faculty of Graduate Studies, University of Sri Jayewardenepura, Nugegoda 10250, Sri Lanka*

ARTICLE INFO

Received: 6 Sep 2021
Received in revised: 7 Jan 2022
Accepted: 12 Jan 2022
Published online: 4 Feb 2022
DOI: 10.32526/ennrj/20/202100171

Keywords:
Textile dye/ Decolorization/ Fungi/ *Aspergillus niger*/ Bioremediation/ Laccase

*** Corresponding author:**
E-mail: pathmalal@sjp.ac.lk

ABSTRACT

Textile dyes that persist in the environment are highly resistant to the natural degradation processes that occur in the environment. Therefore, the present study isolated, identified, and optimized textile dye decolorization by fungi and elucidated the dye decolorization pathway to develop a low-cost biotechnological approach for decolorization and detoxification of textile dyes. Within 36 hours of incubation at temperatures ranging from 28 to 40°C, pH 7, and shaking at 100 rpm, *Aspergillus niger* MN990895, which was selected from a total of 77 fungal isolates, completely decolorized the model dye CI Direct Blue 201 (DB 201). *A. niger* biosorbed 8.4±1.2% of the dye used where live biomass showed complete dye removal. It was found that extracellular crude enzymes were more involved in DB 201 dye decolorization (72.7±3.3%) than intracellular crude enzymes. The enzymatic studies suggested that the primary enzyme involved in DB 201 textile dye decolorization was lacccase, which was further confirmed by the presence of distinct protein bands around 75-100 kDa on the SDS-PAGE. The FTIR spectra and seed germination assays confirmed that *A. niger* proved successful in DB 201 textile dye degradation and detoxification. The present study suggests that *A. niger* may have promising implications in the future for the development of an enzyme-based textile wastewater treatment system.

1. INTRODUCTION

Water is the ultimate receiver of the most pollutants and therefore, the hydrosphere is being polluted at an alarming level compared to the lithosphere and geosphere (Gadallah and Sayed, 2014). The chemical composition of water changes mainly due to wastewater generated by manufacturing or chemical processing industries such as leather, textile, and distilleries (Mahagamage and Manage, 2014; Xing et al., 2010). When it comes to these industries, the textile industry is the most significant polluter of surface and groundwater because it uses a large amount of water during the dyeing and finishing processes and generates large amounts of dye-containing wastewater (Bankole et al., 2018; Goud et al., 2020).

When chemical dyes adhere to compatible surfaces, they form complexes or covalent bonds with the metals, imparting a permanent or temporary color to the substrate (Ekanayake and Manage, 2017). When it relates to the annual production of synthetic dyes, azo dyes account for more than half of the total output (71×10^5 tons) (Fernando et al., 2012; Gupta et al., 2016). These synthetic textile dyes showed significant resistance to natural degradation processes, as well as a long half-life in laboratory tests (Brillas and Martínez-Huitle, 2015). For example, the half-life of the hydrolyzed Reactive Blue 19 at pH 7 and 25°C is approximately 46 years (Hao et al., 2000). It has been founded that the dyes themselves, as well as some of their breakdown daughter compounds, are toxic, carcinogenic, and mutagenic to plants and animals, including humans (Almeida and Corso, 2014; Kagalkar et al., 2009; Vairavela and Murtyb, 2020, Khan and Malik, 2014). Apart from the health implications, dye contamination in receiving environments, particularly inland water bodies or the ocean, has resulted in widespread public outcry and protest (Kalyani et al., 2008).

Citation: Ekanayake MS, Manage P. Mycoremediation potential of synthetic textile dyes by *Aspergillus niger* via biosorption and enzymatic degradation. Environ. Nat. Resour. J. 2022;20(3):234-245. (https://doi.org/10.32526/ennrj/20/202100171)

To address the issue, different wastewater treatment guidelines have been established to reduce the toxicity of the textile dye effluent generated (Abdelgalil et al., 2018; Fernando et al., 2012). Although the overwhelming amount of the world's leading apparel suppliers are still facing environmental pollution issues as a result of the substantial use of textile dyes in the apparel industry, they are being forced to investigate alternative novel treatment methods to obtain the necessary wastewater consent limits and to expand their manufacturing operations (Khan and Malik, 2014). When compared to physicochemical methods such as coagulation, flocculation, and ion exchange, which are currently in use across the world (Gupta et al., 2016; Módenes et al., 2019), the use of fungal strains for textile wastewater treatment via adsorption or degradation is a promising tool for textile wastewater treatment (Bankole et al., 2018). The majority of fungi, once established, thrive and reproduce well even in harsh environments, and they can adapt their metabolism to utilize a variety of carbon and nitrogen sources in their quest for survival (Almeida and Corso, 2014; Bankole et al., 2018).

Most studies have focused on using fungi as bio-sorption agents to bind the surface of biomass, which has resulted in the bioaccumulation of toxins (Bhattacharjee et al., 2020; Mishra et al., 2021). Therefore, the use of a live biomass and their enzymes for bioremediation is a growing concern. Recent studies have documented the use of laccase-like enzymes in bioremediation processes in the presence of various chemical mediators (Shah et al., 2021). Therefore, research into the use of fungal enzymes without additional chemicals is a timely requirement. As a result, the present study is intended to isolate textile dye decolorizing fungi from water and soil in textile wastewater effluent sites and determine the mechanism of dye decolorization using the CI Direct Blue 201 (DB 201) textile dye as the model.

2. METHODOLOGY

2.1 Textile dyes and chemicals

Considering the textile dye usage in Sri Lanka, five structurally different textile dyes were selected for primary screening. These included two direct dyes: DB 201 ($C_{30}H_{16}C_{l2}N_4Na_2O_8S_2$), and Moxilon Blue GRL (MBG) ($C_{30}H_{16}C_{l2}N_4Na_2O_8S_2$), two Vat dyes: Cibanone Gold Yellow RK (CGY) ($C_{24}H_{10}Br_2O_2$), and Vat Green FFB (VG) ($C_{36}H_{20}O_4$), and a Reactive dye: Cibacron Blue FR (CB FR) ($C_{29}H_{20}ClN_7O_{11}S_3$). All of the dyes were sourced from small-scale textile dyeing operations in Sri Lanka. Considering the complexity of its chemical group, structure, and application in Sri Lanka's textile industries, the DB 201 textile dye was selected as the model dye for the study (Ekanayake and Manage, 2020b). The textile dyes used in the study were of industrial grade with 98% purity, and all of the other chemicals used in the study were of high purity and of the analytical and molecular grade.

2.2 Isolation and identification of fungi and appropriate culture conditions

Samples of water and soil were collected from seven textile wastewater effluent sites located in Western Province, Sri Lanka, and enriched for 14 days using modified Kirk's medium (pH 7.0; medium in g/L; glucose: 2, potassium: 0.20, magnesium: 0.05, calcium: 0.01, copper: 0.08, manganese: 0.05, zinc: 0.033, iron: 0.05 (Placido et al., 2016)) supplemented with a mixture of all five dyes (100 rpm). Isolated on Potato Dextrose Agar (PDA) plates following the standard spread plate method, fungi with varying morphological characteristics were identified after 14 days of incubation. Pure cultures were obtained after several inoculations.

2.3 Decolorization of textile dyes

In this experiment, the dye decolorization process was conducted in two stages. First, a solid medium screening procedure was carried out by placing a fungal mycelium disc (5 mm) on a PDA medium overlaid with 5 mL of PDA containing 0.01% (w/v) textile dye mixture and incubating for seven days at 28°C (Rani et al., 2014). The fungal isolates with the highest dye Decolorization Zone (DZ) on the overlaid textile dye mixture (DZ>5 cm) were subjected to the liquid medium screening. Following the liquid medium screening, four discs of (5 mm) fungal mycelium (0.5±1.0 g of wet weight) were introduced into 50 mg/L of each textile dye; DB 201, CGY, CB FR, MBG, and VG which dissolved in modified Kirk's medium (Ekanayake and Manage, 2020b), and the changes of the absorbance were recorded at maximum wavelengths of 570, 420, 605, 620, and 690 nm, respectively. According to Bankole et al. (2018), the percentage of dye decolorization in each experimental set-up was calculated using the equation below. In each experimental set-up, A0 and A1 denote the initial and final absorbance of dye, respectively.

$$DP\ (\%) = [(A0 - A1)/A0] \times 100$$

Following the findings, the most efficient fungal isolate was selected for further optimization studies using DB 201 textile dye as the model dye. The ITS region was used for fungal identification, and the sequence data was deposited on the GENE Bank.

2.4 The optimization of selected external parameters in the fungal decolorization of DB 201 textile dye

Following the methods described in Bankole et al. (2017), Bankole et al. (2018), Ekanayake and Manage (2017), Ekanayake and Manage (2020a), and El-Rahim et al. (2009) temperatures (24, 28, 32, 36, and 40°C), pH (5, 6, 7, 8, 9, and 10), initial dye concentrations (25, 50, 75, 100, 150, and 200 mg/L) as well as agitation conditions (0, 25, 50, 75, 100, and 125 rpm) were scaled up to determine the dye decolorization efficiency. There were three replicates of each experiment, and no fungal inoculation was used to maintain control conditions. The repeated batch decolorization experiment was carried out by repeatedly adding 50 mg/L DB 201 textile dye to the experimental setup without supplement of nutrients or fungal biomass further (Cui et al., 2014; Jadhav et al., 2012). To determine the long-term applicability of isolated fungi for textile dye decolorization, a number of cycles were carried out several times.

2.5 Biosorption assay

Using triplicates, the activity of live and dead biomasses of a fungal isolate on the dye decolorization process was evaluated, and controls were maintained without the addition of fungi to the dye. Biosorption tests were carried out using 5-day-old live, and autoclaved fungal cultures (5.0±0.5 cm diameter) that were introduced into 50 mL of dye DB 201 at a final concentration of 50 mg/L and incubated at 28°C under shaking at 100 rpm until complete dye decolorization was achieved (Erdem and Cihangir, 2018).

2.6 Enzymes that are involved in the decolorization of DB 201 textile dye

To obtain the crude extracellular source of enzymes, the decolorized dye solution was filtered through 0.22 µm filter paper. The filtrate was lyophilized and used as an extracellular source of enzymes. The fungi that remained on the filter paper were washed with sterilized distilled water. The crude intracellular enzymes were extracted using a Proteo Prep-Universal Protein Extraction Kit (Sigma Aldrich, USA), following the manufacturer's instructions. DB 201 textile dye (pH 7.0) was treated with crude extracts from each enzyme source (5% v/v), which was incubated at 28°C for 24 h. At 6-hour intervals, the absorbance was measured to see how it changed. The controls were made up of crude extracts that had been heat-inactivated.

The activity of laccase, azoreductase, lignin Peroxidase (LP), manganese peroxidase (MnP), and tyrosinase enzymes were determined spectrophotometrically, using protocols optimized for each enzyme (Kalyani et al., 2008; Placido et al., 2016; Saratale et al., 2010; Watharkar et al., 2013). In this study, total protein concentration was determined using the Bicinchoninic Acid Protein Assay kit (BCA1 AND B9643; Sigma-Aldrich) and Bovine Serum Albumin as the protein standard (Sigma Aldrich, Germany). One unit of enzyme activity was defined as a change in absorbance unit per minute per mg protein of the enzyme (both from Sigma Aldrich, Germany). All enzyme assays were performed in triplicates, and the average rates of enzyme activity were calculated for each sample.

The most promising enzymes that were found to be involved in the decolorization of DB 201 textile dye solution were studied in greater depth. The dye decolorization experiments were carried out in bulk (1 L) for selected biological agents, and the decolorized dye solutions were lyophilized and re-suspended in 10 mL of potassium phosphate buffer (50 mM, pH 7.4) for use as an extracellular source of the enzymes in the experiments (Wijesekara et al., 2011). The supernatant of each enzyme extract was partially purified with $(NH_4)_2SO_4$ precipitation, dialysis in the potassium phosphate buffer, and ultrafiltration (Amicon, USA) with a 10 kDa cut-off membrane (Arabaci and Usluoglu, 2014; Bagewadi et al., 2017; Chen et al., 2005). The concentrated enzyme solution was further purified by DEAE-anion exchange column and Sephadex G-100 column chromatography using 50 mM of phosphate buffer (pH 7.4) and sodium acetate buffer (pH 5.6) as mobile phase, respectively (Telke et al., 2010; Wijesekara et al., 2011). The putative laccase enzyme was determined through SDS-PAGE.

2.7 Toxicity evaluation of the decolorized dye solutions

Seed germination assay was employed to assess the decolorized dye solutions' toxicity after the myco-remediation process. To summarize, 5 mL of the original DB 201 dye and 5 mL of the decolorized dye solutions were sprayed on thirty seeds of two

agricultural crop seeds, *Oryza sativa* (monocot) and *Vigna radiate* (dicot), once a day for five days. After five days, the length of the shoot (plumule), the length of the root (radicle), and the percentage of seeds that germinated were measured (Ekanayake and Manage, 2020a; Kalyani et al., 2008). The experiments were carried out in triplicate.

2.8 Analysis of the decolorized DB 201 textile dye

According to the method described by Kalyani et al. (2008) the color changes were measured using an ultraviolet-visible (UV-Vis) spectrophotometer and Fourier Transform Infrared Spectroscopy (FTIR) was used to study the changes in the dye before and after treatment.

2.9 Data analyses

One-way analysis of variance (ANOVA) with Tukey-Kramer multiple comparison test, two-sample T-test, and Balanced ANOVA tests were used. When the p-value was less than 0.05, the results were considered significant.

3. RESULTS

3.1 Isolation and identification of textile dye decolorizing fungi

In the present study, out of 77 fungal isolates with different morphological features, only six isolates showed highest dye decolorization when tested on solid medium. *Aspergillus niger* MN990895 indicated by the reference number FBWB/06/S, was the most efficient fungal species for complete decolorization of all five dyes tested in liquid medium compared to the other five isolates (Table 1). The dye decolorization pathway of *A. niger* was evaluated in detail using DB 201 dye as the model dye (Figure 1).

Table 1. Decolorization of five textile dyes by most efficient fungi selected from solid medium screening

Reference No.	Dye decolorization percentages (%) and time (days)				
	DB 201	MB GRL	CBY RK	VG FFB	CB FR
Control	0.1 (14)	0.2 (14)	0.1 (14)	0.1 (14)	0.3 (14)
FPWA/07/S	CD (03)	CD (06)	CD (08)	CD (08)	CD (10)
FPWA/09/S	CD (03)	CD (04)	CD (12)	CD (07)	CD (12)
FPWB/22/S	98.65 (14)	CD (08)	88.2 (14)	95.4 (14)	CD (07)
FBWB/06/S	CD (02)	CD (02)	CD (02)	CD (04)	CD (05)
FBWB/07/S	CD (03)	CD (03)	CD (08)	CD (12)	CD (08)
FBWC/26/S	CD (03)	CD (05)	CD (07)	CD (14)	CD (09)

CD: Complete decolorization (>99%)

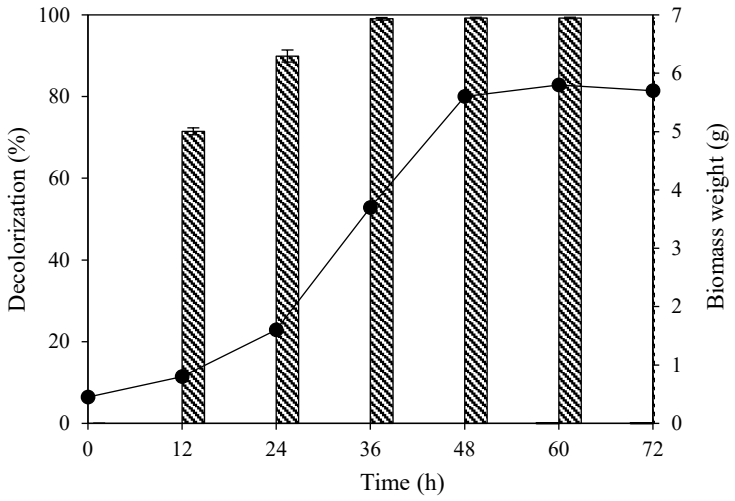

Figure 1. Decolorization of DB 201 dye by *A. niger* and growth of cell biomass (When error bars are not shown, the standard deviation was less than the width of the symbol)

3.2 Optimization of DB 201 dye decolorization by *A. niger*

When incubated for 36 h at temperatures ranging from 28 to 40°C, *A. niger* evidenced 99% dye decolorization (visually complete dye decolorization), with no statistically significant difference ($p>0.05$). The dye decolorization was slightly reduced at 24°C (Figure 2). DB 201 dye decolorization was found to be most effective under neutral pH (7) and vigorous agitation at 100 rpm (Figure 2). A descending order of dye decolorization was discovered as a result of the increasing initial dye concentrations. Throughout the study, the dye decolorization of the controls were less than 1% under all conditions tested. The repeated addition of dye into the same initial biomass resulted in over 99% dye removal up to the 5th cycle, after which the dye removal was recorded in descending order (Table 2).

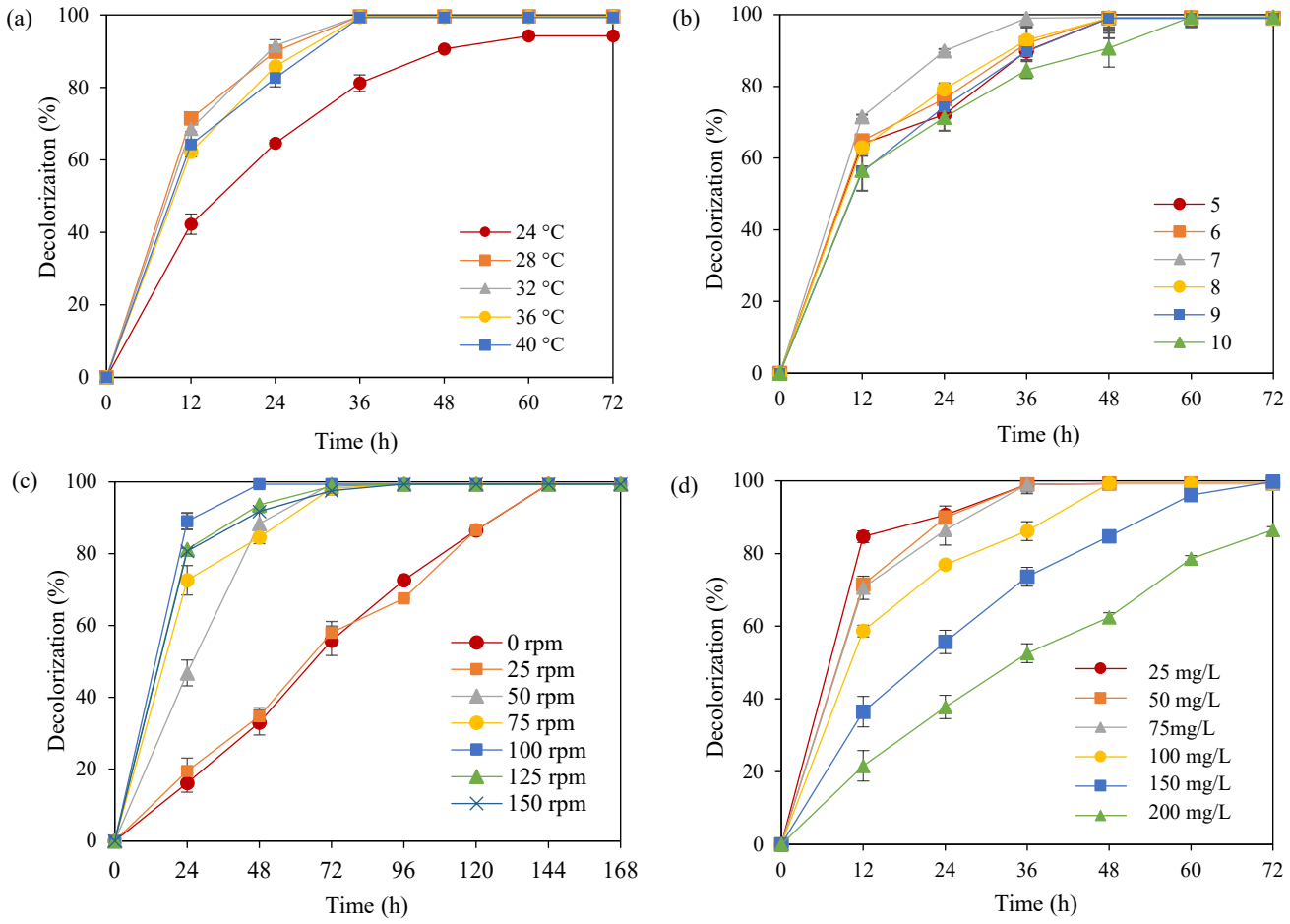

Figure 2. Effect of (a) temperature, (b) pH, (c) agitation, (d) initial dye concentrations on decolorization of DB 201 dye by *A. niger* (When error bars are not shown, the standard deviation was less than the width of the symbol)

Table 2. Effect of repetitive addition of DB 201 textile dye into the same *A. niger* biomass

Biological agent	Decolorization percentages (%) at the end of each cycle and time						
	1st cycle	2nd cycle	3rd cycle	4th cycle	5th cycle	6th cycle	7th cycle
A. niger	CD (36 h)	CD (12 h)	CD (12 h)	CD (12 h)	CD (12 h)	92.5±1.3 (12 h)	88.1±1.7 (12 h)

CD: Complete decolorization (>99%)

3.3 Evaluation of the DB 201 dye decolorization pathway by of *A. niger*

In the present study, the dead biomass of *A. niger* showed 8.4±1.2% biosorption of the DB 201 dye after 12 h of incubation whereas the live biomass showed complete removal of the dye. The amount of DB 201 textile dye decolorized by extracellular crude enzymes (72.7±3.3%) was higher than the amount of DB 201 textile dye decolorized by the crude extract of intracellular enzymes (Figure 3).

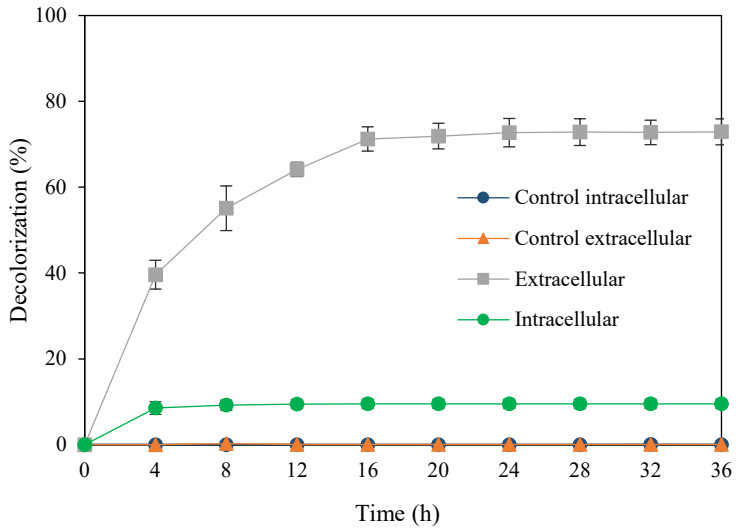

Figure 3. Effect of fungal enzymes on decolorization of DB 201 dye (When error bars are not shown, the standard deviation was less than the width of the symbol)

When the involvement of five different enzymes produced by *A. niger* was evaluated at the end of the dye decolorization process (Table 3), LP and laccase were found to be significantly enhanced ($p \leq 0.05$). Based on the preliminary studies and the literature, laccase was selected for further studies and subjected to further purification and confirmations. Table 4 illustrates the yield and the purification levels of putative laccase enzyme secreted by *A. niger* with the presence of DB 201 textile dye. The putative laccase enzyme obtained after purification was comprised of several distinct proteins (bands around 75-100 kDa) which indicated the presence of laccase enzyme (Figure 4). However, some minor bands were also detected in purified enzyme extract suggesting the importance of further optimizations to remove all the other unwanted enzymes.

Spectral comparison of original DB 201 textile dye solution and those subjected to myco-degradation by *A. niger* is depicted in Figure 5. Changes of transmittance in original dye and formation of new peaks at 3,389.64, 1,734.81, 1,653.53, 1,449.59 which may be responsible for O-H stretching, N=H vibration, N=N stretching, and N-O stretching, respectively, were recorded. Further, the changes in transmittance and peak patterns in the fingerprint region: 1,449.59, 1,400.34, 1,288.71, 1,190.28, 1,122.33, and 1,021.66 suggested formation of new bonds, especially C-O single bonds, after the myco-remediation process.

Table 3. Activity of the major enzymes recorded during the dye decolorization process

Enzyme	Enzyme activity (Umin/mg/protein)	
	Control	Decolorized solution
LP	1.153±0.128	LP
MnP	0.005±0.001	MnP
Tyrosinase	0.002±0.001	Tyrosinase
Laccase	0.090±0.014	Laccase
Azoreductase	0.140±0.026	Azoreductase

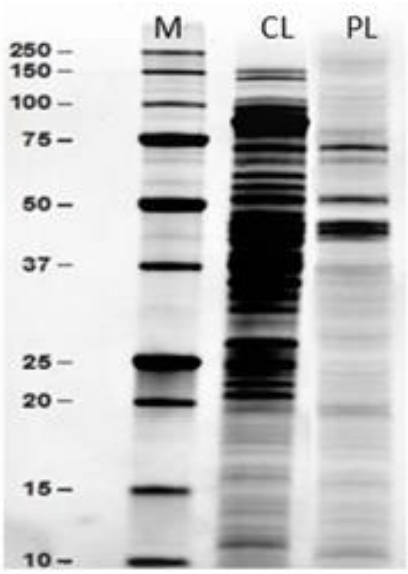

Figure 4. Molecular mass estimation of crude and putative laccase enzymes after dialysis via anion exchange chromatography (M: Marker, CL: Crude laccase, PL: putative laccase)

Table 4. Protein yield and enzyme activity of the purified laccase enzyme

Enzyme source	Purification step	Total protein (mg)	Enzyme activity (U)	Specific activity (U/mg)	Yield (%)	Purification
A. niger laccase	Crude	23.44	17.65	0.77	100.00	1.00
	Dialysis	10.52	10.65	1.02	60.33	1.32
	Ultra filtration	7.47	8.63	1.16	48.89	1.51
	DEAE	1.53	4.40	2.93	24.93	3.82
	Sephadex	1.01	3.20	3.17	18.13	4.13

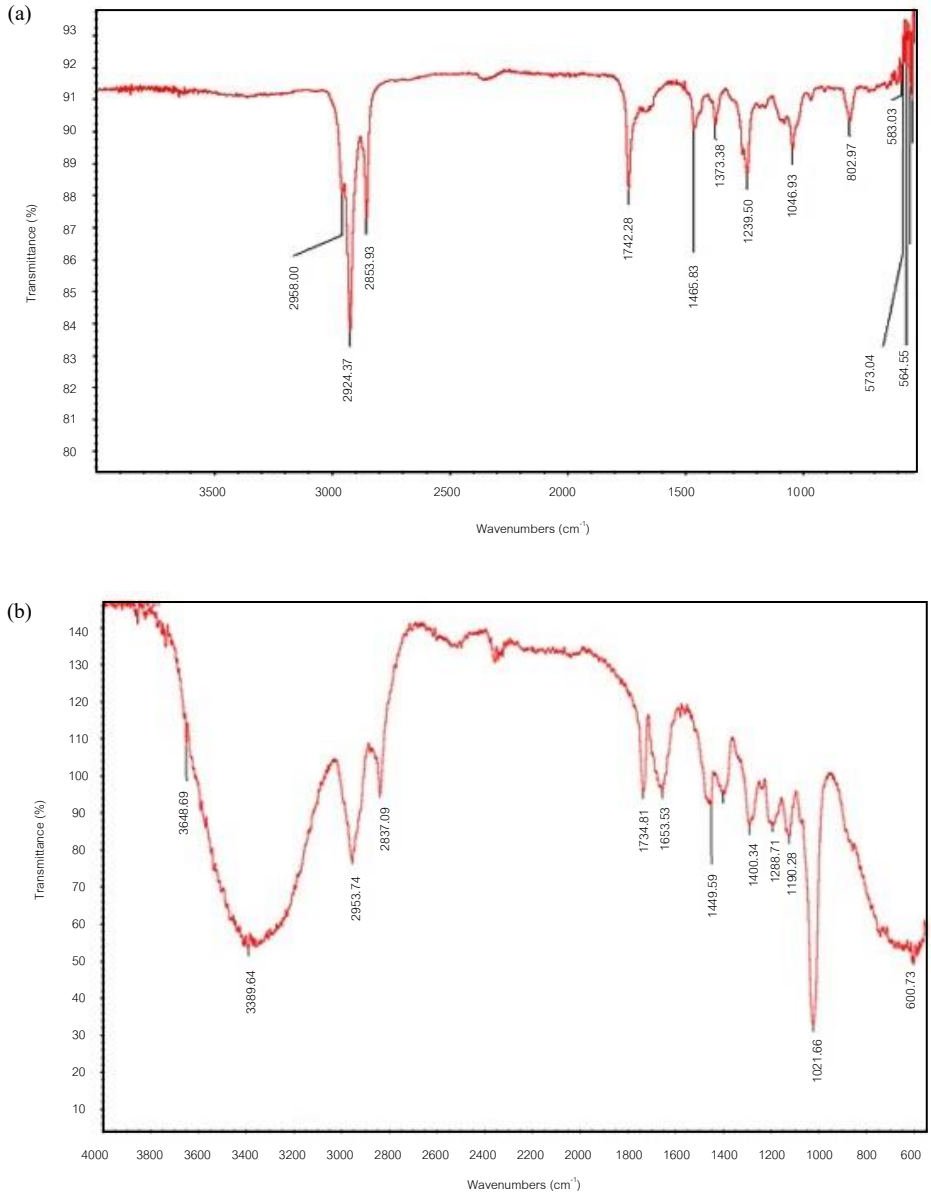

Figure 5. FTIR spectrum for (a) original DB 201 textile dye, decolorized DB 201 textile dye by (b) *A. niger*

The toxicity of the original DB 201 dye and treated dye by *A. niger* was evaluated to confirm whether the treated effluent has detoxified or not (Table 5). The results revealed that both *O. sativa* and *V. radiate* seeds treated with decolorized dye solution had significantly more seed germination, plumule and radicle growth, compared to the seeds treated with the original DB 201 textile dye ($p \leq 0.05$).

Table 5. Assessment of the toxicity of DB 201 textile dye and decolorized products

Parameter	*O. sativa*			*V. radiate*		
	Control	Dye (50 ppm)	Decolorized dye solution	Control	Dye (50 ppm)	Decolorized dye solution
Germination (%)	98.8±0.0	22.2±5.0	100±0	100±0	10.0±3.3	100±0
Plumule (cm)	2.6±0.2	0.6±0.2	2.3±0.1	1.4±0.2	0.3±0.3	1.2±0.3
Radicle (cm)	1.5±0.3	0.3±0.2	1.4±0.1	0.7±0.1	0.2±0.1	0.5±0.1

4. DISCUSSION

The textile dye DB 201, a di-azo direct dye, was selected as the model dye for the study as it had not been previously investigated in relation to decolorization by *A. niger*. DB 201 textile dye (834 g/mol) is complex, with two azo bonds and three sulfur groups on seven aromatic rings (Chemical Book, 2017) and highly resistant to photolysis degradation in the natural environment (Ekanayake and Manage, 2016). Moreover, the breakdown of aromatic components by biological degradation processes is slowed dramatically by textile dyes that contain azo and sulfo groups on the aromatic components (Saratale et al., 2010).

4.1 Isolation and identification of textile dye decolorizing fungi

Isolation of textile dye decolorizing fungi from the natural environment is highly challenging. Out of 77 total isolates studied in the present study, only one isolate, *A. niger*, was able to complete decolorization of all five selected textile dyes efficiently. A few studies have recorded the potential applicability of *A. niger* on decolorization of some other textile dyes; 99% of Rubine Toner 12 (Dhanjal et al., 2013), 92% of Direct Violet dye (El-Rahim et al., 2009), 88% of Synazol dye (Khalaf, 2008) and most of these studies discussed the application of *A. niger* as a bio-sorption agent instead using the organism as its live biochemical activities. The study by Seyis and Subasioglu (2008) recorded 45% and 38% decolorization of Methyl Orange dye by live and dead fungal biomass of *A. niger*, respectively. Fu and Viraraghavan (2002) reported the decolorization of Congo red by *A. niger* with 14.16 mg/g of adsorption capacity into fungal biomass while Rani et al. (2014) recorded the decolorization of malachite green by the fungi; *A. niger* via incorporation activities of the extracellular enzyme, absorption and adsorption. Therefore, comparison of dye decolorization potential of one species to the other is highly intricate as the dye decolorization by the same microorganism may fall under various mechanisms. Further, application of microorganisms used in one country for decolorization of textile dyes being used in their industry may not be applicable for another (Bankole et al., 2017; Seyis and Subasioglu, 2008). Consequently, the isolation and identification of potential microorganisms from the native environment where it will be used is critical for the experiment's success.

4.2 Optimization of textile dye decolorization by *A. niger*

Many external parameters, including temperature, pH and agitation conditions, as well as additional nutrients and the initial dye concentration, are known to have an impact on dye decolorization by biological agents, particularly for the growth, viability and enzymatic activities of the agents (Ekanayake and Manage, 2020b; Jadhav et al., 2012; Kalyani et al., 2008; Saratale et al., 2010). Thus, the present study explored the effect of such factors on the decolorization of DB 201 textile dye by *A. niger*. The results revealed that *A. niger* demonstrated efficient decolorization of DB 201 textile dye under shaking conditions in the temperature range of 28 to 40°C and pH 7.

The temperature range chosen was more or less similar to the optimum temperature for fungal growth (25°C to 35°C) found by Fu and Viraraghavan (2002). As a result, it is possible that *A. niger*'s dye decolorization will not be affected by temperature changes and will continue to function normally within the selected temperature range of 28 to 40°C. At the same time, Bankole et al. (2018) observed that the rate of decolorization of Scarlet R dye by *Peyronellaea prosopidis* was greatly decreased at both lower (15-25°C) and higher temperatures (>45°C), suggesting that this may be due to the reduction of lygnolytic enzymes combined with negligible cell apoptosis at high temperature. El-Rahim et al. (2009) found that pH 2, 3, 8, and 9 were the most effective pH values for dye removal by *A. niger*, and that these pH values were also the ones where the fungi produced the most biomass yield. However, in the present study, the

highest dye decolorization by *A. niger* was observed at a neutral pH value of 7. Many researchers, including Asad et al. (2007), Bankole et al. (2018), and Shah et al. (2012), have highlighted the relationship between oxygen and cell growth as well as the decolorization of textile dyes, identifying it as one of the most important factors that must be optimized. When Rani et al. (2014) investigated the decolorization of dyes by fungi under differing agitation conditions, they revealed that *A. niger* prefers static conditions for the rapid decolorization of Nigrosin and Malachite Green dyes. According to Ali et al. (2008), the *A. niger* preferred shaking conditions for its rapid growth and decolorization of Acid Red 151 and Sulfer Black dyes, implying the effect of agitation conditions on dye decolorization may be dependent on the type of textile dye used in the treatment process. As per the results of this study, *A. niger* was more efficient in dye decolorization under shaking conditions than in under static conditions ($p \leq 0.05$). The results of the present study were in agreement with Przystas et al. (2015) and Yesilada et al. (2003) for a consortium of *Pleurotus ostreatus*, *Gloeophyllum odoratum* and *Fusarium oxysporum* on decolorization of Brilliant Green dye and *Funalia trogii* on decolorization of Astrazone Blue dye. Bankole et al. (2018) hypothesized that the preference for shaking conditions could be attributed to the aerophilic nature of most fungi for enzyme activities and that the opposite results could be due to the involvement of azoreductase-like enzymes, which are inhibited by the presence of oxygen, as previously reported.

Jadhav et al. (2012) hypothesized that the reduction in dye decolorization may be due to the negative impacts occurred into the enzyme system that is involved in the dye decolorization process and the statement was confirmed by showing that the activities of laccase, vertryl alcohol, NADH-DCIP reductase were reduced at higher initial dye concentrations (250 mg/L), compared to the low concentrations (5 mg/L). Similar to the present study, Yesilada et al. (2003) recorded that decolorization of Astrazone Blue dye by *F. trogii* was successful up to five cycles and then declined sharply. Decreasing of dye decolorization after a few cycles may depend on the reduction of cell viability due to the depletion of essential minerals in the medium or entry of cells into the stationary phase followed by death phase, which results in a reduction in metabolic and enzymatic activities that are related to the dye decolorization (Jadhav et al., 2012).

4.3 Evaluation of the DB 201 dye decolorization pathway by *A. niger*

Fungal dye decolorization may occur via two different pathways: bio-sorption or biodegradation (Dhaneshwar, 2016). Polman and Breckenridge (1996) put forward that the interaction of dyes to biomass depends on the chemistry of the particular dye and the specific chemistry of the microbial biomass. Therefore, decolorization rate and behavior may vary from one species to the other as well as from the type of dye employed. Further, Modak and Natarajan (1995) recorded that most biological agents showed bio-sorption of dyes where the environmental conditions are not favorable for their growth, especially when the textile effluent is toxic.

According to the findings of the present study, both bio-sorption and biodegradation appear to be important components of the fungal dye decolorization mechanism, and this may be dependent on the complex structural nature of the dye as well as the heavy weight of biomass and the surface area of the fungi (Fu and Viraraghavan, 2002). Furthermore, Sumathi and Phatak (1999) reported complete decolorization of Remazole Red, Remazole Dark Blue, and Brilliant Orange dyes by *Aspergillus foetidus* within two days of incubation, while Fu and Viharaghavan (2002) reported complete decolorization of Basic Blue and Acid Blue dyes by dead *A. niger* biomass taking 2-30 days to complete. As per the findings of these studies, the dye decolorization behavior of the same species may differ depending on the textile dye used.

According to the present study's results, crude extracellular enzymes from *A. niger* were significantly more involved in DB 201 dye decolorization than the intracellular enzyme extract tested. As far as the authors are aware, the present study is the first study that a crude extracellular enzyme extract secreted by fungi during the previous dye decolorization cycle has been used to evaluate textile dye decolorization. Laccase enzyme, secreted by *A. niger*, was the most prominent enzyme involved in the decolorization of textile dye DB 201, as indicated by bands between 50 and 75 kDa on the SDS-PAGE. Bankole et al. (2018) and Vasdev et al. (1995) have found lignin modifying enzymes such as laccase, lignin peroxidase, and manganese peroxidase, among others, are involved in the biodegradation of textile dyes by live fungi. Bagewadi et al. (2017) recorded that the laccase enzyme produced by *Trichoderma harzianum* was

engaged in the decolorization of Methylene Blue and Congo Red dyes, with 90% of Methylene Blue and 60% of Congo Red dyes decolorized. According to the authors, 163 U/mg of specific laccase activity and a 25-fold purification after two anion exchange chromatographies (DEAE Sepharose and Sephadex G-50) were observed with protein bands around 56 kDa being responsible for the laccase enzyme being identified. In the present study, decolorized dye solution was obtained as the crude enzyme source to measure the enzyme activity, while other studies which recorded so far have used Solid State Fermented (SSF) fungi as the source of crude extract. This may be the reason for detection of low enzyme activity in the present study, compared to the previous studies. The FTIR spectra for original dye and decolorized dye solution by *A. niger* showed significant changes in peak patterns and the transmittance which confirm the myco-degradation potential of the dye.

Altogether, results of the present study suggested that decolorization of DB 201 textile dye was mainly taking place by biodegradation through extracellular activity of *A. niger* laccase enzyme with minor contribution of bio-sorption. Similar mechanism is suggested by Placido et al. (2016) for decolorization of Novacron Red and Remazol Black dyes by activity of laccase enzyme produced by *Leptosphaerulina* sp. and bio-sorption on to the cellular biomass. Laccase, benzenediol: oxygen oxidoreductase (EC 1.10.3.2), is a well-known enzyme with great advantages of being extracellular, inducible, low substrate specificity and an inexpensive cofactor (oxygen) (Placido et al., 2016; Zouari-Mechichi et al., 2006). Hence, isolation and identification of such enzyme producing fungi from native environment of Sri Lanka, with special reference to the textile dye decolorization, appear to be a green light for future biotechnological applications on textile dye decolorization.

Colored textile dyes are associated with a number of environmental hazards. The majority of these effluents eventually find their way into natural water bodies. In some cases, the secondary byproducts of some synthetic chemicals are more toxic than the original forms of the substances in question (Almeida and Corso, 2014; Guruge et al., 2007). Almeida and Corso (2014) discovered that the formation of toxic metabolites by *Aspergillus terreus* following the decolorization of Procion Red MX-5B dye was more harmful than the dye in its original form, which was due to the incomplete degradation. The formation of these metabolites during microbiological treatments is highly undesirable due to the increase in toxicity, which can have a detrimental effect on the surrounding environment. As a result of the present study, *A. niger* demonstrated complete detoxification of the dye, highlighting the potential applicability of the selected species for green and environmentally safe approaches. To design a bioreactor, the isolate can be used as live biomass, and the optimized factors can be used to simulate the process at an industrial scale. Further investigation into the role of the laccase enzyme in textile wastewater treatment may lead to the development of an enzyme-based treatment method for the treatment of textile wastewater as an intelligent approach in textile wastewater treatment.

5. CONCLUSION

Out of the 77 different fungal strains tested, *A. niger* demonstrated the most significant potential for decolorization of the selected model dye DB 201. The toxicity assay confirmed that *A. niger* could be used for textile dye decolorization without forming hazardous intermediate products. The decolorization of DB 201 textile dye occurred primarily through biodegradation, which was mediated by an extracellular enzyme: laccase. To ensure the textile wastewater treatment plant's ease of application and maintenance, additional research is required to develop an environmentally friendly, biotechnological approach to decolorize textile dyes using such enzymes rather than directly applying live biomass.

ACKNOWLEDGEMENTS

Central Instrumental Centre in University of Sri Jayewardenepura would be acknowledged for providing the sample analysis facilities for FTIR and University of Sri Jayewardenepura, Sri Lanka (Research Grant ASP/01/RE/SCI/2016/10) for financial support.

CONFLICTS OF INTEREST

The manuscript was written collaboratively and has not been submitted simultaneously for publication elsewhere; the authors declare that they have no conflicts of interest to disclose.

REFERENCES

Abdelgalil SA, Attia AM, Reyed RM, Soliman NA, El Enshasy HA. Application of experimental designs for optimization the production of *Alcaligenes faecalis* Nyso laccase. Journal of Scientific and Industrial Research 2018;77(1):713-27.

Ali N, Hameed A, Ahmed S, Khan AG. Decolorization of structurally different textile dyes by *Aspergillus niger* SA1. World Journal of Microbiology and Biotechnology 2008;24(7):1067-72.

Almeida EJR, Corso CR. Comparative study of toxicity of azo dye Procion Red MX-5B following biosorption and biodegradation treatments with the fungi *Aspergillus niger* and *Aspergillus terreus*. Chemosphere 2014;112:317-22.

Arabaci G, Usluoglu A. The enzymatic decolorization of textile dyes by the immobilized polyphenol oxidase from quince leaves. Scientific World Journal. 2014;2014:Article No. 685975.

Asad S, Amoozegar MA, Pourbabaee A, Sarbolouki MN, Dastgheib SMM. Decolorization of textile azo dyes by newly isolated halophilic and halotolerant bacteria. Bioresource technology 2007;98(11):2082-8.

Bagewadi ZK, Mulla SI, Ninnekar HZ. Purification and immobilization of laccase from *Trichoderma harzianum* strain HZN10 and its application in dye decolorization. Journal of Genetic Engineering and Biotechnology 2017;15(1):139-50.

Bankole PO, Adekunle AA, Obidi OF, Olukanni OD, Govindwar SP. Degradation of indigo dye by a newly isolated yeast, *Diutina rugosa* from dye wastewater polluted soil. Journal of Environmental Chemical Engineering 2017;5(5):4639-48.

Bankole PO, Adekunle AA, Obidi OF, Chandanshive VV, Govindwar SP. Biodegradation and detoxification of Scarlet RR dye by a newly isolated filamentous fungus, *Peyronellaea prosopidis*. Sustainable Environment Research 2018;28(5): 214-22.

Bhattacharjee C, Dutta S, Saxena VK. A review on biosorptive removal of dyes and heavy metals from wastewater using watermelon rind as biosorbent. Environmental Advances 2020:2:Article No.100007.

Brillas E, Martínez-Huitle CA. Decontamination of wastewaters containing synthetic organic dyes by electrochemical methods. An updated review. Applied Catalysis B: Environmental 2015;166:603-43.

Chemical Book. CI direct blue 201 basic information [Internet]. 2017 [cited 2017 Mar 6]. Available from: https://www.chemicalbook.com/ProductChemicalPropertiesCB01453522_EN.htm.

Chen H, Hopper SL, Cerniglia CE. Biochemical and molecular characterization of an azoreductase from *Staphylococcus aureus*, a tetrameric NADPH-dependent flavoprotein. Microbiology 2005;151:1433-41.

Cui D, Li G, Zhao M, Han S. Decolourization of azo dyes by a newly isolated *Klebsiella* sp. strain Y3, and effects of various factors on biodegradation. Biotechnology and Biotechnological Equipment 2014;28(3):478-86.

Dhaneshwar A. Decolorisation of Methylene Blue Using Lactuca and Sophora species [dissertation]. New Zealand: University of Canterbury; 2016.

Dhanjal NIK, Mittu B, Chauhan A, Gupta S. Biodegradation of textile dyes using fungal isolates. Journal of Environmental Science and Technology 2013;6(2):99-105.

Ekanayake EMMS, Manage PM. Decoloriztion of textile dye (CI Direct Blue 201) by selected aquatic plants. Proceedings of the 2nd Environment and Natural Resources International Conference; 2016 Nov 16-17; Bangkok: Thailand; 2016.

Ekanayake EMMS, Manage PM. Decolorization of CI Direct Blue 201 textile dye by native bacteria. International Journal of Multidisciplinary Studies 2017;4(1):49-58.

Ekanayake EMMS, Manage PM. Decolorization and detoxification of CI Direct Blue 201 textile dye by two fungal strains of genus *Aspergillus*. Journal of National Science Foundation Sri Lanka 2020a;48(1):69-80.

Ekanayake EMMS, Manage PM. Green approach for decolorization and detoxification of textile dye - CI direct blue 201 using native bacterial strains. Environment and Natural Resource Journal 2020b;18(1):1-8.

El-Rahim WMA, El-Ardy OAM, Mohammad FH. The effect of pH on bioremediation potential for the removal of direct violet textile dye by *Aspergillus niger*. Desalination 2009; 249(3):1206-11.

Erdem Ö, Cihangir N. Color removal of some textile dyes from aqueous solutions using *Trametes versicolor*. Hacettepe Journal of Biology and Chemistry 2018;45(4):499-507.

Fernando E, Keshavarz T, Kyazze G. Enhanced bio-decolourisation of acid orange 7 by *Shewanella oneidensis* through co-metabolism in a microbial fuel cell. International Biodeterioration and Biodegradation 2012;72:1-9.

Fu Y, Viraraghavan T. Removal of Congo red from an aqueous solution by fungus *Aspergillus niger*. Advances in Environmental Research 2002;7(1):239-47.

Gadallah MAA, Sayed SA. Impacts of different water pollution sources on antioxidant defense ability in three aquatic macrophytes in Assiut Province, Egypt. Journal of Stress Physiology and Biochemistry 2014;10(3):47-61.

Goud BS, Cha HL, Koyyada G, Kim JH. Augmented biodegradation of textile azo dye effluents by plant endophytes: A sustainable, eco-friendly alternative. Current Microbiology 2020;77:3240-55.

Gupta N, Kushwaha AK, Chattopadhyaya MC. Application of potato (*Solanum tuberosum*) plant wastes for the removal of methylene blue and malachite green dye from aqueous solution. Arabian Journal of Chemistry 2016;9(1):707-16.

Guruge KS, Taniyasu S, Yamashita N, Manage PM. Occurrence of perfluorinated acids and fluorotelomers in waters from Sri Lanka. Marine Pollution Bulletin 2007;54(10):1667-72.

Hao OJ, Kim H, Chiang PC. Decolorization of wastewater: Critical reviews. Environmental Science and Technology 2000;30(4):449-505.

Jadhav SB, Yedurkar SM, Phugare SS, Jadhav JP. Biodegradation studies on acid violet 19, a triphenylmethane dye, by *Pseudomonas aeruginosa* BCH. CLEAN-Soil, Air, Water 2012;40(5):551-8.

Kagalkar AN, Jagtap UB, Jadhav JP, Bapat VA, Govindwar SP. Biotechnological strategies for phytoremediation of the sulfonated azo dye Direct Red 5B using *Blumea malcolmii* Hook. Bioresource Technology 2009;100(18):4104-210.

Kalyani DC, Patil PS, Jadhav JP, Govindwar SP. Biodegradation of reactive textile dye Red BLI by an isolated bacterium *Pseudomonas* sp. SUK1. Bioresource Technology 2008; 99(11):4635-41.

Khalaf MA. Biosorption of reactive dye from textile wastewater by non-viable biomass of *Aspergillus niger* and *Spirogyra* sp. Bioresource Technology 2008;99(14):6631-4.

Khan S, Malik A. Environmental and health effects of textile industry wastewater. In: Environmental Deterioration and Human Health. Dordrecht: Springer; 2014. p. 55-71.

Mahagamage MGYL, Manage PM. Water quality index (CCME-WQI) based assessment study of water quality in Kelani River Basin, Sri Lanka. International Journal of Environment and natural resources 2014;1:199-204.

Mishra S, Cheng L, Maiti A. The utilization of agro-biomass/byproducts for effective bio-removal of dyes from dyeing wastewater: A comprehensive review. Journal of Environmental Chemical Engineering 2021;9(1):Article No. 104901.

Modak JM, Natarajan KA. Biosorption of metals using nonliving biomass: A review. Mining, Metallurgy and Exploration 1995;12(4):189-96.

Módenes AN, Hinterholz CL, Neves CV, Sanderson K, Trigueros DE, Spinoza-Quiñones FR, et al. A new alternative to use soybean hulls on the adsorptive removal of aqueous dyestuff. Bioresource Technology Reports 2019;6:175-82.

Placido J, Chanaga X, Ortiz-Monsalve S, Yepes M, Mora A. Degradation and detoxification of synthetic dyes and textile industry effluents by newly isolated *Leptosphaerulina* sp. from Colombia. Bioresources and Bioprocessing 2016;3(6):2-14.

Polman K, Breckenridge CR. Biomass-mediated binding and recovery of textile dyes from waste effluents. Textile Chemist and Colorist 1996;28(4):116-21.

Przystas W, Zablocka-Godlewska E, Grabinska-Sota E. Efficacy of fungal decolorization of a mixture of dyes belonging to different classes. Brazilian Journal of Microbiology 2015;46(2):415-24.

Rani B, Kumar V, Singh J, Bisht S, Teotia P, Sharma S, et al. Bioremediation of dyes by fungi isolated from contaminated dye effluent sites for bio-usability. Brazilian Journal of Microbiology 2014;45(3):1055-63.

Saratale RG, Saratale GD, Chang JS, Govindwar SP. Decolorization and biodegradation of reactive dyes and dye wastewater by a developed bacterial consortium. Biodegradation 2010;21(6):999-1015.

Seyis I, Subasioglu T. Comparison of live and dead biomass of fungi on decolorization of methyl orange. African Journal of Biotechnology 2008;7(13):2212-6.

Shah PD, Dave SR, Rao MS. Enzymatic degradation of textile dye Reactive Orange 13 by newly isolated bacterial strain *Alcaligenes faecalis* PMS-1. International Biodeterioration and Biodegradation 2012;69:41-50.

Shah H, Yusof F, Alam MZ. A new technique to estimate percentage decolorization of synthetic dyes on solid media by extracellular laccase from white-rot fungus. Bioremediation Journal 2021:1-9 (In press).

Sumathi S, Phatak V. Fungal treatment of bagasse based pulp and paper mill wastes. Environmental Technology 1999;20(1):93-8.

Telke AA, Kadam AA, Jagtap SS, Jadhav JP, Govindwar SP. Biochemical characterization and potential for textile dye degradation of blue laccase from *Aspergillus ochraceus* NCIM-1146. Biotechnology and Bioprocess Engineering 2010;15(4):696-703.

Vairavela P, Murtyb VR. Decolorization of Congo red dye in a continuously operated rotating biological contactor reactor. Desalin Water Treat 2020:196:299-314.

Vasdev K, Kuhad RC, Saxena RK. Decolorization of triphenylmethane dyes by the bird's nest fungus *Cyathus bulleri*. Current Microbiology 1995;30(5):269-72.

Watharkar AD, Khandare RV, Kamble AA, Mulla AY, Govindwar SP, Jadhav JP. Phytoremediation potential of *Petunia grandiflora* Juss., an ornamental plant to degrade a disperse, disulfonated triphenylmethane textile dye Brilliant Blue G. Environmental Science and Pollution Research 2013;20(2):939-49.

Wijesekara I, Pangestuti R, Kim SK. Biological activities and potential health benefits of sulfated polysaccharides derived from marine algae. Carbohydrate Polymers 2011;84(1):14-21.

Xing Y, Liu D, Zhang LP. Enhanced adsorption of methylene blue by EDTAD-modified sugarcane bagasse and photocatalytic regeneration of the absorbent. Desalination 2010;259:187-91.

Yesilada O, Asma D, Cing S. Decolorization of textile dyes by fungal pellets. Process Biochemistry 2003;38(6):933-8.

Zouari-Mechichi H, Mechichi T, Dhouib A, Sayadi S, Martinez AT, Martinez MJ. Laccase purification and characterization from *Trametes trogii* isolated in Tunisia: Decolorization of textile dyes by the purified enzyme. Enzyme and Microbial Technology 2006;39(1):141-8.

Social Life Cycle Assessment of Green and Burnt Manual Sugarcane Harvesting in the Northeastern Thailand

Thiwaporn Thuayjan[1], Jittima Prasara-A[1*], Pornpimon Boonkum[2], and Shabbir H. Gheewala[3,4]

[1]*Energy and Environment for Sustainable Development Research and Training Center, Faculty of Environment and Resource Studies, Mahasarakham University, Mahasarakham 44150, Thailand*

[2]*Technology and Informatics Institute for Sustainability (TIIS), National Science and Technology Development Agency (NSTDA), 114 Thailand Science Park, Phahonyothin Road, Khlong Nueng, Khlong Luang, Pathum Thani 12120, Thailand*

[3]*Joint Graduate School of Energy and Environment, King Mongkut's University of Technology Thonburi, Bangkok 10140, Thailand*

[4]*Centre of Excellence on Energy Technology and Environment, Ministry of Higher Education, Science, Research and Innovation, Bangkok 10400, Thailand*

ARTICLE INFO

Received: 29 Sep 2021
Received in revised: 11 Jan 2022
Accepted: 18 Jan 2022
Published online: 11 Feb 2022
DOI: 10.32526/ennrj/20/202100190

Keywords:
Social life cycle assessment/ S-LCA/ Social performance/ Sugarcane/ Green and burnt sugarcane

*** Corresponding author:**
E-mail: jittima.p@msu.ac.th

ABSTRACT

Despite green sugarcane harvesting being promoted in Thailand, with some limitations on the use of harvesting machines, green sugarcane harvesting is practiced manually in many sugarcane fields. Although the environmental benefit seems clear, this harvesting practice's social implications are yet unknown. This study assessed social performances of green and burnt manual sugarcane harvesting in North-Eastern Thailand, the region hosting the largest sugarcane plantation area, using the Social Life Cycle Assessment technique. Data collection was undertaken by surveys. The performance reference points method was applied to assess the different stakeholder's social performances. Key stakeholder groups examined were workers, local community, and farm owners. The main social issues included in this study are fair wages, working conditions, health and safety, local employment, economic development, social responsibility, and satisfaction of occupation. The results showed that the social performances of green and burnt sugarcane harvesting were generally similar except for the local community group. This is mainly due to the health impact of sugarcane burning on the local community. Different issues cause the farmers to harvest the burnt sugarcane; for example, labor shortage in the harvesting season and the difficult working conditions for green harvesting, causing the farm owners to bear higher costs. For these reasons, mechanized harvesting is suggested to help promote green harvesting to reduce local air pollution. However, technology development is in urgent need to make the harvesting machines more affordable and applicable to all geographical conditions.

1. INTRODUCTION

Sugarcane plays a vital role in the Thai economy; the country is the world's third-largest sugar exporter (Workman, 2020). Sugarcane is not only a feedstock for food; it is also a source of bio-energy such as bagasse-based electricity and molasses-based ethanol (Gheewala et al., 2019). Every year, Thailand produces a large amount of sugarcane to serve the sugar industry. In 2021, the nation grew more than 66 million tonnes of sugarcane (OCSB, 2021).

Despite its economic importance, the sugar industry has come under scrutiny for its impact on air quality, caused by burning sugarcane tops and leaves before harvesting-so-called "burnt harvesting". For this reason, via the office of the cane and sugar board, the Thai government has promoted "green harvesting", which requires no sugarcane burning before harvesting by means of mechanized sugarcane harvesting (Thansettakij Multimedia, 2019). However, to date, there are still some issues associated with using harvesting machines for the Thai sugarcane farmers, including the high cost of machines and the required conditions of sugarcane fields to use the harvesting machines (Chaya et al., 2019). Therefore,

Citation: Thuayjan T, Prasara-A J, Boonkum P, Gheewala SH. Social life cycle assessment of green and burnt manual sugarcane harvesting in the Northeastern Thailand. Environ. Nat. Resour. J. 2022;20(3):246-256. (https://doi.org/10.32526/ennrj/20/202100190)

in many sugarcane plantations in Thailand, green sugarcane harvesting still depends on manual labor.

Sustainable agriculture is one of the main goals emphasized in Thailand's sustainable development goals (Department of International Organizations, 2021). Life cycle thinking considers every stage of a product/service, from acquiring raw materials, transportation and distribution of product, use, reuse/processing, and waste management after use. This concept helps prevent shifting problems from one stage to another. Life cycle thinking is a useful concept for considering the environmental, economic, and social dimensions along the life cycle of a product or service, leading to sustainable development (Valdivia et al., 2013). The life cycle approach can thus support the transition to sustainable agriculture. Moreover, human well-being is identified as the main scope of sustainable development. Therefore, social consideration in the life cycle of the product is promoted to enhance sustainability (Rezaei Kalvani et al., 2021).

Some previous studies compared the life cycle environmental impacts of green and burnt sugarcane harvesting practices. They showed that green harvesting could help reduce the environmental impacts (de Oliveira Bordonal et al., 2013; Pongpat et al., 2017). Some studies assessed the health impacts of burnt sugarcane harvesting on workers and locals living near the sugarcane fields (Barbosa et al., 2012; Matsuda et al., 2020). Although there have been some studies on the environmental and health aspects of green and burnt sugarcane harvesting, research on the social issues of these harvesting approaches on a variety of stakeholder groups is still limited.

Social Life Cycle Assessment (S-LCA) is a technique used to assess socio-economic and social effects (both positive and negative) that may occur throughout the product's life cycle, involving different stakeholders (UNEP, 2020). This method could help identify the social effects of green and burnt manual sugarcane harvesting on different stakeholders involved. A few previous S-LCA studies on sugarcane reported some social issues in sugarcane cultivation such as low wages, health and safety for workers, and air pollution for the local community (Prasara-A and Gheewala, 2018; Sawaengsak et al., 2019). However, the social effects of stakeholders involved in specific sugarcane harvesting practices, i.e., green and burnt harvesting, are yet unknown. This study compares the socio-economic and social performances of green and burnt manual sugarcane harvesting approaches using the S-LCA technique. The results of this study can help identify the social hotspots where improvement is needed, to help endorse green harvesting in order to reduce air pollution from cane trash burning. Moreover, it can be used to make recommendations to improve the social conditions of the stakeholders involved. In addition, the methodology used in this study could be applied to other agricultural products.

2. METHODOLOGY

The methods used for this study are detailed in the following sub-sections.

2.1 Context of the site studied

The selected study area was in Udon Thani Province, as this province has the largest sugarcane plantation area in the nation (OCSB, 2021). The location map of the study site is presented in Figure 1. This study site is located at the top of the North-Eastern Region of Thailand, near the Laos border. This implies that the problem of cane trash burning from this site would not only affect the local area, but it could also affect the neighboring country. Therefore, there is an urgent need to address the air emission problem of this study site. Most of the sugarcane farms in this area are small-scale farms. Both green and burnt sugarcane harvesting are prevalent in the area. Although the government is promoting harvesting machines, there are issues of them not being able to enter the fields due to the size of farms and the landscape not being suitable for their use. Therefore, human labor was primarily used to harvest green and burnt sugarcane.

2.2 Goal and scope

The goal of this study was to compare the socio-economic and social performances of green and burnt sugarcane harvesting using the Social Life Cycle Assessment (S-LCA) technique. The S-LCA study was conducted following the guidelines of UNEP (2020). There were three main groups of stakeholders included in this study, viz., workers, local community, and farm owners. The three key stakeholder groups were selected based on their relation to sugarcane cultivation and their relationships with each other. Based on the previous study on the S-LCA of sugarcane by Prasara-A and Gheewala (2018), these groups are most affected by sugarcane cultivation. Hence, they were selected to examine. In the site studied, the farm owners worked on their own farms and hired local workers. Most workers also owned sugarcane farms themselves.

Figure 1. Location map of the study site [Source: WordPress (2021)]

The system boundary of this study is shown in Figure 2. The reference unit is one rai of sugarcane plantation. Rai is an area unit used in Thailand; it equals 0.16 hectares. The system boundary of this study is cradle-to-gate, including land preparation, planting, fertilization, weed and pest management, harvesting, and transportation stages. These stages were included in the system boundary due to their significant contribution to the social effects of the sugarcane industry (Prasara-A and Gheewala, 2018).

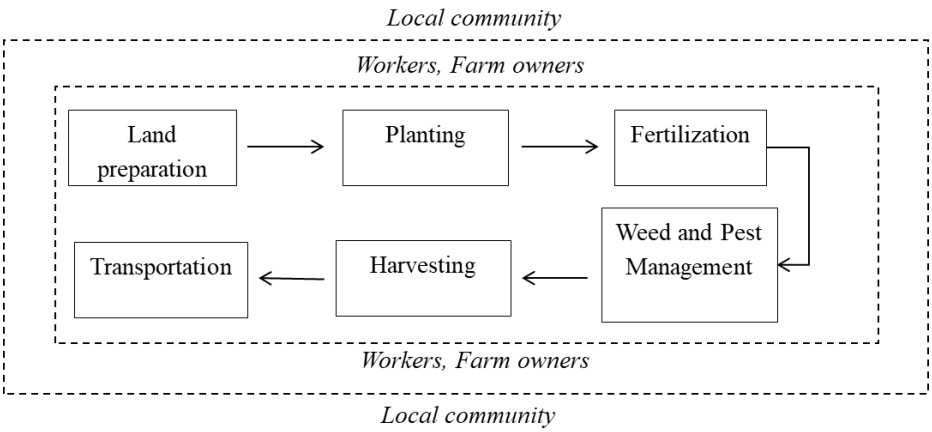

Figure 2. System boundary

2.3 Inventory analysis

A list of social issues and indicators examined are presented in Table 1. These key social issues were selected from the relevant guidelines and standards such as S-LCA guidelines of UNEP (2013), Sustainability Assessment of Food and Agriculture Systems Indicators (SAFA) (FAO, 2013), and Bonsucro standards (Bonsucro, 2014). The authors developed the social indicators (questions to ask interviewees) using definitions of social issues from the aforementioned guidelines and standards, together with discussion with experts and representatives of stakeholders involved. The Item Objective Congruence (IOC) was used to test the validity of indicators used; the indicators with IOC of 0.5 to 1.0 were acceptable. The IOC was obtained by asking three experts to provide validity scores ranging from -1 to 1. The IOC for each social indicator was calculated by dividing the sum of scores from all experts for each indicator with number of experts. The IOC calculated for each indicator used in this study are presented in Table 1.

Table 1. Social inventory analysis

Stakeholder group	Social issue	Social indicator/question	IOC[b]	Unit of indicator	Best performance
Workers	Fair wage	Do you receive a minimum wage (9 USD[a] per day)?	1.0	Yes or No	100 percent of workers answering "yes"
	Working conditions	Have you ever been forced to work at risk of danger?	1.0	Yes or No	100 percent of workers answering "no"
		Do workers of different genders working on the same kind of work receive the same wage?	1.0	Yes or No	100 percent of workers answering "yes"
	Health and Safety	Do all workers present on the field have access to first aid?	1.0	Yes or No	100 percent of workers answering "yes"
		Is there protective equipment in the workplace?	1.0	Yes or No	100 percent of workers answering "yes"
Community	Economic development	Does sugar cultivation contribute to local employment?	1.0	Yes or No	100 percent of people answering "yes"
		Does sugar cultivation help to reduce migration for other jobs outside the community?	0.6	Yes or No	100 percent of people answering "yes"
	Health and Safety	Are you exposed to pollution from sugarcane cultivation?	1.0	Yes or No	100 percent of people answering "no"
Farm owners	Social responsibility	Do you participate in a group of organic agriculture farmers or other groups that save the environment?	0.6	Yes or No	100 percent of farmers answering "yes"
		Do you cultivate organic sugarcane in your farm?	0.6	Yes or No	100 percent of farmers answering "yes"
		Are hazardous chemicals such as Furadan used in the sugarcane farms?	1.0	Yes or No	100 percent of farmers answering "no"
	Health and Safety	Do you prepare first aid equipment for employees?	1.0	Yes or No	100 percent of farmers answering "yes"
	Satisfaction of occupation	Are you satisfied with being a sugarcane farmer as a career?	1.0	Yes or No	100 percent of farmers answering "yes"

[a]as of October 2021
[b]IOC is Item Objective Congruence

Data collection was done using face-to-face surveys with stakeholders in 2018. Data were collected from farm owners, workers, and locals living in the community nearby. The number of samples for each stakeholder group was fixed to at least 30 persons. According to the study of Manik et al. (2013), the suggested minimum sample size for statistical significance is 30. The sample sizes for the different stakeholder groups are shown in Table 2. The farm owners included in this study were small-scale farmers as they are the majority of sugarcane farmers in the site studied. All stakeholders surveyed were asked questions about both green and burnt sugarcane harvesting because they were affected by both harvesting practices.

Data collection approach for this study has been granted ethics approval by the Mahasarakham University Ethics Committee for Research Involving Human Subjects (approval number: 118/2018), with exemption review method. To protect the interviewees' identity, verbal consents were granted

before starting the surveys. Hence, paper-based consent forms were not used in this study.

2.4 Impact assessment

This study applied the performance reference points method because it is suggested for use when undertaking an S-LCA study at a site-specific level as the results are more accurate (Chhipi-Shrestha et al., 2015). The performance reference point method assesses social performances by comparing a product's current social performance with the performance reference points based on internationally accepted minimum performance levels, relevant guidelines, and standards (Russo Garrido et al., 2018). The characterization, weighting, and interpretation of results are described in the following sub-sections.

Table 2. Number of samples of different stakeholder groups

Stakeholder group	Description	No. of samples	
		Green harvesting	Burnt harvesting
Workers	Employees working in sugarcane fields	41	41
Community	People who live in the nearby area	30	30
Farm owners	Farmers who own sugarcane plantations	34	34

2.4.1 Characterization

The inventory data for each indicator were characterized into the percentage of respondents answering yes or no following social criteria (see details in Table 1). This was adapted from the characterization method used in Aparcana and Salhofer (2013) and Manik et al. (2013). The characterized score for each indicator was in the range of 0-100. In addition, the statistical analysis technique, "Cochran's Q test" was used to assess whether the proportion of respondents answering yes and no for the green and burnt sugarcane harvesting options were significantly different. The analysis was undertaken for each social indicator at a confidence level of 0.50. Cochran's Q test was used because it is possible for use when response is two possible outcomes (in this case, yes or no).

2.4.2 Weighting

The weighting step was undertaken to aggregate the social performance values of different social indicators belonging to the same social issue into a single value. The same principle also applies to the values for different social issues belonging to the same stakeholder group. Weighting was done at the levels of social indicators and social issues. The weighting factors were based on stakeholders' perceptions and were obtained using surveys. Stakeholders were asked to rate the importance of social indicators/issues using a score of 1-100. Zero refers to least important, while 100 refers to most important. The weighting factors were calculated using the following Equations 1 and 2.

$$\text{Weighting factor}_i = \text{AI}_i / \Sigma \text{I}_i \quad (1)$$

Where; Weighting factor$_i$ is weighting factor for each social indicator; AI$_i$ is average of importance scores from all stakeholders for that particular social indicator; ΣIi is sum of the average of importance scores of all social indicators within the same social issue.

$$\text{Weighting factor} = \text{AI}/\Sigma\text{I} \quad (2)$$

Where; Weighting factor is weighting factor for each social issue; AI is average of importance scores from all stakeholders for that particular social issue; ΣI is sum of average of importance scores of all social indicators within the same stakeholder group.

After getting the weighting factors for social indicators and social issues, the weighted social performances of social indicators and social issues were calculated using the following Equations 3 and 4.

$$\text{WIN} = \text{AIN}_i \times \text{Weighting factor}_i \quad (3)$$

Where; WIN is weighted social performance of social indicator; AIN$_i$ is average of indicator results; Weighting factor$_i$ is weighting factor for that particular indicator.

$$\text{WIS} = \Sigma\text{WIN} \times \text{Weighting factor} \quad (4)$$

Where; WIS is weighted social performance of social issue; ΣWIN is Sum of weighted social performances of social indicators within the same social issue; Weighting factor is weighting factor for that social issue.

After getting the weighted social performance of all social issues, given that all stakeholder groups

are equally important, the social performance of each stakeholder group was calculated by simply summing up weighted social performances of all the social issues for each stakeholder group as shown in Equation 5.

$$SPS = \Sigma WIS \quad (5)$$

Where; SPS is social performance of stakeholder group; ΣWIS is sum of weighted social performances of social issues within the same stakeholder group.

2.4.3 Interpretation of results

To ease the interpretation of results, the classification system shown in Figure 3 was used in this study. This classification system was adapted from Sawaengsak et al. (2019). The social performances calculated from the previous section were classified into five groups, with the scores in each group ranging between 0-100.

Poor	Fair	Medium	Good	Very good
0-20	21-40	41-60	61-80	81-100

Figure 3. Classification of results

3. RESULTS AND DISCUSSION

The social indicator results, weighting factors, and the weighted social performances of social indicators, for the green and burnt sugarcane harvesting, are shown in Table 3. In addition, Table 3 also indicates whether there was a difference in proportion (between the green and burnt harvesting groups) of stakeholders answering yes or no for each social indicator, using Cochran's Q test, measured at 95 percent confidence.

Table 3. Social indicator results, weighted performance of social indicators, and weighting factors

Stakeholder groups	Social issues	Social indicators	The average of indicator results		Weighting factor	Weighted performance of social indicator for green harvesting	Weighted performance of social indicator for burnt harvesting
			Green harvesting	Burnt harvesting			
Workers	Fair wage	• Minimum wage (9 USD/day)	59[b]	76[b]	1.00	59	76
			Social performance of fair salary			59	76
	Working conditions	• Absence of forced labor to work at risk of danger	100[a]	100[a]	0.50	50	50
		• Workers of all genders working on the same kind of work receive the same remuneration	100[a]	100[a]	0.50	50	50
			Social performance of working conditions			100	100
	Health and Safety	• All workers present on the field have access to first aid	49[b]	44[b]	0.49	24	22
		• There is protective equipment in the workplace	54[b]	46[b]	0.51	27	24
			Social performance of health and safety			51	45
Community	Economic development	• Local employment	75[a]	75[a]	0.68	51	51
		• No migration for other occupations outside the community	81[a]	81[a]	0.32	26	26
			Social performance of economic development			77	77
	Health and Safety	• None of the exposure of pollution from sugarcane farming	100[b]			38[b]	0.86
			Social performance of health and safety			86	32

[a]Analysis of Cochran's Q test to find the proportion of each group of stakeholders answering yes/no at $p<0.05$, indicating that there was no significant difference at 95% confidence.

[b]Analysis of Cochran's Q test to find the proportion of each stakeholder group answering yes/no at $p>0.05$, indicating a significant difference at 95% confidence.

Table 3. Social indicator results, weighted performance of social indicators, and weighting factors (cont.)

Stakeholder groups	Social issues	Social indicators	The average of indicator results		Weighting factor	Weighted performance of social indicator for green harvesting	Weighted performance of social indicator for burnt harvesting
			Green harvesting	Burnt harvesting			
Farm owners	Social responsibility	• Participation in a group of organic agriculture members or other groups that save the environment	100[a]	100[a]	0.24	24	24
		• Organic sugarcane is cultivated	16[a]	16[a]	0.38	6	6
		• Avoid the use of hazardous chemicals prohibited for use in sugarcane farms such as Furadan	100[a]	100[a]	0.38	38	38
			Social performance of social responsibility			68	68
	Health and Safety	• The first aid equipment is prepared for employees	39[a]	39[a]	1.00	39	39
			Social performance of health and safety			39	39
	Satisfaction of occupation	• Satisfaction in sugarcane planting career	82[a]	82[a]	1.00	82	82
			Social performance of satisfaction of occupation			82	82

[a]Analysis of Cochran's Q test to find the proportion of each group of stakeholders answering yes/no at $p<0.05$, indicating that there was no significant difference at 95% confidence.
[b]Analysis of Cochran's Q test to find the proportion of each stakeholder group answering yes/no at $p>0.05$, indicating a significant difference at 95% confidence.

3.1 Workers

The wages for all stages of sugarcane cultivation were not different between the green and the burnt harvesting except for harvesting. In sugarcane harvesting, the workers are paid wages based on the amount of sugarcane they can cut. Fifty-nine percent of workers in the green sugarcane harvesting reported that they were paid at least the minimum daily wages (Minimum wage is 9 USD/day, based on local general wage). Seventy-six percent of workers in the burnt sugarcane harvesting reported that they received at least the minimum wage.

Green sugarcane harvesting requires expertise and strength. The green sugarcane farms have dense sugarcane leaves and grass. Workers have to peel off the sugarcane leaves before cutting, resulting in longer working hours. In addition, in Thailand, the hot weather can slow down the work. Sawaengsak et al. (2021) reported that workers who are more skilled and healthy could cut sugarcane in large quantities, resulting in wages greater than or equal to the minimum wage. In the study area, the workers reported that the maximum amount of green sugarcane that a worker could cut was about 100 bales a day (the wage equals 9 USD/day). This means that some of them earned less than the minimum wage. While for burnt sugarcane, a worker could cut at least 150 bales (the wage equals 9 USD/day). This implies that every worker could secure the minimum wage by cutting the burnt sugarcane. This information corresponds to reports about the sugarcane harvesting in the Eastern Region of Thailand, where the workers could cut about 100 bales green sugarcane a day but about 300 bales of burnt sugarcane (Kijjakosol, 2019).

There was no difference between the result indicators of the green and burnt sugarcane harvesting for working conditions. There was no report on forced labor to work at risk of danger and wage discrimination among different genders of workers. Therefore, the social performance score for this social issue is 100 for both harvesting approaches. A similar study by Prasara-A and Gheewala (2018) in a different province in the North-Eastern Region of Thailand also reported that there was no wage discrimination among different genders in sugarcane cultivation.

The social performance for the health and safety issue for green and burnt harvesting is at a "Medium" level. Compared to other social aspects, this issue did

not perform very well. A study by Du et al. (2019) also identified health and safety as one of the impact categories with the highest risks for sugarcane production in Brazil. In the green sugarcane fields, forty-nine percent of workers reported access to first aid equipment, and fifty-four percent of workers said there was some equipment in the farms. Some added that they often prepared the first aid and the protective equipment themselves. For workers in the burnt sugarcane fields, forty-four percent reported that they had access to first aid supplies and forty-six percent said there was protection equipment in the farm. These results show that more first aid kits and protective gear were provided in the green sugarcane harvesting farms. This is because the working conditions in the green sugarcane farms are more complex. However, the calculated social performances of this social issue are at the same level (medium) for both green and burnt harvesting.

3.2 Community

Social indicator results for local employment and migration for other occupations outside the community issues are the same for both green and burnt sugarcane harvesting. Seventy-five percent of the locals surveyed reported that the sugarcane farm owners hire local workers. In comparison, twenty-five percent of locals said that workers were from other regions (employed in the harvesting season only). Eighty-one percent of the locals responded that there was no migration of people for jobs outside the community. The performance for this social issue is at the "Good" level. This result is supported by a study in Brazil where a positive relationship was found between sugarcane and economic development (Tomei et al., 2020). For health and safety issues, all of the locals surveyed responded that they were not affected by the green sugarcane harvesting. Sixty-two percent of locals reported being affected by sugarcane burning, as the dust and smoke from burning sugarcane blew into their houses. Thirty-eight percent of the locals said they were not affected because their houses were quite far from the sugarcane fields.

3.3 Farm owners

Regarding the social responsibility issues, the results for both green and burnt sugarcane harvesting are the same as their cultivation practices were similar. Even though all of the farm owners surveyed claimed that they had participated in a group of organic agriculture farmers or other groups that save the environment, only sixteen percent of them grew organic sugarcane. Some of the farm owners interviewed commented that the reason for not opting to grow organic sugarcane is that the organic sugarcane has lower yields than conventional sugarcane. However, a study by Coulis (2021) revealed that organic sugarcane farming has a beneficial effect on soil biological processes even after a short period of conversion from conventional farming. However, all farm owners surveyed claimed that they did not use any prohibited chemicals in their sugarcane farms.

For health and safety issues, thirty-nine percent of the farm owners reported providing some first aid facilities to employees. They added that the employees were always careful in their work and often prepared the first aid equipment they needed. Regarding career satisfaction, eighty-two percent of both harvesting groups responded that they were satisfied with their career as sugarcane growers and will continue to grow in the future. They commented that the area was suitable for sugarcane cultivation, and they have expertise in sugarcane growing and that selling sugarcane could earn a living. However, several of the farm owners surveyed commented that if the price of sugarcane falls in the future, they might change to grow other crops instead.

From Table 3, when considering each social issue, both green and burnt harvesting have social performance scores at the same level, except for fair wages for workers and health and safety for the community. The green harvesting has lower social performance for fair salary (medium level) than that of the burnt harvesting (good level) because of the lower wages for workers. Lower wages in green harvesting were caused by challenging working conditions for green harvesting, making some of the workers unable to earn the minimum wage. The social performance of health and safety for the community for burnt harvesting (fair level) is lower than green harvesting (very good level). This resulted from the lower rate of locals affected by the pollution from sugarcane burning. The results shown in Table 3 suggest that the social issue that needs urgent attention is all stakeholder groups' health and safety. This includes the problems of sugarcane burning and first aid kits provided to the workers.

Table 4 shows weighted social performances of different social issues, weighting factors, and the social performances of different stakeholders for green and burnt sugarcane harvesting

Table 4. Weighted social performances of different social issues and social performances of stakeholders, and weighting factors

Stakeholder groups	Social issues	Weighting factor	Performance of social issues		Weighted performance of social issues	
			Green harvesting	Burnt harvesting	Green harvesting	Burnt harvesting
Workers	Fair wages	0.32	59	76	19	24
	Working conditions	0.33	100	100	33	33
	Health and safety	0.35	51	45	18	16
	Social performance of workers				70	73
Community	Economic development	0.49	77	77	38	38
	Health and safety	0.51	86	32	44	16
	Social performance of community				82	54
Farm owners	Social responsibility	0.22	68	68	15	15
	Satisfaction of occupation	0.39	39	39	15	15
	Health and safety	0.39	82	82	32	32
	Social performance of farm owners				62	62

From Table 4, when considering the overall social performances of different stakeholder groups for green and burnt harvesting, the social performances of workers and farm owners are at the same level (good) except for the community. For the community stakeholder group, the social performance of green harvesting is at the "very good" level, while the one for burnt harvesting is at the "medium" level. This is mainly due to the problem of sugarcane trash burning.

The root cause of this burnt sugarcane harvesting is related to manual harvesting. Burning sugarcane before cutting is practiced to ease the productivity of manual harvesting. Another issue in sugarcane cultivation is a shortage of labor for harvesting. The farmers have to get the harvested sugarcane to the sugar factories in time. Therefore, a large number of sugarcane cutters are needed at the same time. This results in a labor shortage in some areas (Thansettakij Multimedia, 2019). However, the problem of sugarcane burning has to be addressed urgently as it causes a negative health impact on locals and also other stakeholders who also live in the community in the long term.

To solve the problem of sugarcane burning, the government has started to educate the farmers about the health impact of particulate matter caused by sugarcane burning. They have also provided loans for farmers at a low-interest rate to buy sugarcane cutting machines (Khaosod, 2019). However, as mentioned earlier in the introduction section, there are still issues about using sugarcane harvesting machines, such as the high cost of machines and conditions of sugarcane fields for using harvesting machines, such as proper interval distance between sugarcane rows and size of sugarcane fields. For this reason, the majority of the Thai sugarcane farmers (mostly small-scale farmers) seem not yet ready to use the harvesting machines (Chaya et al., 2019).

Another reason for burnt sugarcane harvesting is that it has more productivity. This issue also causes higher production costs for green sugarcane burning. Kijjakosol (2019) reported that the cost of harvesting 1 tonne of burnt sugarcane for manual harvesting was 2.1-2.4 USD lower than that of the green sugarcane. On the other hand, the selling price of green sugarcane per 1 tonne was 0.9 USD higher than burnt sugarcane (Mitr Phol Group, 2020). Obviously, the cost of manual harvesting of green sugarcane is more than that of burnt sugarcane. The farm owners are disadvantaged by using labor to cut the green sugarcane.

As discussed earlier, the issues that need urgent attention are the problem of sugarcane trash burning and the low rate of first aid kits provided to the workers. The first problem seems to bear enormous pressure on the sugarcane farm owners. Different factors are causing the sugarcane farmers to harvest the burnt sugarcane. These include the need to harvest sugarcane quickly to send to the sugar mills, lack of labor to harvest sugarcane, the workers prefer cutting burnt sugarcane, and harvesting burnt sugarcane having lower production cost for harvesting. With social pressure about the impacts of sugarcane trash burning on all stakeholders, mechanized green sugarcane harvesting seems appropriate. However, there is an urgent need for technology development for cheaper machines to make them more affordable for

sugarcane farmers. Moreover, the equipment needs to be developed for use in any geographical condition.

4. CONCLUSION

The social life cycle assessment results of green and burnt sugarcane harvesting using a case in Udon Thani Province in the North-Eastern Region of Thailand were presented. This study site was selected as it hosts the largest sugarcane plantation area in the country. In addition, it is near the border of a neighboring country, which means that the social and environmental impacts caused by sugarcane production from this area may affect the locality and another country. This study compares the social performances of the two different sugarcane harvesting practices used at the site study, i.e., green and burnt harvesting. Both approaches of sugarcane harvesting in this area still mainly rely on human labor as the geographical conditions are not suitable for the use of harvesting machines. The stakeholder groups included workers, the community, and farm owners. Moreover, it identifies hotspots needing improvement to help reduce environmental impact and improve the social conditions of stakeholders involved in sugarcane production.

The main findings reveal that the social performance scores for most of the social issues for green and burnt harvesting are at the same level, except fair wages for workers and health and safety for the community. For the fair wages aspect, green harvesting has “medium” social performance, while burnt harvesting has “good” social performance. The main issue lowering the social performance for green harvesting is the difficult working conditions for workers to make at least the minimum wage. This is because the sugarcane harvesting is paid per amount of the sugarcane they could cut.

For the health and safety of the community, burnt harvesting has lower social performance than green harvesting. This impact is caused by the cane trash burning before harvesting. Considering all the social issues examined, the problems that need urgent attention are the sugarcane trash burning and first aid kits provided to the workers. However, the overall social performances of workers and farm owners are at the same level (good level) except for the community. The social performance of green harvesting for the community group is in the “very good” level, while it is in the “medium” level for burnt harvesting.

In summary, burnt harvesting has lower social performance; the difference is mainly from the problem of sugarcane trash burning. To address this problem, factors making the farm owners choose burnt harvesting are needed to be understood and resolved. This includes the necessity to harvest sugarcane quickly to be delivered to sugar mills, a scarcity of labor to harvest sugarcane, employees preferring to cut burnt sugarcane, and cheaper cost for burnt harvesting. Moreover, the current issue of air pollution from cane trash burning, mechanized sugarcane harvesting appears to be the best option. However, technology development for less expensive machines is critical to make them accessible to all sugarcane producers. Furthermore, the equipment must be designed to work in any environment.

ACKNOWLEDGEMENTS

This work was supported by the Research Chair Grant of the National Science and Technology Development Agency, Ministry of Science and Technology, Thailand under grant number (P-16-51880); Thailand Research Fund and the Office of the Higher Education Commission (OHEC) under grant number (MRG6180276). All the anonymous stakeholders providing inputs for this research are gratefully acknowledged.

REFERENCES

Aparcana S, Salhofer S. Development of a social impact assessment methodology for recycling systems in low-income countries. International Journal of Life Cycle Assessment 2013;18(5):1106-15.

Barbosa CMG, Terra-Filho M, Albuquerque ALP, de Giorgi D, Di Grupi C, Negrão CE, et al. Burnt sugarcane harvesting-cardiovascular effects on a group of healthy workers, Brazil. PLoS ONE 2012;7(9):e46142.

Bonsucro. Bonsucro Production Standard Version 4.01. London, UK: Bonsucro; 2014.

Chaya W, Bunnag B, Gheewala SH. Adoption, cost and livelihood impact of machinery services used in small-scale sugarcane production in Thailand. Sugar Tech 2019;21(4):543-56.

Chhipi-Shrestha GK, Hewage K, Sadiq R. ‘Socializing’ sustainability: A critical review on current development status of social life cycle impact assessment method. Clean Technologies and Environmental Policy 2015;17(3):579-96.

Coulis M. Abundance, biomass and community composition of soil saprophagous macrofauna in conventional and organic sugarcane fields. Applied Soil Ecology 2021;164:Article No. 103923.

Department of International Organizations. Thailand’s Voluntary National Review on the Implementation of the 2030 Agenda for Sustainable Development. Bangkok, Thailand: Department of International Organizations; 2021.

de Oliveira Bordonal R, Barretto de Figueiredo E, Aguiar DA, Adami M, Theodor Rudorff BF, La Scala N. Greenhouse gas

mitigation potential from green harvested sugarcane scenarios in São Paulo State, Brazil. Biomass and Bioenergy 2013; 59:195-207.

Du C, Ugaya C, Freire F, Dias LC, Clift R. Enriching the results of screening social life cycle assessment using content analysis: A case study of sugarcane in Brazil. International Journal of Life Cycle Assessment 2019;24(4):781-93.

Gheewala SH, Silalertruksa T, Pongpat P, Bonnet S. Biofuels production from sugarcane in Thailand. In: Khan MT, Khan IA, editors. Sugarcane Biofuels: Status, Potential, and Prospects of the Sweet Crop to Fuel the World. Springer, Cham; 2019. p. 157-74.

Khaosod. Move forward to solve the sugarcane problem with hope to reduce the air pollution [Internet]. 2019 [cited 2021 Oct 31]. Available from: https://www.khaosod.co.th/economics/news_2184918 (in Thai).

Kijjakosol T. Sugarcane planters federation explains the necessity to burn sugarcane [Internet]. 2019 [cited 2022 Jan 5]. Available from: https://www.77kaoded.com/news/thanapat/289029 (in Thai).

Manik Y, Leahy J, Halog A. Social life cycle assessment of palm oil biodiesel: A case study in Jambi Province of Indonesia. International Journal of Life Cycle Assessment 2013;18(7): 1386-92.

Matsuda M, Braga ALF, Marquezini MV, Monteiro MLR, Saldiva PHN, de SantosU. Occupational effect of sugarcane biomass burning on the conjunctival mucin profile of harvest workers and residents of an adjacent town-A Brazilian panel study. Experimental Eye Research 2020;190:Article No. 107889.

Mitr Phol Group. Stop burning sugarcane! what are benefits of green harvesting? [Internet]. 2020 [cited 2020 Jan 24]. Available from: https://www.mitrphol.com/news_detail.php?topic=263 (in Thai).

Food and Agriculture Organization of the United Nations (FAO). Sustainability Assessment of Food and Agriculture Systems Indicators. Rome, Italy: Food and Agriculture Organization of the United Nations; 2013.

Office of the Cane and Sugar Board (OCSB). Situation Report on Sugarcane Planting: Producion year 2020/2021. Bangkok, Thailand: Office of the Cane and Sugar Board; 2021. (in Thai).

Pongpat P, Gheewala SH, Silalertruksa T. An assessment of harvesting practices of sugarcane in the central region of Thailand. Journal of Cleaner Production 2017;142(Part3): 1138-47.

Prasara-AJ, Gheewala SH. Applying social life cycle assessment in the Thai sugar industry: Challenges from the field. Journal of Cleaner Production 2018;172:335-46.

Rezaei Kalvani S, Sharaai AH, Abdullahi IK. Social consideration in product life cycle for product social sustainability. Sustainability 2021;13:Article No. 11292.

Russo Garrido S, Parent J, Beaulieu L, Revéret JP. A literature review of type I SLCA-making the logic underlying methodological choices explicit. International Journal of Life Cycle Assessment 2018;23(3):432-44.

Sawaengsak W, Olsen SI, Hauschild MZ, Gheewala SH. Development of a social impact assessment method and application to a case study of sugarcane, sugar, and ethanol in Thailand. International Journal of Life Cycle Assessment 2019;24:2054-72.

Sawaengsak W, Prasara-AJ, Gheewala SH. Assessing the socio-economic sustainability of sugarcane harvesting in Thailand. Sugar Tech 2021;23(2):263-77.

Thansettakij Multimedia. Why burn sugarcane?...insight stories that outsiders don't know about! [Internet]. 2019 [cited 2021 Oct 31]. Available from: https://www.thansettakij.com/content/379992 (in Thai).

Tomei J, de Oliveira L, de Oliveira Ribeiro C, Lee Ho L, Montoya LG. Assessing the relationship between sugarcane expansion and human development at the municipal level: A case study of Mato Grosso do Sul, Brazil. Biomass and Bioenergy 2020;141:Article No. 105700.

United Nations Environment Programme (UNEP). The Methodological Sheets for Subcategories in Social Life Cycle Assessment (S-LCA) (Pre-Publication Version). Paris, France: United Nations Environment Programme; 2013.

United Nations Environment Programme (UNEP). Guidelines for Social Life Cycle Assessment of Products and Organizations 2020. Paris, France: United Nations Environment Programme; 2020.

Valdivia S, Ugaya CML, Hildenbrand J, Traverso M, Mazijn B, Sonnemann G. A UNEP/SETAC approach towards a life cycle sustainability assessment-our contribution to Rio+20. International Journal of Life Cycle Assessment 2013; 18(9):1673-85.

WordPress. Udonthani, Thailand [Internet]. 2021 [cited 2021 Oct 31]. Available from: https://udonthailand.files.wordpress.com/2015/10/2558-09-25-11_52_19-udon-thani-google-maps.png?fbclid=IwAR0_4uWkhhGkinAjDiWlbPXQVvmn_Efn36wtTsbfG3SEZWZLA9nCZZTqGM8.

Workman D. Sugar exports by country [Internet]. 2020 [cited 2021 Oct 31]. Available from: http://www.worldstopexports.com/sugar-exports-country/.

Plant Growth Promoting Activities of Spore-Forming and Vegetative Cells of Salt-Tolerant Rhizobacteria under Salinity Condition

Tiptida Kidtook[1], Jindarat Ekprasert[2], and Nuntavun Riddech[2*]

[1]*Graduate School of Microbiology Program, Department of Microbiology, Faculty of Science, Khon Kaen University, Khon Kaen 40002, Thailand*

[2]*Department of Microbiology, Faculty of Science, Khon Kaen University, Khon Kaen 40002, Thailand*

ARTICLE INFO

Received: 29 Oct 2021
Received in revised: 18 Jan 2022
Accepted: 23 Jan 2022
Published online: 17 Feb 2022
DOI: 10.32526/ennrj/20/202100211

Keywords:
Spore forming rhizobacteria/
Vegetative cell rhizobacteria/
Salinity condition

*** Corresponding author:**
E-mail: nunrid@kku.ac.th

ABSTRACT

Plant growth promoting rhizobacteria are able to enhance plant growth. This study isolated spore-forming rhizobacteria from vegetable rhizosphere soil samples. These isolates were tested for their abilities to promote plant growth and to be used in bio-fertilizers. Thirty-nine isolates with different characteristics were obtained. Three isolates, TYS1.1, TYS3.3, and TYS3.5, showed multifunctional activities on nitrogen fixation and potassium solubilization. They were tested for IAA production in liquid medium supplemented with tryptophan and NaCl, with the vegetative cells of isolate TYS3.5 showing the highest IAA production. The colonization of the three isolates on okra roots was checked by spread plate technique and scanning electron microscope. It was found that rhizobacteria could colonize plant roots with a concentration of 8.19 log CFU/g in the presence of 50 mM NaCl solution. Bio-fertilizer was produced by immobilizing the mixture of three isolates on carriers. The viable cells were enumerated during the storage at room temperature for 60 days. The results showed that the highest number of survival cells in the form of vegetative and spore-forming cells were obtained when using rice husk ash and vermiculite as a carrier. The concentration of viable cells was in a range of 8.14-8.44 log CFU/g. These isolates were *Bacillus* sp. according to the 16S rDNA sequencing analysis.

1. INTRODUCTION

Saline soil is an unfertile soil. In saline soil, salt ions accumulate and affect the growth and productivity of plants, especially in the dry season. Moreover, the imbalance of nutrient-uptake by plants in saline soil might be caused by salt ions. Where agriculture is undertaken, it is therefore necessary to improve the quality of saline soils. Chemical fertilizer is commonly utilized, yet its continuous use over prolonged periods can lead to negative effects on the soil, the wider environment and the organisms present. Consequently, the availability of an ecofriendly alternative such as a bio fertilizer would be beneficial

Plant growth promoting rhizobacteria (PGPR) are genetically diverse microorganisms found in soil. They are an important factor in the decomposition and turnover of minerals and also promote plant growth and provide protection. There are many types of soil microorganisms, including bacteria, fungi and actinomycetes which are classified as PGPR. PGPRs have the ability to convert unavailable forms of soil nutrients into available forms for plant growth. Soil microbes have naturally versatile functional relationships. In the environment, interaction between microbes show both positive and negative effects. Thus, to apply and also to keep a long shelf-life of microbial products in the natural soils, it is necessary to immobilize microbes on supporting material such as organic or inorganic carriers.

The production of microbial inoculants as bio-fertilizers requires development. The first step of the simple production process is the propagation of microbial cells in a culture broth. Next is the immobilization of microorganisms on sterile carrier materials and the last step is the incubation of immobilized products at room temperature for 1-2 weeks. Many types of carriers can be used for bio-fertilizer production. For instance, organic carriers

Citation: Kidtook T, Ekprasert J, Riddech N. Plant growth promoting activities of spore-forming and vegetative cells of salt-tolerant rhizobacteria under salinity condition. Environ. Nat. Resour. J. 2022;20(3):257-265. (https://doi.org/10.32526/ennrj/20/202100211)

such as peat, bagasse and rice husk ash, and inorganics carriers such as alginate and vermiculite are normally used as carrier materials. To reduce the cost of bio-fertilizer and to realize zero waste for agricultural sectors, the residues or waste from agro-industries could be used as carriers. The microbial inoculant can be both in the form of vegetative cells and endospores. However, the use of microbial vegetative cells in bio-fertilizer is less recommended due to both their intolerance to soil abiotic and biotic stresses and their short shelf-life. Thus, to enhance microbial survival rates under stress environments, utilizing endospores is most preferable.

Bacillus spp. is classified as a plant growth promoting bacteria (PGPB). It has the ability to promote plant growth through its nitrogen fixation activity, phosphate and potassium solubilization activities and also phytohormone production, such as IAA and gibberellic acid (Shen et al., 2016). The role of *Bacillus* in the ecosystem is as a decomposer of organic matter in soil, which can become nutrients for plant growth. *Bacillus* is characterized as an aerobic gram-positive bacterium. It is spore-forming and so able to tolerate stress conditions. Therefore, *Bacillus* can be found in heat, cold, drought, nutrient-lacking conditions, and in saline soil. Under suitable conditions for growth, *Bacillus* endospores can turn into vegetative forms of bacterial cells. Moreover, it has the ability to survive and proliferate in various environments (Lyngwi and Joshi, 2014). A previous report found that *Bacillus* alleviates the harmful effects of salt stress and enhances the growth of peanuts grown in sodium chloride-adjusted soils with various plant growth-promoting microbial properties such as phosphate solubilization, ammonia, IAA and siderophore production (Goswami et al., 2014). For this reason, *Bacillus* sp. can be utilized as a bio-fertilizer and applied to cultivation areas with stress conditions. The aim of this study was to compare the abilities of vegetative cells and endospores of rhizobacteria for use as a bio-fertilizer to promote plant growth. The results obtained from this study can be used as a model to produce bio-fertilizers suitable for plant cultivation in saline soil.

2. METHODOLOGY

2.1 Screening of spore-forming microorganisms from rhizosphere soils

Rhizosphere soil samples of vegetable plants (*Brassica rapa* L., *Apium graveolens* L., *Lactuca sativa* L., *Brassica alboglabra*, and *Coriandrum sativum* L.) were collected from agricultural fields in Khon Kaen Province. Rhizobacteria were isolated from soil samples using spread plate technique according to a modified method of Bal and Adhya (2012). Five grams of soil was suspended in 45 mL of distilled water and then incubated in a water bath at 80°C for 12 min (Watterson et al., 2014) to stimulate spore germination. After that, the flasks were immediately transferred to incubate in a water bath at room temperature. Soil suspensions were diluted to 10^{-4}-10^{-6} and then spread on the Nutrient Agar (NA) and Tryptone Yeast Extract (TYE) agar media in order to screen for spore forming colonies (Verma et al., 2013). Plates were incubated at 30°C for 24-48 h. Single colonies were subsequently subcultured onto fresh media for purification. Cultures of pure isolates were stored in 20% glycerol and kept at -20°C for PGPR activity test and biofertilizer production.

2.2 Gram Staining and Endospore staining

Colonies of the isolates were gram-stained for visualization under a microscope and their Gram types classified. Gram-positive bacterial isolates were stained with malachite green solution in order to visualize spore formation under a microscope. Spore-forming bacteria were selected for use in further experiments.

2.3 Preparation of vegetative cells and endospores

To cultivate vegetative cells, bacterial isolates were cultured in nutrient broth (NB) and incubated at 30°C with shaking at 150 rpm for 18 h. Then, cell suspensions were centrifuged at 7,000 rpm for 20 min at 4°C to remove supernatants. Cell pellets were washed twice with 0.85% NaCl. Bacterial cells were dissolved in a 0.85% NaCl solution to obtain a cell density of 10^8 CFU/mL.

Endospores were prepared by using the modified method of Omer (2010). Bacterial isolates were cultured in TYE medium and incubated with shaking at 150 rpm at 30°C for 48 h. Then culture broth was boiled at 80°C for 12 min, afterward the endospores were harvested by centrifugation at 7,000 rpm for 20 min and subsequently washed twice with 0.85% NaCl solution. Concentrations of endospores were adjusted to 10^8 CFU/mL. The number of endospores was determined by counting on agar plate and the formation of spores confirmed using a spore staining technique.

2.4 Determination of plant growth promoting abilities of the vegetative cells and spore-forming cells of the selected bacterial isolates

2.4.1 Screening for nitrogen fixation activity

To determine the nitrogen fixation activity, vegetative and spore-forming cell suspensions were diluted to 10^{-1}-10^{-6} and spread onto a nitrogen free culture medium (Ashby's agar). Plates were incubated at 30°C for seven days. Colonies grown on Ashby's agar were indicative of positive nitrogen fixing activity. This was also confirmed by the inoculation of bacterial suspension into 10 mL Ashby's broth, and incubation by shaking at 150 rpm, at 30°C, for three days. The uninoculated media served as a control. Microbial growth in the nitrogen-free culture broth (Kumar et al., 2014) indicates a positive activity.

2.4.2 Phosphate solubilization activity

Phosphate solubilization activity of the bacterial isolates was evaluated using the National Botanical Research Institute's Phosphate growth medium (NBRIP) according to the modified method of Roslan et al. (2020). Bacterial cultures were point-inoculated onto NBRIP agar supplemented with tricalcium phosphate as an inorganic phosphate source. Plates were then incubated at 30°C for seven days. Clear zones around the colonies indicated the ability of bacteria to solubilize the inorganic phosphates.

2.4.3 Potassium solubilization activity

Potassium solubilization activity (Sun et al., 2020) was determined by point inoculation of the bacterial isolates onto the Aleksandrov agar medium containing potassium aluminum silicate as a source of inorganic potassium. Plates were then incubated at 30°C for seven days. Clear zones around the colonies showed the inorganic potassium-solubilizing ability.

2.5 IAA production

IAA-producing activity of the bacterial isolates was tested using the modified method of Ozdal et al. (2017). One mL of vegetative cells and spore forming cells of bacteria was inoculated into 10 mL of Tryptic soy broth (TSB) supplemented with tryptophan 1,000 mg/L and NaCl at a concentration of 0, 50, and 100 mM. Bacterial culture was incubated at 30°C with shaking at 150 rpm for three days. Two mL of the suspension was centrifuged at 10,000 rpm for 2 min. Supernatants were mixed with 2 mL of Salkowski reagent and then incubated in the dark for 25 min. A pink color appearing in the solution is an indicator of positive IAA production. The amount of IAA produced was determined by measuring absorbance at a wavelength of 530 nm using a spectrophotometer and then compared to an IAA standard curve.

2.6 Determination of root colonization of rhizobacteria under salinity condition using a conventional method and a scanning electron microscope (SEM)

According to the conventional method, seeds were grown on 6% water agar supplemented with 0, 50, and 100 mM of sodium chloride solution under a sterile condition for 7-15 days at room temperature. Root colonization was checked using a spread plate technique on tryptic soy agar.

For the determination of root colonization by SEM (Gajbhiye et al., 2019) the initial concentration of vegetative cells was 10^8 CFU/mL. Seeds were surface-sterilized by using 70% ethanol for 5 min and soaking with 3% (v/v) sodium hypochlorite for 5 min. Then, they were rinsed five times with sterile water, and soaked in rhizobacterial suspension for 30 min. Seeds were transferred into Hoagland's solution containing 0, 50, and 100 mM of sodium chloride solution under a sterile condition. Seeds were then incubated at room temperature for 7-15 days. Root samples were rinsed with 0.1 M phosphate buffered saline (PBS) pH 7.0 and then fixed with 2.5% glutaraldehyde, the samples were stored at 4°C for 2 h. The root samples, sized 3-5 mm, were soaked in PBS solution for 10 min three times. Then, the roots were soaked with different concentrations of ethanol (50, 60, 70, 80, and 90%) for 15 min of each concentration and finally soaked with absolute ethanol for 30 min at 4°C. Root samples were dried by critical point dryer (CPD). These samples were gold-coated prior to observation under SEM.

2.7 Bio-fertilizer production in the form of vegetative cells and spore-forming cells

In this study, bio-fertilizer was produced by immobilizing the vegetative cells and spore-forming cells on the carriers such as rice husk ash, bagasse, vermiculite and sodium alginate. The carrier materials (rice husk ash, bagasse and vermiculite) were prepared by autoclave sterilization. The humidity of carrier materials was then adjusted to be in the range 40-50%. Bacterial cells were inoculated at a concentration of 10% into each carrier material, mixed with 15% of starch and 2% PEG to make the granular bio-fertilizer, and then incubated at 50°C for 24 h.

The immobilization of bacteria on sodium alginate was performed by the method of Bashan et al. (2002). One hundred mg of skimmed milk powder was dissolved in hot water at 90°C and 1.6 g of sodium alginate (NaAlg) was added before sterilization. The solution was left to cool down at room temperature. Then, 10% (v/v) of a bacterial suspension was inoculated into the solution of sodium alginate under a sterilized condition. The mixture of rhizobacterial and immobilization solution was transferred into a 10 mL syringe and added dropwise into the 0.1 M $CaCl_2$ solution with stirring. After 30 min, alginate granules were separated from 0.1 M $CaCl_2$ solution and washed twice with 0.85% NaCl solution under a sterilized condition. Surviving vegetative and spore-forming cells of microorganisms immobilized on the carriers as bio-fertilizers were studied for the eight treatments: T1: alginate mixed with vegetative cells, T2: alginate mixed with spores, T3: bagasse mixed with vegetative cells, T4: bagasse mixed with spores, T5: rice husk ash mixed with vegetative cells, T6: rice husk ash mixed with spores, T7: vermiculite mixed with vegetative cells, T8: vermiculite mixed with spores. Survival of bacterial cells and spore-forming cells was determined for 60 days at 30°C (sampled at day 0, 15, 30, 45, and 60) by spread plate technique. The pH and electrical conductivity (EC) values were measured.

2.8 Statistical analysis

The significant differences among the data were analyzed using ANOVA and the Least Significant Difference (LSD) by using the Statistic 10 program ($p<0.5$).

3. RESULTS AND DISCUSSION

3.1 Isolation of rhizobacteria and determination of plant growth promoting activities in vegetative and spore-forming cells

The spore-forming rhizobacteria was isolated from rhizosphere soil samples of five types of vegetable. Soil samples were pre-treated by heating at 80°C in a water bath for 12 min, then spread onto tryptone yeast extract (TYE) and nutrient agar (NA) for culturing microbes, and incubated at 30°C. For thirty-nine isolates of rhizobacteria with different characteristics, it was found that 12 isolates were able to produce IAA and three isolates (TYS1.1, TYS3.3, and TYS3.5) showed the highest potential for IAA production. Nitrogen fixation, phosphate solubilization and potassium solubilization were also determined for these isolates. The results revealed that isolates TYS1.1, TYS3.3, and TYS3.5 exhibited nitrogen fixation and potassium solubilization activities (data shown in Table 1); all three isolates were *Bacillus* sp. according to the 16S rDNA sequencing analysis.

Table 1. Characterization of rhizobacterial isolates for nitrogen fixation, phosphate and potassium solubilization and Gram types

Isolates	Nitrogen fixing activity		Phosphate solubilization		Potassium solubilization		Gram stain	
	Vegetative cells	Spores	Vegetative cells	Spores	Vegetative cells	Spores	Gram positive	Endospores
TYS1.1	+	+	–	–	+	+	+	+
TYS3.3	+	+	–	–	+	+	+	+
TYS3.5	+	+	–	–	+	+	+	+

+ or – indicate positive and negative results, respectively

PGPRs have great potential to promote plant growth (Bashan et al., 2014). In this experiment, we isolated rhizobacteria from rice rhizosphere soil and used these bacteria to produce bio-fertilizers. *Bacillus* spp. is in a genus of bacteria that have properties for enhancing plant growth, such as phytohormones production (IAA and gibberellic acids), inorganic nutrient solubilization and nitrogen fixation (Gharib et al., 2015). In addition, *Bacillus* spp. are able to form endospores when grown under stress conditions, resulting in tolerance to heat and unfertile soils (Bressuire et al., 2018). The exhibition of endospore formation ability was reported by Pesce et al. (2014), which applied *Bacillus* spp. to environments and found that they were able to survive under stress environments. Our results were similar to Kumar et al. (2012), who screened 7 rhizobacterial isolates belonging to the genus *Bacillus* from bean rhizosphere samples. Their study found isolates that had IAA producing activity, siderophore production, organic acid production, ACC deaminase activities, and the dissolution of inorganic phosphate and potassium.

3.3 IAA production under different levels of salinity conditions

Auxin can promote plant growth through several mechanisms such as stimulating root elongation of primary or lateral roots, cell

enlargement, cell division, and root germination (Spaepen et al. 2007).

Three isolates of rhizobacteria (TYS1.1, TYS3.3, and TYS3.5) in the form of vegetative cells and spore-forming cells were tested for IAA production activity under various salinity conditions (0, 50, and 100 mM NaCl solution). It was found that at salinity concentrations greater than 100 mM of NaCl, three rhizobacterial isolates were able to produce IAA after 72 h of incubation, especially in the form of vegetative cells. The range of IAA production by vegetative cells of three TYS1.1, TYS3.3, and TYS3.5 were 69.78, 62.18, and 84.78 µg/mL, respectively. In the case of spore-forming cells, IAA was produced in a range of 23.17, 25.85, and 28.70 µg/mL, respectively, as shown in Figure 1. On the other hand, Rojas-solis et al. (2020) found that the amount of IAA produced from *Bacillus* sp. E25 was reduced from 31.18 µg/mL (control condition, without NaCl solution) to 20.51 and 20.46 µg/mL in the presence of NaCl solutions at concentrations of 100 and 200 mM, respectively. Moreover, an increase of salinity level in the culture broth of *Bacillus* sp. CR71 did not show a significant effect on IAA production. This is similar to the experiment of Ansari et al. (2019) which found that IAA production of *Bacillus pumilus* FAB10 was 105.8, 87.8, 73.3, 60.4, and 51.2 µg/mL, respectively, in the presence of NaCl concentrations of 0, 75, 125, 250, and 500 mM.

3.4 Root colonization

In this experiment, okra was selected for study because it is a popular vegetable for consumers in Thailand. Okra contains high levels of vitamins and minerals which are healthy for humans (Oyelade et al., 2003). Normally, okra can grow in every season and can tolerate moderate salinity. However, when it is cultivated in saline soil, the germination and the productivity of okra is reduced (Khan et al., 2001).

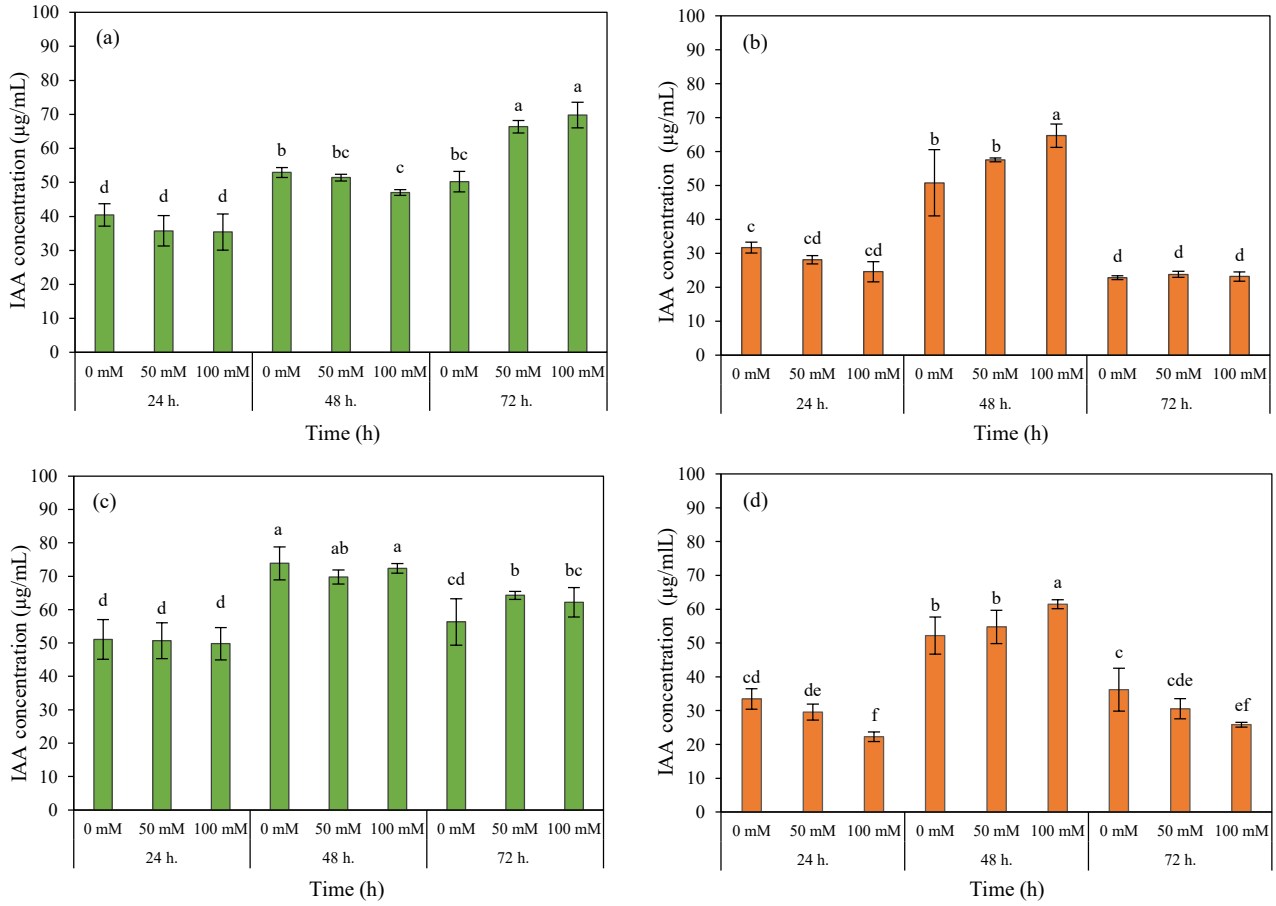

Figure 1. The IAA (indole-3-acetic acid) content produced by the isolate TYS1.1 including vegetative cells (a) and spore-forming cells (b), isolate TYS3.3; vegetative cells (c) and spore-forming cells (d), isolate TYS3.5; vegetative cells (e) and spore-forming cells (f) under different concentrations of NaCl solution (mM)

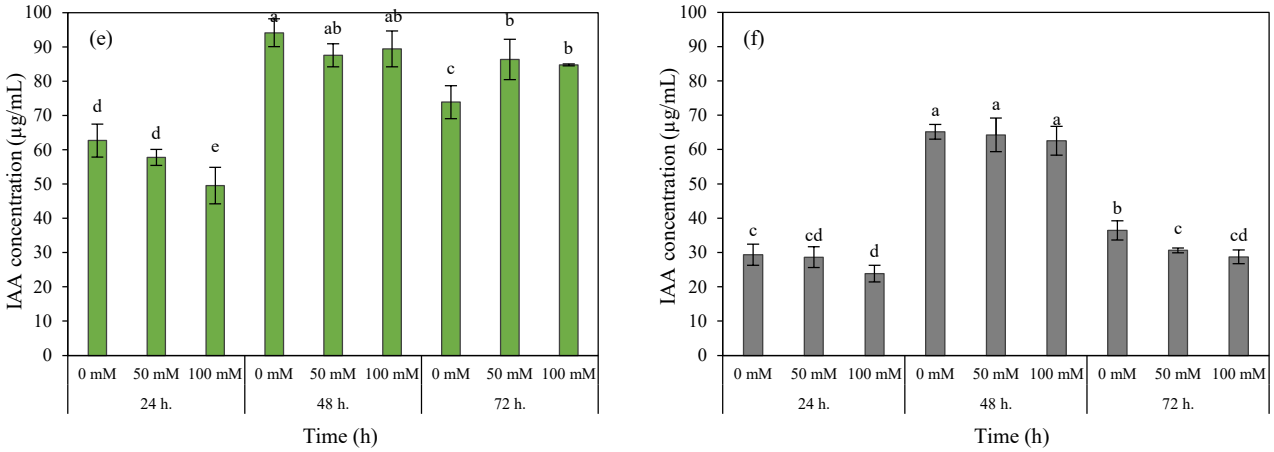

Figure 1. The IAA (indole-3-acetic acid) content produced by the isolate TYS1.1 including vegetative cells (a) and spore-forming cells (b), isolate TYS3.3; vegetative cells (c) and spore-forming cells (d), isolate TYS3.5; vegetative cells (e) and spore-forming cells (f) under different concentrations of NaCl solution (mM) (cont.)

Microbial colonization on okra roots under varying salinity conditions was studied using scanning electron microscopy (SEM). The results showed that the three isolates (TYS1.1, TYS3.3, and TYS3.5) of rhizobacteria lived on the surface of okra roots (Figure 2). Root colonization was quantified by counting the microorganisms that adhered around the roots. It was found that at the salinity concentrations of 0, 50, 100 mM, the amount of bacteria were 10^8 CFU/g, 10^8 CFU/g and 10^7 CFU/g, respectively (Figure 3). This result was similar to the report of Sathya et al. (2016) showing that motility-related features of the bacterium *Bacillus amyloliquefaciens* VB7 was found on the roots of chili seeds when visualized on a scanning electron microscopy (SEM). The results revealed that the bacterial cells had adhesion around the roots at a concentration of 3.8×10^5 CFU/g.

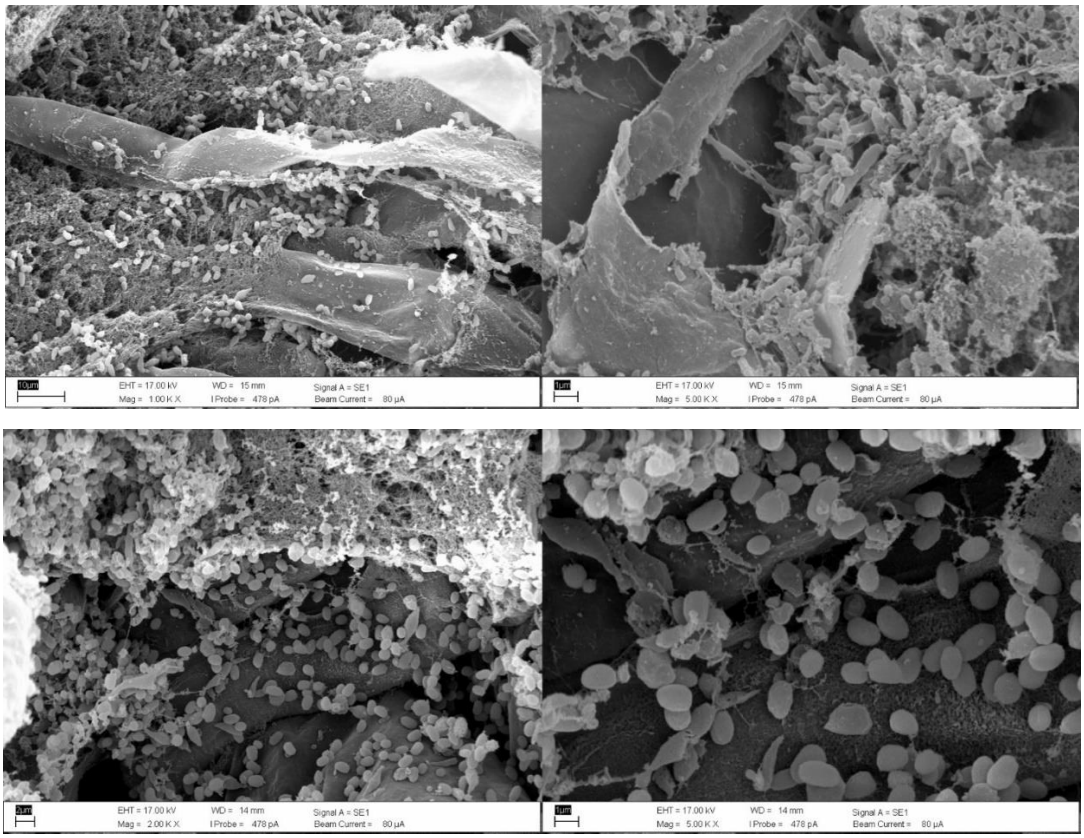

Figure 2. The colonization of rhizobacteria on the root surface of okra under various salinity conditions, on: 0 mM NaCl solution, center: 50 mM NaCl solution, and lower:100 mM NaCl solution

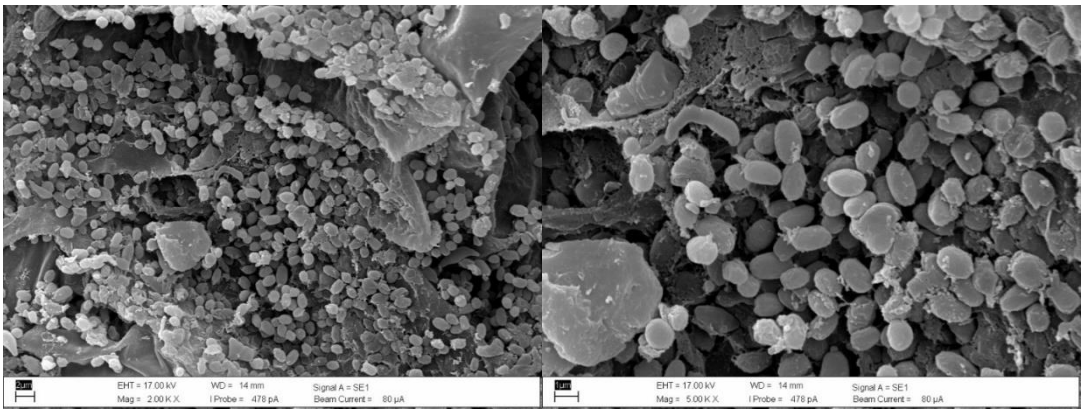

Figure 2. The colonization of rhizobacteria on the root surface of okra under various salinity conditions, on: 0 mM NaCl solution, center: 50 mM NaCl solution, and lower:100 mM NaCl solution (cont.)

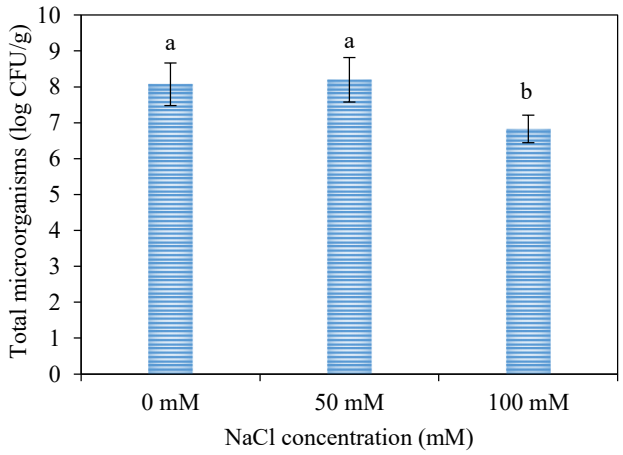

Figure 3. The viable cells of total microorganisms on the root surface determined by a conventional method (spread plate technique)

3.5 Bio-fertilizer production from vegetative cells and spore-forming cells

Surviving vegetative cells and spore-forming cells in the bio-fertilizer product, which was stored at room temperature for 60 days, were counted. The mixture of rhizobacteria was immobilized on four kinds of carrier materials (alginate, bagasse, rice husk ash, and vermiculite). The greatest amount of both forms of microbial cells was found in two carrier materials, rice husk ash and vermiculite, (T5: rice husk ash+vegetative cell, T6: rice husk ash+spores, T7: vermiculite+vegetative cell, T8 vermiculite+spores). The survival numbers in treatments T5-T8 were consistent on the carriers in all sampling days (15, 30, 45, and 60 days) as shown in Figure 4.

The pH and EC of the bio-fertilizer did not change during storage at room temperature for 60 days. The pH and EC values for the alginate carrier were in a range of 6.37-7.85 and 1.79-4.17 dS/m, respectively. In the case of the bagasse carrier, the pH was at 3.58-4.69, and EC was at 0.40-0.60 dS/m. Rice husk ash had a pH in a range of 7.71-8.73, and EC of 0.69-12.47 dS/m. The pH and EC of vermiculites were 8.34-9.27 and 0.31-0.55 dS/m, respectively. The neutral pH and slight salinity conditions in sodium alginate carrier made it the best carrier for immobilizing rhizobacterial cells and growing plants. Our results showed a high rate of surviving cells in rice husk ash and vermiculite. This might be due to the porous structures of both these carriers, causing the microbes to adhere to and live within these materials.

One of the major concerns when applying microbial inoculants to saline soil in the form of vegetative cells is the survivability of the microbial cells under salinity stresses. Abiotic stress might suppress the growth of bacterial cells in inappropriate environments. Therefore, the use of spore-forming rhizobacteria that tolerate salinity could be an alternative option for applying microbial inoculants into saline soil. These microbes are able to solubilize nutrients in saline soil, increasing their availability for plant uptake and growth. Moreover, this method provides a long shelf-life in natural fields under stress conditions when compared with vegetative cells (El-Sayed et al., 2014).

The quality of the carrier materials is an important factor for supporting rhizobacterial cells. Desirable properties of carrier materials are being rich in nutrients, structurally porous, and non-toxic. The quality of the carrier material is an important factor for supporting rhizobacterial cells. Enumeration of the total microorganisms immobilized on four types of carrier materials, alginate, bagasse, rice husk ash and vermiculite, was determined after 60 days of biofertilizer production. The highest numbers of total

microorganisms (in the form of vegetative and spore-forming cells) were found in rice husk ash and vermiculite. It showed a consistent survival rate. Both kinds of carriers are agricultural materials popularly used in cultivation. Rice husk ash has a porous structure allowing good air-circulation and high-water absorption ability (Ogbo and Odo., 2011), while vermiculite is a natural biological stimulant for plant growth which can maintain soil moisture content and has high porosity (Marinova et al., 2012). These carrier materials have promising physical, chemical and biological properties for use in soils and support bacterial growth, especially in stress conditions. This bio-fertilizer should be tested and developed as an alternative product for use in both fertile and unfertile soils under stress and non-stress condition.

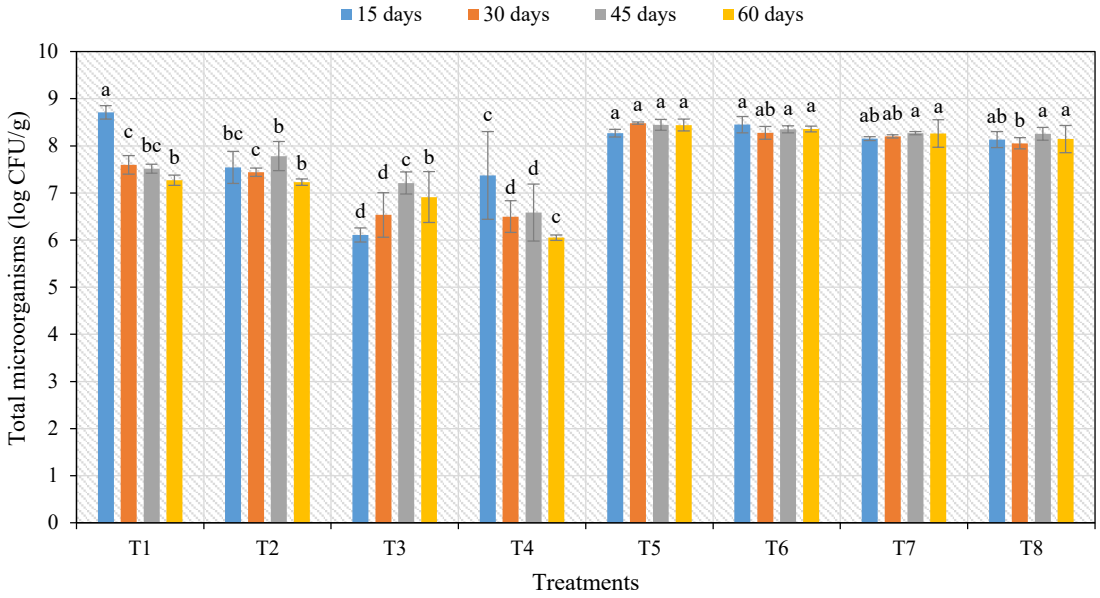

Figure 4. The survival of vegetative and spore-forming cells of microorganisms in bio-fertilizers for 8 treatments were as followed T1: alginate+vegetative cells, T2: alginate+spores, T3: bagasse+vegetative cells, T4: bagasse+spores, T5: rice husk ash+vegetative cells, T6: rice husk ash+spores, T7: vermiculite+vegetative cells, T8: vermiculite+spores

4. CONCLUSION

PGPRs demonstrated great potential on the promotion of plant growth in both forms (vegetative and spore forming cells). They showed similar abilities on the promotion of plant growth under salinity conditions such as fixed the nitrogen, solubilized phosphate and potassium on the agar plate. Moreover, both forms of rhizobacterial cells were able to produce IAA product. However, our data showed evidence that to maintain the survival rate of rhizobacterial cells under stress conditions, immobilization of rhizobacterial cells on a carrier is recommended. The microbial inoculum must be prepared on supporting material before application to the soil. In this study, rice husk ash and vermiculite were suitable carriers for protecting both forms of bacterial cells from salinity stress. These two carriers are widely found in Thailand and would increase in importance and value due to their role in bio-fertilizer production in the agro-industry.

ACKNOWLEDGEMENTS

This project was supported by the research capability enhancement program through graduate student scholarship in the year 2018, Faculty of Science, Khon Kaen University. Finally, thanks to the members of Microbial Fertilizer Laboratory, Department of Microbiology, Faculty of Science, Khon Kaen University, Thailand for assisting the laboratory works. We would like to thank Mr. Matthew Savage, Head of English (Upper Level), Khonkaen Wittayayon EP School, Khon Kaen Province for proofing on English writing of this manuscript.

REFERENCES

Ansari FA, Ahmad I, Pichtel J. Growth stimulation and alleviation of salinity stress to wheat by the biofilm forming *Bacillus pumilus* strain FAB10. Applied Soil Ecology 2019;143:45-54.

Bal HB, Adhya TK. Diversity of plant growth promoting rhizobacteria (PGPR) in rice soil of Odisha. Plant Science Research 2012;34:27-33.

Bashan Y, de-Bashan LE. Prabhu SR, Hernandez JP. Advance in plant growth-promoting bacterial inoculants technology:

Formulations and practical perspectives (1998-2013). Plant and Soil 2014;378:1-33.

Bashan Y, Hernandez JP, Leyva LA, Bacillio M. Alginate microbeads as inoculant carriers for plant growth promoting bacteria. Biology and Fertility of Soils 2002;35:359-68.

Bressuire IC, Broussolle V, Carlin F. Sporulation environment influences spore properties in *Bacillus*: Evidence and insights on underlying molecular and physiological mechanisms. FEMS Microbiology Reviews 2018;42(5):614-26.

El-Sayed WS, Akhkha A, El-Naggar MY, Elbadry M. In vitro antagonistic activity, plant growth promoting traits and phylogenetic affiliation of rhizobacteria associated with wild plants grown in arid soil. Frontiers in Microbiology 2014;5:Article No. 651.

Gharib AA, Shahen MM, Ragab AA. Influence of Rhizobium inoculation combined with *Azotobacter chrococcum* and *Bacillus megaterium* var phosphaticum on growth nodulation, yield and quality of two snap bean (*Phasealus vulgaris* L.) cultivers. Annals of Agricultural Sciences 2015;53(2):249-61.

Gajbhiye T, Pandey SK, Lee SS, Kim KH. Size fractionated phytomonitoring of airborne particulate matter (PM) and speciation of PM bound toxic metals pollution through *Calotropis procera* in an urban environment. Ecological Indicators 2019;104:32-40.

Goswami D, Dhandhukia P, Patel P, Thakker JN. Screening of PGPR from saline desert of Kutch: Growth promotion in *Arachis hypogea* by *Bacillus licheniformis* A2. Microbiological Research 2014;169:66-75.

Khan AA, McNeilly T, Azhar FM. Stress tolerance in crop plants. International Journal of Agriculture and Biology 2001; 3(2):250-5.

Kumar A, Maurya BR, Raghuwanshi R. Isolation and characterization of PGPR and their effect on growth, yield and nutrient content in wheat (*Triticum aestivum* L.). Biocatalysis and Agricultural Biotechnology 2014;3(4):121-8.

Kumar P, Dubey RC, Maheshwari DK. *Bacillus* strains isolated from rhizosphere showed plant growth promoting and antagonistic activity against phytopathogens. Microbiological Research 2012;167(8):493-9.

Lyngwi NA, Joshi SR. Economically important *Bacillus* and related genera: A mini review. Biology of Useful Plants and Microbes 2014;3:33-43.

Marinova SV, Toncheva R, Zlatareva E, Pchelarova H. Characteristics of vermiculite and its influence on the yield of lettuce in greenhouse experiments. Proceedings of the 5th Water Observation and information System for Decision Support Conference; 2012 May 27- Jun 2; Ohrid, Republic of Macedonia, Bulgaria; 2012.

Ogbo FC, Odo MO. Potential of rice husk and cassava peel as carriers for bio-fertilizer production. Nigerian Journal of Biotechnology 2011;23:1-4.

Omer AM. Bioformulations of *Bacillus* spores for using as biofertilizer. Life Science Journal 2010;7(4):124-31.

Oyelade OJ, Ade-Omowaye BIO, Adeomi VF. Influence of variety on protein, fat contents and some physical characteristics of okra seeds. Journal of Food Engineering 2003;57(2):111-4.

Ozdal M, Ozdal OG, Sezen A, Algur OF, Kurbanoglu EB. Continuous production of indole-3-acetic acid by immobilized cells of *Arthrobacter agilis*. 3 Biotech. 2017;7(1):Article No. 23.

Pesce G, Rusciano G, Sasso A, Isticato R, Sirec T, Ricca E, et al. Surface charge and hydrodynamic coefficient measurements of *Bacillus subtilis* spore by optical tweezers. Colloids and Surfaces B: Biointerfaces 2014;116:568-75.

Rojas-Solis D, Vences-Guzman MA, Sohlenkamp C, Santoyo G. Antifungal and plant growth-promoting *Bacillus* under saline stress modify their membrane composition. Journal of Soil Science and Plant Nutrition 2020;20(3):1549-59.

Roslan MAM, Zulkifli NN, Sobri ZM, Zuan ATK, Cheak SC, Abdul Rahman NA. Seed biopriming with P- and K-solubilizing *Enterobacter hormaechei* sp. improves the early vegetative growth and the P and K uptake of okra (*Abelmoschus esculentus*) seedling. Public Library of Science One 2020;15(7):e0232860.

Sathya S, Nakkeeran S, Lakshmi S. Effect of biopriming on populations of *Bacillus amyloliquefaciens* VB7 in chilli seeds. The Bioscan: An International Quarterly Journal of Life Sciences 2016;11(2):907-10.

Shen H, He X, Liu Y, Chen Y, Tang J, Guo T, et al. A complex inoculant of N_2-fixing, P- and K-solubilizing bacteria from a purple soil improves the growth of kiwifruit (*Actinidia chinensis*) plantlets. Front Microbiol 2016;7:Article No. 841.

Spaepen S, Vanderleyden J, Remans R. Indole-3-acetic acid in microbial and microorganism-plant signaling. Federation of European Microbiological Societies 2007;31(4):425-48.

Sun F, Ou Q, Wang N, xuan Guo Z, Ou Y, Li N, et al. Isolation and identification of potassium-solubilizing bacteria from *Mikania micrantha* rhizospheric soil and their effect on *M. micrantha* plants. Global Ecology and Conservation 2020;23:e01141.

Verma N, Singh NA, Kumar N, Raghu HV. Screening of different media for sporulation of *Bacillus megaterium*. International Journal of Microbiology Research 2013;1(4):68-73.

Watterson MJ, Kent DJ, Boor KJ, Wiedmann M, Martin NH. Evaluation of dairy powder products implicates thermophilic sporeformers as the primary organisms of interest. Journal of Dairy Science 2014;97(4):2487-97.

Use of Bayesian, Lasso Binary Quantile Regression to Identify Suitable Habitat for Tiger Prey Species in Thap Lan National Park, Eastern Thailand

Paanwaris Paansri[1], Warong Suksavate[1], Aingorn Chaiyes[2], Prawatsart Chanteap[3], and Prateep Duengkae[1*]

[1]*Special Research Unit for Wildlife Genomics (SRUWG), Department of Forest Biology, Faculty of Forestry, Kasetsart University, Bangkok 10900, Thailand*

[2]*School of Agriculture and Cooperatives, Sukhothai Thammathirat Open University, Nonthaburi 11120, Thailand*

[3]*Department of National Parks, Wildlife and Plant Conservation, Prachinburi 25220, Thailand*

ARTICLE INFO

Received: 19 Dec 2021
Received in revised: 23 Jan 2022
Accepted: 1 Feb 2022
Published online: 22 Feb 2022
DOI:10.32526/ennrj/20/202100244

Keywords:
Wildlife habitat/ Spatial model/ Bayesian/ Quantile regression/ Thap Lan National Park

*** Corresponding author:**
E-mail: prateepd@hotmail.com

ABSTRACT

A Bayesian approach was used to develop binary quantile regression models featuring the lasso penalty. The models afford the advantages of all quantile regression models, such as robustness and detailed insights into covariate effects; they also handle issues associated with overfitting well. Thus, this model was used to investigate habitat suitability for the management of tiger prey species. Field data were collected from 150 sampling sites (2,416 sub-plots) in Thap Lan National Park of the Dong Phayayen-Khao Yai Forest Complex (DPKY) from August 2019 to March 2021. We focused on sambar deer (*Rusa unicolor*) and gaur (*Bos gaurus*) because they are the principal prey species of tigers. Vegetation was sampled for biomass and nutrient content to identify suitable habitat. The "bayesQR" package of R was used to identify habitats appropriate for these species. The correlation between forage crop biomass and the normalized difference vegetation index (NDVI) was significantly associated with tiger prey species presence. The habitat can be improved by increasing grass and forb biomasses as the prey species prefer open habitats, such as grassland and open areas of dry evergreen forest. Habitat management has ensured that the grass biomass of open forest is significantly higher than that of dense forest. In addition, the hemicellulose content of open forest was significantly greater than that of dense forest. We found that spatial modeling combined with Bayesian, lasso binary quantile regression could aid wildlife habitat management in a Thai National Park.

1. INTRODUCTION

The statistical theory of regression quantiles has been developed by econometricians over the past 40 years (Bassett and Koenker, 1986; Koenker and Bassett Jr, 1982), but ecological applications have been published only recently (Brennan et al., 2015; Cade and Noon, 2003; Chamaillé-Jammes and Blumstein, 2012; Muggeo et al., 2013). The statistical properties of the regression quantile estimates are used to test hypotheses and construct confidence intervals that reveal the effects of ecological limiting factors; the models find many ecological applications (Krause et al., 2002). The statistical distributions of ecological data often exhibit unequal variation given the complex interactions among factors affecting various organisms; not all can be measured and incorporated into statistical models (Brennan et al., 2015). Thus, to obtain a more complete picture of the relationships among variables missed by other quantile regression methods, we initially used the binary quantile regression model of Manski (1985). However, Kordas (2006) found that quantile regression afforded a much more comprehensive view than binary regression for how predictor variables influence the responses of even binary cases. However, most studies of binary quantile regression have employed median binary regression. Bayesian binary quantile regression estimates, and the associated variable selection procedures, are insensitive

Citation: Paansri P, Suksavate W, Chaiyes A, Chanteap P, Duengkae P. Use of Bayesian, lasso binary quantile regression to identify suitable habitat for tiger prey species in Thap Lan National Park, Eastern Thailand. Environ. Nat. Resour. J. 2022;20(3):266-278. (https://doi.org/10.32526/ennrj/20/202100244)

to outliers, and the methods thus identify variables that are important predictors of the various response distribution quantiles of the dependent variable (Benoit et al., 2013). We used this model to investigate habitat suitability for tiger prey species.

This study is the first wildlife habitat management work to employ Bayesian, lasso binary quantile regression to investigate habitat suitability and factors affecting habitat quality and quantity in Southeast Asia. We used foraging resource productivity and composition data to seek associations between ecological factors and the quality of wildlife habitat. Protein and digestibility value have been especially emphasized as major factors for pasture quality evaluation for animal performance (Seven and Cerci, 2006). Information on nutritive value of these pastures is scarce and in fragmented form and often assumptions are made for estimating feed contribution from this important source. We employed a spatial distribution model to examine the associations among underlying characteristics and to predict the quality of wildlife habitat at several levels (Cushman and McGarigal, 2002). We created a decision-support model that yields deep insights into wildlife habitat composition and configuration at the landscape and regional levels. This will inform decision-making and policy.

2. METHODOLOGY

2.1 Study site

Thap Lan National Park, part of the Dong Phayayen-Khao Yai Forest Complex (DPKY), was declared a UNESCO World Heritage Site in 2005. Ash et al. (2021), Duangchatrasiri et al. (2017), and Ngoprasert and Gale (2017) studied the status of the tiger (*Panthera tigris*) and tiger prey species in the DPKY. Tiger density was high in Thap Lan and Pang Sida National Parks but no tigers were found in Khao Yai National Park. The principal tiger prey species [sambar deer (*Rusa unicolor*) and gaur (*Bos gaurus*)] were widespread in the DPKY. Areas with high densities of tigers and their prey must be protected from human interference. The study was conducted in a 1,638 km^2 area of Thap Lan National Park that lies in the provinces of Nakhon Ratchasima, Buri Ram, and Prachin Buri (14º05′-14º33′N, 101º50′-102º40′E) (Figure 1). The elevation range is 37-925 m.a.s.l.

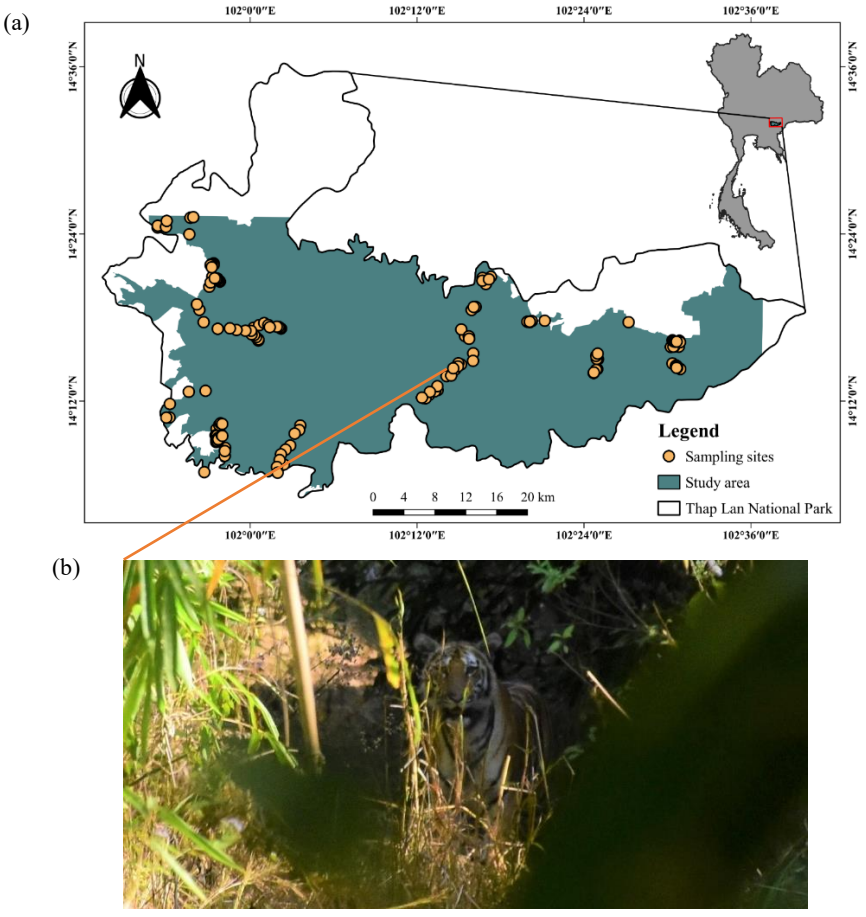

Figure 1. (a) The study area (Thap Lan National Park, part of the Dong Phayayen-Khao Yai Forest Complex (DPKY)). We focused on the areas that are habitats for tiger prey species. Therefore, the village part and agricultural areas were excluded. (b) Tiger at Thap Lan National Park from direct observation, was taken on December 19, 2019.

2.2 Survey design

Sampling sites were surveyed in terms of forage resources and the abundance of sambar deer and gaur (the principal tiger prey). The sampling sites were randomly selected over the study area. The following factors were considered when selecting sites: the occurrences/distributions (and densities) of tigers and their prey, the forest type (evergreen, deciduous, and mixed deciduous) (RFD, 2018), and the topography (elevation and slope) created from Google Earth Engine (Gorelick et al., 2017). The study area was divided into 10 strata by reference to the scores for each factor. The value of each factor was normalized from 0 to 100. The study area was then divided into 10 clusters according to the scores of each factor using K-means clustering, following Paansri et al. (2021) (Figure 2).

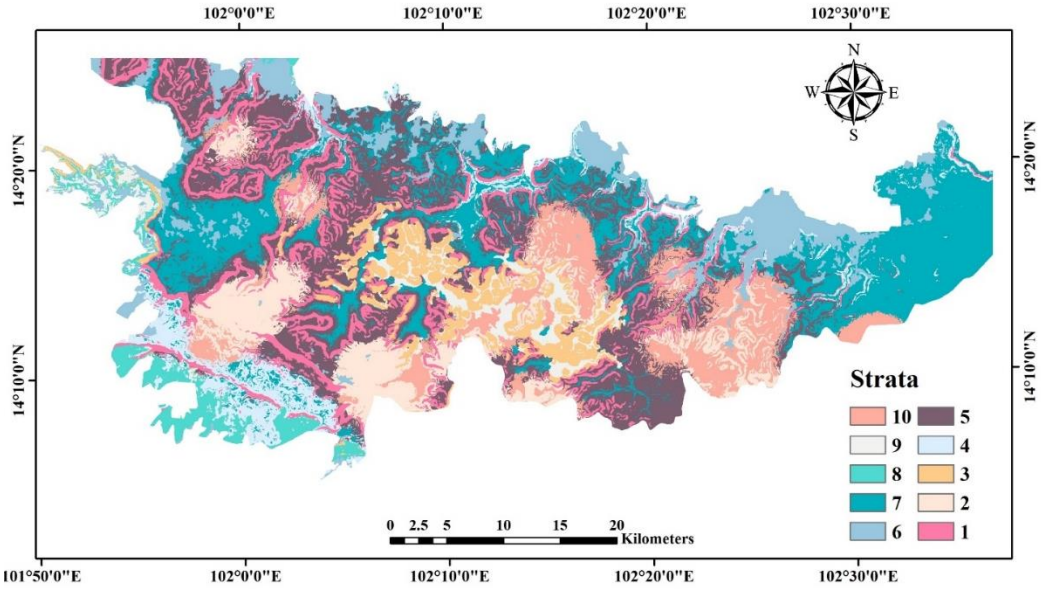

Figure 2. A map of the 10 strata of the study area derived using the K-means method

2.3 Field data collection

Forage crop data were collected from 20 sub-plots per each sample site (Figure 3), and all aboveground biomass was cut and separated into forbs, grasses, and shrubs following Holechek (1984). All specimens were dried in an oven at 70°C for 48 h or until the weights became stable. Dry weights and moisture contents (percentages) were calculated following Pattanakiat (1988). Then, analysis of forage crops used by sambar deer and gaur was conducted; the crude protein (CP), neutral detergent fiber (NDF), acid detergent fiber (ADF), acid detergent lignin (ADL), cellulose, and hemicellulose levels were measured in the Animal Nutrition Laboratory, Department of Animal Science, Kasetsart University. Presence data from habitat use of sambar deer and gaur with sightings, tracks, and fresh dung (the way an animal uses the physical and biological resources in a habitat) was recorded for every sub-plot at each sample site.

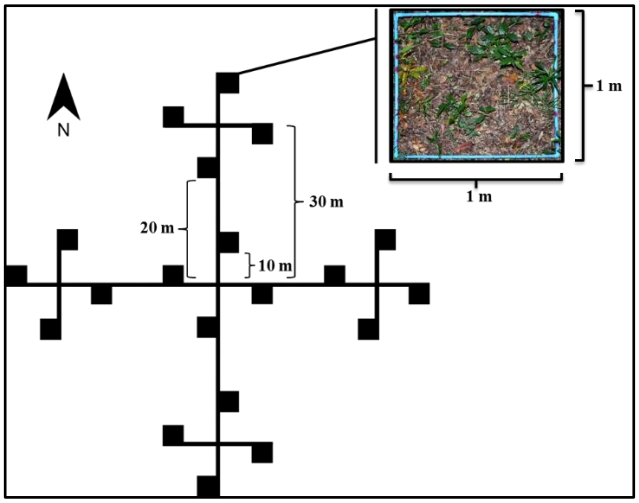

Figure 3. 20 Sub-plots (each 1×1 m) at each sample site (An inaccessible sub-plots are excluded from data collection and analysis)

2.4 Statistical analysis

Gaussian and Poisson generalized mixed models (GLMs) were used to link limiting factors to

environmental variables (all at resolutions of 30×30 m). The logistic regression analysis (featuring a GLM with a binomial distribution and a logit-link function; McCullagh and Nelder, 2019) included the limiting factors of shrub, forb, and grass biomasses; sambar deer and gaur occurrences; and environmental variables such as the slope (in degrees); elevation; distances from a road, a stream, and villages; canopy cover; and normalized difference vegetation index (NDVI) data from the Landsat 8 satellite. All analyses were performed using the MASS package (Venables and Ripley, 2013) of R (R Core Team, 2017). Automatic stepwise selection was used to derive the model with the lowest Akaike Information Criterion (Akaike 1998). The processing workflow for the spatial modeling is presented in Figure 4. The "bayesQR" package (Benoit and Van den Poel, 2017) was used to investigate habitat suitability by wildlife occurrence; estimations and inferences were made employing Bayesian, lasso binary quantile regression following Li et al. (2010). Both the frequentist approach and a more recent Bayesian approach based was used on an asymmetric Laplace distribution (ALD) (Benoit and Van den Poel, 2012). Bayesian-binary quantile regression yields estimates and variables, and is insensitive to outliers, heteroskedasticity, and other anomalies that challenge existing assumptions. The regression identifies variables that are important predictors of the various quantiles of the dependent variable response distributions (Benoit and Van den Poel, 2017). The processing workflow for the Bayesian, lasso binary quantile regression modeling is presented in Figure 5.

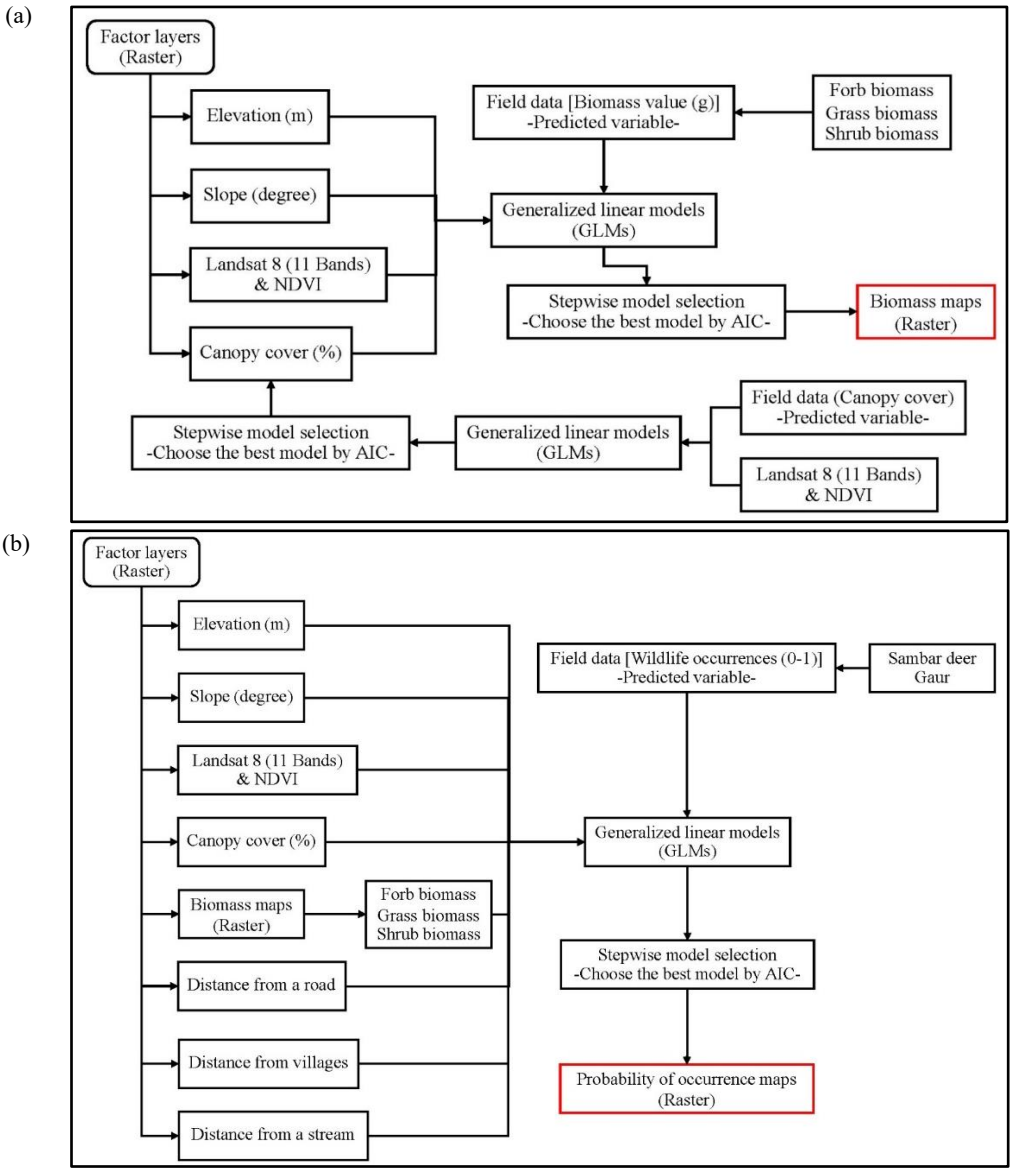

Figure 4. Flowchart of the processing performed for the (a) forage-crop models and (b) habitat-suitability models

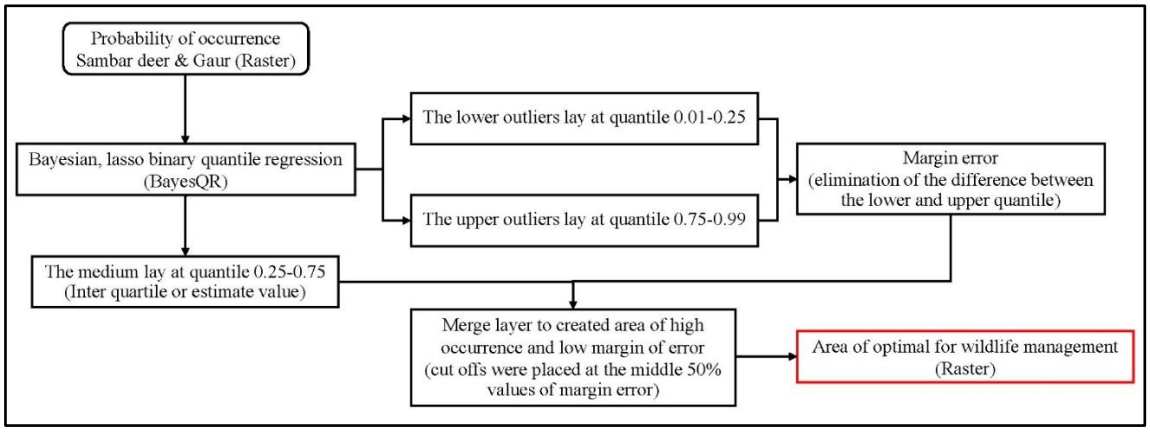

Figure 5. Flowchart of the processing performed for the Bayesian, lasso binary quantile regression modeling to create the area of optimal for wildlife management

3. RESULTS AND DISCUSSION

3.1 The abundance of tiger prey species

A total of 150 sampling sites (2,416 Sub-plots) were surveyed. The presence of tiger prey species was recorded at 1,466 points (60.68%), composed of 740 points of sambar deer (30.63%), and 726 points of gaur (30.05%) (Figure 6). The presence of tiger prey species in each the strata is summarized in Table 1.

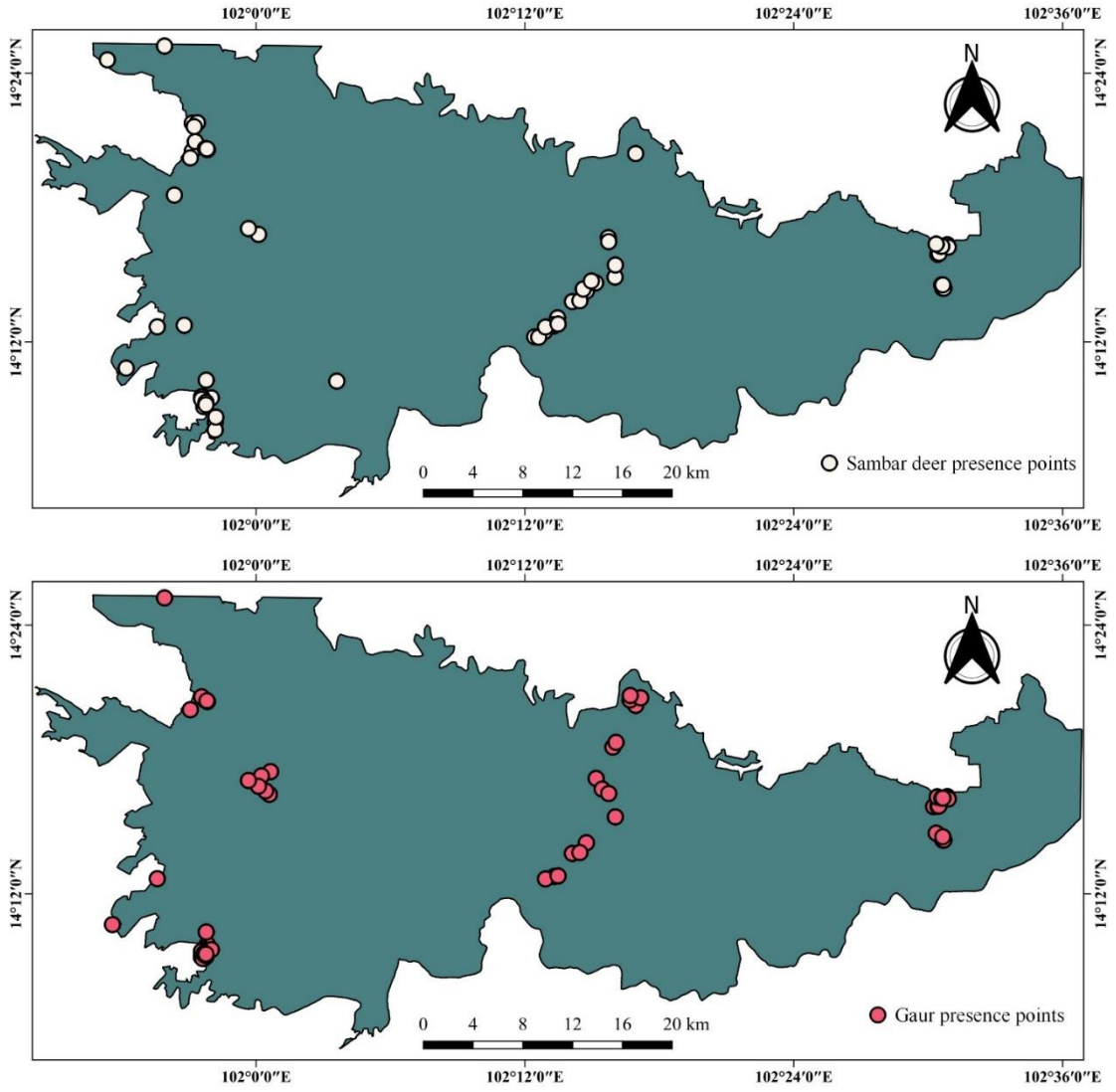

Figure 6. A map of the tiger prey species distribution from habitat use of sambar deer and gaur for every sub-plots

Table 1. The number of sub-plots (each 1×1 m) and presence points of tiger prey species in the strata

Strata	Sub-plots	Sambar deer		Gaur	
	Count	Presence	%	Presence	%
1	163	53	32.52	24	14.72
2	78	24	30.77	48	61.54
3	44	40	90.91	12	27.27
4	213	36	16.90	36	16.90
5	191	48	25.13	24	12.57
6	676	235	34.76	366	54.14
7	467	98	20.99	132	28.27
8	373	36	9.65	12	3.22
9	130	98	75.38	36	27.69
10	82	72	87.80	36	43.90
Sum	2,416	740	30.63	726	30.05

3.2 Spatial prediction models

The spatial prediction models (Table 2) were those with the lowest AICs. A canopy cover model with six variables exhibited the highest efficiency. The spatial predictions lay between 0-100%; the model exhibited a stronger predictive ability than did the NDVI data ($p<0.01$), as in Li and Mao (2020) and Wu et al. (2013), who nonetheless found that the NDVI was a good predictor of, and the most important variable affecting, canopy cover. The NDVI values vary between dense and open forests in terms of vegetation greenness (Moreno-de las Heras et al., 2015). Moreover, the differences in the Landsat 8 reflectances of band 2 (Blue), band 3 (Green), band 9 (Cirrus), band 10 (Thermal Infrared 1), and band 11 (Thermal Infrared 2) imagery, were all significant at $p<0.01$.

The forage crop model indicated that forb biomass varied directly with only the NDVI ($p<0.01$). Grass biomass varied directly with slope and the NDVI (both $p<0.01$) but inversely with elevation and canopy cover (both $p<0.01$). Shrub biomass varied directly with elevation and canopy cover (both $p<0.05$) but inversely with elevation ($p<0.01$). The forb biomass was 0-262.4 kg/ha, the grass biomass was 0-2,998 kg/ha, and the shrub biomass was 0-440.4 kg/ha. The model of shrub biomass exhibited a negative relationship with elevation, consistent with the data of Ensslin et al. (2015) on tropical forests and Paansri et al. (2021) on areas surrounding highway 304 in the region of our study. Shrub biomass decreased significantly with elevation. The models for forage crops included the additive and interactive effects of canopy cover. In forested habitats, the relationship between canopy cover and ground vegetation biomass was positive for shrubs but negative for grass, consistent with Aranha et al. (2020), who reported that canopy closure is positively correlated with shrub biomass because photosynthetic capacity is more strongly related to canopy cover (Kaur 2007; Moreno-de las Heraset al., 2015). Canopy cover was a strong (negative) predictor of grass biomass; increasing canopy cover significantly reduced grass (Randle, 2018). Most grasses were C4 grasses that were exposed to frequent fires (Hoffmann, 1999), and were therefore restricted to high-light-intensity open ecosystems; such grasses are shade-intolerant and thus very susceptible to competitive exclusion as woody cover increases (Sage and Kubien, 2003).

The habitat-suitability models (HSMs) showed that the probability of sambar deer presence (a value between 0 and 0.87) varied directly by slope, the forb and grass biomasses, and distances from villages (all $p<0.01$) but inversely with elevation, shrub biomass, the distance from a road, and the NDVI (all $p<0.05$). The probability of gaur presence (a value between 0 and 0.9) varied directly by slope, forb and grass biomasses, the distance from a stream, and distances from villages (all $p<0.05$) but inversely by elevation, shrub biomass, and the NDVI (all $p<0.05$). The relationships are analyzed in the next section.

3.3 Investigation of habitat suitability via Bayesian, lasso binary quantile regression

The factors yielded by the models (with the lowest AICs) of tiger prey presence (Table 2) were subjected to Bayesian-binary quantile regression analysis. The lower outliers lay at quantile 0.01-0.25 and the upper outliers are at quantile 0.75-0.99; the medium (interquartile or estimate value) lay at quantile 0.25-0.75 (this is the probability of a value between 0 and 1) (Dicker et al., 2006; Wan et al., 2014) (Figure 7). The medium quantiles indicate the relationships between environmental factors and tiger prey presence, as shown by Ji et al. (2012), and afford a very comprehensive insight into how predictor variables influence the response of a binary case. Thus, for every performance measure and every type of data-generation process, the lasso afforded the best performance (Benoit et al., 2013).

Table 2. The spatial predictions of the generalized linear model using the predictor variables with the lowest AICs

Model	Predictor	Coefficient	Standard error	P-value	AIC
Canopy cover	Intercept	9.42E+01	4.28E+01	<0.05	1161.6
	Band 2	4.56E-03	6.94E-04	<0.01	
	Band 3	-4.82E-03	5.42E-04	<0.01	
	Band 9	-2.35E-02	8.40E-03	<0.01	
	Band 10	-1.96E-03	5.83E-04	<0.01	
	Band 11	2.85E-03	8.29E-04	<0.01	
	NDVI	1.71E+01	1.12E+00	<0.01	
Forb biomass	Intercept	3.88E+00	1.99E+00	0.05	26312
	NDVI	4.11E+01	6.22E+00	<0.01	
Grass biomass	Intercept	1.17E+02	8.66E+00	<0.001	32690
	Slope	2.07E+00	4.72E-01	<0.001	
	Elevation	-8.92E-02	2.19E-02	<0.001	
	NDVI	4.14E+02	4.64E+01	<0.001	
	Canopy cover	-3.11E+02	1.86E+01	<0.001	
Shrub biomass	Intercept	1.04E+01	1.82E+00	<0.01	25477
	Slope	3.10E-01	1.15E-01	<0.01	
	Elevation	-4.32E-02	5.35E-03	<0.01	
	Canopy cover	3.51E+01	2.39E+00	<0.01	
Probability of occurrence (Sambar deer)	Intercept	-1.06E+01	2.52E+00	<0.001	2875.1
	Slope	1.22E-01	3.55E-02	<0.001	
	Elevation	-1.42E-02	4.18E-03	<0.001	
	Forb biomass	1.49E+00	3.22E-01	<0.001	
	Grass biomass	3.46E-02	1.06E-02	<0.01	
	Shrub biomass	-4.88E-01	1.03E-01	<0.001	
	Distance from a road	-6.01E-05	1.58E-05	<0.001	
	Distance from villages	3.72E-05	1.27E-05	<0.001	
	NDVI	-1.31E+01	6.13E+00	<0.05	
Probability of occurrence (Gaur)	Intercept	-7.93E+00	2.58E+00	<0.01	2791.9
	Slope	1.24E-01	3.38E-02	<0.001	
	Elevation	-2.36E-02	3.91E-03	<0.001	
	Forb biomass	1.80E+00	3.09E-01	<0.001	
	Grass biomass	2.58E-02	1.09E-02	<0.05	
	Shrub biomass	-6.96E-01	9.47E-02	<0.001	
	Distance from a stream	8.35E-05	3.07E-05	<0.01	
	Distance from villages	3.57E-05	1.33E-05	<0.01	
	NDVI	-1.58E+01	6.26E+00	<0.05	

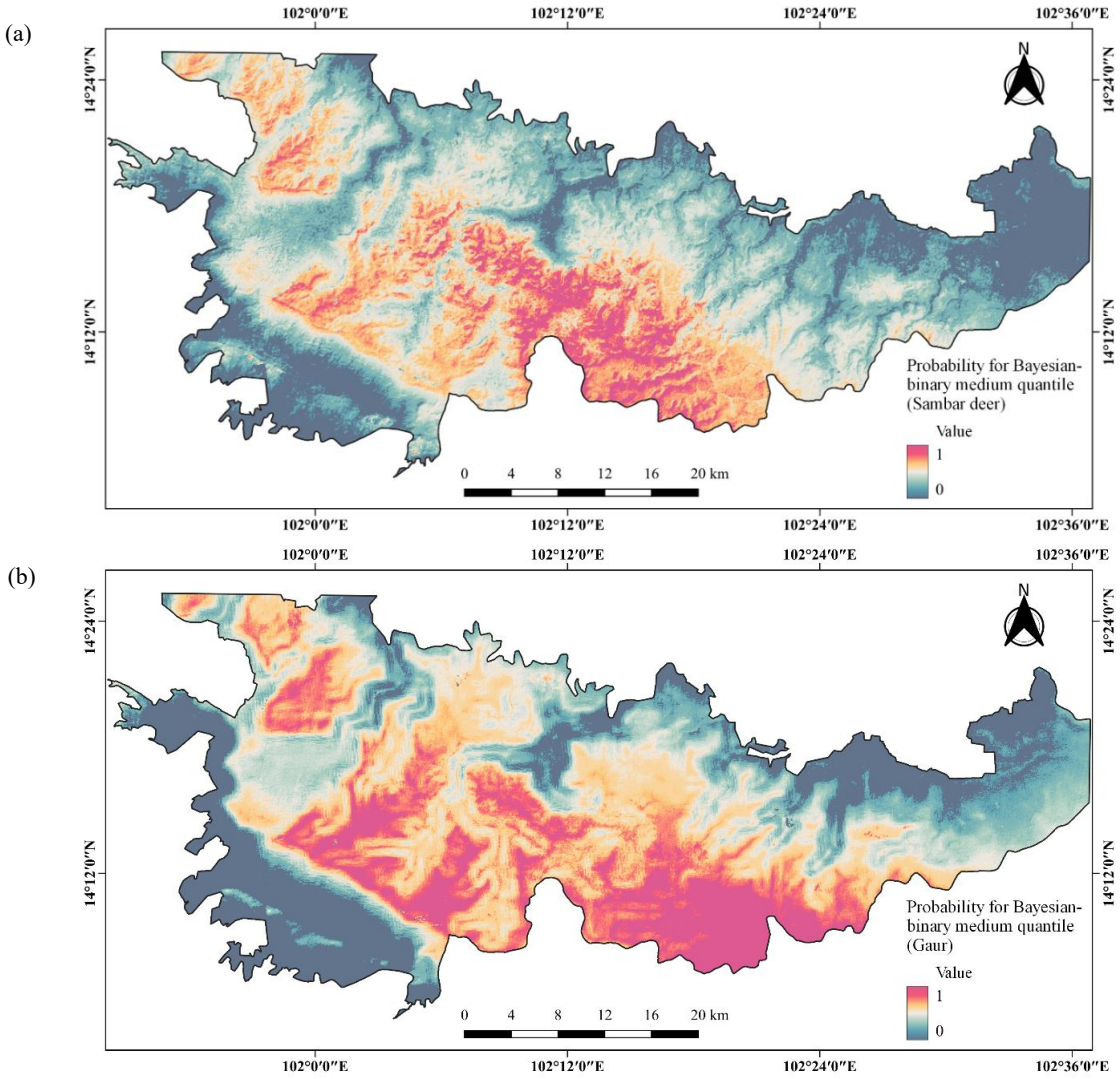

Figure 7. Probabilities yielded by the Bayesian-binary medium quantile (0-1) for (a) sambar deer and (b) gaur presence

Therefore, the region occupied by tiger prey species requires a low margin of error (thus elimination of the difference between the upper and lower quartile; represents the low-risk area of variability) and a high model estimate for the medium quantile (John, 2015) (Figure 7). Cutoffs were placed at the middle 50% values of the margin errors, and the model estimates formed the medium quantile when ordered from lowest to highest (Dodge, 2008). The stable areas available to manage and increase the populations of sambar deer and gaur were 296.7 km^2 and 385.7 km^2, respectively (Figure 8); gaur require more (and better connected) habitat than sambar deer (Chetri, 2006), consistent with McShea and Bhumpakphan (2011), who found that gaur in Thailand prefer grassland and open areas of moist evergreen, dry evergreen, semi-evergreen, and mixed deciduous forests. Gaur used both closed and open forest. The habitat preferences of sambar deer were higher in areas close to the main river at lower elevations, where the predominant habitat was mixed deciduous forest (Chatterjee, 2014; Rai, 2019; Simcharoen et al., 2014); sambar deer preferred the more open habitat (Lynam et al., 2012). The regression coefficients for the NDVI data in the HSMs of sambar deer and gaur were -13.1 and -15.8, respectively (Table 2), indicating that both prey species lived in open areas. Thus, both species preferred grassland (of low NDVI reflectivity). NDVI-based models yielded different results for forest and grassland (Borowik et al., 2013). Grass cover decreased as canopy cover increased because of lower transmission of light to the understory; grass requires light (Widenfalk and Weslien, 2009). The grass biomass increased significantly with a reduction in the canopy cover (Table 2) in the conservation area, which has more open than dense forest (Paansri et al., 2021), particularly in Thap Lan National Park.

The habitat suitabilities derived via Bayesian, lasso binary quantile regression are presented in Figure 7. Next, we focused on manageable environmental factors (Table 2). In both models, the relationships between manageable environmental factors and sambar deer and gaur presence were all statistically correlated (grass and forb biomasses positively but shrub biomass negatively), consistent with Lamont et al. (2019), who found that ungulates select grassy areas well away from disturbances (Duangchatrasiri et al., 2019). Therefore, an increased grass biomass, associated with a more open canopy, promotes habitat use by ungulates. However, in certain areas, sambar deer and gaur consume large amounts of forbs and shrubs, primarily when green grass is unavailable. Such ungulates strongly avoid shrubs high in volatile oils because they lack mechanisms to reduce the toxic effects of such substances (Cappai and Aboling, 2020).

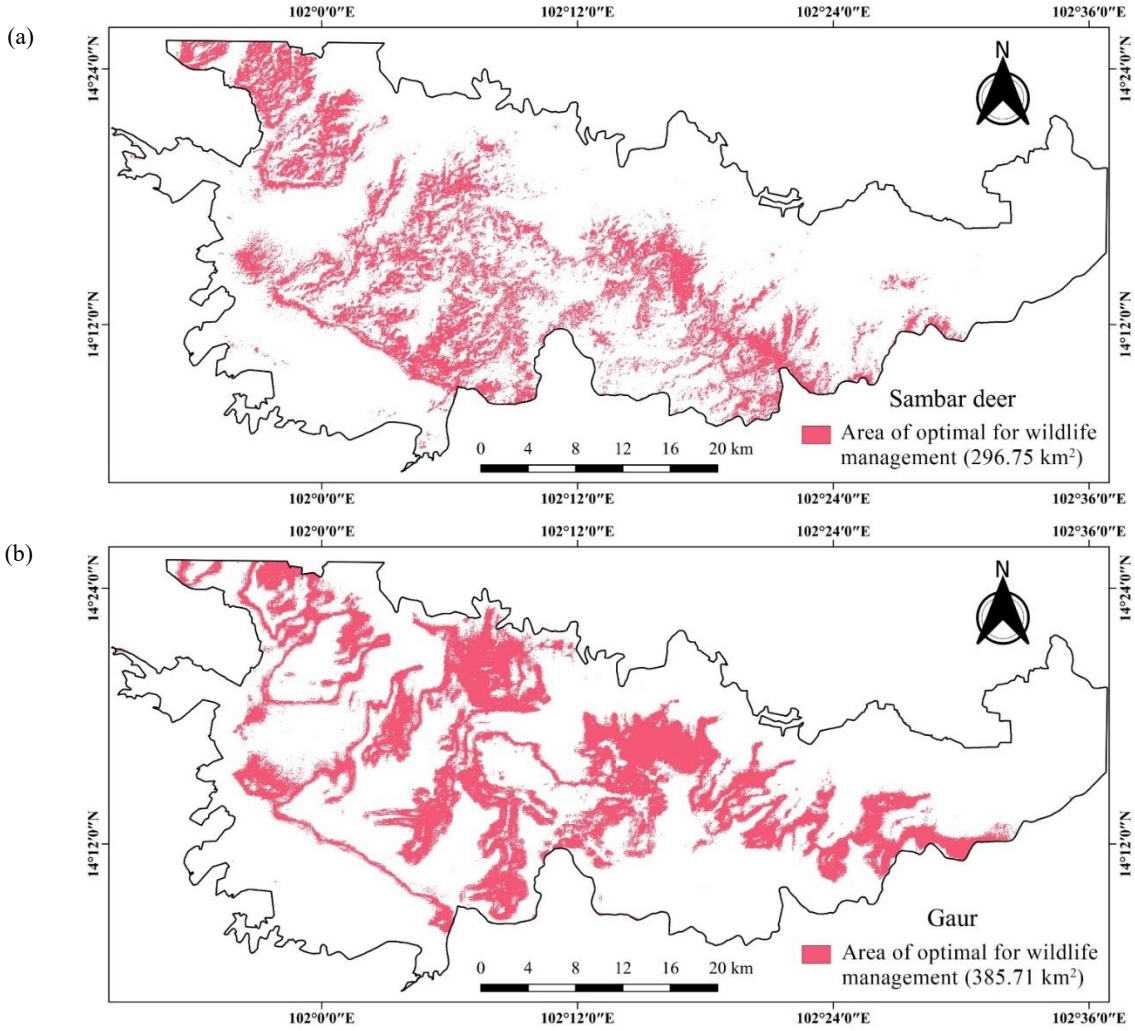

Figure 8. Area of optimal for wildlife management of (a) sambar deer (296.75 km)^2 and (b) gaur (385.71 km)^2; High abundance of tiger prey species, high-quality habitat, and the region occupied by tiger prey species requires a low margin of error; represents the low-risk area of variability and worth for habitat management

3.4 Biomass production and nutritional characteristics of forage crops

The results of forage crop biomass by canopy cover revealed 1,645 dense forest plots (0-40% of the sky was obstructed by tree canopies) and 415 open forest plots (≥40% of the sky obstructed). In dense forest, the forb biomass was 18.73±0.78 g/m^2, the grass biomass was 9.24±1.19 g/m^2, and the shrub biomass was 22.08±1.01 g/m^2; the figures for open forest were 12.46±2.25, 164.15±9.60, and 35.27±0.71 g/m^2, respectively (Table 3). The forb and shrub biomasses of dense forest were significantly higher than those of open forest (both $p<0.05$) but the grass biomass of dense forest was lower than that of open forest ($p<0.05$).

Table 3. Forage crop biomasses by the extents of canopy cover as revealed by the SFR (2001)

Life form	Dense forest (n=1,489)			Open forest (n=415)		
	Mean±SE	95% CI		Mean±SE	95% CI	
	(g/m^2)	lower	upper	(g/m^2)	lower	upper
Forb biomass	18.73±0.78*	17.19	20.27	12.46±2.25*	8.04	16.88
Grass biomass	9.24±1.19*	6.91	11.57	164.15±9.6*	145.31	182.99
Shrub biomass	22.08±1.01*	20.1	24.05	5.27±0.71*	3.89	6.66

*=Significantly different at the statistical level <0.05 of two sample t-test

Eighty-seven forage crop species of habitat use by sambar deer and gaur in the study area. Of these, 38 were grasses, 27 were shrubs, and 22 were forbs. The nutritional parameters of forbs and shrubs growing in either dense or open forest did not significantly differ. For grasses, however, the NDF and hemicellulose percentages of dense forest species (59.96±3.14 and 16.76±2.15%, respectively) were significantly lower than those of species of open forest (68.53±1.44 and 23.70±0.90%, respectively) (both $p<0.05$) and the CP percentage of dense forest grasses (8.76±0.60%) was significantly higher than that of open forest grasses (5.68±0.53%; $p<0.05$; Table 4, Figure 9).

This study focused on Crude protein and hemicellulose; these are good estimators of ungulate food quality (Bukombe et al., 2019) and hemicellulose are the main fuel for ruminants, typically providing up to 80% of their energy (Barboza et al., 2009; Rautiainen et al., 2021). The CP and hemicellulose data in this study were consistent with Mobashar et al. (2017); shrubs and forbs have higher CP contents than grasses. Our CP values are similar to those of Jasra and Johnson (2000), who studied shrubs, forbs, and grasses of Baluchistan grasslands. In general, plant CP content is high in the vegetative stage and declines later (Mountousis et al., 2008; Tufarelli et al., 2010). The CP of forbs is of particular importance to ruminants, both ensuring appropriate rumen function and providing biosynthetic substrates. Wallmo et al. (1977) showed that a minimum CP level of 7% is required to maintain ruminant herbivores. Cook et al. (2001) and Verme and Ullrey (1972) reported that dry matter CP levels in fawn forage or a diet should be 13% and 20%, respectively to ensure optimal growth, and recommended supplementary feeding, because percentages of 16-17% are needed to meet the maximum requirements of most ungulates including lactating dose. Thus, the CP concentrations in the forbs and shrubs that we studied met the protein requirements of all ungulates. In terms of hemicellulose, Mobashar et al. (2017) reported that the hemicellulose contents of grasses ranged from 18.4% to 29.4%, being lowest at one month of age and highest at three months. For other plants, the season and extent of plant maturity affect the levels of complex carbohydrates. Ruminants efficiently use cellulose and hemicellulose; rumen microbes readily digest these materials (Holechek et al., 1998).

Table 4. Nutritional parameters of the forage crops of dense forest (DF) and open forest (OP)

% Nutrient	Forb		Grass		Shrub	
	DF (n=18)	OF (n=4)	DF (n=12)	OF (n=26)	DF (n=24)	OF (n=3)
NDF	51.91±1.50	51.67±7.34	59.96±3.14*	68.53±1.44*	51.10±1.40	49.36±4.27
ADF	44.97±1.17	45.58±5.49	43.20±2.43	45.99±1.07	45.61±1.23	42.88±3.32
ADL	12.38±0.89	9.67±1.54	6.95±0.69	8.28±0.90	15.18±1.23	15.29±1.72
Crude protein	10.83±0.61	9.65±1.58	8.76±0.60*	5.68±0.53*	10.89±0.57	13.00±1.09
Cellulose	32.59±1.48	34.99±4.21	36.26±1.98	37.71±0.91	30.44±1.08	27.58±1.86
Hemicellulose	7.39±0.68	6.09±1.93	16.76±2.15*	23.70±0.90*	6.10±0.95	6.49±1.19

*=Significantly different at the statistical level <0.05 of two sample t-test

3.5 Integrated habitat management; habitat suitability and forage crops

This study of tiger prey habitat, biomass production, and the nutritional characteristics of forage crops indicates that increases in the populations of tiger prey species require increases in the grass and forb biomasses of open forest. For gaur, this may also be the case for some closed forest. In terms of forage crop management efficiency, an increase in grass biomass is more achievable in open than in dense

forest (Table 3). The hemicellulose content of open forest grass was significantly higher than that of dense forest grass (Table 4). Hemicellulose is important in terms of the ungulate diet; wild herbivores similarly process plant tissues with high concentrations of cellulose and hemicellulose (Capoani, 2019). Specifically, as sambar deer exhibit a well-developed gastrointestinal structure, they can use plant materials that are high in cellulose and hemicellulose, such as leaves, bark, and woody twigs; these are efficiently digested (Tajchman et al., 2018). Such materials are the principal ruminant fuels, typically providing up to 80% of energy (Barboza et al., 2009). González-Hernández and Silva-Pando (1999) reported that the CP level was a good estimator of food quality. Fiber quality greatly affects the rumen microbiome and the amount of energy that is produced (Van Soest et al., 1991); CP is an essential component of an ungulate diet (Bayoumi and Smith, 1976). The CP content of open forest is significantly less than that of closed forest, because the biomass is less. Open habitat management is more efficient than closed habitat management (Chaiyarat et al., 2021; Frank et al., 2016; Ofstad et al., 2016; Tschöpe et al., 2011). Suggested pilot area optimal for tiger prey species are shown in Figure 8.

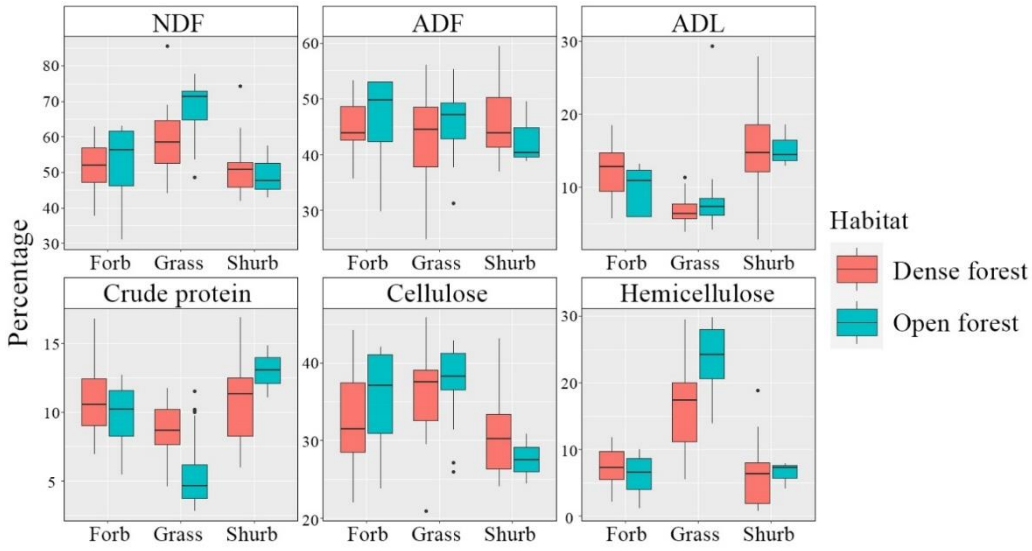

Figure 9. Nutritional parameters of forage crops by the extent of canopy cover

4. CONCLUSION

Identification of suitable habitats via Bayesian, lasso binary quantile regression can be used to facilitate optimal management of large areas. The models in this study show correlations between NDVI and grass, forb, and shrub biomasses significantly influenced the probabilities that sambar deer and gaur would be present. These factors can be managed/controlled. If an area is conducive to open habitat, it should be regularly managed as a grassland (to ensure good prey species nutrition). Pilot management of optimal areas in Thap Lan National Park should be selected according the stable areas available to manage; such areas are shown in Figure 8. However, further study of the forage crop quality of local plants is required to enhance the management of tiger prey species.

ACKNOWLEDGEMENTS

This research was supported by "Study of wildlife habitat quality for prey species of tiger in Dong Phayayen-Khao Yai Forest Complex" project (P-18-51249) of the National Science and Technology Development Agency (NSTDA), the Department of National Parks, Wildlife and Plant Conservation, the Geo-Informatics and Space Technology Development Agency (Public Organization), Wildlife Conservation Society (WCS)-Thailand Program, Thap Lan National Park. Finally, our special thanks for all fieldwork assistance.

REFERENCES

Akaike H. Information theory and an extension of the maximum likelihood principle. In: Parzen E, Tanabe K, Kitagawa G, editors. Selected Papers of Hirotugu Akaike. New York, USA: Springer; 1998.

Aranha J, Enes T, Calvão A, Viana H. Shrub biomass estimates in former burnt areas using sentinel 2 images processing and classification. Forests 2020;11(5):Article No. 555.

Ash E, Kaszta Ż, Noochdumrong A, Redford T, Chanteap P, Hallam C, et al. Opportunity for Thailand's forgotten tigers: Assessment of the Indochinese tiger *Panthera tigris corbetti* and its prey with camera-trap surveys. Oryx 2021;55(2):204-11.

Barboza PS, Parker KL, Hume ID. Integrative Wildlife Nutrition. Berlin, Germany: Springer; 2009.

Bassett GW, Koenker RW. Strong consistency of regression quantiles and related empirical processes. Econometric Theory 1986;2(2):191-201.

Bayoumi MA, Smith AD. Response of big game winter range vegetation to fertilization. Journal of Range Management Archives 1976;29(1):44-8.

Benoit DF, Van den Poel D. Binary quantile regression: A Bayesian approach based on the asymmetric Laplace distribution. Journal of Applied Econometrics 2012;27(7):1174-88.

Benoit DF, Alhamzawi R, Yu K. Bayesian lasso binary quantile regression. Computational Statistics 2013;28(6):2861-73.

Benoit DF, Van den Poel D. bayesQR: A Bayesian approach to quantile regression. Journal of Statistical Software 2017; 76(1):1-32.

Borowik T, Pettorelli N, Sönnichsen L, Jędrzejewska B. Normalized difference vegetation index (NDVI) as a predictor of forage availability for ungulates in forest and field habitats. European Journal of Wildlife Research 2013;59(5):675-82.

Brennan A, Cross PC, Creel S. Managing more than the mean: Using quantile regression to identify factors related to large elk groups. Journal of Applied Ecology 2015;52(6):1656-64.

Bukombe J, Kittle A, Senzota RB, Kija H, Mduma S, Fryxell JM, et al. The influence of food availability, quality and body size on patch selection of coexisting grazer ungulates in western Serengeti National Park. Wildlife Research 2019;46(1):54-63.

Cade BS, Noon BR. A gentle introduction to quantile regression for ecologists. Frontiers in Ecology and the Environment 2003;1(8):412-20.

Capoani L. Variations in Nutritional Content of Key Ungulate Browse Species in Sweden [dissertation]. Sweden: Swedish University of Agricultural Sciences; 2019.

Cappai MG, Aboling S. Toxic or harmful components of aromatic plants in animal nutrition. In: Feed Additives. Massachusetts, USA: Academic Press; 2020.

Chamaillé-Jammes S, Blumstein DT. A case for quantile regression in behavioral ecology: Getting more out of flight initiation distance data. Behavioral Ecology and Sociobiology 2012;66(6):985-92.

Chaiyarat R, Prasopsin S, Bhumpakphan N. Food and nutrition of Gaur (*Bos gaurus* CH Smith, 1827) at the edge of Khao Yai National Park, Thailand. Scientific Reports 2021;11:Article No. 3281.

Chetri M. Diet analysis of gaur (*Bos gaurus gaurus* smith, 1827) by micro-histological analysis of fecal samples in parsa wildlife reserve, Nepal. Our Nature 2006;4(1):20-8.

Chatterjee D, Sankar K, Qureshi Q, Malik PK, Nigam P. Ranging pattern and habitat use of sambar (*Rusa unicolor*) in Sariska Tiger Reserve, Rajasthan, Western India. DSG Newsletter 2014;26:60-71.

Cook RC, Murray DL, Cook JG, Zager P, Monfort SL. Nutritional influences on breeding dynamics in elk. Canadian Journal of Zoology 2001;79(5):845-53.

Cushman SA, McGarigal K. Hierarchical, multi-scale decomposition of species-environment relationships. Landscape Ecology 2002;17(7):637-46.

Dicker RC, Coronado F, Koo D, Gibson PR. Principles of Epidemiology in Public Health Practice: An Introduction to Applied Epidemiology and Biostatistics. Atlanta, GA, USA: Centers for Disease Control and Prevention, 2006.

Dodge Y. The Concise Encyclopedia of Statistics. Berlin, Germany: Springer; 2008.

Duangchatrasiri S, Shadshan D, Kernklang P, Jornburom P, Vinitpornsawan S, Habitat occupancy for a tiger (*Panthera tigris*) in the Dong Phayayen-Khao Yai Forest Complex. Proceedings of the 38th Wildlife in Thailand Seminar, 2017 December 14-15; Kasetsart University, Bangkok: Thailand; 2017.

Duangchatrasiri S, Jornburom P, Jinamoy S, Pattanvibool A, Hines JE, Arnold TW, et al. Impact of prey occupancy and other ecological and anthropogenic factors on tiger distribution in Thailand's western forest complex. Ecology and Evolution 2019;9(5):2449-58.

Ensslin A, Rutten G, Pommer U, Zimmermann R, Hemp A, Fischer M. Effects of elevation and land use on the biomass of trees, shrubs and herbs at Mount Kilimanjaro. Ecosphere 2015;6(3):1-5.

Frank DA, Wallen RL, White PJ. Ungulate control of grassland production: Grazing intensity and ungulate species composition in Yellowstone Park. Ecosphere 2016;7(11):e01603.

González-Hernández MP, Silva-Pando FJ. Nutritional attributes of understory plants known as components of deer diets. Journal of Range Management Archives 1999;52(2):132-8.

Gorelick N, Hancher M, Dixon M, Ilyushchenko S, Thau D, Moore R. Google earth engine: Planetary-scale geospatial analysis for everyone. Remote Sensing of Environment 2017;202:18-27.

Hoffmann WA. Fire and population dynamics of woody plants in a neotropical savanna: Matrix model projections. Ecology 1999;80(4):1354-69.

Holechek JL. Comparative contribution of grasses, forbs, and shrubs to the nutrition of range ungulates. Rangelands Archives 1984;6(6):261-3.

Holechek JL, Pieper RD, Herbel CH. Range Management: Principles and Practices. 3rd ed. New Jersey, USA: Prentice Hall; 1998.

Jasra AW, Johnson DE. Nutritional constraints on the productivity of sheep and goats grazing a degraded grassland of highland Balochistan, Pakistan. Pakistan Journal of Agricultural Research 2000;16(1):64-7.

Ji Y, Lin N, Zhang B. Model selection in binary and tobit quantile regression using the Gibbs sampler. Computational Statistics and Data Analysis 2012;56(4):827-39.

John OO. Robustness of quantile regression to outliers. American Journal of Applied Mathematics and Statistics 2015;3(2):86-8.

Kaur R. Carbon Pool Assessment in Govind Wildlife Sanctuary and National Park [dissertation]. Dehradun: Forestry and Ecology Division, Indian Institute of Remote Sensing; 2007.

Koenker R, Bassett Jr G. Robust tests for heteroscedasticity based on regression quantiles. Econometrica 1982:50(1);43-61.

Kordas G. Smoothed binary regression quantiles. Journal of Applied Econometrics 2006;21(3):387-407.

Krause J, Ruxton GD, Ruxton G, Ruxton IG. Living in Groups. Oxford, England: Oxford University Press; 2002.

Lamont BG, Monteith KL, Merkle JA, Mong TW, Albeke SE, Hayes MM, et al. Multi-scale habitat selection of elk in response to beetle-killed forest. The Journal of Wildlife Management 2019;83(3):679-93.

Li J, Mao X. Comparison of canopy closure estimation of plantations using parametric, semi-parametric, and non-parametric models based on GF-1 remote sensing images. Forests 2020;11(5):Article No. 597.

Li Q, Lin N, Xi R. Bayesian regularized quantile regression. Bayesian Analysis 2010;5(3):533-56.

Lynam AJ, Tantipisanuh N, Chutipong W, Ngoprasert D, Baker MC, Cutter P, et al. Comparative sensitivity to environmental variation and human disturbance of Asian tapirs (*Tapirus indicus*) and other wild ungulates in Thailand. Integrative Zoology 2012;7(4):389-99.

Manski CF. Semiparametric analysis of discrete response: Asymptotic properties of the maximum score estimator. Journal of Econometrics 1985;27(3):313-33.

McCullagh P, Nelder J. Generalized Linear Models, 2nd ed. London, UK: Chapman and Hall; 2019.

McShea WJ, Davies SJ, Bhumpakphan N. The Ecology and Conservation of Seasonally Dry Forests in Asia. Washinton, DC, USA: Smithsonian Institution Scholarly Press; 2011.

Mobashar M, Habib G, Anjum MI, Gul I, Ahmad N, Moses A, et al. Herbage production and nutritive value of alpine pastures in upper Kaghan valley, Khyber Pakhtunkhawa, Pakistan. Journal of Animal and Plant Sciences 2017;27(5):1472-8.

Moreno-de las Heras M, Díaz-Sierra R, Turnbull L, Wainwright J. Assessing vegetation structure and ANPP dynamics in a grassland-shrubland Chihuahuan ecotone using NDVI-rainfall relationships. Biogeosciences Discussions 2015;12(1):51-92.

Mountousis I, Papanikolaou K, Stanogias G, Chatzitheodoridis F, Roukos C. Seasonal variation of chemical composition and dry matter digestibility of rangelands in NW Greece. Journal of Central European Agriculture 2008;9(3):547-55.

Muggeo VM, Sciandra M, Tomasello A, Calvo S. Estimating growth charts via nonparametric quantile regression: A practical framework with application in ecology. Environmental and Ecological Statistics. 2013;20(4):519-31.

Ngoprasert D, Gale GA. The status of Tiger and Dhole and their Prey in the Dong Phayayen-Khao Yai Forest Complex. Proceedings of the 38th Wildlife in Thailand Seminar, 2017 December 14-15; Kasetsart University, Bangkok: Thailand; 2017.

Ofstad EG, Herfindal I, Solberg EJ, Seather BE. Home ranges, habitat and body mass: Simple correlates of home range size in ungulates. Proceedings of the Royal Society B: Biological Sciences 2016;283(1845):Article No. 1234.

Paansri P, Sangprom N, Suksavate W, Chaiyes A, Duengkae P. Spatial modeling of forage crops for tiger prey species in the area surrounding highway 304 in the Dong Phayayen-Khao Yai Forest Complex. Environment and Natural Resources Journal 2021;19(3):220-9.

Pattanakiat S. Vegetation pattern and soil relationship in a tropical grassland of Khao Yai National Park. Bangkok, Thailand: FAO; 1988. (in Thai).

Randle M, Stevens N, Midgley G. Comparing the differential effects of canopy shading by *Dichrostachys cinerea* and *Terminalia sericea* on grass biomass. South African Journal of Botany 2018;119:271-7.

Rai D. Opinion survey on the ecology of Sambar, *Rusa unicolor* (Artiodactyla, Cervidae) and its status with respect to crop damage in districts Jhunjhunu and Churu, Rajasthan (India). Journal of Applied and Natural Science 2019;11(2):468-77.

Rautiainen H, Bergvall UA, Felton AM, Tigabu M, Kjellander P. Nutritional niche separation between native roe deer and the nonnative fallow deer: A test of interspecific competition. Mammal Research 2021;66(3):1-13.

R Core Team. R: A Language and Environment for Statistical Computing. Vienna, Austria: R Foundation for Statistical Computing; 2017.

Royal Forest Department, Ministry of Natural Resources and Environment (RFD). Preparation of Information on Forest Area 2017-2018. Bangkok, Thailand: Ministry of Natural Resources and Environment; 2018.

Sage RF, Kubien DS. Quo vadis C 4? An ecophysiological perspective on global change and the future of C 4 plants. Photosynthesis Research 2003;77(2):209-25.

Seven PT, Cerci IH. Relationships between nutrient composition and feed digestibility determined with enzyme and nylon bag (in situ) techniques in feed resources. Bulgarian Journal of Veterinary Medicine 2006;9(2):107-13.

Simcharoen A, Savini T, Gale GA, Roche E, Chimchome V, Smith JL. Ecological factors that influence sambar (*Rusa unicolor*) distribution and abundance in western Thailand: Implications for tiger conservation. Raffles Bulletin of Zoology 2014; 62:100-6.

Tajchman K, Steiner-Bogdaszewska Ż, Żółkiewski P. Requirements and role of selected micro and macro elements in nutrition of cervids (Cervidae). Applied Ecology and Environmental Research 2018;16(6):7669-86

Tschöpe O, Wallschläger D, Burkart M, Tielbörger K. Managing open habitats by wild ungulate browsing and grazing: A case-study in North-Eastern Germany. Applied Vegetation Science 2011;14(2):200-9.

Tufarelli V, Cazzato E, Ficco A, Laudadio V. Evaluation of chemical composition and in vitro digestibility of Appennine pasture plants using yak (*Bos grunniens*) rumen fluid or faecal extract as inoculum source. Asian-Australasian Journal of Animal Sciences 2010;23(12):1587-93.

Van Soest PJ, Robertson JB, Lewis BA. Symposium: Carbohydrate methodology, metabolism, and nutritional implications in dairy cattle. Journal of Dairy Science 1991;74(10):3583-97.

Venables WN, Ripley BD. Modern Applied Statistics with S. 4th ed. New York, USA: Springer; 2013.

Verme LJ, Ullrey DE. Feeding and nutrition of deer. Digestive Physiology and Nutrition of Ruminants 1972;3:275-91

Wallmo OC, Carpenter LH, Regelin WL, Gill RB, Baker DL. Evaluation of deer habitat on a nutritional basis. Journal of Range Management 1977;30(2):122-7.

Wan X, Wang W, Liu J, Tong T. Estimating the sample mean and standard deviation from the sample size, median, range and/or interquartile range. BMC Medical Research Methodology 2014;14(1):1-3.

Widenfalk O, Weslien J. Plant species richness in managed boreal forests: Effects of stand succession and thinning. Forest Ecology and Management 2009;257(5):1386-94.

Wu W, De Pauw E, Helldén U. Assessing woody biomass in African tropical savannahs by multiscale remote sensing. International Journal of Remote Sensing 2013;34(13):4525-49.

Environmental Factors Modulating Indole-3-Acetic Acid Biosynthesis by Four Nitrogen Fixing Bacteria in a Liquid Culture Medium

Le Thi Xa[1], Nguyen Khoi Nghia[2*], and Hüseyin Barış Tecimen[3]

[1]School of Education, Soc Trang Community College, Soc Trang Province, Vietnam
[2]Department of Soil Science, College of Agriculture, Can Tho University, Can Tho City, Vietnam
[3]Soil Science and Ecology Department, Faculty of Forestry, Istanbul University-Cerrahpaşa, Istanbul, Turkey

ARTICLE INFO

Received: 29 Nov 2021
Received in revised: 30 Jan 2022
Accepted: 3 Feb 2022
Published online: 28 Feb 2022
DOI: 10.32526/ennrj/20/202100233

Keywords:
Biological nitrogen fixing bacteria/ Indole-3-acetic acid biosynthesis/ Plant growth promotion/ pH/ Sodium chloride/ Tryptophan

*** Corresponding author:**
E-mail: nknghia@ctu.edu.vn

ABSTRACT

This study evaluated the effects of some environmental conditions on IAA biosynthesizing capacity of four nitrogen fixing bacteria, namely *Paenibacillus cineris* TP-1.4, *Bacillus megaterium* MQ-2.5, *Klebsiella pneumoniae* OM-17.2, and *Pseudomonas boreopolis* CP-18.2. Carbon source, pH, NaCl, and tryptophan supplement treatments were set to investigate the effects of those environmental factors on IAA synthesis. The IAA synthesizing capacity of bacterial strains in liquid medium was measured spectroscopically following incubation by Salkowski's reagent method. The results showed that, under the sucrose amendment, the IAA concentrations produced by all four bacterial strains were significantly higher than those of the other four carbon source added treatments. Two of the four bacterial strains produced the highest yield of IAA in liquid medium at pH 7 (TP-1.4 and OM-17.2), whereas pH 8 was optimum for the other two strains (MQ-2.5 and CP-18.2). The MQ-2.5 strain could synthesize IAA fairly well in up to 5% NaCl and produced the highest amount of IAA with 1% NaCl. Furthermore, IAA synthesizing capability of tested bacterial strains increased sharply along with increasing tryptophan content in culture medium except for the TP-1.4 strain. From the current study, these isolates emerged as possible alternatives for future IAA production for plant growth and yield enhancement. Hence, they have a great potential to be used as bio-inoculants for plant growth promotion in eco-friendly and sustainable agriculture.

1. INTRODUCTION

The agriculture industry has applied numerous measures for intensive crop production, such as using chemical fertilizers, pesticides, and plant growth stimulants, which have become widespread to increase productivity and ensure global food security. However, the long term impacts of applying these cultivation techniques made a dramatic decrease in the productivity of some crops (Sirivastava and Singh, 2017), degradation of the soil, and water pollution (Stinner, 2007). Therefore, implementation of sustainable, eco-friendly agriculture and climate change adaptive methods is of utmost concern and has a priority.

Nowadays, chemical fertilizer costs have risen all over the world and this fact has become a big disadvantage for farmers as they suffer from higher input costs and get low profits accordingly. Therefore, the use of plant growth promoting microorganisms in crop cultivation is preferred and encouraged worldwide in order to reduce or partly replace applying chemical fertilizers, or plant growth stimulants which would reduce the input costs and protect the agri-ecosystems, environment, and human health. In particular, the isolation, selection and application of multi-functional microorganisms has shown a significantly higher stimulation on crop growth and yields compared to those of single-function ones (Tewari and Arora, 2014). Among them, the growth functions stimulating microorganisms, including biological nitrogen fixation and synthesis of indole-3-acetic acid, have attracted remarkable attention (Shokri and Emtiazi, 2010; Defez et al., 2017), because nitrogen and indole-3-acetic acid are the two most essential factors that have a strong impact on growth and yield of plants.

Citation: Xa LT, Nghia NK, Tecimen HB. Environmental factors modulating indole-3-acetic acid biosynthesis by four nitrogen fixing bacteria in a liquid culture medium. Environ. Nat. Resour. J. 2022;20(3):279-287. (https://doi.org/10.32526/ennrj/20/202100233)

In a previous study, Xa and Nghia (2019) isolated and selected strains of bacteria that possess significant nitrogen fixation and IAA synthesis functions to be tools for agricultural production. However, it was suggested that environmental factors greatly influence their ability to activate IAA synthesizing functions (Scarcella et al., 2017; Bhutani et al., 2018). Therefore, to ensure the efficacy of these strains when they are inoculated in the greenhouse and field conditions, the environmental and cultural conditions of these strains should be well known. Therefore, within this study, we examined the IAA production capacities of four different selected bacteria against various amended culture mediums in the laboratory. Our findings are expected to broaden the knowledge over the natural and environmentally friendly solutions for sustainable agricultural development under environmental stresses.

2. METHODOLOGY

2.1 Microorganism source

Four nitrogen fixing bacteria, namely *Paenibacillus cineris* TP-1.4, *Bacillus megaterium* MQ-2.5, *Klebsiella pneumoniae* OM-17.2, and *Pseudomonas boreopolic* CP-18.2 were isolated and selected from indigenous microorganisms of different cropping systems in Soc Trang Province, Vietnam (Xa and Nghia, 2019). Four bacterial isolates were maintained in N-free Burks liquid medium under laboratory conditions. N-free Burks liquid medium contained sucrose 10 g, $K_2HPO_4 \cdot 4H_2O$ 0.41 g, KH_2PO_4 1.05 g, $CaCl_2 \cdot 2H_2O$ 0.1 g, $MgSO_4 \cdot 7H_2O$ 0.1 g, $FeSO_4 \cdot 7H_2O$ 0.015 g, H_3BO_3 0.0025 g, and Mo 0.0025 g per liter (Mehta and Nautiyal, 2001).

2.2 Environmental factors on IAA production

2.2.1 Effect of different carbon sources on IAA synthesis by four bacterial strains in Burks liquid medium

Five different carbon sources composed of fructose, glucose, glycerol, mannose and sucrose at the concentration of 1% were considered as different treatments and the control treatment was without bacteria. Each treatment had three replicates, corresponding to three different incubation flasks. Bacterial strains were grown in 100 mL Erlenmeyer flasks containing 50 mL fresh N-free Burks liquid medium for four days. Then, an aliquot of 300 µL bacterial suspension was transferred to 50 mL Erlenmeyer flasks containing 30 mL fresh N-free Burks liquid medium, pH 7, 100 mg/L tryptophan and different carbon sources as different treatments to achieve bacterial numbers of 10^6 CFU/mL. The flask samples were put on an orbital shaker at 100 rpm in the dark and under laboratory conditions for ten days. The synthesized IAA concentrations were determined after 0, 2, 4, 6, 8, and 10 days of incubation by Salkowski's reagent method at a wavelength of 530 nm followed by the modified method described by Bric et al. (1991).

2.2.2 Effect of different pH values on IAA synthesis

To determine the effect of different pH values of N-free Burk's medium on IAA production, an experiment was conducted at pH values of 3, 5, 7, 8, and 9. Each pH level had their own corresponding control treatment without bacterial inoculation. The carbon form providing the highest IAA production from the results of the test in section 2.2.1 was added as an energy source to the bacteria. Concentration of IAA production was measured at 0, 2, 4, 6, 8, and 10 days after inoculation according to Bric et al. (1991).

2.2.3 Effect of different NaCl concentrations

The experiment was established to evaluate the effect of different concentrations of NaCl on IAA production of four bacterial strains. The 0%, 1%, 2%, 3%, 4%, and 5% NaCl concentration series was used as individual treatments. Each NaCl concentration treatment accordingly had a corresponding control treatment without microbial inoculation. The best pH value and carbon source from the results of the tests in section 2.2.1 and 2.2.2 were applied in the liquid culture medium of this experiment. The synthesized IAA concentrations were determined after 0, 2, 4, 6, 8, and 10 days of incubation by the method of Bric et al. (1991).

2.2.4 Effect of different concentrations of tryptophan

This experiment was conducted to find out the best concentration of tryptophan added in N-free Burks liquid medium for optimizing IAA production using tryptophan concentrations of 100, 200, 300, 400, and 500 mg/L. The control treatment was without tryptophan with pH 7. Each IAA concentration treatment, accordingly, had a corresponding control treatment without microbial inoculation. The optimal pH, carbon source, and NaCl concentration achieved from section 2.2.1, 2.2.2, and 2.2.3 were adjusted in the cultured medium of this experiment.

2.3 Data analysis

The data were analyzed by ANOVA with MINITAB software with 16.2 versions.

3. RESULTS AND DISCUSSION

3.1 Effects of different carbon sources on IAA production synthesized by four bacterial isolates

The results presented in Figure 1 reveal that the different carbon sources caused variation in the production of IAA by four bacterial isolates. During the experiment period, sucrose was observed to be the best carbon source at supporting the four bacterial strains to boost the IAA synthesis, and OM-17.2 was the highest IAA producing strain compared to the other three isolates. The OM-17.2 strain reached its maximum IAA production amount after four days of incubation at 93.9 mg IAA/L in the sucrose amended treatment, followed by the treatments with glycerol, glucose, mannose, and fructose. Two other strains, MQ-2.5, and CP-18.2 synthesized up to 32.8 mg/L and 43.0 mg/L IAA in sucrose added medium after 6 and 4 days of incubation, respectively, slightly higher than glucose, glycerol, mannose, and fructose added treatments. The TP-1.4 strain reached its highest IAA production rate of 26.3 mg/L in the sucrose added treatment after the 10 days incubation. To sum up, from this result, sucrose can be considered as the best carbon source for the four tested bacteria to synthesize at a worthy amount of IAA in liquid culture.

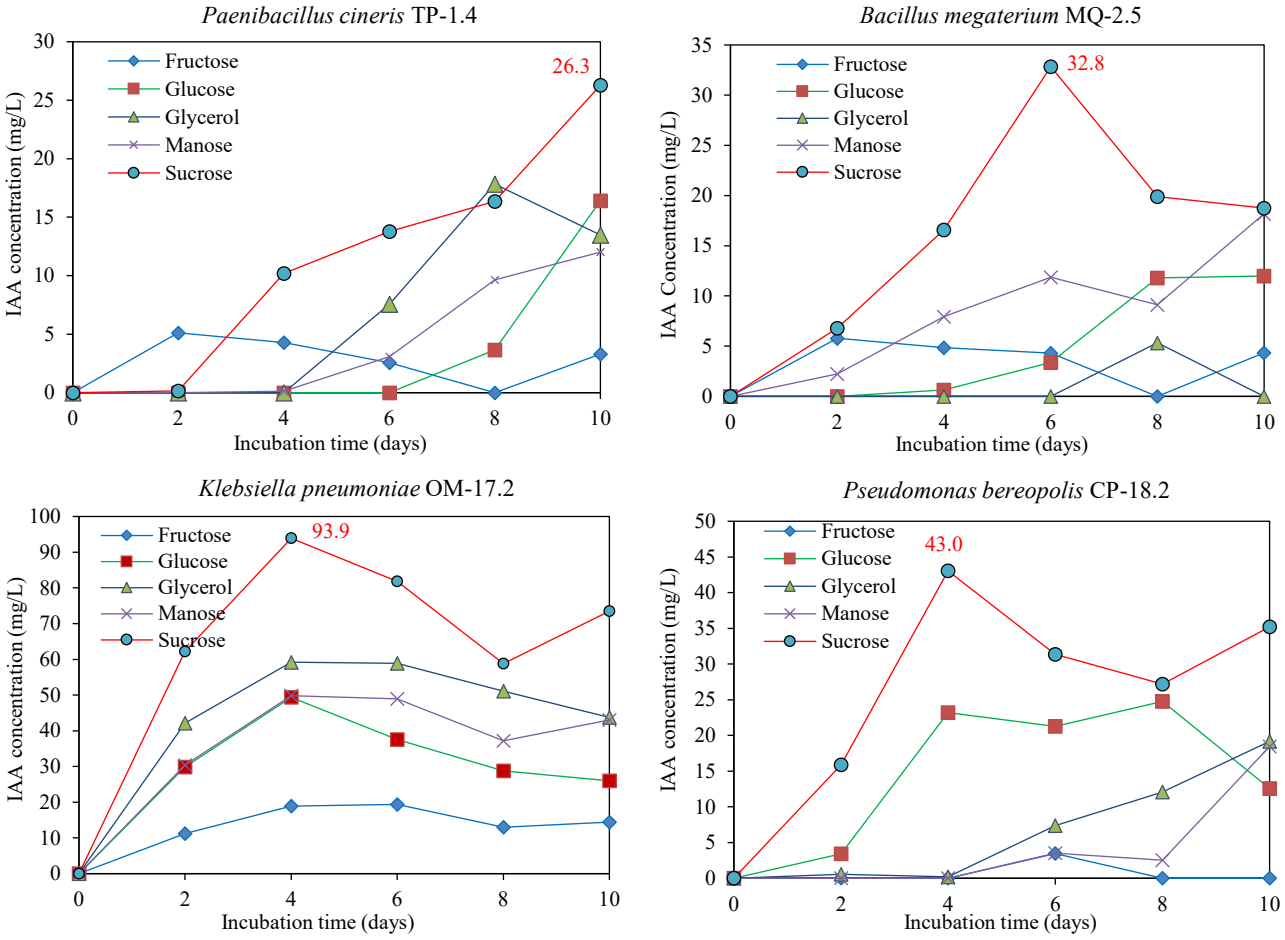

Figure 1. Effects of different carbon sources on the IAA production by four bacterial strains in Burks liquid medium during 10 days of incubation

This result is consistent with the study of Nutaratat et al. (2015) who recorded that the strain of *Rhodosporidium paludigenum* synthesized the highest amount of IAA in liquid culture medium containing 1% sucrose compared to arabinose, dextrose, fructose, galactose, glycerol, lactose, maltose, mannitol, mannose, my-inositol, raffinose, sorbitol, sorbose, starch, xylitol, and xylose. Similarly, Kucuk and Cevheri (2016) also detected that among glucose, fructose, mannitol, and sucrose, the highest IAA synthesis by the strain of *Rhizobium* sp. P2 was found to be in sucrose-amended culture medium. In this case,

it is clear that sucrose is the best carbon source for IAA synthesis. However, in the study of Scarcella et al. (2017) on *Trichosporon asahii,* a yeast strain showed that IAA production in the sucrose added treatment was superior at pH 6.0, but the pH of 4.5 in this study gave the highest IAA production in the glucose added treatment. These results indicate an association between the carbon source and medium pH. For *Rhodotorula mucilaginosa*, the highest IAA production was observed at pH 6.0 with glucose. In a research study of Bhutani et al. (2018) on *Bacillus aryabhattai*, the MBN3, MJHN1, and MJHN10 strains, the most suitable carbon sources were found to be mannitol, sucrose, and glucose, respectively. This result is consistent with the results of Wagi and Ahmed (2019) for *Bacillus cereus* (So3II) and *B. subtilis*. Alfonso et al. (2021) also noted that although the highest growth rate was achieved when glucose was the carbon source, the lowest IAA concentration was found in the glucose added medium. Upon the findings from reviewed studies, we can postulate that different types of sugar sources in a media have basal differences due to varied utilization of sugars by bacteria during their growth (Shanti et al., 2007; Sridevi et al., 2008).

3.2 Effects of different pH levels

The IAA production performances by four bacterial strains in different pH levels are presented in Figure 2. It was clear that, for *Paenibacillus cineris* TP-1.4 and *Klebsiella pneumoniae* OM-17.2 strains, the best pH value for IAA synthesis was pH 7, while for the two others was pH 8. The TP-1.4 and OM-17.2 strains showed their maximum IAA production after eight days of incubation with a value of 33.8 and 76.6 mg/L, respectively. The MQ-2.5, and CP-18.2 strains performed the maximum IAA production at rates 40.0, and 25.0 mg/L after eight and 10 days of incubation, respectively. The IAA production by four bacterial strains showed the same trend as following the order as pH 8>pH 9>pH 5>pH 3. It was clear to see that under the acidic environment of liquid culture (pH=3, and pH=5) the IAA production of bacterial strains decreased dramatically.

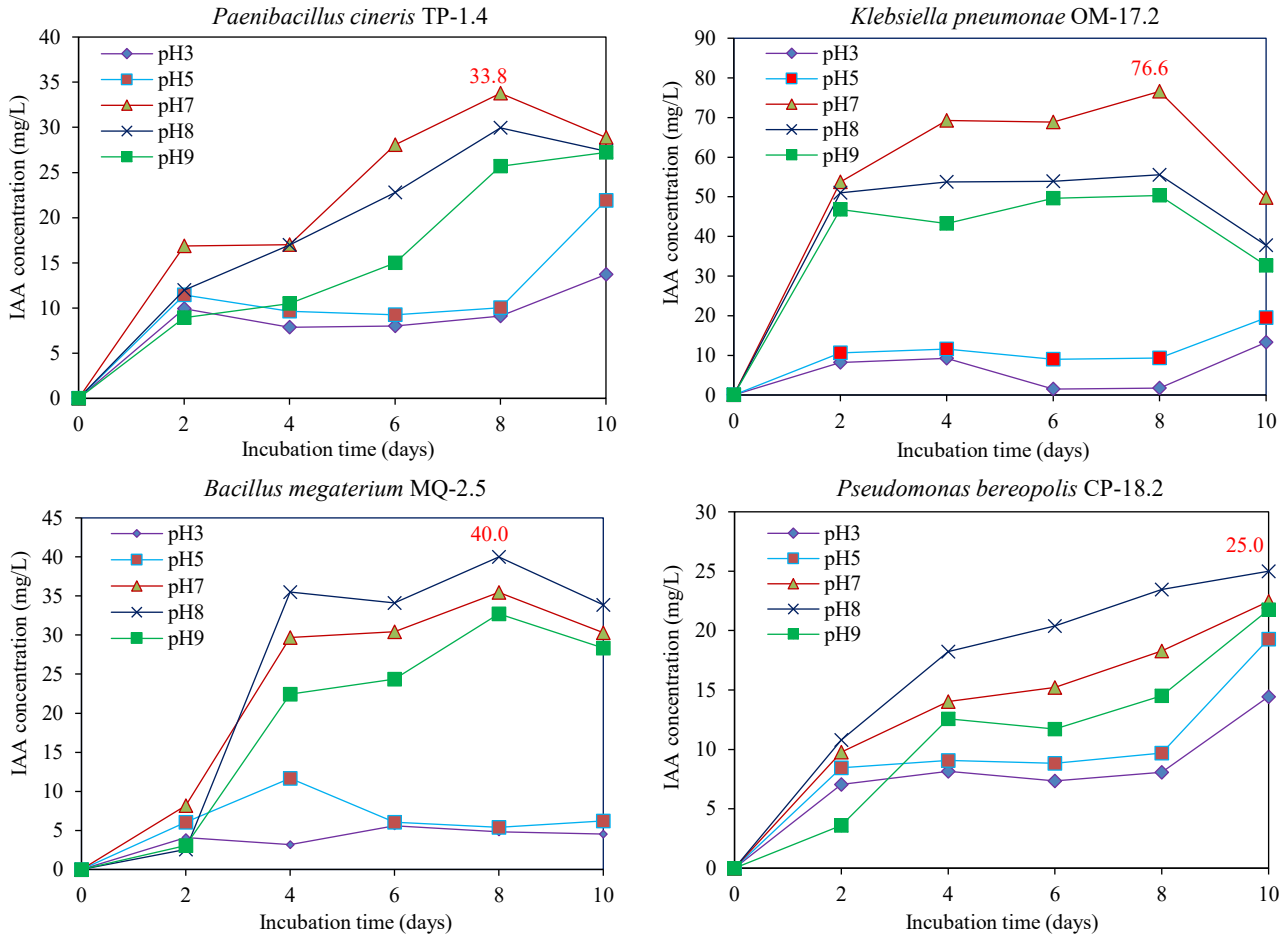

Figure 2. Effects of different pH levels of liquid medium on the IAA production by four bacterial strains in Burks liquid medium during 10 days of incubation

Our results showed similarity with findings of Nutaratat et al. (2015) who suggested that pH 7 was suitable for IAA synthesizing performance of *Rhodosporidium paludigenum*. In addition, Khamna et al. (2010) reported that, pH 7.0 was suitable for maximum IAA production by *Streptomyces* sp. or *Bacillus subtilis* (Kumari et al., 2018), pH 7.2 was the optimum range for IAA production of *Rhizobium* strain VMA 301 (Mandal et al., 2007), pH 7.5 was best for *Pseudomonas putida* UB-1 (Bharucha et al., 2013) and pH 7.2 was the optimum IAA production range (Shanti et al., 2007). However the best IAA production was found at pH 8 (Sachdev et al., 2009). In the study by Chandra et al. (2018), three different isolates were tested and the isolate CA2003 showed maximum IAA production at pH 5 and decreased towards the pH range of 6-9; while CA2001 was opposite. The maximum IAA production of this strain was observed at pH 9 and CA2004 produced maximum IAA at pH 6, but lower IAA production was recorded at pH 5, 7, 8, and 9. Overall, the acid medium is not suitable for IAA synthesis of bacteria (Ona et al., 2005; Mohite, 2013).

3.3 Effects of different sodium chloride concentrations

The results of the effects of different NaCl concentration on the IAA production are presented in Figure 3. It is obvious that the highest IAA production by strains MQ-2.5 and OM-17.2 was found in the 1% NaCl added treatments, while the highest IAA production by strains TP-1.4 and CP-18.2 was found in the no NaCl added treatment. For both with and without NaCl treatments, the most efficient IAA synthesis was done by OM-17.2. The highest amount of IAA production was recorded in the 1% NaCl added and no NaCl added treatments after the fourth day of incubation at rates 97.2 mg/L and 82.7 mg/L, respectively. However, with increasing NaCl concentration, the synthesized IAA amount by the strain OM-17.2 decreased accordingly from 97.2 mg/L to 80.1, 57.8, 32.8, and 10.1 mg/L in treatments supplied with 2%, 3%, 4%, and 5% NaCl, respectively.

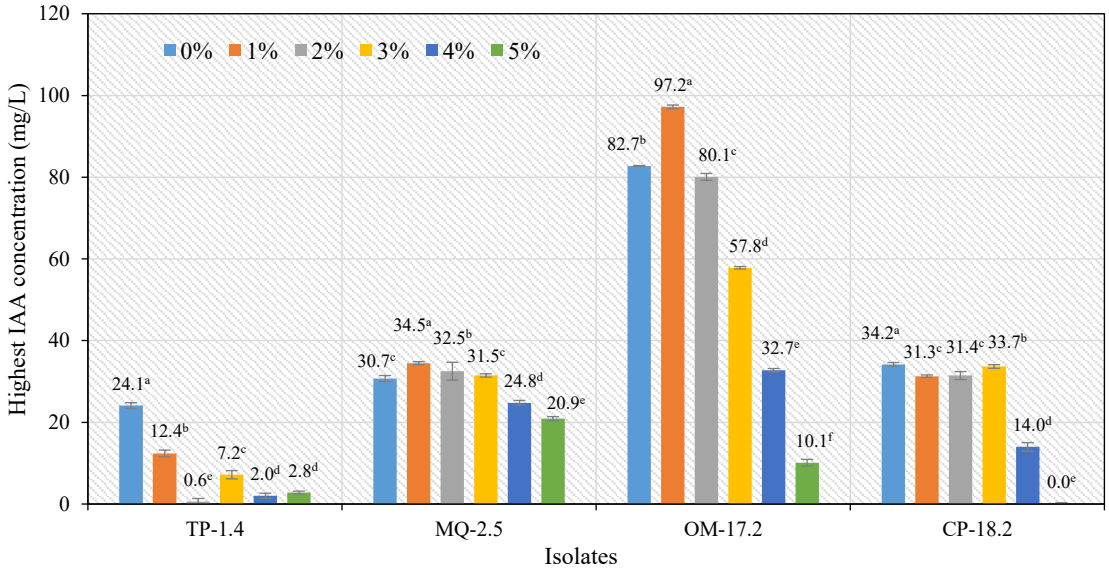

Figure 3. The highest concentration of IAA in Burks liquid medium synthesized by four bacterial strains in the different NaCl concentrations

Although the MQ-2.5 strain did not produce IAA as high as the strain OM-17.2, the amount of IAA produced by MQ-2.5 varied between 20.9 and 34.5 mg/L. The highest IAA amount synthesized by MQ-2.5 was in the treatment of 1% NaCl, however with gradually increased NaCl content to 2, 3, 4, and 5%, the synthesis of IAA decreased very slightly and still remained at a high level (over 20 mg/L IAA in the treatment of 5% NaCl). In short, under the NaCl stress, the MQ-2.5 strain showed the optimum IAA synthesis at 1% NaCl treatment and it tolerated NaCl concentration up to 5% which allowed MQ-2.5 to be assessed as a halotolerant bacteria (Willey et al., 2009). Turning to the strain CP-18.2, the results showed its best capacity of IAA synthesis in the treatment of 3% NaCl supplementation. However, under 5% NaCl conditions, this bacterial strain was completely suppressed in producing IAA. Unfortunately, with the

presence of NaCl in liquid culture, the IAA synthesizing process by strain TP-1.4 was strongly inhibited while the content of IAA produced by this strain was found to be highest at the treatment without NaCl addition (24.1 mg/L). However, when NaCl concentration in the liquid culture increased to 1%, 2%, 3%, 4%, and 5%, the IAA content synthesized by strain TP-1.4 sharply decreased.

The halophilic bacteria identified as *Bacillus megaterium* ST2-9 synthesized the highest amount of IAA at the treatment supplied with 3% NaCl (Nghia et al., 2017). Similarly, Sarkar et al. (2018) observed a sharp decline in IAA production produced by *Enterobacter* sp. P23 strain with gradually increasing NaCl concentration (160 µg/mL at 150 mM NaCl and <20 µg/mL at 600 mM NaCl). Egamberdiyeva (2009) reported that IAA-producing bacteria supported plant growth under salt stress with a significantly increased plant growth. Additionally, Nakbanpote et al. (2014) proved that *Pseudomonas* sp. PDMZnCd2003 isolated from a Zn/Cd contaminated soil was classified as a salt-tolerant bacteria. This strain also indicated a good capacity of IAA synthesis, biological nitrogen fixation, and phosphate solubilization in liquid medium containing 8% (w/v) NaCl. Smith (2000) inferred that, IAA was an auxin hormone required by most plant cells for proliferation and root initiation. Badawy et al. (2021) showed that *Aspergillus ochraceus* produced 146 and 176 µg/mL IAA in a medium provided with 15 and 30% seawater, respectively. Therefore, this fungus was considered as a plant growth promoting and salt tolerant agent under seawater irrigation conditions. From the result of this experiment we can conclude that three strains, MQ-2.5, OM-17.2, and CP-18.2 can be considered as salt tolerant plant growth promoting bacteria. This had implications for agriculture in the Mekong Delta region of Vietnam where it is currently affected by salinity and drought.

3.4 Effects of different L-tryptophan concentrations

The test results to evaluate the effects of different L-tryptophan concentrations on IAA synthesizing ability of four bacterial strains presented in Figure 4 manifested that all four isolates preferred tryptophan for IAA production. Maximum IAA production was found in the treatments amended with 500 mg/L tryptophan for MQ-2.5, and CP-18.2, 400 mg/L tryptophan for TP-1.4, and 300 mg/L tryptophan for OM-17.2. Among four bacterial strains, CP-18.2 was found to be the most sensitive with tryptophan precursor. In the 100 mg/L tryptophan added treatment, the synthesized IAA was 32 mg/L, with a dramatic increase in the 500 mg/L tryptophan added treatment (128 mg/L IAA). A similar trend was observed for the MQ-2.5 strain with the highest IAA concentration of 84.6 mg/L. In particular, the OM-17.2 strain showed its highest concentration of IAA (123.4 mg/L) in the 300 mg/L tryptophan treatment, however, the IAA content dropped sharply when tryptophan content increased to 400 or 500 mg/L. The IAA synthesis of TP-1.4 was less affected by the tryptophan content than the other three isolates and TP-1.4 did not synthesize IAA as good as the other three bacteria under the same tryptophan supplementation conditions.

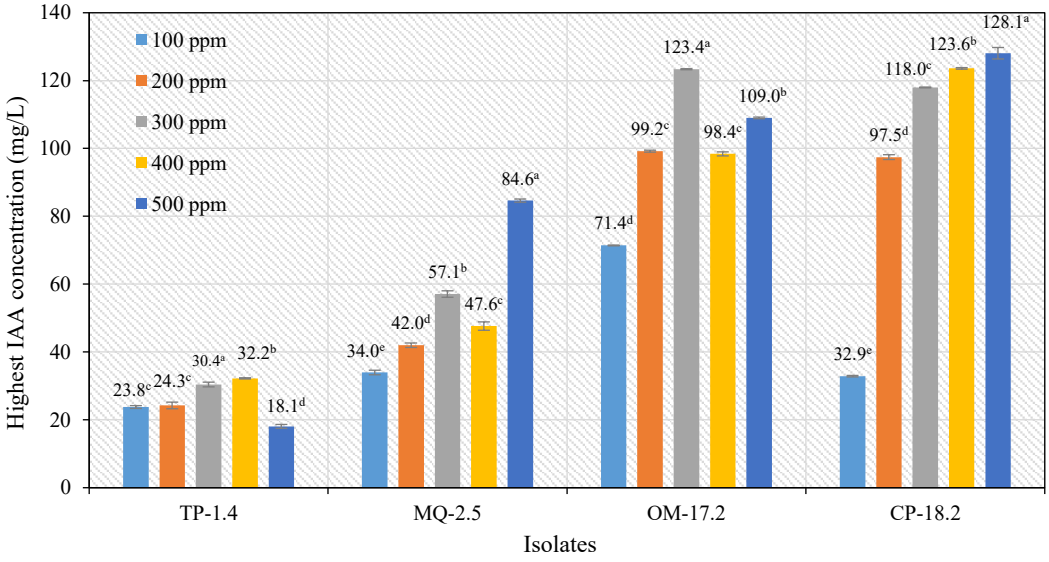

Figure 4. The highest concentrations of IAA synthesized by four different bacterial strains in Burks liquid medium containing different tryptophan concentrations

The IAA synthesis behaviors of four isolates when cultivated in Burks media supplied with or without tryptophan were varied. No IAA production at tryptophan-free medium for all four bacterial strains proved the dependency of those isolates on the tryptophan pathway for IAA synthesis.

Our results showed consistency with Ahmad et al. (2005) who tested IAA synthesizing capacity of 10 *Azotobacter* spp. strains and 11 strains of *Pseudomonas* sp. in liquid media containing 0, 1, 2, and 5 mg/mL tryptophan and observed lower IAA (2.68-10.80 mg/mL) yield in the liquid media without tryptophan addition. Seven *Azotobacter* strains produced IAA at ranges between 7.3 to 32.8 mg/mL and *Pseudomonas* sp. strains produced 41.0 to 53.2 mg/mL with 5 mg/mL tryptophan. In addition, Ahmad et al. (2008) showed that *Azotobacter* sp., *Pseudomonas* sp., and *Bacillus* sp. strains could not synthesize IAA properly without tryptophan, and they showed their highest IAA production ranged from 7.03 µg/mL to 22.02 µg/mL when the culture medium included 500 µg/mL tryptophan. Bhutani et al. (2018) indicated a gradual increase in the IAA production with an increase in L-tryptophan concentration. *Bacillus aryabhat* MBN3 and *Bacillus aryabhat* MJHN1 had a maximum IAA production in the treatment provided with 500 µg/mL tryptophan while *Bacillus aryabhat* MJHN10 produced the highest IAA in the treatment added with 300 µg/mL tryptophan. The study of Suliasih and Widawati (2020) illustrated that maximum IAA production by *Bacillus siamensis* was achieved after 96 h of incubation in a medium supplemented with 250 µg/mL of tryptophan, pH 8 and sucrose as carbon. In addition, Mohite (2013) suggested that IAA was not produced in negligible quantities of L-tryptophan. There were significantly different demand levels of L-tryptophan for varying microorganisms. For many bacteria, the conversion of tryptophan into IAA is of uppermost importance (Costacurta and Venderleyden, 1995). Manulis et al. (1994) reported that various *Streptomyces* spp. could secrete IAA when fed with tryptophan, while according to the results of Swain et al. (2007), IAA producing *Bacillus* spp. were tryptophan dependent and several other bacteria strains as well (Patten and Glick, 2002).

The results of four experiments in this study allowed us to conclude that different strains of bacteria also have different abilities in synthesizing IAA, and sucrose is the best carbon source for IAA synthesis for all four bacterial strains. In particular, the OM-17.2 strain has the highest ability to synthesize IAA in an environment with pH 7, 1% NaCl, and 300 mg/L tryptophan. Strain CP-18.2 showed optimum IAA production at pH 8, and 500 mg/L tryptophan. Notably, the MQ-2.5 strain was a salt-tolerant bacteria and can synthesize IAA in saline conditions up to 5% and this strain produced the highest IAA under pH 8, NaCl 1%, and 500 mg/L tryptophan. Meanwhile, the TP-1.4 strain had a stable IAA production and was least affected by environmental conditions. It produces the highest concentration of IAA in liquid culture medium under pH 7, without and with 400 mg/L tryptophan.

4. CONCLUSION

In summary, the environmental factors of the culture medium such as pH, carbon source, NaCl, and tryptophan concentration strongly influenced the IAA synthesizing capacity of four bacterial isolates. Under the low pH culture medium the IAA synthesizing capacity of the bacterial strains was reduced and increased under high pH culture medium (pH=7 and pH=8). Sucrose was the best carbon source to promote an increase of the IAA synthesis for all four strains. *Bacillus megaterium* MQ-2.5 was considered as the best salt tolerant plant growth promoting bacteria and tryptophan precursors also played an important role in enhancing IAA synthesis by all four strains. All four bacterial strains in this study emerged as potential alternatives for IAA production and they could be applied in the greenhouse and field conditions as bio-inoculants for more sustainable field production. In particular, two strains OM-17.2 and CP-18.2 can be used to produce safe biological IAA products to replace synthetic IAA used widely in agriculture.

ACKNOWLEDGEMENTS

This research was funded by Can Tho University Upgrade Project VN14-P6 with an ODA-A7 loan from the Japanese Government.

REFERENCES

Ahmad F, Ahmad I, Khan MS. Indole acetic acid production by the indigenous isolates of *Azotobacter* and *Pseudomonas fluorescent* in the presence and absence of tryptophan. Turkish Journal of Biology 2005;29(1):29-34.

Ahmad F, Ahmad I, Khan MS. Screening of free-living rhizospheric bacteria for their multiple plant growth promoting activities. Microbiological Research 2008;163(2):173-81.

Alfonso FC, Vigueras-Ramírez G, Rosales-Colunga LM, Monte-Martínez A, Hernández RO. Propionate as the preferred

carbon source to produce 3-indoleacetic acid in *B. subtilis*: Comparative flux analysis using five carbon sources. Molecular Omics 2021;17:554-64.

Badawy AA, Alotaibi MO, Abdelaziz AM, Osman MS, Khalil AMA, Saleh AM, et al. Enhancement of seawater stress tolerance in barley by the endophytic fungus *Aspergillus ochraceus*. Metabolites 2021;11:Article No. 428.

Bharucha U, Trivedi UB, Patel K. Optimization of indole acetic acid production by *Pseudomonas putida* UB1 and its effect as plant growth-promoting rhizobacteria on Mustard (*Brassica nigra*). Agricultural Research 2013;2(3):215-22.

Bhutani N, Maheshwari R, Negi M, Suneja P. Optimization of IAA production by endophytic *Bacillus* spp. from *Vigna radiata* for their potential use as plant growth promoters. Israel Journal Plant Science 2018;65(1-2):83-96.

Bric JM, Bostock RM, Silverstone SE. Rapid insitu assay for indole acetic acid production by bacteria immobilized on nitrocellulose membrane. Applied and Environmental Microbiology 1991;57:535-8.

Chandra S, Askaria S, Kumaria M. Optimization of indole acetic acid production by isolated bacteria from *Stevia rebaudiana* rhizosphere and its effects on plant growth. Journal of Genetic Engineering and Biotechnology 2018;16:581-6.

Costacurta A, Vanderleyden J. Synthesis of phytohormones by plant associated bacteria. Critical Reviews in Microbiology 1995;21:1-18.

Defez R, Andreozzi A, Bianco C. The overproduction of indole-3-acetic acid (IAA) in endophytes upregulates nitrogen fixation in both bacterial cultures and inoculated rice plants. Microbial Ecology 2017;74(2):441-52.

Egamberdiyeva D. Alleviation of salt stress by plant growth regulators and IAA producing bacteria in wheat. Acta Physiologiae Plantarum 2009;31:861-4.

Khamna S, Yokota A, Peberdy JF, Lumyong S. Indole-3-acetic acid production by *Streptomyces* sp. isolated from some Thai medicinal plant rhizosphere soils. EurAsian Journal of BioSciences 2010;4:23-32.

Kucuk C, Cevheri C. Indole acetic acid production by *Rhizobium* sp. isolated from Pea (*Pisum sativum* L. ssp. arvense) Bezelye (*Pisum sativum* L. ssp. arvense)'den İzole edilen *Rhizobium* sp. Tarafından İndol Asetik Asit Üretimi. Turkish Journal of Life Sciences 2016;1(1):43-5.

Mandal SK, Mondal KC, Dey S, Pati BR. Optimization of cultural and nutritional conditions for indole-3-acetic (IAA) production by a *Rhizobium* sp. isolated from root nodules of *Vigna mungo* (L.) Helpper. Research Journal of Microbiology 2007;2:239-46.

Manulis S, Shafri RH, Epstein E, Lichter A, Barash I. Biosynthesis of Indole 3-acetic acid via the indole 3-acetamide pathway in *Streptomyces* spp. Microbiology 1994;140:1045-50.

Mehta S, Nautiyal CS. An efficient method for qualitative screening of phosphate-solubilizing bacteria. Current Microbiology 2001;43:51-6.

Mohite B. Isolation and characterization of indole acetic acid (IAA) producing bacteria from rhizospheric soil and its effect on plant growth. Journal of Soil Science and Plant Nutrition 2013;13(3):638-49.

Nakbanpote AW, Panitlurtumpaia N, Sangdeea A, Sakulponea N, Sirisoma P, Pimthong A. Salt-tolerant and plant growth promoting bacteria isolated from Zn/Cd contaminated soil: Identification and effect on rice under saline conditions. Journal of Plant Interactions 2014;32:37-41.

Nghia NK, Tien TTM, Oanh NTK, Nuong NHK. Isolation and characterization of indole acetic acid producing halophilic bacteria from salt affected soil of rice-shrimp farming system in the Mekong Delta, Vietnam. Agriculture, Forestry and Fisheries 2017;6(3):69-77.

Nutaratat P, Amsri W, Srisuk N, Arunrattiyakorn P, Limtong S. Indole-3-acetic acid production by newly isolated red yeast *Rhodosporidium paludigenum*. Journal of General and Applied Microbiology 2015;61:1-9.

Ona O, Impe JV, Prinsen E, Vanderleyden J. Growth and indole-3-acetic acid biosynthesis of *Azospirillum brasilense* Sp245 is environmentally controlled. FEMS Microbiology Letters 2005;246:125-32.

Patten CL, Glick BR. Role of *Pseudomonas putida* indo lactic acid in development of the host plant root system. Applied and Environmental Microbiology 2002;68:3795-801.

Sachdev DP, Chaudhari HG, Kasture VM, Dhavale DD, Chopade BA. Isolation and characterization of indole acetic acid (IAA) producing *Klebsiella pneumonia* strains from rhizosphere of wheat (*Triticum aestivum*) and their effect on plant growth. Indian Journal of Experimental Biology 2009;47:993-1000.

Sarkar A, Ghosh PK, Pramanik K, Mitra S, Sorent, Pandey S, et al. A halotolerant *Enterobacter* sp. displaying ACC deaminase activity promotes rice seedling growth under salt stress. Research in Microbiology 2018;169:20-32.

Scarcella ASA, Junior RB, Bastos RG, Magri MMR. Temperature, pH and carbon source affect drastically indole acetic acid production of plant growth promoting yeasts. Brazilian Journal of Chemical Engineering 2017;34(02):429-38.

Shanti M, Keshab C, Dey S. Optimization of cultural and nutritional conditions for indole acetic acid production by a *Rhizobium* sp. isolated from root nodules of *Vigna mungo* (L.) Hepper. Research Journal of Microbiology 2007;2:239-46.

Shokri D, Emtiazi G. Indole-3-acetic acid (IAA) production in symbiotic and non-symbiotic nitrogen-fixing bacteria and its optimization by Taguchi design. Current Microbiology 2010;61(3):217-25.

Sirivastava A, Singh A. Plant growth promoting rhizobacteria (PGPR) for sustainable agriculture. International Journal of Agricultural, Science and Research 2017;7(4):2250-321.

Smith H. Phytochromes and light signal perception by plants: An emerging synthesis. Nature 2000;407:585-91.

Kumari S, Prabha C, Singh A, Kumari S, Kiran S. Optimization of indole-3-acetic acid production by diazotrophic *B. subtilis* DR2 (KP455653), isolated from rhizosphere of *Eragrostis cynosuroides*. International Journal of Pharma Medicine and Biological Sciences 2018;7(2):20-7.

Sridevi M, Yadav NCS, Mallaiah KV. Production of indole acetic acid by *Rhizobium* isolates from *Crolatariaspecies*. Research Journal of Microbiology 2008;3(4):276-81.

Stinner DH. The science of organic farming. In: Lockeretz W, editor. Organic Farming: An International History. Oxfordshire, UK and Cambridge, Massachusetts: CAB International; 2007. p. 978-1000.

Suliasih, Widawati S. Isolation of Indole Acetic Acid (IAA) producing *Bacillus siamensis* from peat and optimization of the culture conditions for maximum IAA production. IOP Conference Series: Earth and Environmental Science (The 9th International Symposium for Sustainable Humanosphereer) 2020;572:12-25.

Swain MR, Naskar SK, Ray RC. Indole 3-acetic acid production and effect on sprouting of yam. (*Dioscorea rotundata* L.)

minisetts by *Bacillus subtilis* isolated from culturable cowdung microflora. Polish Journal of Microbiology 2007;56:103-10.

Tewari S, Arora NK. Multifunctional exopolysaccharides from *Pseudomonas aeruginosa* PF23 involved in plant growth stimulation, biocontrol and stress amelioration in sunflowers under saline conditions. Current Microbiology 2014;69(4): 484-94.

Wagi S, Ahmed S. *Bacillus* spp.: potent microfactories of bacterial IAA. Peer Journal 2019;7:e7258.

Willey JM, Sherwood LM, Woolverton CJ. Prescott's Principles of Microbiology. New York, USA: McGraw-Hill; 2009.

Xa LT, Nghia NK. Isolation and selection of biological nitrogen fixing and indole-3-acetic acid synthesizing bacteria from different cropping systems in Soc Trang Province, Vietnam. International Journal of Innovative Studies in Sciences and Engineering Technology 2019;5(11):15-23.

Adaptiveness to Enhance the Sustainability of Freshwater-Aquaculture Farmers to the Environmental Changes

Anawach Saithong[1], Suvaluck Satumanatpan[2*], Kamalaporn Kanongdate[2], Thiyada Piyawongnarat[3], and Poonyawee Srisantear[4]

[1]United Nations Development Programme, United Nations Building, Rajdamnern Nok Avenue, Bangkok 10200, Thailand
[2]Faculty of Environment and Resource Studies, Mahidol University, Nakhon Pathom 73170, Thailand
[3]Research, Innovation and Partnership Office, King Mongkut's University of Technology Thonburi, Bangkok 10140, Thailand
[4]Foundation for Environmental Education for Sustainable Development (Thailand), Bangkok 10900, Thailand

ARTICLE INFO

Received: 5 Nov 2021
Received in revised: 1 Feb 2022
Accepted: 6 Feb 2022
Published online: 22 Feb 2022
DOI: 10.32526/ennrj/20/202100217

Keywords:
Adaptation/ Perception/ Aquaculture satisfaction/ Freshwater farmers, Thailand

*** Corresponding author:**
E-mail:
suvaluck.nat@mahidol.ac.th

ABSTRACT

Two alternative physical adaptations of freshwater-aquaculture farmers were observed along the upstream Bangpakong Watershed, Thailand. First was the modification of aquaculture types: (1) completely changing former species to others; (2) mixing freshwater prawn with current cultured species; (3) mixing fish with *L. vannamei*, and second was the direct reaction to environmental changes, including adding freshwater into cultured ponds to reduce temperature and dilute salt concentration; modifying pond-depth; aeration application; and reducing the amount of food or net covering on the water surface during flooding. Principal component analysis revealed that four key components (Options, Learning, Competitiveness, and Plan) reflected the perceived adaptive capacity of farmers to environmental changes. However, culture types have no significant effect on these four components. Farmers with an alternative source of income and practicing monoculture fish farming tend to have a greater ability to change occupation. Old age and more extended experience in aquaculture indicated a low ability to change occupation. The well-educated farmers and farmers who preferred to pass on aquaculture occupation to their children showed higher ability to learn and adapt, but this is not the case for older farmers. Thus, understanding the adaptations of the farmers may assist in promoting appropriate development programs based on their contexts as well as helping decision-makers to have a better plan for strengthening their adaptive capacities based on their perceptions.

1. INTRODUCTION

The frequency and severity of environmental changes may lead to uncertainty in aquaculture production (Handisyde et al., 2017; Lazard, 2017) and likely to a decline in freshwater-aquaculture production in Thailand (Department of Fishery, 2019). Over the past two decades, aquaculture production at the global scale and in Asia has shown an increasing trend (FAO, 2017), which indicates upward demand in the future. On the other hand, adaptation to environmental changes of aquaculture farmers as food producers could be another dimension of food security of concern that needs to be studied. Especially, important are freshwater farmers that play a role in stabilizing the food supply as the primary protein source of reasonable price that tends to be easily accessible. Most of the aquaculture production on the global scale tends to be concentrated in Asian countries (Dubey et al., 2017), especially China, India, and Southeast Asian countries, with their combined production projected to reach 93.6 million tons by 2030 (The World Bank, 2013).This may lead to uncertainty in sustainability and food security with regards to accessibility of protein sources. In addition, unusual average annual precipitation and temperature related to climate change has affected environmental conditions around Thai Bay. This includes the Bangpakong Watershed, which comprises Nakhon Nayok River and Prachinburi River as dominant freshwater zones, and the Bangpakong River, which

Citation: Saithong A, Satumanatpan S, Kanongdate K, Piyawongnarat T, Srisantear P. Adaptiveness to enhance the sustainability of freshwater-aquaculture farmers to the environmental changes. Environ. Nat. Resour. J. 2022;20(3):288-296. (https://doi.org/10.32526/ennrj/20/202100217)

serves as a brackish water zone. During the dry season (1st November to 30th April), salt intrusion spreads landward a long distance from the Bangpakong River to the freshwater areas in Nakhon Nayok and Prachinburi Rivers, resulting in salinity increasing over 0.5 ppt. Whereas, during the wet season (1st May to 31st October), a high amount of freshwater spread from Nakhon Nayok and Prachinburi Rivers to Bangpakong River results in salinity decreasing by around 0.5-5.0 ppt. Specifically, flooding is known to cause significant loss in shrimp production (Lebel et al., 2019; Seekao and Pharino, 2016a; Seekao and Pharino, 2016b). Thus, adaptation to environmental changes by freshwater-aquaculture farmers (called "farmers" in this paper) is increasingly becoming an important key for sustaining their livelihood, income generation, and food security in this sector. In this study, two forms of adaptation are described: physical adaptation and perceived adaptive capacity. The farmers were interviewed along the upstream of the Bangpakong Watershed (Nakhon Nayok province) where the salinity of the freshwater in the main river fluctuates periodically depending on the magnitude of saltwater intrusion (Srisurat, 2020). The farmers were hypothesized to have a variety of adaptations and likely have different perceptions on their adaptation capacities. Basically, these farmers, to some extent, have learned and adapted from time to time. For instance, they tend to preferentially culture Pacific White Shrimp (*Litopeneaus vannamei*) instead of *Penaeus monodon* due to its higher tolerance to diseases (Wyban, 2007) and high salinity from salt intrusion and may be a benefit derived for the farmers. Nevertheless, this shrimp species is still prone to many diseases during unfavorable conditions (Zhou et al., 2010; Han et al., 2018; Xu et al., 2021; Estrada-Cárdenas et al., 2021), causing farmers to change to other species or different aquatic fauna for culturing.

Most studies have focused on the physical adaptations of farmers, whereas few studies (e.g., Lebel et al., 2018) have focused on the perceived adaptive capacity of farmers. For instance, Lebel et al. (2018) revealed short-term reactions, seasonal tactics, and long-term adaptation strategies for fish farmers in northern Thailand in order to manage climate-related risks and market risks. Lebel et al. (2021) suggested that the perception of fish farmers against climate-related risks is also vital and indicated that wealthier and more educated farmers in the Mekong Basins tend to have better adaptive strategies for dealing with current risks. Thus, perceptions are a relatively strong factor that influences the motivation of farmers to adapt to environmental changes based on their history of understanding situations and experience in management practices. This study provides more insight into the adaptation and perceived adaptive capacity of the farmers in this area to cope with environmental changes and to maintain security of food production to meet the needs of the country. The objective of this study was to investigate farmers' adaptation (physical adaptation) and their perceived adaptive capacity (perspective of "how to adapt") against environmental changes due to saltwater intrusion, flood, drought, and fluctuation in temperature.

2. METHODOLOGY

Study participants were selected from households in four districts of Nakhon Nayok Province, located in central Thailand. The areas along Nakhon Nayok River were claimed as suitable for freshwater aquaculture, but marine intrusion was observed to affect these areas. Aquaculture activities observed around the study area consisted of monoculture of fish, monoculture of White-Leg Shrimp (*L. vannamei*), polyculture between *L. vannamei* and Freshwater Prawn (*Macrobrachium rosenbergii*), polyculture between fish and *L. vannamei* or *M. rosenbergii*, and polyculture fish (Figure 1). There are no complete lists of names and addresses of farmers in the study areas. Hence, snowball sampling and purposive representative sampling were applied from one farm to other farms with a minimum of 30 cases of each culture type existing in the study areas (i.e., monoculture of *L. vannamei*, monoculture fish, polyculture fish, polyculture between *L. vannamei* and *M. rosenbergii*, and polyculture between fish and *L. vannamei*) (Pollnac and Crawford, 2000). We sampled a total of 206 cases, which were statistically sufficient to represent a surrogate of farmers in the study sites. Face-to-face interviews were conducted from March 2017 to January 2018, using a semi-structured questionnaire approved by the Central Institutional Review Board of Mahidol University.

2.1 Dependent variables, independent variables, and data analysis

Adaptation was measured in two forms: (1) physical adaptation was observed and farmers were interviewed with open end questions on how frequently they adapt to changes or stresses using

descriptive explanations that directed reactions to environmental stresses including salinity change, drought, flood, and fluctuation in water temperature; (2) perceived adaptive capacity on the changes: farmers were asked to indicate their level of agreement with 12 variables (Supplementary data) modified from Marshall and Marshall (2007). A 4-level Likert scale ranging from strongly disagree to strongly agree was applied to measure these variables. This study used the same scales suggested by Marshall and Marshall (2007). In this case, a mid-point was not comparable after data analysis.

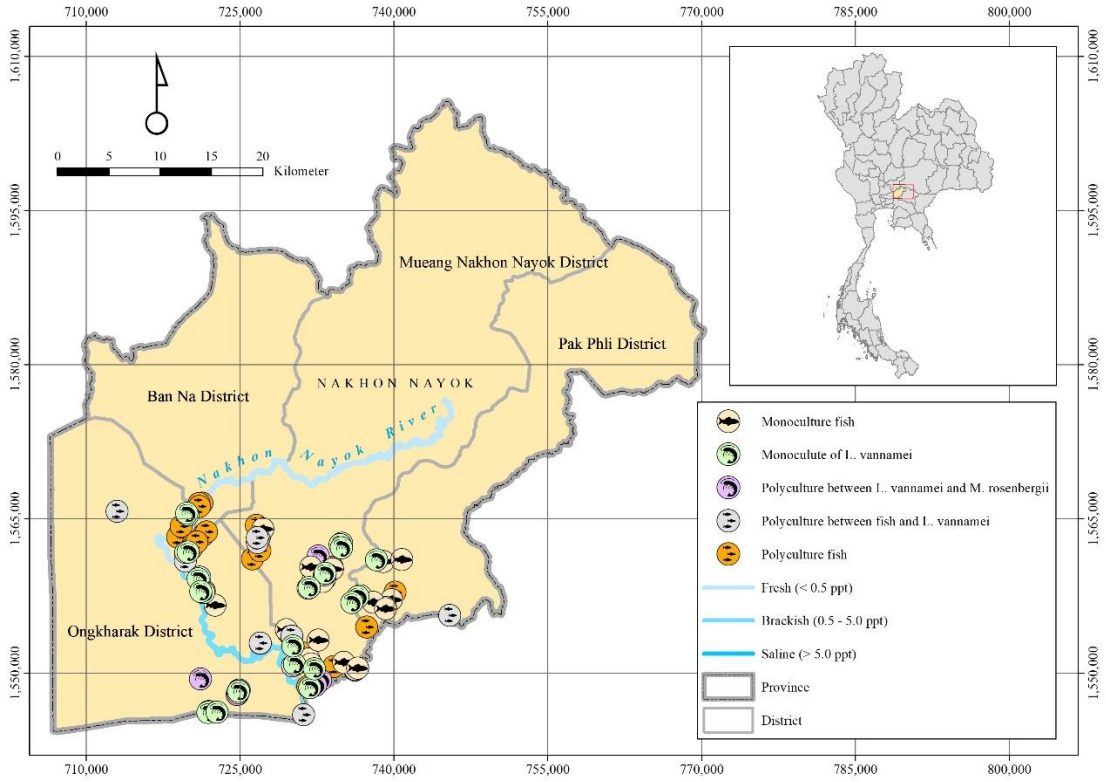

Figure 1. Distribution of existing aquaculture activities around Nakhon Nayok Province

Another set of questions was used to gather demographic information (i.e., age, education, aquaculture experience, household size, gender, religion, number of kin involved in aquaculture, marital status, aquaculture ownership, type of aquaculture, official registration, income from aquaculture, satisfaction with income, climate change awareness, and job satisfaction). These were variables related to perceived adaptive capacity.

Descriptive results on physical adaptation of farmers were provided with regard to the classification of aquaculture types and the grouping of environmental stresses. The perceived adaptive capacity was analyzed using Principal Component Analysis (PCA). The relationship between dependent and independent variables was analyzed using Pearson's correlation (Freedman et al., 2007) and Student's t-test (Kalpić et al., 2011). Statistical software, SPSS version18 was used for the analysis.

3. RESULTS AND DISCUSSION

3.1 Demographic results

Based on a total of 206 respondents, the male: female ratio was close to 1:1 (56.8% male). Most respondents were married (91.7%). The average age and education level was 53.3±12.9 and 6.9±4.1 years, respectively. Households had an average of four members. Respondents had an average of 13.9±8.5 year-experiences in aquaculture. On average, one person in each household assisted in aquaculture. Most of them (81.6%) shared that they have relatives engaged in aquaculture. About 60.7% of respondents depended on income not only from aquaculture but also other jobs such as farming, employment, trading, and raising animals.

When asked for opinions on income, it was found that most respondents earned enough income to cover their family's food expenses (51.9%), family expenses (50.4%), children education (52.4%), and

36.4% had insufficient income to save for future necessities. Respondents said they had uncertain income in each production cycle. For instance, making profits in some years, and losses in other years. Thus, they do not have enough money to save. In addition, some had debts from the mega-flood disasters in 2011 and 2013 that resulted in huge losses of aquaculture profits. Concerning the opinions on job satisfaction, most farmers (94.7%) were satisfied with aquaculture and willing to continue it in the future. About 53.4% of respondents agreed with recommending their children to pursue working in aquaculture because they already have land and they have experience to pass on, while 27.7% said they do not want their children to work in aquaculture, because it is a difficult and high-risk career. They wanted their children to have a good education and pursue other occupations to gain more stable income. About 18.9% did not know whether they should or should not recommend their children to do aquaculture.

3.2 Physical adaptation to environmental stresses

The majority of respondents owned farms (94.7%) and were observed having two alternatives of physical adaptation: (1) three modifications of aquaculture type, and (2) direct reaction to environmental changes (salt intrusion, drought, flood, and water temperature change).

The three modification of aquaculture type for adaptation were classified as

(A) Modification by completely changing the former species to others: The complete conversion from monoculture of *L. vannamei* to polyculture fish was mentioned, which has higher resistance to diseases and environmental changes. Polyculture fish reduces the risk of diseases through feeding behaviors of different kinds of species throughout the aquaculture system. Waste elimination leads to the better water quality and environmental conditions resulting in preventing diseases. The polyculture fish was observed for 37.9% of the farmers, while monoculture *L. vannamei* was observed for 24.3% of the farmers. Nevertheless, the observed 37.9% does not represent all of the farms converted from monoculture of *L. vannamei*.

(B) Modification by mixing Freshwater Prawn (*M. rosenbergii*) with former cultured species: The polyculture between *M. rosenbergii* and *L. vannamei* was observed for 18% of the aquaculture farms. Among these farms there were some that had converted from monoculture *L. vannamei*. In this case, farmers tend to have less risk of potential loss of entire profits by selling *M. rosenbergii* in situations where there is loss in yield of *L. vannamei* owing to adverse environmental impact. In addition, polyculture between *L. vannamei* and *M. rosenbergii* resulted in higher yield compared to a monoculture of *L. vannamei,* which seems consistent with that reported by Chuchird et al. (2009) for Ratchaburi Province.

(C) Modification by mixing fish with *L. vannamei*: The culture mixing between polyculture fish and *L. vannamei* was observed in 20.4% of the farms. In this modification type, farmers did not want to mention the former species they cultured before conversion. Probably, the farmers were suspicious about the rationale behind the question, and thus unwilling to share the details of the previously cultured species. Farmers can harvest *L. vannamei* 2-3 times per one harvest of the polyculture fish, providing them with additional income. This observation is in line with Dailynews (2015) for polyculture between Tilapia and *L. vannamei* in Chonburi Province where the farmers harvested *L. vannamei* every 2-3 months during 10 months of Tilapia culturing and earned income higher than usual (the price of *L. vannamei* was 250 Baht/ kg vs. Tilapia 35-40 Baht/kg in 2015).

Other culture types which do not fall into the three modification types mentioned above were also observed. These other farms had various monoculture fish (i.e., Fry Catfish 12.1%; Red Tilapia 5.8%, Catfish 3.4%, Tilapia 3.4%, Snapper 1%, and others 0.5%) that were not related to adaptation strategies in this area.

Among these three types of modification around 59.2% were semi-intensive, including polyculture fish, polyculture fish with *L. vannamei*, and monoculture of Fry Catfish. Approximately 40.3% were intensive; monoculture of *L. vannamei*, polyculture between *L. vannamei* and *M. rosenbergii*, and Red Tilapia fish cages. A minority of farmers (0.5%) applied extensive culture.

In terms of direct response to the environmental changes, respondents revealed adjustment of environmental conditions when facing undesirable stresses (salt intrusion, drought, flood, high and low water temperature) in several ways. A common method applied against environmental stresses was adding freshwater into the ponds but not in the case of low water temperature. Aeration increase was also

commonly applied against flooding and temperature changes. Details of adaptations are as follows.

During periods of salt intrusion, salinity in the ponds also increased through pipelines or outlets. All types of aquacultures would pump freshwater into the culture ponds. For the *L. vannamei* culture, farmers pumped saltwater out of the ponds then diluted the salt concentration in the ponds with freshwater and controlled the salinity to not exceed 10 ppt. In some cases, farmers would change from culturing *L. vannamei* to Sea Bass fish during the period of high salinity in the river and later change back to the former culture type. The results were in line with De Silva and Soto (2009) who reported that farmers have an adaptive strategy during salt intrusion by shifted stenohaline species to euryhaline species to reduce costs, and Cruz (2016) who reported that a mono-sex Tilapia fish was an alternative to culture of Tiger shrimps during unfavorable conditions.

For the drought condition, the first mechanism for response in all aquaculture types was the pumping of freshwater from storage ponds into culture ponds. Read (2007) and De Silva and Soto (2009) also suggested that rainwater storage, dry-plant covering on water surface, regular maintenance of a pond structure, and keeping deeper pond depths can help prevent the loss in aquaculture production during drought conditions. However, this is different from the culture of Fry Catfish and Red Tilapia in cages, which in this study, farmers tended to temporarily stop culturing due to unsuitable water content consistent with the findings of Flaherty et al. (1999).

During flooding, all aquaculture types use nets to cover the ponds and increase the pond dikes to prevent aquatic animals from slipping into the flooded water similar to that observed by other studies (Shameem et al., 2015; Seekao and Pharino, 2016a; Seekao and Pharino, 2016b), whereas covering discharge pipe outlets with a net was applied with the culture of Giant Catfish (Teongphukeao, 2012). Some farms may harvest before the planned schedule (Shameem et al., 2015). In addition, running water could have been changed temporarily to stagnant water during flooding that caused low oxygen. Thus, increasing aeration would be applied. Those who cannot afford any prevention would have changed species or culture methods after flooding (Nguyen et al., 2015). Aside from the flooding, storm surge in some areas can adversely affect water quality in the culture ponds (Ahmed and Diana, 2015) and raise water levels higher than usual, so almost the same techniques used during flooding are also applied.

Water temperature change, both high and low degrees affected adaptation of farmers differently. All aquaculture types pumped freshwater from storage ponds into culture ponds when water temperature increased, but not during the low temperature. Instead, they reduce the amount of food and feeding time during cold conditions due to the low rate of shrimp metabolism and to prevent anoxia conditions caused by food waste at the bottom of the ponds. These adaptations were different from a reported common technique elsewhere which is to modify the depth of a pond to be deeper than usual, especially in shrimp farms (Shameem et al., 2015). In our studies, farmers would increase aeration during both high and low temperatures for the culture type of monoculture *L. vannamei*, and polyculture between *L. vannamei* and *M. rosenbergii* that can reduce the heat and prevent stratification of water temperature. In other studies, farmers adopt the higher tolerant species instead of providing aeration (De Silva and Soto, 2009). Another adaptation technique observed in our studies to reduce the heat was to pave straws in the ponds on the water surface.

3.3 The perception and perceived adaptive capacity to environmental changes

Most farmers (93.7% of total respondents) were aware of climate change and perceived that, over the past 10 years, climate change may have had an impact and threatened aquaculture production through several changes. However, farmers' perception on the stresses that most affect aquaculture production were salinity increase (55.3%), drought (54.9%), and flood (51.5%), respectively. This was followed by increasing water temperature in the hot season (44.7%), decreasing water temperature in the winter season (40.3%), water pollution (23.3%), first rainfall (22.2%), water acidification (19.9%), increasing rainfall (10.7%), climate variability (6.3%), and air pollution (5.8%), respectively.

The PCA with varimax rotation of the 12 variables resulted in four components, explaining 65.74% of the variance in the dataset (Table 1). The components were named "Options" (opportunities and confidence to get work elsewhere), "Learning" (change work, cope with small changes, more likely to adapt, and learn new skills), "Competitiveness" (can survive more changes, things will turn out well) and "Plan" (plan for finance security and competitive),

based on the content of variables loading highest on the component, a common practice associated with the use of this technique. The "Options" component explained 24.46% of the variance in the dataset, followed by "Learning", "Competiveness", and "Plan" (18.82%, 12.82% and 10.24%, respectively) (Table 1). These four components were used as indicators of farmers perceived adaptive capacity to deal with the future changes. In this study, the "Plan" component explained the least variance in perceived adaptive capacity of farmers. However, the higher the plan perception, the better planned farming that contributes to improve *L. vannamei* farmers' benefits in the south and east of Thailand (Sanrak, 2010). For instance, using good quality breeders as one of the farming plans could be one alternative of the adaptation methods (Boonstra and Hanh, 2015).

Table 1. Components as indicators illustrate perceived adaptive capacity of the farmers

Items	Components			
	Options	Learning	Competitiveness	Plan
Confident to get work elsewhere	**0.888**	0.203	0.139	0.100
Many options available	**0.852**	-0.062	0.034	0.008
Not nervous trying something else	**0.820**	0.167	0.089	0.018
Not too old to find work elsewhere	**0.748**	0.386	0.087	0.098
Plan to make change work for me	-0.005	**0.779**	0.227	0.068
Can cope with small changes	0.170	**0.719**	0.039	0.108
More likely to adapt to change than others	-0.072	**0.624**	0.173	0.307
Interested in learning new skill	0.303	**0.554**	-0.063	-0.093
If more changes will survive	0.222	-0.011	**0.868**	0.077
Confident things will turn out well	0.031	0.302	**0.813**	-0.069
Planned for financial security	0.111	-0.039	-0.008	**0.799**
Competitive enough to survive much longer	0.019	0.306	0.012	**0.664**
Percent total variance	24.46**%**	18.22%	12.82%	10.24%

3.4 Factors influencing perceived adaptive capacity

Demographic information on farmers age, years of aquaculture experiences, and education level averaged 53.3±12.9, 13.9±8.5, and 6.9±4.1 years, respectively. These are the three main variables that tend to affect farmers perceived adaptive capacity and seem to be consistent with other studies (Satumanatpan and Pollnac, 2020; Satumanatpan and Pollnac 2017). The older adults have lower ability to work ($r=-0.249$, $p<0.01$) and learn ($r=-0.222$, $p<0.01$) compared to the younger ones. In addition, the results indicate that farmers engaged in aquaculture for a longer period of time tend to have significantly less adaptation with regards to other forms of occupation ($r=-0.157$, $p<0.05$). Gender (more males than females), marital status (most married 91.7%), and family members engaged in aquaculture (averaged four per household) appear to have no significant influence on perceived adaptive capacity of farmers.

Farmers with higher education level had the ability to learn and adjust better than those with lower education ($r=0.299$, $p<0.01$) implying higher perceived adaptive capacity. This seems to be in line with Rattanadechakorn (2012) who suggested that local fishermen who have higher indigenous wisdom may have better adaptive strategies of survive and thus, tend to lower their vulnerability to seasonal alteration in climatic conditions. In addition, the good knowledge on environmental changes may enhance perceived adaptive capacity. This could be explained with the study of Sanrak (2010) who suggested that farmers of *L. vannamei* in southern and eastern Thailand tend to have higher production and earn more profits through sharing of knowledge and experience.

Aquaculture types have no significant effect on the four components of the perceived adaptive capacity (Table 2) that were compared between monoculture of *L. vannamei* vs monoculture fish (Part B1), monoculture *L. vannamei* vs polyculture between *L. vannamei* and *M. rosenbergii* (Part B3), polyculture fish vs polyculture fish with *L. vannamei* (Part B4). However, an indication of small effect (effect size=0.028) revealed that the monoculture fish perceived higher ability on work options than the polyculture fish (Table 2 part B2, $t=1.997$, $p<0.05$).

Farmers who earned income only from aquaculture (39.3%) have significantly lower flexibility in work options than those having income from both aquaculture and other occupations (Table 2 Part A, t=-3.883, p<0.01). Diverse alternative incomes were also reported as one significant adaptation option of rice and fish farming households in Vietnam (Tri et al., 2019), and for small-scale fishermen in Thailand (Satumanatpan and Pollnac, 2020; Satumanatpan and Pollnac, 2017; Tongpli, 2011).

Analysis of aquaculture satisfaction towards adaptation (Table 2 Part C), indicates significantly higher ability to learn and adapt (*Learning* component) among those who prefer their children to continue aquaculture (effect size=0.073, t=3.265, p<0.05). Probably, their perceived adaptive learning could help them overcome any problems and enable their children to also learn how to adapt. Moreover, most of them already owned well equipped farms, thus they likely felt learning and adaptation could be an easy task. In contrast, those who did not advise their children to continue aquaculture, raised concerns that they were unable to cope with environmental stresses and felt difficulties with their own jobs, i.e., working hard, risky, and uncertain income. In this respect, the *Learning*-perceived adaptive capacity of the farmers seems to be in line with Lebel et al. (2021) who suggested that wealthier and more educated farmers could better deal with current risks related to climate change as well as recognizing the need for adaptation strategies for future changes in climate. Finally, official registration as being freshwater-aquaculture farmers with the fishery provincial office did not influence the level of perceived adaptive capacity. Farmers indicated that they did not receive assistance when they encountered stress.

Table 2. The t-test analysis between independent and dependent variables

Part	Independent variables	Values	Dependent variables			
			Options	Learning	Competitiveness	Plan
A	Income aquaculture vs income aquaculture +	t	-3.883	1.651	-1.025	-1.661
	others	P	0.000**	0.100	0.307	0.098
B1	Monoculture of *L.vannamei* vs Monoculture fish	t	-0.455	0.239	1.488	-0.109
		P	0.649	0.811	0.138	0.913
B2	Monoculture fish vs Polyculture fish	t	1.997	0.144	0.539	0.668
		P	0.048*	0.886	0.591	0.506
B3	Monoculture *L.vannamei* vs Polyculture of	t	-1.253	0.336	-0.832	1.579
	L.vannamei and *M. rosenbergii*	P	0.214	0.738	0.408	0.119
B4	Polyculture fish vs Polyculture fish	t	1.004	-0.965	-1.293	-0.195
	with *L. vannamei*	P	0.318	0.337	0.199	0.846
C	Advise vs Not advise to do aquaculture	t	-1.560	3.265	-0.309	0.244
		P	0.121	0.001*	0.758	0.807
D	Registered vs Non-register	t	-0.244	-0.701	0.621	-0.116
		P	0.808	0.484	0.535	0.908

*p<0.05, **p<0.01; Effect size: small=0.01, moderate=0.06, large=0.14;
A (n=81:125), B1 (n=69:137), B2 (n=44:93), B3 (n=38:31), B4 (n=57:36), C (n=110:57), D (n=174:32)

4. CONCLUSION

The study indicates that farmers in Nakhon Nayok Province tends to show different adaptive capacity to environmental changes depending on species-reared, environmental stresses, and their perception. Salt intrusion in the freshwater zone of Nakhon Nayok River appears not to be a major problem for the farmers to modify their aquaculture activities and sustain their livelihoods. However, the marketing mechanism and severe change in environmental conditions drive the farmers to adapt from time to time, which has become natural habits expressed through their physical reactions either by culturing modifications or reacting directly to the specific stresses.

Our findings suggest that understanding adaptations of the farmers should not only be restricted to physical adaptation, but also perceived adaptive capacity which is in part significant to designing aquaculture-development programs. Based on the preference of most respondents, supplemental sources of income are recommended to help farmers sustain their aquaculture practice. In this respect, complete change of job skills is not recommended, instead,

farmers should be trained for upskills, for instance, in polyculture and advanced technology application.

ACKNOWLEDGEMENTS

We are grateful for the funding received from the Agricultural Research Development Agency (ARDA) under the project, development of model for predicting impact of climate change on aquaculture zones and adaptation of aquaculture farmers in the upper Gulf of Thailand year 2016. Besides, we are thankful to the Department of Fishery, Thailand, for the unpublished information on freshwater-aquaculture farmers obtained from the department's data base. Furthermore, we extend our gratitude to Mr. Theerawut Chiyanon for mapping the study site. Finally, we thank Dr. Seth Nii-Annang and Dr. Thomas Neal Stewart for editing the manuscript.

REFERENCES

Ahmed N, Diana JS. Coastal to inland: expansion of prawn farming for adaptation to climate change in Bangladesh. Aquaculture Reports 2015;2:67-76.

Boonstra WJ, Hanh TTH. Adaptation to climate change as social-ecological trap: A case study of fishing and aquaculture in the Tam Giang Lagoon, Vietnam. Environment, Development and Sustainability 2015;17:1527-44.

Cruz A. Swimming toward adaptation with climate-smart aquaculture [Internet]. 2016 [cited 2021 Sep 26]. Available from: https://ccafs.cgiar.org/news/swimming-towards-adaptation-climate-smart-aquaculture#.WCkz4BJ96qA.

Chuchird N, Limsuwan C, Prasertsir S, Limhang K, Supyoudkaew P. Pacific white shrimp (*Litopenaeus vannamei*) culture for maximum profit: Monoculture, mixed culture with giant freshwater prawn (*Macrobrachium rosenbergii*) in low salinity water. Proceedings of the 47th Kasetsart University Annual Conference; 2009 Mar 17-20; Kasetsart University, Bangkok: Thailand; 2009.

Dailynews. Polyculture between *L. vannamei* and Tilapia enhance daily income [Internet]. 2015 [cited 2021 Dec 12]. Available from: https://d.dailynews.co.th/agriculture/292035/ (in Thai).

De Silva SS, Soto D. Climate change and aquaculture: Potential impacts, adaptation, and mitigation. In: Cochrane K, De Young C, Soto D, Bahri T, editors. FAO Fisheries and Aquaculture Technical Paper (530): Climate Change Implications for Fisheries and Aquaculture: Overview of Current Scientific Knowledge. Rome, Italy: Food and Agriculture Organization of the United Nations; 2009. p. 151-212.

Department of Fishery (DOF). Fisheries Statistics of Thailand 2017: No. 9/2019. Thailand: Ministry of Agriculture and Cooperatives; 2019.

Dubey SK, Trivedi RK, Chand BK, Mandal B, Rout SK. Farmers' perceptions of climate change, impacts on freshwater aquaculture and adaptation strategies in climatic change hotspots: A case of the Indian Sundarban delta. Environmental Development 2017;21:38-51.

Estrada-Cárdenas P, Cruz-Moreno D, González-Ruiz R, Perigrino-Uriarte AB, Leyva-Carrillo L, Camacho-Jiménez L, et al. Combined hypoxia, and high temperature affect differentially the response of antioxidant enzymes, glutathione and hydrogen peroxide in the white shrimp *Litopenaeus vannamei.* Comparative Biochemistry and Physiology, Part A 2021;254:Article No. 110909.

Flaherty M, Vandergeest P, Miller P. Rice paddy or shrimp pond: Tough decisions in rural Thailand. World Development 1999;27(12):2045-60.

Food and Agriculture Organization of the United Nations (FAO). The state of world fisheries and aquaculture: Sustainability in action [Internet]. 2017 [cited 2021 Dec 12]. Available from: https://doi.org/10.4060/ca9229en.

Freedman D, Pisani R, Purves R. Statistics (International Student Edition). 4th Ed. New York: W.W. Norton and Company; 2007.

Han SY, Wang MQ, Wang BJ, Liu M, Jiang KY, Wang L. A comparative study on oxidative stress response in the hepatopancreas and midgut of the white shrimp *Litopenaeus vannamei* under gradual changes to low or high pH environment. Fish and Shellfish Immunology 2018;76:27-34.

Handisyde N, Telfer TC, Ross LG. Vulnerability of aquaculture-related livelihoods to changing climate at the global scale. Fish and Fisheries 2017;18(3):466-88.

Kalpić D, Hlupić N, Lovrić M. Student's t-tests. In: Lovric M, editor. International Encyclopedia of Statistical Science. Berlin, Heidelberg, Switzerland: Springer Nature; 2011.

Lazard J. Aquaculture systems facing climate change. Cahiers Agricultures 2017;26(3):Article No. 34001.

Lebel L, Jutagate T, Phuong NT, Akester MJ, Rangsiwiwat A, Lebel P, et al. Climate risk management practices of fish and shrimp farmers in the Mekong Region. Aquaculture Economics and Management 2021:25(4):388-410.

Lebel L, Lebel P, Chitmanat C, Uppanunchai A, Apirumanekul C. Managing the risks from the water-related impacts of extreme weather and uncertain climate change on inland aquaculture in Northern Thailand. Water International 2018;43(2):257-80.

Lebel L, Lebel P, Chuah CJ. Water use by inland aquaculture in Thailand: Stakeholder perceptions, scientific evidence, and public policy. Environmental Management 2019;63:554-63.

Marshall N, Marshall P. Conceptualizing and operationalizing social resilience within commercial fishers in Northern Australia. Ecology and Society 2007;12(1):Article No. 1.

Nguyen AL, Truong MH, Verreth JA, Leemans R, Bosma RH, De Silva SS. Exploring the climate change concerns of striped catfish producers in the Mekong Delta, Vietnam. SpringerPlus 2015;4(1):Article No. 46.

Pollnac R, Crawford R. Assessing Behavioral Aspects of Coastal Resources Use. Coastal Resource Center, Naranganset. Rhode Island: University of Rhode Island; 2000.

Rattanadechakorn J. Roles of Local Wisdom to Reduce Vulnerability of Climate Changes on Artisanal Fishers' Households in Palean Watershed, Trang Province [dissertation]. Technology of Environmental Management, Mahidol University; 2012.

Read P. Aquaculture and Drought. New South Wales, Australia: NSW Department of Primary Industries; 2007.

Sanrak P. The Study of Farm Management and Modelling for Planning the Culturing of *Litopeneaus vannamei* in Thailand [dissertation]. Management of Agro-Industrial Technology, Kasetsart University; 2010 (in Thai).

Satumanatpan S, Pollnac R. Factors influencing the well-being of small-scale fishers in the Gulf of Thailand. Ocean and Coastal Management 2017;142:37-48.

Satumanatpan S, Pollnac R. Resilience of small-scale fishes to declining fisheries in the Gulf of Thailand. Coastal Management 2020;48:1-22.

Seekao C, Pharino C. Key factors affecting the flood vulnerability and adaptation of the shrimp farming sector in Thailand. International Journal of Disaster Risk Reduction 2016a; 17:161-72.

Seekao C, Pharino C. Assessment of the flood vulnerability of shrimp farms using a multicriteria evaluation and GIS: A case study in the Bangpakong Sub-Basin, Thailand. Environmental Earth Sciences 2016b;75(4):Article No. 308.

Shameem MIM, Momtaz S, Kiem AS. Local perceptions of and adaptation to climate variability and change: The case of shrimp farming communities in the coastal region of Bangladesh. Climatic Change 2015;133:253-66.

Srisurat S. Morphological analysis of Bangpakong Watershed using geo-informatics technique. Proceeding of the 12th NPRU National Academic Conference; 2020 July 9-10; Nakhon Pathom Rajabhat University, Nakhon Pathom: Thailand; 2020.

Teongphukeao N. Culturing of Mekong Giant Catfish (*Pangasianodon gigas*) [Internet]. 2012 [cited 2016 May 14]. Available from: http://nuch-and-chan.blogspot.com/2012/01/blog-post_24.html (in Thai).

The World Bank. FISH TO 2030: Prospects for Fisheries and Aquaculture. World Bank Report Number 83177-GLB: Agriculture and Environmental Services Discussion Paper 3; 2013.

Tongpli S. Cost and Beneficial Gain Analysis from *Litopeneaus vannamei* Culturing between Monoculture and Polyculture [dissertation]. Faculty of Business Administration, Rajamangala University of Technology Thanyaburi; 2011 (in Thai).

Tri NH, Choowaew S, Ni DV, Kansantisukmongkol K. Impact of saline intrusion and adaptation options on rice- and fish-farming households in the Mekong Delta of Vietnam. Kasetsart Journal of Social Science 2019;40:427-33.

Wyban J. Thailand's white shrimp revolution: 2021 Global Seafood Alliance [Internet]. 2007 [cited 2021 Dec 10]. Available from: https://www.globalseafood.org/advocate/thailands-white-shrimp-revolution/.

Xu D, Wu J, Sun L, Qin X, Fan X, Zheng X. Combined stress of acute cold exposure and waterless duration at low temperature induces mortality of shrimp *Litopenaeus vannamei* through injuring antioxidative and immunological response in hepatopancreas tissue. Journal of Thermal Biology 2021;100:Article No. 103080.

Zhou J, Wang L, Xin Y, Wang WN, He WY, Wang AL, et al. Effect of temperature on antioxidant enzyme gene expression and stress protein response in white shrimp *Litopenaeus vannamei*. Journal of Thermal Biology 2010;35:284-9.

Water Turbidity Determination by a Satellite Imagery-Based Mathematical Equation for the Chao Phraya River

Wilaiporn Pimwiset[1], Kanita Tungkananuruk[1], Thitima Rungratanaubon[1], Pratin Kullavanijaya[2], and Chalisa Veesommai Sillberg[1*]

[1]Department of Environmental Science, Faculty of Environment, Kasetsart University, Bangkok 10900, Thailand
[2]Excellent Center of Waste Utilization and Management, Pilot Plant Development and Training Institute, King Mongkut's University of Technology Thonburi, Bangkok 10150, Thailand

ARTICLE INFO

Received: 3 Dec 2021
Received in revised: 14 Feb 2022
Accepted: 20 Feb 2022
Published online: 16 Mar 2022
DOI: 10.32526/ennrj/20/202100237

Keywords:
Environmental data and information analysis/ Sentinel-2/ Chao Phraya River/ Statistical analysis/ Remote sensing data analysis

*** Corresponding author:**
E-mail: chali-h@hotmail.com; chalisa.v@ku.th

ABSTRACT

Turbidity is a standard water quality parameter that indicates its optical property in scattering light along the column containing suspended particles. The satellite imagery information of Sentinel-2 and the Chao Phraya River turbidity data from December 2016 to February 2021 was applied to develop a mathematical equation for turbidity determination. This practical and straightforward approach eliminates some constraints of traditional laboratory analysis, which is labour-intensive and time-consuming in monitoring the entire river. Four studied steps were implemented: data pre-processing, correlating analysis of numerical turbidity and satellite image reflectance, developing the mathematic equations for turbidity estimation, and its validation of use. Four different bands (B2, B3, B4, and B8) and three selection methods were investigated; single-band, combination band, and ratio band. The obtained results depicted that the reflectance of B4 in the single-band process promoted the highest correlation with turbidity compared to the others. The reflectance in visible wavelengths increased when the turbidity of river water increased, particularly B4. The mathematical power equation was a more suitable function for evaluating turbidity than linear regression, quadratic, and exponential functions. A similar concentration was obtained for measured and estimated turbidity in the validation. This finding demonstrated the potential application of remotely sensed data to estimate river water turbidity with high capability and accuracy that adequately supports spatial data continuity acquisition.

1. INTRODUCTION

The Chao Phraya River is the main river of Thailand that begins in the North and flows through the central provinces, including Phra Nakhon Si Ayutthaya, Pathum Thani, Nonthaburi, and Bangkok, and exits into the Gulf of Thailand at Samut Prakan. The river is an essential resource of raw water for various usages along its waterways; water for daily consumption, industrial processes, livestock farming, and conserving ecosystems downstream. The quality of the Chao Phraya River's water is reflected in its relative contamination and proportion that affects sequentially human health and aquatic life involved (Sillberg et al., 2021). Therefore, the entire monitoring of river water quality is essential in developing its usage efficiently and cost-effectively delivering to end-users.

A standard water parameter that reflects its optical quality and is commonly used in water supply processes is turbidity. This parameter can easily be visualized for the initial assessment. The turbidity is the light scattering and absorbing property of water when containing suspended solids and colloidal matters, i.e., clay, silt, planktons, and other organisms (Mulliss et al., 1996). The high turbidity of river water is often found after heavy rain, run-off water and flooding (Marina et al., 2020). This high turbidity in water resources limits light transmission and dissolved oxygen, impacting consequently aquatic plants and animals (Güttler et al., 2013). Turbidity also affects

Citation: Pimwiset W, Tungkananuruk K, Rungratanaubon T, Kullavanijaya P, Sillberg CV. Water turbidity determination by a satellite imagery-based mathematical equation for the Chao Phraya River. Environ. Nat. Resour. J. 2022;20(3):297-309. (https://doi.org/10.32526/ennrj/20/202100237)

water supply systems by increasing the use of chemical agents and the amount of sludge generated. This contamination increases costs due to a higher concentration of suspended solids in raw water (Gikas and Tchobanoglous, 2009). Monitoring and evaluating turbidity are essential to perform regularly or map the waterway entirely (Alvado et al., 2021). However, the turbidity concentration is assessed experimentally using the traditional gravimetric method (Pavelsky and Smith, 2009). This chemical and indirect measurement method is helpful for point or spot information, but several aspects such as time-consumed, skilled-labour need, and cost must be considered when river water quality measurements encompass the entire distribution over a specified time (Giardino et al., 2001).

In recent years, a remote sensing data-based application is considered a beneficial method that provides significant syntrophic coverage to comprehensive information that can be applied practically to water quality monitoring. It offers direct contactless survey data from aerial and satellite images to estimate the turbidity and is used in many applications, i.e., water usage planning, water quality tracking, and situation assessment (Yunus et al., 2020). Remote sensing technology is an alternative method to assess the turbidity that increases the efficiency of measuring and assessing water quality along a river from gathering a wide range of data. This method reduces time and human resources for data collection with up-to-date information provided (Acharya et al., 2018). Several studies used remote sensing-based imagery to develop mathematical equations for water quality prediction. Various linear and nonlinear regression equations have been applied (Elhag et al., 2019; Li et al., 2020). This study applied remotely sensed multispectral satellite image reflection to develop a mathematical equation for estimating turbidity in the lower part of the Chao Phraya River. Four different mathematic functions and three expression processes of Sentinel-2 satellite imagery were systematically studied.

2. METHODOLOGY

The mathematical equation for the determination of water turbidity was developed based on the surface reflectance of remote sensing data. Satellite images were studied to determine their correlation to the experimental turbidity data set of the Cho Phraya River. Processes were implemented in four steps; (1) pre-processing of satellite image and numerical data, (2) analysis of the relationship between turbidity data and satellite image data, (3) developing mathematical equations for estimation of turbidity in the river, and (4) validating the obtained equations for estimation of turbidity entirely for the river. In Figure 1, the system design method of this study is summarized.

2.1 Source of data

Two datasets were used as input sources: satellite image and measured turbidity data. The satellite image data source was the Sentinel-2 satellite of the European Space Agency. The Sentinel-2 images (https://www.sentinel-hub.com/) were in wavelengths between 496.6-835.1 nm, specifically Band 2-Blue (B2), Band 3-Green (B3), Band 4-Red (B4), and Band 8-NIR (B8). These bands are in the visible and near-infrared spectrum, and their sensitivity appropriation to reflect suspended solids causing turbidity of river water has been reported (Neukermans et al., 2012). The scattering ability of bands was found relatively high even in clear, turbid, and chlorophyll-rich water (Gohin et al., 2020). Specifically, the red region was reported increase when sediment concentrations in the water or turbidity increased (Caballero et al., 2019). In this study, the used spatial resolution was at 10 meters. These satellite image data were collected in 29 scenes from December 2016 to February 2021. The data were used differently as input data for equation development and validation, respectively; data from December 2016 to December 2020 was used for developing mathematical equations and February 2021 for validating the process. The criteria from images data collection are specific times and locations. The selected images were recorded simultaneously as automatically measured turbidity data strictly, or less than 10 min differently, when no exact image matched each paired data.

The turbidity data of the Chao Phraya River was sourced from the water quality information system (https://rwater.mnre.go.th/) of the Office of the Environment Region 1-16, Phase 2; and automatic water quality measurement stations (http://rwc.mwa.co.th/page/home/) from the real-time water quality monitoring system of the Metropolitan Waterworks Authority. These measured turbidity data are automatic measurements from the monitoring station. There is a cycle of recording data in real-time every 10 min, following the Pollution Control Department criterion to measure the water source class 3. The level installation of the water quality sensor at

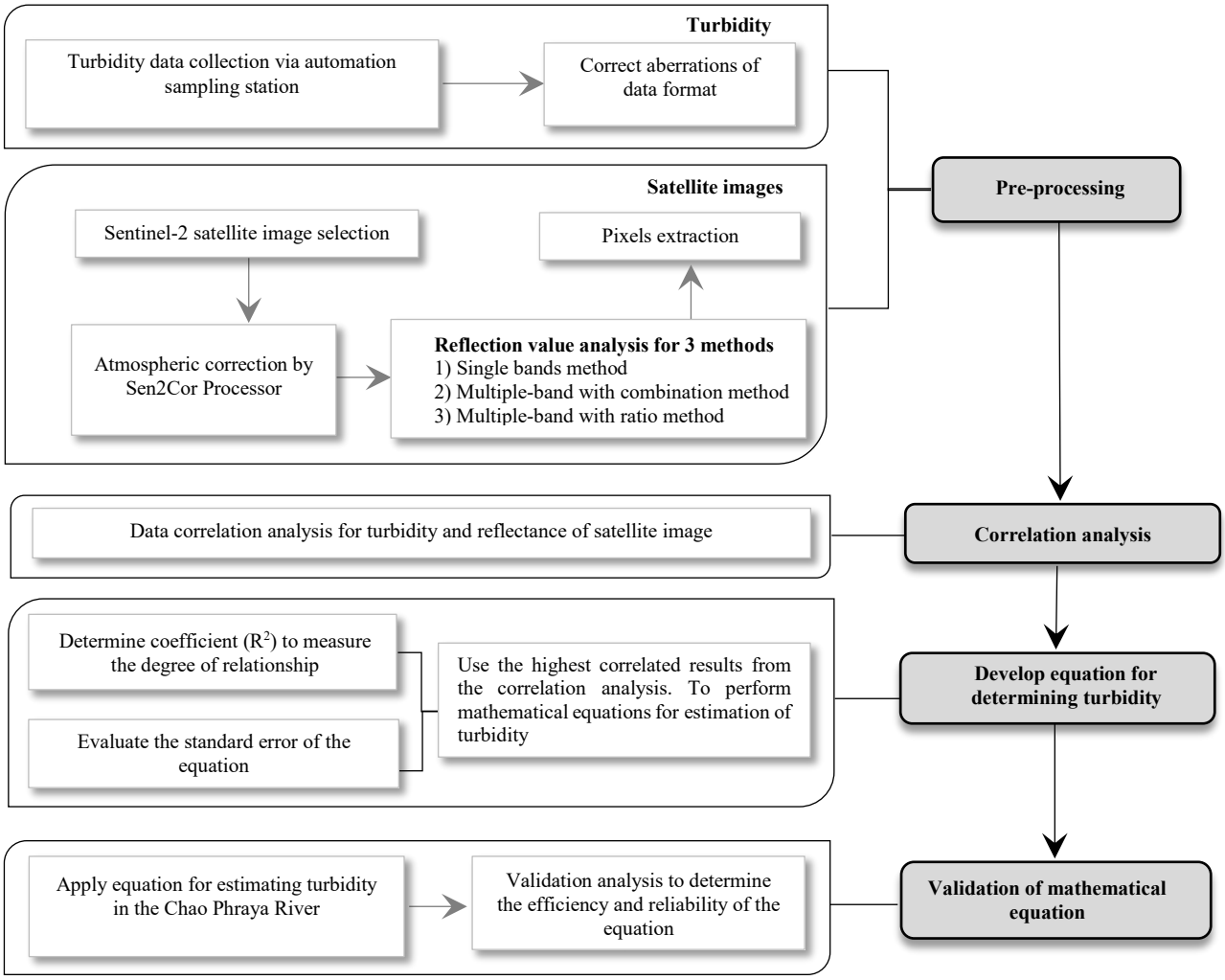

Figure 1. System design method of this study

each station is approximately 4-10 m from the bank, and the depth of the probe from the water surface to the probe is about 100-150 cm, which is below the low water level. The locations of the monitoring stations covered approximately 130 km. Geographical coordinates of the study area start at the latitude of 14.23775N, the longitude of 100.57571E, and the end coordinates of the section at the latitude of 13.54403N the longitude of 100.58935E. These monitoring stations are located at the river's width between 200-500 m. The turbidity data focused on automatic sampling installed stations at only eight stations along the lower part of Chao Phraya River, namely Saphan Krungthep; Wat Chankapo; Samlae Pathum Thani; Samut Prakan; Wat Pho Taeng Nuea, Phra Nangklao Bridge; Wat Ban Paeng; Wat Makham station. Collected data for correlation analysis were coordinates, location, date, and time of turbidity measurement and pictorial information recorded at the nearest time. Therefore, 45 data sets were obtained. The location of each water monitoring station is shown in Figure 2.

2.2 Pre-processing of satellite image and numerical data

The collected turbidity data and satellite imagery were pre-processed to correct their aberrations and eliminate incompletion and noise. There are two steps of data correction in their format, type and location between the satellite image and turbidity data.

Step 1. Fixing the turbidity data from the two data sources, numeric and imagery, into the same numeric data format. Then, showing the spatial data in the form of coordinates from the riverbank to the water quality sensor probe of the eight automatic water quality monitoring stations in the form of Point data. Moreover, set as the representative position of the water quality monitoring station to extract the reflection value in the pixel of the satellite image data to obtain data from both data sets at the same coordinate position.

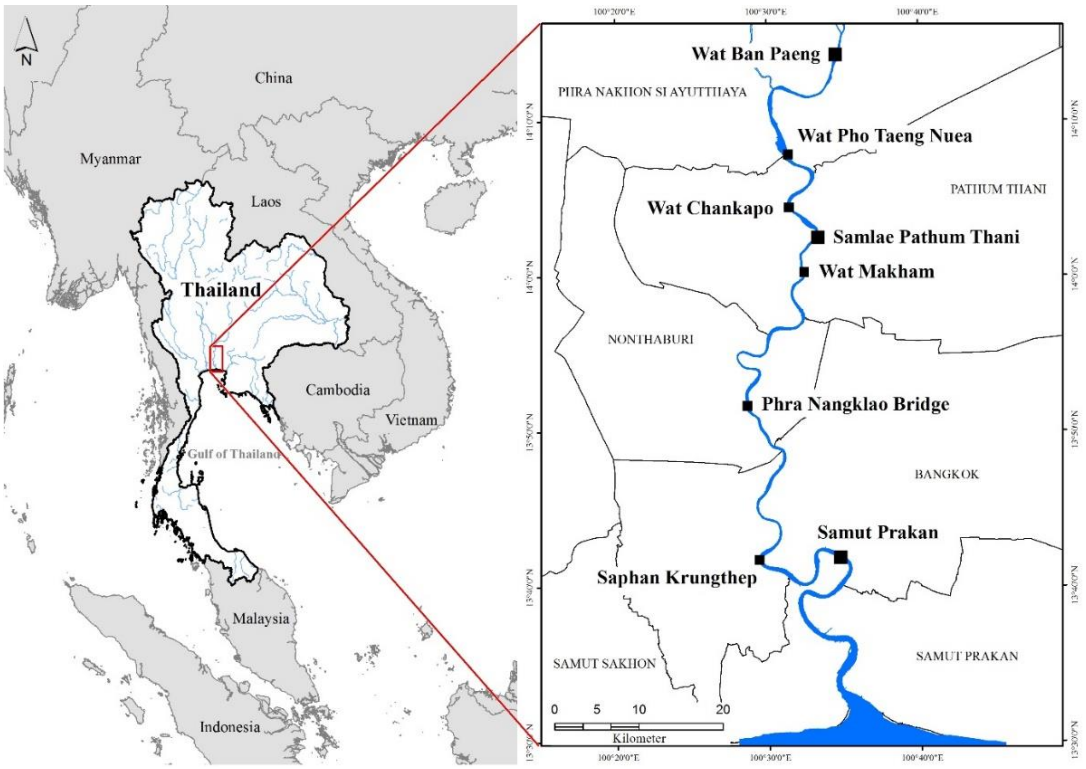

Figure 2. The study area and water quality monitoring stations of the Chao Phraya River

Step 2. Importing and correcting the satellite image data from Sentinel-2. This second step selected the paths and rows of satellite images to cover the study area and corrected aberrations due to atmospheric error correction using the Plugin Sen2Cor Processor of Sentinel Application Platform (Louis et al., 2019; Raiyani et al., 2021). Therefore, the corrected data for atmospheric error were used to analyze reflection values in multiple and single wavelengths. Then, the geographical coordinate system was corrected to define the surface water. The calculation of the reflectance value of the satellite image was conducted using three mathematical methods comparatively: Singer-band analysis, which analyzes only the reflectance values of each wavelength individually as shown as Equation (1). The multiple-band analysis was a combination method using multi-wavelength reflectance of different bands for calculation. This combination of bands is correlated well with in-situ measurements of different water quality conditions; total suspended matter, inorganic fraction, and an organic fraction (Toming et al., 2016). The additional function was applied to calculate the reflectance values from single and combined wavelengths, as shown in Equation (2). The last processing function was a multiple-band analysis. This method used the ratio of the specific band with specific wavelength reflections to calculate the reflection value by permutation between wavelengths. Therefore, the noises such as irradiance, atmospheric, and air-water surface influences in the remotely sensed signal can be minimized (Aisabokhae and Oresajo, 2018; Twumasi et al., 2019), as shown in Equation (3).

The concentration of suspended particulate matter influenced mainly the reflectance of a water body and the magnitude of the backscattering, which directly affects each band's reflectance ability (Wernand et al., 2013). Therefore, in the study, various types of reflectivity must be considered. The computational results obtained from all three methods were used to select the band processing method promoting the best correlation of imagery reflectance and turbidity data.

$$R_{rs}(\lambda)_i \quad (1)$$

$$R_{rs}(\lambda)_i + R_{rs}(\lambda)_i + , \ldots + R_{rs}(\lambda)_i \quad (2)$$

$$R_{rs}(\lambda)_i \, / \, R_{rs}(\lambda)_i \quad (3)$$

Where; $R_{rs}(\lambda)_i$ is the wavelength of band n; n is the number of bands.

2.3 Correlation analysis of turbidity and satellite image data

The statistical technique was adopted in this study. An analysis via Pearson correlation coefficient was applied to perform the relative strength of correlation between measured turbidity data and satellite image data reflectance values prior to building a regression model (Li et al., 2020; Shi et al., 2018). Pearson's correlation analysis had been applied variously to examine correlation patterns between two variables. There is a tendency of correlation patterns in linear regression (Chen et al., 2020; Jayaweera and Aziz, 2018), as shown in Equation (4). The correlation coefficient was depicted as an R-value, which indicated low when it approached -1 and high when a value was closed to 1.

$$R = \frac{\sum X_i Y_i - n\bar{X}\bar{Y}}{\sqrt{\left[\sum X_i^2 - n\bar{X}^2\right]\left[\sum Y_i^2 - n\bar{Y}\right]}} \quad (4)$$

Where; X is a turbidity value in units of NTU; Y is the reflected satellite image data; i is the number of measurements 1, 2, 3,..., n.

2.4 Mathematical equations development for turbidity estimation

The results from process 2.3 were applied to develop the mathematical equations to estimate the river water turbidity. The regression analysis was implemented for linear, quadratic, power, and exponential equations, as described in Equations (5)-(8). To investigate the most suitable mathematical equation, the 95% confidence level was determined with the coefficient of determination (R^2) in a better fit condition, and a higher value was obtained.

$$Y_1 = A \times R_{rs}(\lambda) + B \quad (5)$$

$$Y_2 = A \times R_{rs}(\lambda)^2 + B \times R_{rs}(\lambda) + C \quad (6)$$

$$Y_3 = A \times R_{rs}(\lambda)^B \quad (7)$$

$$Y_4 = Ae^{B \times R_{rs}(\lambda)} \quad (8)$$

Where; A, B, and C are constant values of variables in each equation; $R_{rs}(\lambda)$ is the reflected data of the satellite image; e^B is an exponential function; λ is the wavelength of band 4; Y_1, Y_2, Y_3, and Y_4 are the estimated turbidity value from the linear regression equation, quadratic equation, power equation, and exponential equation.

The R^2 value was used to measure the degree of the relationship between the dependent and independent variables, as shown in Equation (9).

$$R^2 = \frac{\left(\sum XY - n\bar{X}\bar{Y}\right)^2}{\left(\sum X^2 - n\bar{X}^2\right)\left(\sum Y^2 - n\bar{Y}^2\right)} \quad (9)$$

Where; Y is the dependent variable; X is the independent variable; n is the number of data points

To select the appropriate equation for estimating the river's turbidity, the standard error of the estimation method was applied to the reflectance value from the satellite image data as described in Equation (10).

$$SEE = \sqrt{\frac{\sum_{i=1}^{n}\left(Y_i - \hat{Y}\right)^2}{n-k-1}} \quad (10)$$

Where; SEE is the standard error of an estimation; Y is the dependent variable from equations (5), (6), (7), and (8); $\hat{Y}$ is an approximation of Y obtained from equations (5), (6), (7), and (8); n is the number of data points; k is the number of independent variables

2.5 Validation of obtained equation

The obtained mathematic equation in 2.3 was validated using satellite image information and turbidity dataset collected on February 2021 of three automatic sampling stations of the Chao Phraya River, namely Wat Ban Paeng station, Samlae Pathum Thani station, and Samut Prakan station. The equations used to calculate the reflectance of the wavelengths were compared with the measurement data.

The validation analysis of the efficiency and reliability of the equations to estimate turbidity was determined by the Root Mean Square Error (RMSE), as described in Equation (11).

$$RMSE = \sqrt{\frac{1}{n}\sum_{i=0}^{n}(error)^2} \quad (11)$$

Where; error is the actual result minus the predicted result; n is the number of data points

In comparison, the results from the calibration of the turbidity data were obtained from the measurement, and the turbidity value of calculating by the reflectance in the wavelength that most closely related to the turbidity value was plotted in the Geographic information system (GIS) process, The Kriging method estimates the distance or direction

between each sample point. This plot of reflected spatial relation can explain changes occurring on the surface (Ali and Ahmad, 2020).

3. RESULTS AND DISCUSSION

3.1 Pre-processed satellite image and turbidity data

This step of pre-processing satellite images and automatic collecting turbidity data was conducted to minimize the discontinuity and noise. The satellite images were recorded about 3-4 images a month. Among the studied images, a good quality condition was selected. For turbidity data, it was collected from eight automatic measurement stations that were selected by criterion condition if it had been recorded at the same date, time, and coordinates of the location that match the satellite data recording. About 28 sets of numeric data and satellite images collected from December 2016 to 2020 were studied. To sharpen the imagery, the satellite image was corrected for atmospheric discrepancies effect when recording under atmospheric conditions-comparing the satellite image data before the aberrated correcting from the normalizing position. The position used to check the reflectance after the correction was Wat Pho Taeng Nuea station (latitude 14.13939N, longitude 100.51654E), which had a lower reflectance value from the reduction of light scattering conditions. At this condition, there was now free of aerosol optical thickness and water vapour that affected the satellite image data (Fujiwara and Takeuchi, 2020) and had been reported that was the best condition in reflection ability of water bodies at the wavelength of 500-700 nm. In Figure 3, an original satellite image corrected atmospheric condition and spectrum view.

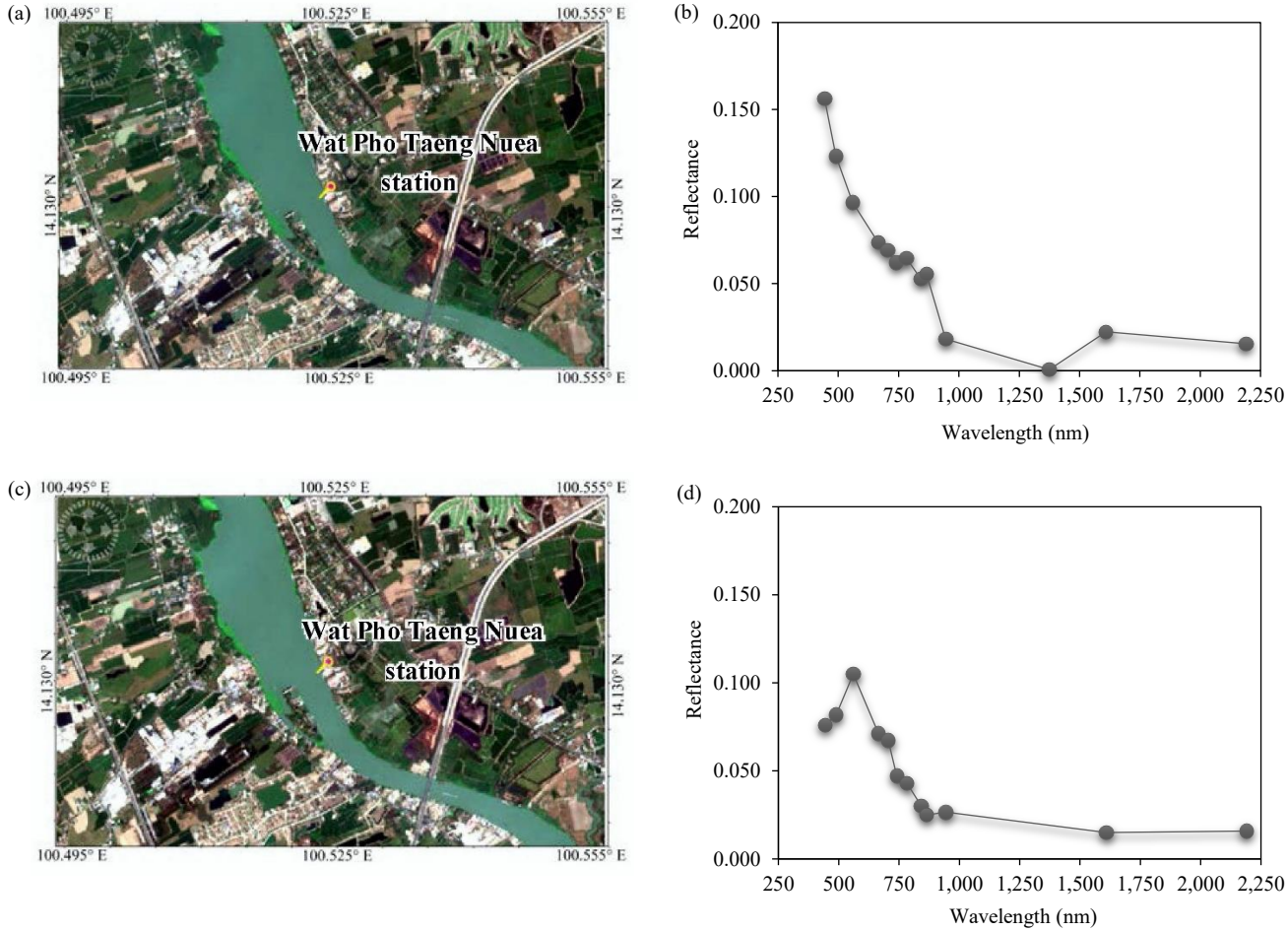

Figure 3. Top-view of satellite image and spectrum view before (a-b) and after (c-d) atmospheric correction

3.2 Correlation analysis of turbidity and reflection data of satellite image

In this step, three different conditions for the spectrum section were investigated for the correlation analysis to turbidity data. These methods were a single band, a multispectral method with a combination of wavelength, and a multispectral method with a wavelength ratio. The best correlation depicted as

Person's coefficient of band method was applied for the mathematic equation development.

3.2.1 Single-band method

The single band method uses a single wavelength, like the B2, B3, B4, and B8, in correlation with the turbidity. The obtained results depicted that spectrum B4 (central wavelength of 665 nm) was correlated maximally to turbidity concentration of the Chao Phraya River water data promoting the highest coefficient of 0.956. The following correlation was found for B3, B2, and B8 with correlation coefficients of 0.807, 0.564, and 0.146, respectively. The correlation results are provided in Table 1.

Table 1. Correlation of turbidity and satellite image reflection of single wavelength analysis

Resolution (m)	Band (B)	Correlation
		Pearson correlation
10	B2	0.564*
	B3	0.807*
	B4	0.956*
	B8	0.146**

Remark * Correlation is significant at the 0.01 level (2-tailed).
** Correlation is significant at the 0.05 level (2-tailed).

There was a significant relationship between the turbidity values in the water and the satellite image reflectance data in each wavelength. Band 4 had the best relationship because its wavelength is in visible light (red), which technically promoted the highest resolution image. Thus, better reflection values were obtained properly related significantly to the turbidity of water (Soria et al., 2017). Furthermore, this satellite provides images at 10 m resolution providing more explicit spatial information enough for relation analysis (Wang et al., 2016). It was found that the reflectance in visible light (red) increased corresponding to sediment or turbidity in the water increased. This finding was similar to the previous result (Trinh et al., 2017).

3.2.2 Multiple-band with the combination method

The second band method using a combined wavelength for relating reflectance and turbidity data was investigated. The results from multiple-band analysis indicated that the combination of band 3 and 4 (B3+B4) provided the best correlation of turbidity with the highest coefficient of 0.907, followed by bands 2 and 4 (B2+B4) and then bands 2, 4, and 3 (B2+B3+B4) with a correlation coefficient of 0.867 and 0.852, respectively, which shown as Table 2.

Table 2. Correlation of turbidity and satellite image reflection of combination method

Resolution (m)	Rating	Band (B)	Correlation
			Pearson coefficient*
10	1	B3+B4	0.907
	2	B2+B4	0.867
	3	B2+B3+B4	0.852
	4	B3+B4+B8	0.839
	5	B4+B8	0.822
	6	B2+B3+B4+B8	0.792
	7	B2+B4+B8	0.764
	8	B2+B3	0.726
	9	B3+B8	0.646
	10	B2+B3+B8	0.628

Remark * Correlation is significant at the 0.01 level (2-tailed).

It was found that multiple-band analysis based on a combination of the wavelength of B3 and B4 can identify significant relationships for turbidity and the reflectance data from satellite imagery. Those bands represent green and red colours, reflecting plant cover and chlorophyll absorption (Clevers and Gitelson, 2013). It had been reported that the visible region of the spectrum promoted an excellent correlation of reflectance and turbidity, mainly when water bodies contained high concentrations of suspended sediment particles (Garg et al., 2020). Therefore, when these two wavelengths were combined, the correlation coefficient regarding predicting water turbidity was the highest, similar to Ouma et al. (2020).

3.2.3 Multiple-band with ratio method

The results from multiple-band analysis with the ratio method indicated that the ratio between band 4 and band 3 (B4/B3) provided the best relationship or turbidity prediction with the highest correlation coefficient of 0.884, followed by bands 4 and 2 (B4/B2) and then bands 4 and 8 (B4/B8) with a correlation coefficient of 0.774 and 0.430, which shown as Table 3.

Compared to the previous method, it was found that the single band method of B4 promoted correlation efficiency of 0.956 ($p<0.01$), which is higher than the combination band method (Band 3 and Band 4; B3+B4) and multiband with ratio method (B4/B3). The result indicated data distribution model was a linear and nonlinear correlation between mathematically calculated reflection values and

Table 3. Relationship between turbidity and reflection data based on multiple-band with ratio method

Resolution (m)	Rating	Band (B)	Correlation
			Pearson coefficient
10	1	B4/B3	0.884*
	2	B4/B2	0.774*
	3	B4/B8	0.430*
	4	B3/B2	0.373**
	5	B3/B8	0.266
	6	B2/B8	0.192
	7	B8/B2	-0.136
	8	B8/B3	-0.184
	9	B8/B4	-0.331**
	10	B2/B3	-0.367**

Remark * Correlation is significant at the 0.01 level (2-tailed).
** Correlation is significant at the 0.05 level (2-tailed).

turbidity data obtained from the measurement station, as shown in Figure 4, reflected well in the B4 wavelength, which related significantly to turbidity in water (Ouma et al., 2018). This reflectance of light increased when the suspended solid increased, particularly in the visible (red) band (Vanhellemont, 2019).

3.3 Development of mathematic equation for turbidity estimation

To develop a mathematical equation for estimating river turbidity, B4 was selected as the analytical variable. This process used 45 datasets applied to four mathematical equations (linear regression, quadratic, power, and exponential mathematical equation). The mathematical power equation was the most suitable for the assessment of the turbidity because (1) the equation had a correlation coefficient (R^2) greater than 0.8; (2) the relationship was significant ($p<0.01$); (3) the standard error of estimates was less than for the other equations. The power equation was also the best for estimating sea-surface suspended particulate matter concentrations of the southern North Sea (Eleveld et al., 2008) and for dispersion analysis of suspended river sediment concentration (Yao et al., 2020).

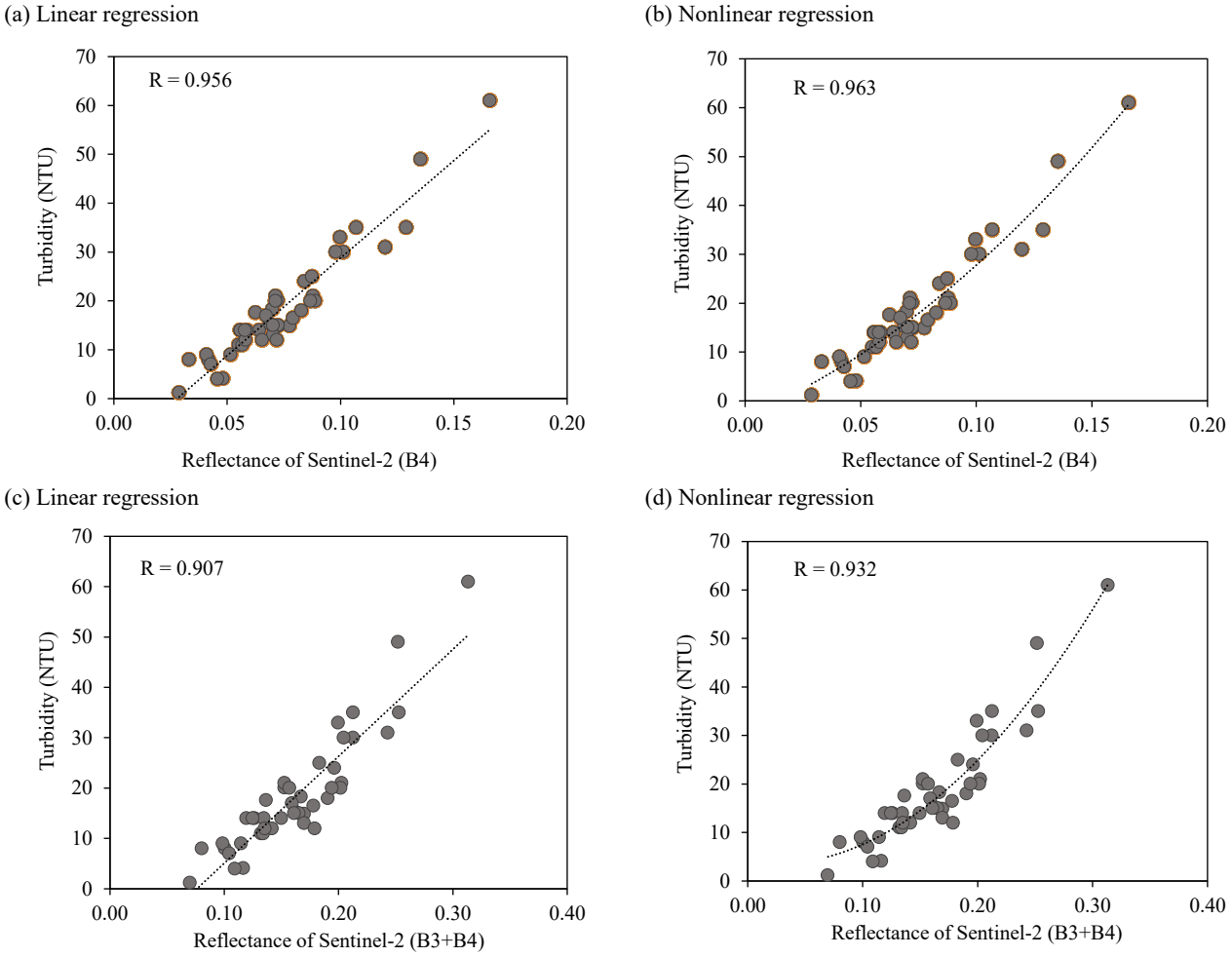

Figure 4. Linear and nonlinear regression plotted of the single-band method (a-b), multiple-band with combination method (c-d), multiple-band with ratio method (e-f)

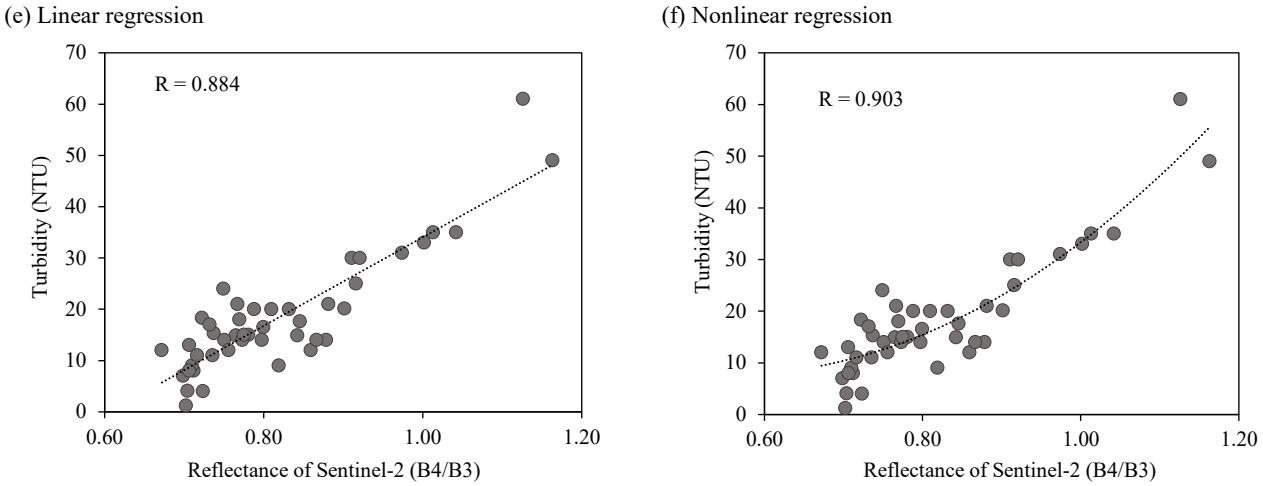

Figure 4. Linear and nonlinear regression plotted of the single-band method (a-b), multiple-band with combination method (c-d), multiple-band with ratio method (e-f) (cont.)

Linear regression is the most feasible and straightforward mathematical equation for correlation analysis, whereas quadratic and exponential equations use nonlinear regression that may be difficult in modelling, but nonlinear can explain more variation. These methods have been used to evaluate water quality (Quang et al., 2017; Sebastia-Frasquet et al., 2019). In some cases, the R^2 value may not reflect a good indicator for the accuracy of the prediction equation (Dixon, 2020; Gani et al., 2021). In this case, a standard error is considered a more suitable proportion (Li and Wong, 2001; Schumacker and Lomax, 2004). In this study, the standard error value was applied as a selecting criterion for the most suitable equation of turbidity estimation. The results are shown in Table 4.

Table 4. Model summary and parameter estimated

Dependent variable: Turbidity (NTU)									
Equation	Model summary					Parameter estimates			
	R^2	F	df1	df2	Sig.	Constant	b1	b2	Std. error of the estimate
Linear	0.913	453.565	1	43	0.00	-11.131	398.952	-	3.387
Quadratic	0.927	267.436	2	42	0.00	-2.961	191.619	1,156.961	3.142
Power	0.823	199.626	1	43	0.00	1,509.984	1.724	-	0.288
Exponential	0.727	114.474	1	43	0.00	3.182	21.173	-	0.358

The independent variable is B4.

From the analysis, the power equation was the best at the 95% confidence level with an R^2 coefficient of 0.823, having a significant relationship ($p<0.01$) and a standard error of 0.288, which was lower than for the other equations. The distribution characteristics of the data are shown in Equation (12). It was found that the turbidity values calculated using the Power equation and the turbidity data from the measurement station were similarly ($p<0.05$).

$$\text{Turbidity (NTU)} = 1{,}509.984\ (\lambda)^{1.7241} \quad (12)$$

Where; λ_4 is the reflected value from the B4 satellite imagery data from the Sentinel-2 satellite, it was consistent with the study by Hossain et al. (2021) using power equations to estimate turbidity in the river and using Landsat 8 satellite imagery data that had a high coefficient (R^2=0.95) and a significant correlation ($p<0.05$). The resulting equation had a high R^2 value and a standard error of 0.288, considered a low value. Comparing the result, the reflectance value via the Linear equation differed from (Suwanlertcharoen et al., 2020) a nonlinear (Power equation) calculation. The power equation could generate a minor variation of measured and estimated data properly.

3.4 Validation of mathematical equations for estimating river water turbidity

The satellite reflectance data of B4 was used to validate the mathematical equations for estimating river turbidity based on the turbidity values from turbidity stations in the Chao Phraya River obtained on February 2021, corrected aberrations due to atmospheric correction using the Plugin Sen2Cor Processor. This method was also applied for multi-wave rectification. The turbidity values calculated from remote sensing imagery compared to the ground truth data from the three water quality monitoring stations: Wat Ban Paeng, Samlae Pathum Thani, and Samut Prakan were the difference in the range 4.03-4.61 NTU. In detail, Table 5 and Figure 5 shows these validation results using the RMSE, with the predicted results being more significant than the data values from the three stations (4.03, 4.20, and 4.61 NTU, respectively). Similarly, RMSE was an appropriate measurement of accuracy that depicted the correlation between calculated and measured data (Neill and Hashemi, 2018) differently.

Table 5. Comparison of monitored and estimated turbidity by satellite image reflectance data

Location	Geographic coordinates		Turbidity (NTU)		RMSE
	Latitudes	Longitudes	Field data	Equation estimate	
Wat Ban Paeng	14.23774	100.57570	16	20.20	4.20
Samlae Pathum Thani	14.04192	100.55500	14	18.61	4.61
Samut Prakan	13.69576	100.48930	11.7	15.73	4.03

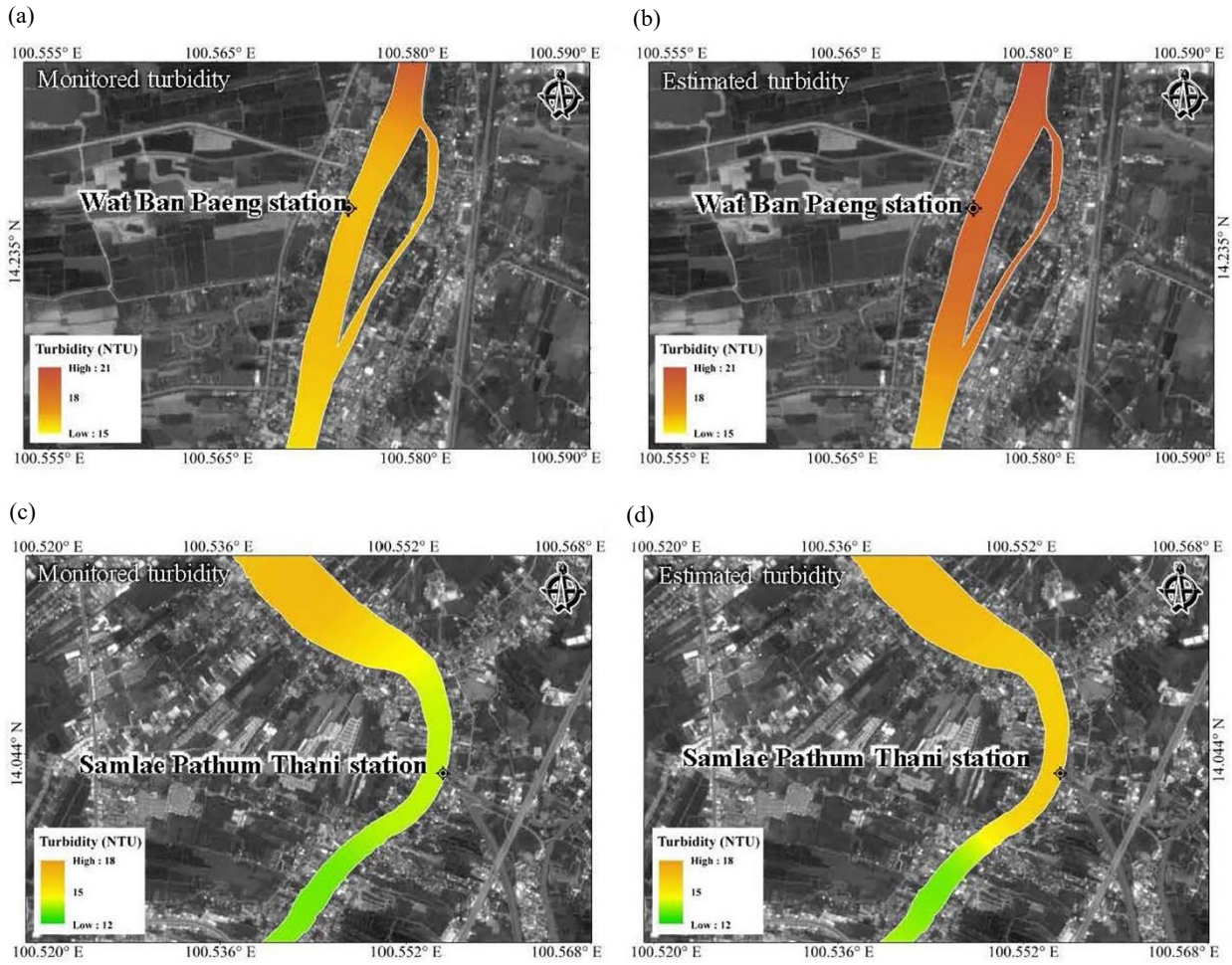

Figure 5. Monitored and estimated turbidity from the obtained equation of the Chao Phraya River at Wat Ban Paeng (a-b), Samlae Pathum Thani (c-d), and Samut Prakan (e-f) stations

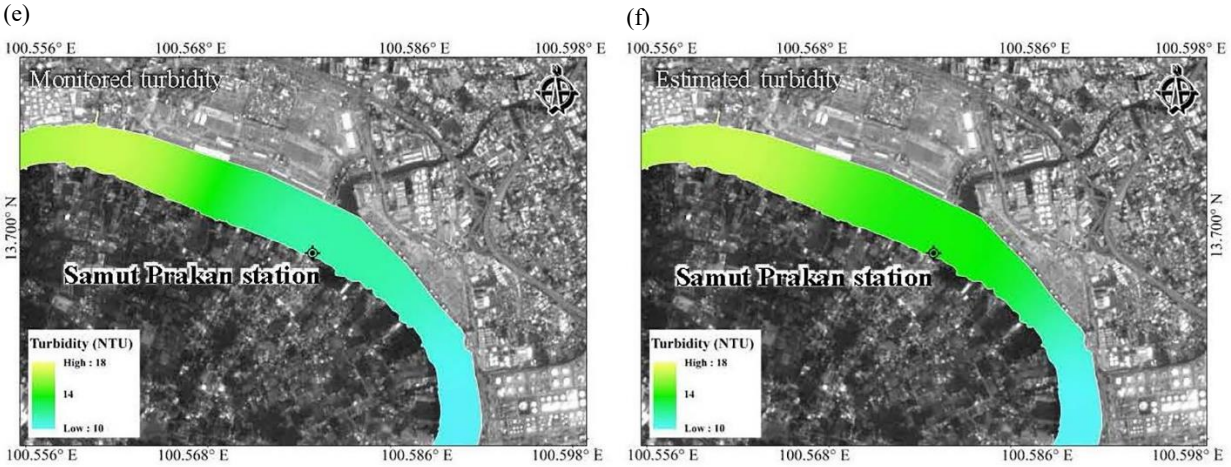

Figure 5. Monitored and estimated turbidity from the obtained equation of the Chao Phraya River at Wat Ban Paeng (a-b), Samlae Pathum Thani (c-d), and Samut Prakan (e-f) stations (cont.)

In Figure 5, the estimated turbidity using obtained equation was compared to the monitored data. It was found that the estimated turbidity of the Chao Phraya River was approximately 18-21 NTU. The higher concentration values were found at the upper part than the river's end, with about 10-16 NTU turbidity. This variation consisted of the land use characteristics around the riverbank differently in the upper through lower river part from agricultural activity and riverbank's physical characteristic, which promoted higher land deposition by the water current (Sahavacharin and Likitswat, 2019). The land use characteristics around the riverbank of the river's end were residential land use, commercial land use, and water transportation use (Ketkeaw, 2019). The flow characteristic of the water current at the end of the river decreased (Chauhan and Singh, 2020) from the decrease of transportation (Tian et al., 2021) and human activities, which beneficially disturbing less of suspended pollution in water (Collivignarelli et al., 2020; Luis et al., 2019). Consequently, the river's end turbidity was less than at the beginning and middle of the river.

From the relationship analysis between the measured turbidity and the predicted results using the three methods (single-band method, combination method, and ratio method), the single-band method with B4 produced the best relationship, with the highest correlation coefficient (0.956) as this visible band (red) is effective at indicating turbidity, as noted in the previous paragraph (Ehmann et al., 2019). It was found that the increase of sediment and turbidity levels in water sources related closely to the increase of reflectance value in the visible band (red) (Gholizadeh et al., 2016). Miller and McKee (2004) also used the visible band (red) to evaluate suspended sediment and turbidity in water sources successfully. The combination method produced the best relationship using B3 and B4 in the current study, with the highest correlation coefficient of 0.907. The ratio method revealed that the ratio between bands with the highest relationship value was between B4/B3, with a correlation coefficient of 0.884. Many studies have indicated that the ratio between the red and green visible bands could be used to assess turbidity or suspended solids (Shen et al., 2017). In the current study, river turbidity equations developed using the power equation had an R^2 value greater than 0.8 and had the lowest standard error from the four tested equations. This finding was similar to Baughman et al. (2015), who used a power equation to estimate turbidity in lakes and used the reflection value of image data from the visible band (red).

4. CONCLUSION

Retrieving turbidity of the Chao Phraya River entirely via remote sensing-based equation was developed successfully in this study. The application of reflectance band 4 in visible wavelength was correlated well with turbidity data of the river. A power equation was a suitable mathematic function fitting significantly to this correlation of satellite image reflected ability and turbidity. This estimation equation via remotely sensed data significantly benefits mapping and monitoring entire rivers by reducing the traditional process's labour-intensive, time-consuming, and analysis cost. This practical determination of water quality parameters was also

valuable in providing data for planning and decision-making associated with continuous monitoring of changes in river water quality.

ACKNOWLEDGEMENTS

Author thanks the Department of Environmental Science, the Faculty of Environment, Kasetsart University, and Kasetsart University Research and Development Institute (KURDI) for the support.

REFERENCES

Acharya TD, Subedi A, Lee DH. Evaluation of water indices for surface water extraction in a Landsat 8 scene of Nepal. Sensors 2018;18(8):Article No. 2580.

Aisabokhae JE, Oresajo SB. Supervised classification of Landsat-8 band ratio images for geological interpretation of Sokoto, Nigeria. South African Journal of Geomatics 2018;7(3):360-71.

Ali SA, Ahmad A. Analysing water-borne diseases susceptibility in Kolkata Municipal Corporation using WQI and GIS based Kriging interpolation. GeoJournal 2020;85(4):1151-74.

Alvado B, Soria-Perpinya X, Vicente E, Delegido J, Urrego P, Ruiz-Verdu A, et al. Estimating organic and inorganic part of suspended solids from Sentinel 2 in different inland waters. Water 2021;13(18):Article No. 2453.

Baughman CA, Jones BM, Bartz KK, Young DB, Zimmerman CE. Reconstructing turbidity in a glacially influenced lake using the Landsat TM and ETM+ surface reflectance climate data record archive, Lake Clark, Alaska. Remote Sensing 2015;7(10):13692-710.

Caballero I, Stumpf RP, Meredith A. Preliminary assessment of turbidity and chlorophyll impact on bathymetry derived from Sentinel-2A and Sentinel-3A satellites in South Florida. Remote Sensing 2019;11(6):Article No. 645.

Chauhan A, Singh RP. Decline in PM2.5 concentrations over major cities around the world associated with COVID-19. Environmental Research 2020;187:Article No. 109634.

Chen J, Zhu W, Tian YQ, Yu Q. Monitoring dissolved organic carbon by combining Landsat-8 and Sentinel-2 satellites: Case study in Saginaw River estuary, Lake Huron. Science of the Total Environment 2020;718:Article No. 137374.

Clevers JG, Gitelson AA. Remote estimation of crop and grass chlorophyll and nitrogen content using red-edge bands on Sentinel-2 and -3. International Journal of Applied Earth Observation and Geoinformation 2013;23:344-51.

Collivignarelli MC, Abbà A, Bertanza G, Pedrazzani R, Ricciardi P, Miino MC. Lockdown for CoViD-2019 in Milan: What are the effects on air quality? Science of the Total Environment 2020;732:Article No. 139280.

Dixon MT. Exploring the Effects of Social Media Use and Avoidant Attachment Style on Marital Satisfaction and Cyber Infidelity [dissertation]. Atlanta, Mercer University; 2020.

Ehmann K, Kelleher C, Condon LE. Monitoring turbidity from above: Deploying small unoccupied aerial vehicles to image in-stream turbidity. Hydrological Processes 2019;33(6):1013-21.

Eleveld MA, Pasterkamp R, van der Woerd HJ, Pietrzak JD. Remotely sensed seasonality in the spatial distribution of sea-surface suspended particulate matter in the southern North Sea. Estuarine, Coastal and Shelf Science 2008;80(1):103-13.

Elhag M, Gitas I, Othman A, Bahrawi J, Gikas P. Assessment of water quality parameters using temporal remote sensing spectral reflectance in arid environments, Saudi Arabia. Water. 2019;11(3):Article No. 556.

Fujiwara T, Takeuchi W. Simulation of Sentinel-2 bottom of atmosphere reflectance using shadow parameters on a Deciduous Forest in Thailand. ISPRS International Journal of Geo-Information 2020;9(10):Article No. 582.

Gani A, Ion W, Yang E. Optimisation of cutting parameters and surface deformation during thin steel sheets plasma processing using Taguchi approach. Advances in Mechanical Engineering 2021;13(7):1-19.

Garg V, Aggarwal SP, Chauhan P. Changes in turbidity along Ganga River using Sentinel-2 satellite data during lockdown associated with COVID-19. Geomatics, Natural Hazards and Risk 2020;11(1):1175-95.

Gholizadeh MH, Melesse AM, Reddi L. A comprehensive review on water quality parameters estimation using remote sensing techniques. Sensors 2016;16(8):Article No. 1298.

Giardino C, Pepe M, Brivio PA, Ghezzi P, Zilioli E. Detecting chlorophyll, Secchi disk depth and surface temperature in a sub-alpine lake using Landsat imagery. Science of the Total Environment 2001;268(1-3):19-29.

Gikas P, Tchobanoglous G. The role of satellite and decentralized strategies in water resources management. Journal of Environmental Management 2009;90(1):144-52.

Gohin F, Bryère P, Lefebvre A, Sauriau P-G, Savoye N, Vantrepotte V, et al. Satellite and in situ monitoring of Chl-a, turbidity, and total suspended matter in coastal waters: Experience of the year 2017 along the French Coasts. Journal of Marine Science and Engineering 2020;8(9):Article No. 665.

Güttler FN, Niculescu S, Gohin F. Turbidity retrieval and monitoring of Danube Delta waters using multi-sensor optical remote sensing data: An integrated view from the delta plain lakes to the western-northwestern Black Sea coastal zone. Remote Sensing of Environment 2013;132:86-101.

Hossain A, Mathias C, Blanton R. Remote sensing of turbidity in the Tennessee River using Landsat 8 satellite. Remote Sensing 2021;13(18):Article No. 3785.

Jayaweera C, Aziz N. Reliability of principal component analysis and pearson correlation coefficient, for application in artificial neural network model development, for water treatment plants. IOP Conference Series: Materials Science and Engineering 2018;458:Article No. 012076.

Ketkeaw T, Thanuttamavong M, Kaveeta R. Effects of land use on water quality in Samrong Canal, Samut Prakan Province. Journal of Science and Technology 2019;21(1):175-83.

Li C, Wong WH. Model-based analysis of oligonucleotide arrays: Model validation, design issues and standard error application. Genome Biology 2001;2(8):1-11.

Li W, Niu Z, Shang R, Qin Y, Wang L, Chen H. High-resolution mapping of forest canopy height using machine learning by coupling ICESat-2 LiDAR with Sentinel-1, Sentinel-2 and Landsat-8 data. International Journal of Applied Earth Observation and Geoinformation 2020;92:Article No. 102163.

Louis J, Pflug B, Main-Knorn M, Debaecker V, Mueller-Wilm U, Iannone RQ, et al. Sentinel-2 global surface reflectance level-2A product generated with Sen2Cor. Proceedings of IEEE International Geoscience and Remote Sensing Symposium; 2019 Jul 28-Aug 2; Yokohama: Japan; 2019.

Luis KM, Rheuban JE, Kavanaugh MT, Glover DM, Wei J, Lee Z, et al. Capturing coastal water clarity variability with Landsat 8. Marine Pollution Bulletin 2019;145:96-104.

Marina P, Snezana M, Maja N, Miroslava M. Determination of heavy metal concentration and correlation analysis of turbidity: A case study of the Zlot source (Bor, Serbia). Water, Air, and Soil Pollution 2020;231(3):1-12.

Miller RL, McKee BA. Using MODIS Terra 250 m imagery to map concentrations of total suspended matter in coastal waters. Remote Sensing of Environment 2004;93(1-2):259-66.

Mulliss RM, Revitt DM, Shutes RB. The impacts of urban discharges on the hydrology and water quality of an urban watercourse. Science of the Total Environment 1996;189: 385-90.

Neill SP, Hashemi MR. Fundamentals of Ocean Renewable Energy: Generating Electricity from the Sea. London, United Kingdom, Elsevier Academic Press; 2018.

Neukermans G, Loisel H, Mériaux X, Astoreca R, McKee D. In situ variability of mass-specific beam attenuation and backscattering of marine particles with respect to particle size, density, and composition. Limnology and Oceanography 2012;57(1):124-44.

Ouma YO, Noor K, Herbert K. Modelling reservoir chlorophyll-a, TSS, and turbidity using Sentinel-2A MSI and Landsat-8 OLI satellite sensors with empirical multivariate regression. Journal of Sensors 2020;2020:Article No. 8858408.

Ouma YO, Waga J, Okech M, Lavisa O, Mbuthia D. Estimation of reservoir bio-optical water quality parameters using smartphone sensor apps and Landsat ETM+: Review and comparative experimental results. Journal of Sensors 2018;2018:Article No. 3490757.

Pavelsky TM, Smith LC. Remote sensing of suspended sediment concentration, flow velocity, and lake recharge in the Peace-Athabasca Delta, Canada. Water Resources Research 2009;45(11):Article No. W11417.

Quang NH, Sasaki J, Higa H, Huan NH. Spatiotemporal variation of turbidity based on landsat 8 oli in cam ranh bay and thuy trieu lagoon, Vietnam. Water 2017;9(8):Article No. 570.

Raiyani K, Gonçalves T, Rato L, Salgueiro P, Marques da Silva JR. Sentinel-2 image scene classification: A comparison between Sen2Cor and a machine learning approach. Remote Sensing 2021;13(2):Article No. 300.

Sahavacharin A, Likitswat F. Landscape ecological structure of Peri-Urban agricultural area in Bangkok Metropolitan Region. Journal of Community Development and Life Quality 2019;7(2);180-91.

Schumacker RE, Lomax RG. A beginner's guide to structural equation modeling. London, United Kingdom: Psychology Press; 2004.

Sebastia-Frasquet M-T, Aguilar-Maldonado JA, Santamaria-Del-Angel E, Estornell J. Sentinel 2 analysis of turbidity patterns in a coastal lagoon. Remote Sensing 2019;11(24):Article No. 2926.

Shen M, Duan H, Cao Z, Xue K, Loiselle S, Yesou H. Determination of the downwelling diffuse attenuation coefficient of lake water with the sentinel-3A OLCI. Remote Sensing 2017;9(12):Article No. 1246.

Shi L, Mao Z, Wang Z, Retrieval of total suspended matter concentrations from high resolution WorldView-2 imagery: a case study of inland rivers. IOP Conference Series: Earth and Environmental Science 2018;121(3):Article No. 032036.

Sillberg CV, Kullavanijaya P, Chavalparit O. Water quality classification by integration of attribute-realization and support vector machine for the Chao Phraya River. Journal of Ecological Engineering 2021;22(9):70-86.

Soria X, Delegido J, Urrego E, Pereira-Sandoval M, Vicente E, Ruiz-Verdu A, et al. Validación de algoritmos para la estimación de la clorofila-a con Sentinel-2 en la Albufera de València. Proceedings of the XVII Congreso de la Asociacion Espanola de Teledeteccion; 2017 Oct 3-7; Murcia, Spain; 2017.

Suwanlertcharoen T, Prukpitikula S, Buakaewa V. Retrieval of water turbidity using sentinel-2 image time series to enhance water quality assessment for consumption. Journal of Environmental Management 2020;16:74-93.

Tian X, An C, Chen Z, Tian Z. Assessing the impact of COVID-19 pandemic on urban transportation and air quality in Canada. Science of the Total Environment 2021;765:Article No. 144270.

Toming K, Kutser T, Laas A, Sepp M, Paavel B, Nõges T. First experiences in mapping lake water quality parameters with Sentinel-2 MSI imagery. Remote Sensing 2016;8(8):Article No. 640.

Trinh RC, Fichot CG, Gierach MM, Holt B, Malakar NK, Hulley G, et al. Application of Landsat 8 for monitoring impacts of wastewater discharge on coastal water quality. Frontiers in Marine Science 2017;4:Article No. 329.

Twumasi N, Shao Z, Altan O. Mapping built-up areas using two band ratio on Landsat imagery of Accra in Ghana from 1980 to 2017. Applied Ecology and Environmental Research 2019;17:13147-68.

Vanhellemont Q. Daily metre-scale mapping of water turbidity using CubeSat imagery. Optics Express 2019;27(20):1372-99.

Wang Q, Shi W, Li Z, Atkinson PM. Fusion of Sentinel-2 images. Remote Sensing of Environment 2016;187:241-52.

Wernand M, Hommersom A, van der Woerd HJ. MERIS-based ocean colour classification with the discrete Forel-Ule scale. Ocean Science 2013;9(3):477-87.

Yao R, Cai L, Liu J, Zhou M. GF-1 Satellite observations of suspended sediment injection of Yellow River Estuary, China. Remote Sensing 2020;12(19):Article No. 3126.

Yunus AP, Masago Y, Hijioka Y. COVID-19 and surface water quality: Improved lake water quality during the lockdown. Science of the Total Environment 2020;731:Article No. 139012.

Dynamic Occupancy of Wild Asian Elephant: A Case Study Based On the SMART Database from the Western Forest Complex in Thailand

Peerawit Amorntiyangkul[1], Anak Pattanavibool[2,3], Weeraya Ochakul[2], Wichien Chinnawong[2], Supalerk Klanprasert[2], Chatwaroon Aungkeaw[2], Prateep Duengkae[1], and Warong Suksavate[1*]

[1]Major Field of Forest Biology, Faculty of Forestry, Kasetsart University, Bangkok, Thailand
[2]Department of National Park, Wildlife and Plant Conservation, Bangkok, Thailand
[3]Wildlife Conservation Society Thailand Program, Bangkok, Thailand

ARTICLE INFO

Received: 3 Jan 2022
Received in revised: 24 Feb 2022
Accepted: 1 Mar 2022
Published online: 21 Mar 2022
DOI: 10.32526/ennrj/20/202200005

Keywords:
Elephas maximus/ Protected area/ Habitat/ SMART Patrol/ Threat/ Thung Yai Naresuan

*** Corresponding author:**
E-mail: wsuksavate@gmail.com

ABSTRACT

Understanding distribution patterns is essential for the long-term conservation of megafauna, particularly the Asian elephant (*Elephas maximus*). We investigated the dynamic occupancy of Asian elephants in the Thung Yai Naresuan West Wildlife Sanctuary in Thailand. Asian elephant occurrences were recorded during patrol activities from 2012 to 2019. We applied a single-species dynamic occupancy model to examine the environmental factors influencing habitat occupancy of Asian elephant across multiple seasons. The best-supported model, based on the Akaike information criterion (AIC), indicated that the normalized difference vegetation index and elevation positively influenced the probability of colonization. In contrast, the distance to the nearest population source sites showed a negative association. The probability of local extinction was positively correlated with the distance to the nearest villages and population source sites. The predictive map indicated a higher probability of colonization in a remote mountainous region of the center of the protected area. Higher extinction probability was associated with areas of dense human activity and far from population source sites connecting the Asian elephant population to the east. This is the first study to utilize a patrol database for assessing the dynamic occupancy of Asian elephants across multiple years. Our model provides insight into the dynamic distribution patterns of Asian elephants within the wildlife sanctuary and the factors that most influence these patterns. Long-term ecological data provide crucial information for assessing biodiversity, population status, and the ecological processes of focal wildlife species and are valuable for both protected area management and conservation efforts.

1. INTRODUCTION

A global conservation crisis has resulted from biodiversity declines and associated threats to various megafauna species (Davis et al., 2018). The Asian elephant (*Elephas maximus*), a terrestrial megafauna species, is a keystone and umbrella species with varied ecological functions (Suksavate et al., 2019). The global population of Asian elephant is in decline, with approximately 40,000-52,000 individuals surviving in the wild, and the species is listed as Endangered in the IUCN Red List (IUCN, 2020). However, Asian elephant have low reproductive output and require large home ranges, making them highly vulnerable to population declines (Cardillo et al., 2005). Increases in human disturbances (Allbrook and Quinn, 2020) threaten wildlife via habitat loss and fragmentation (Leimgruber et al., 2003; Nekaris et al., 2015). Poaching is also a threat to remnant Asian elephant populations due to the high value of body parts in the wildlife trade (McClenachan et al., 2016). The conflict between humans and Asian elephant has increased substantially due to human impacts (Krishnan et al., 2019; Sukumar, 2006).

The wild Asian elephant population in Thailand was estimated to be approximately 3,124 individuals, with 642 individuals inhabiting the Western Forest Complex (WEFCOM) (IUCN, 2017). WEFCOM is the most significant conservation landscape consisting

Citation: Amorntiyangkul P, Pattanavibool A, Ochakul W, Chinnawong W, Klanprasert S, Aungkeaw C, Duengkae P, Suksavate W. Dynamic occupancy of wild Asian elephant: A case study based on the SMART database from the western forest complex in Thailand. Environ. Nat. Resour. J. 2022;20(3):310-322. (https://doi.org/10.32526/ennrj/20/202200005)

of 17 contiguous and strongly protected areas in Thailand (Duangchatrasiri et al., 2019; Simcharoen et al., 2007), particularly in the Huai Kha Kheng Wildlife Sanctuary (HKK). The distribution range of these Asian elephant extends into adjacent protected areas (Sukmasuang, 2009). Large-scale surveys conducted throughout the WEFCOM in 2010 indicate that the Asian elephant populations in these peripheral protected areas are smaller than those in source sites, particularly in the Thung Yai Naresuan West Wildlife Sanctuary (TYW), where the distribution of Asian elephant was clearly limited (DNP, 2013). The Spatial Monitoring and Reporting Tool (SMART) is used for evaluating and improving law enforcement systems in protected areas (Stokes, 2010). SMART has been used to record the on-site patrols, then compile the observations into a systematic database to identify illegal activities and other conservation management issues (Hötte et al., 2015). In TYW, the SMART patrol system has been implemented since 2008 and expanded to 70% (DNP, 2013). SMART can be used in ecological studies of the major wildlife species to gain insight into ecology, threats, and management of the species. Such understanding could facilitate the maintenance of biodiversity and the achievement of conservation objectives (Marescot et al., 2019).

Occupancy models have been employed to investigate areas occupied by target species within a specific region using appropriately scaled predictors to facilitate occurrence predictions (Scott et al., 2002). Factors at the local scale can provide insight into habitat occupancy based on environmental factors. Such implementations are critical for wildlife management and the conservation of endangered species in particular (Duangchatrasiri et al., 2019; Vinitpornsawan, 2013). Using a standard occupancy model for the Asian elephant could elucidate patterns of seasonal dynamic occupancy over a large and diverse landscape that are mainly determined by key anthropogenic and ecological factors (Jathanna et al., 2015), The occupancy modeling framework has been expanded to account for species interactions, imperfect detection, and changes in species distributions (MacKenzie et al., 2003).

The Asian elephant is a megafauna known once to occupy TYW but historically diminished and nearly absent from the area. The re-occupation of the Asian elephant population was recorded in TYW during the last decade due to improved protected area management with the SMART system, wildly applied in protected areas in many African and Asian nations. However, the re-occupation pattern is poorly understood during the transition period in the dynamic landscape context. We used a single-species, dynamic occupancy model to examine the factors influencing Asian elephant occupancy across multiple seasons (Broms et al., 2016). In this study, we hypothesize that socio-ecological factors affected the dynamic of habitat occupancy of the Asian elephant. The dynamic occupancy model was used to quantify associations between covariates and colonization-extinction processes at the landscape scale. Then, we used the optimal model to develop a spatial representation of the colonization-extinction probability. This predictive map could support the conservation of Asian elephant populations in the study area by providing spatial and temporal information on habitat occupancy and evidence of the transboundary re- population process across protected areas in WEFCOM.

2. METHODOLOGY

2.1 Study area

Thung Yai Naresuan West Wildlife Sanctuary (TYW) is located within WEFCOM in the western region of Thailand, connected to the border of Myanmar. The study area was between the latitudes of 14°8'N and 15°49'N; and between the longitudes of 98°33'E and 99°8'E. TYW is connected to HKK and Thung Yai Naresuan East Wildlife Sanctuary (TYE) to the east. The study area was composed of a portion of WEFCOM landscape declared as a world natural heritage site since 1991, encompassing an area of 2,129 km^2 (Kanchanasaka, 1997; Trisurat, 2004) (Figure 1). The study area is mainly hilly terrain with the elevation ranging from 800 to 1,813 m with 10-40% slopes. The climate is characterized by three main seasons composed of rainy season (May-October), winter (November-January) and summer (February-April) (Kanchanasaka, 1997). The majority of landcover is forest ecosystem which varies across elevation, classified as dry evergreen forest, hill evergreen forest, dry dipterocarp forest, and savannah grassland (Duangchatrasiri et al., 2019). TYW is rich in biodiversity, including several endemic and internationally threatened species such as Indochinese tiger (*Panthera tigris*), Gaur (*Bos gaurus*), Banteng (*Bos javanicus*), and Rufous-necked Hornbill (*Aceros nipalensis*). Furthermore, this area has been identified as one of the potential landscapes for the long-term conservation of Asian elephants (Leimgruber et al., 2003; Sukumar, 2006).

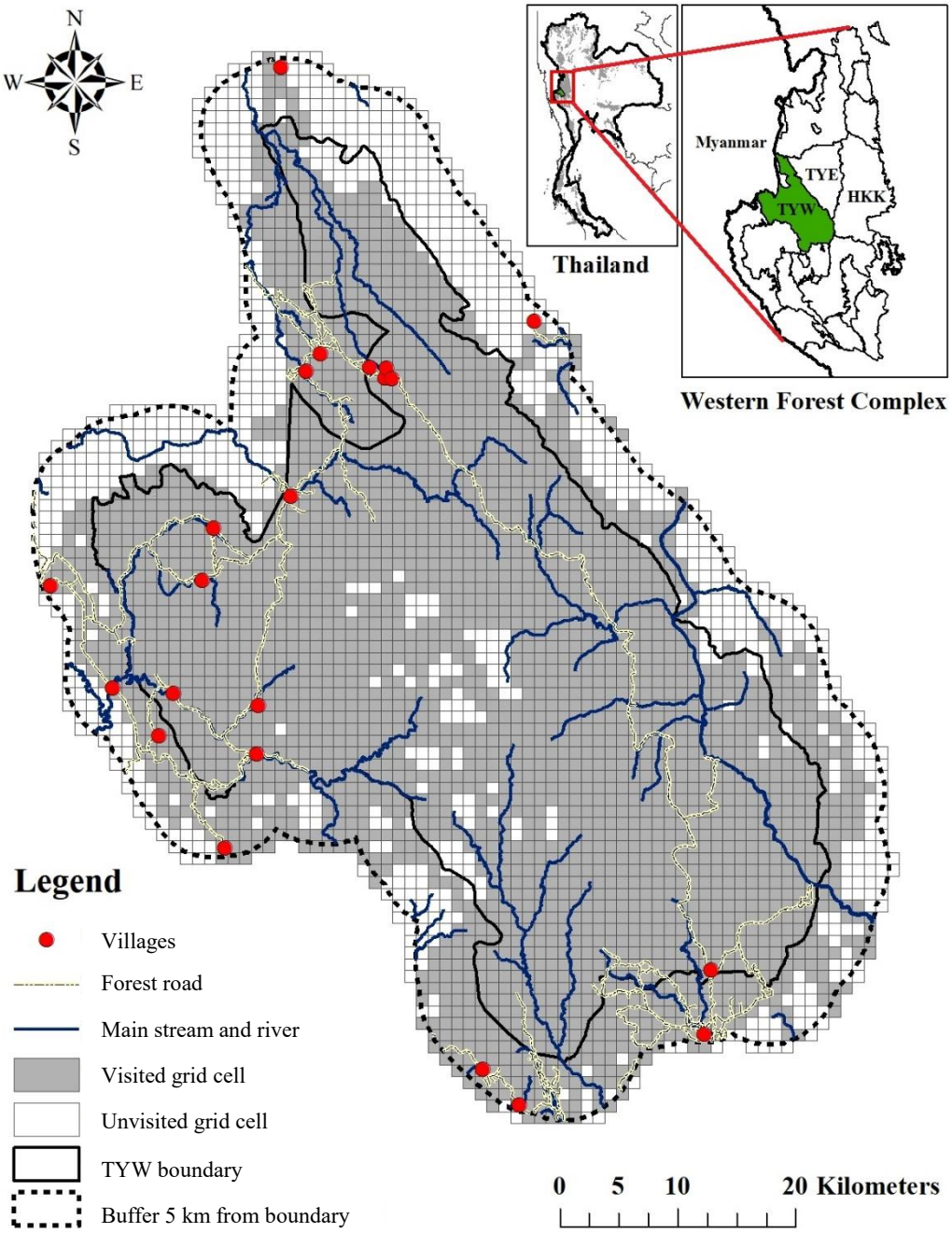

Figure 1. Study area and 1 km^2 spatial grid cell of Asian elephant dynamic occupancy model in Thung Yai Naresuan Wildlife Sanctuary (TYW) from SMART database during 2012-2019

2.2 Data collection and analysis

Occurrence data of Asian elephants was acquired from the SMART database recorded during patrolling routines from 2012 to 2019. The patrol data showed stability of coverage over 90% since 2012 and increase of Asian elephant presence (Figure 2). Data in this study was represented at 1 km^2 grid resolution, following the referenced scale for protected area management (DNP, 2013). Grid cells for the study area were generated to cover the 5 km buffered study area to include the transboundary connection, making the total area of 3,722 km^2 (Figure 1). Direct observation and recent signs, primarily tracks and dungs situated in the grid cell were included as quarterly observing occasions within annual occupancy. Raster of ecological and anthropogenic covariates were obtained from the SMART database and GIS public domain (Figure 1). Eight static covariates were used as the input of the occupancy state model. Geographical covariates comprise the average value of elevation (ELV) and slope (SLP) within a spatial grid (Leimgruber et al., 2003;

Suksavate et al., 2019). The distance from the boundary of HKK and Khuean Srinagarindra National Park (KSR) to the centroid of each grid was used to represent the dispersal fatigue of Asian elephant from the nearest initial population source (PPS) (Vasudev et al., 2021). Average normalized difference vegetation index (NDVI), extracted from Landsat-8 imagery, was used as a critical tool for representing habitat condition, vegetation phenology, and primary production; which many previous studies have shown to correlate with Asian elephant distribution (Jathanna et al., 2015; Pettorelli et al., 2011; Thapa et al., 2019). The presence of the water body was represented by the distance from the grid centroid to the nearest main stream (MST) and secondary stream (SST). The anthropogenic influencing factor was defined by the distance from the grid centroid to the nearest villages (VLG) (Jornburom et al., 2020; Suksavate et al., 2019) (see in Table 1 and Figure 3). Threat intensity (THTyear) was a dynamic covariate to represent the annual kernel density of poaching incidents such as poacher camp, poached animal carcasses, and other belongings (Hötte et al., 2015) (see in Figure 3 and Figure 4). To model the detectability, quarterly patrol frequency (P_{freq}) and distance from the nearest ranger to grid centroid (RGS) was included to represent the effect of sampling intensity and fatigue, respectively. The seasonal and terrain difficulties were also included in modeling detection probability by terrain ruggedness index (TRI) and annual rainfall (R_{avr}) (Table 1).

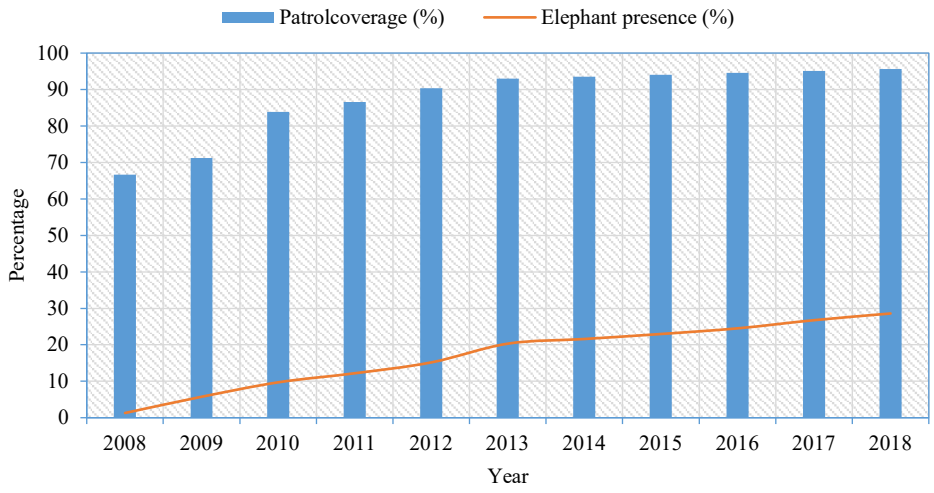

Figure 2. Percentage of patrol coverage compared to Asian elephant sign (orange line) in 1 km^2 grid cell in TYW during 2008-2019

Table 1. Covariates hypothesized to influence patterns of habitat use in spatial (grid cell 1 km^2) and detection probability of Asian elephant in Thung Yai Naresuan wildlife sanctuary

Covariate	Description	Min	Max	Av.	SD
Site level covariates					
PPS	Distance to nearest Asian elephant population source site (km)	0.00	68.35	31.41	17.92
VLG	Distance to nearest villages (km)	0.00	43.86	13.68	9.57
MST	Distance to nearest main stream (km)	0.00	17.46	2.79	2.70
SST	Distance to nearest secondary stream (km)	0.00	12.04	0.50	1.32
ELV	Elevation (m)	118.91	1,633.03	663.66	322.41
NDVI	Normalized difference vegetation index	-0.06	0.46	0.37	0.06
SLP	Slope	0.00	37.16	15.16	5.99
THT12	Threat intensive in 2012, using data from SMART	0.00	0.50	0.01	0.02
Yearly site covariates					
THTyear	Annual threat intensive during 2012-2019, using data from SMART	0.00	0.67	0.005	0.01

Table 1. Covariates hypothesized to influence patterns of habitat use in spatial (grid cell 1 km^2) and detection probability of Asian elephant in Thung Yai Naresuan wildlife sanctuary (cont.)

Covariate	Description	Min	Max	Av.	SD
Observation covariates					
P_{freq}	Patrol frequency (2012-2019), using data from SMART	0.70	39.00	0.00	1.52
R_{avr}	Rainfall average (mm)	14.31	30.67	4.85	4.95
TRI	Terrain ruggedness index	0.00	0.52	0.49	0.03
RGS	Distance to nearest forest ranger station (km)	0.00	19.31	6.62	3.78

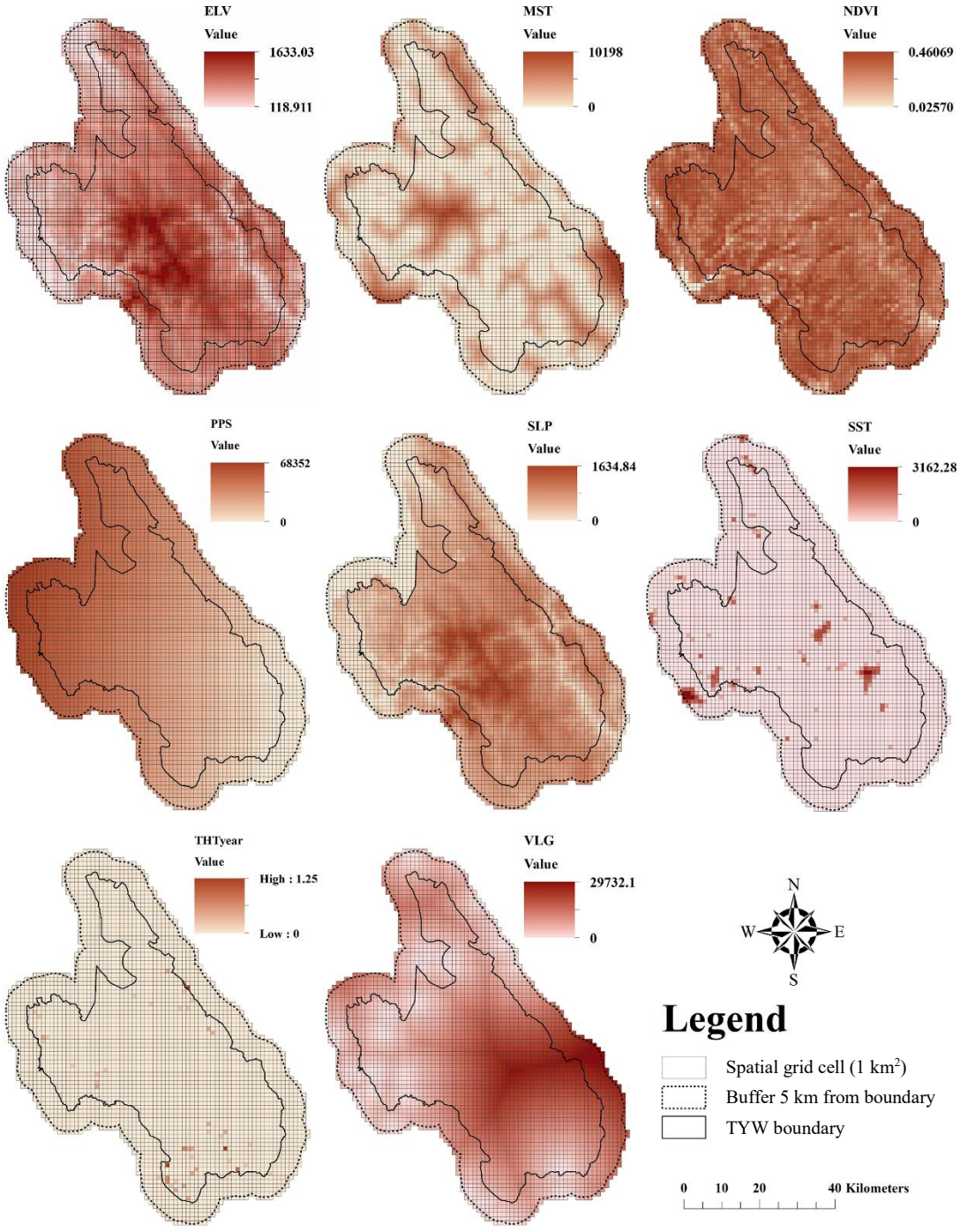

Figure 3. Static covariates (1 km^2 grid cells) of Asian elephant dynamic occupancy model in Thung Yai Naresuan West Wildlife Sanctuary

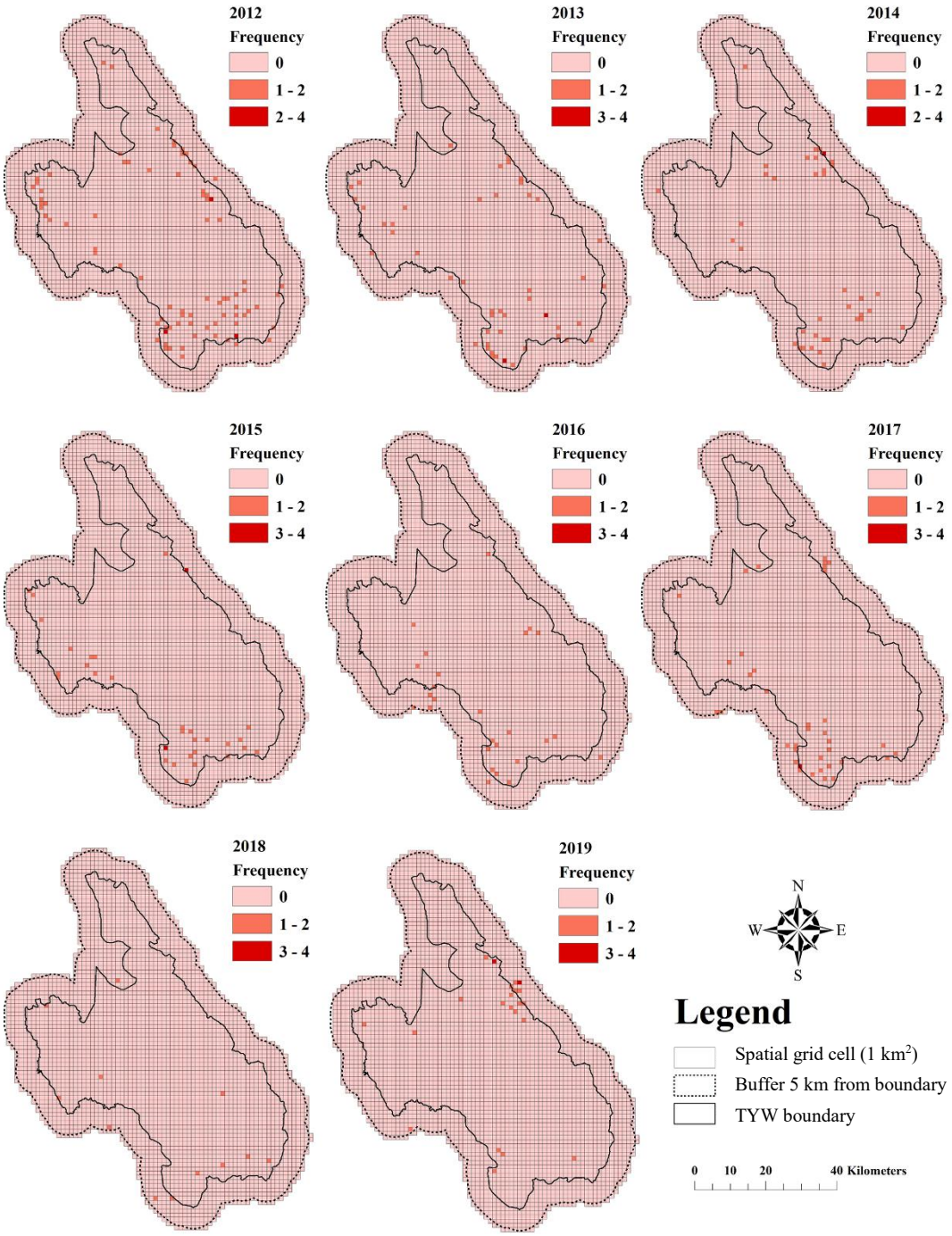

Figure 4. Threat annual intensity (1 km^2 grid cells) during 2012-2019 used for Asian elephant dynamic occupancy model in Thung Yai Naresuan West Wildlife Sanctuary

2.3 Model training and selection

A single species, multi-season, dynamic occupancy modeling framework was used to model the dynamic occupancy of Asian elephants (Broms et al., 2016) in TYW. The model inferred the association between the occupancy states and ecological-anthropogenic covariates. The model was done by introducing probability parameters that justify the changing between states of using of unoccupied habitat, so-called colonization, and the unused of occupied habitat, so-called extinction. The model training was done in R program using unmarked package (Fiske and Chandler, 2011). All exploratory variables were standardized prior to training to improve convergence and interpretability. We firstly identified the most appropriate structure for detection probability parameters (ρ) on the top of full model using Akaike's information criterion (AIC) following Goswami et al. (2014) and Vasudev et al. (2021). Next, the optimal detection probability structure was

fixed to find the optimal initial occupancy (Ψ) based on the full model. Detection and initial state of occupancy were fixed at the optimal form and then selected for the best model combination for colonization probability (γ) and extinction probability (ε). All of the model comparisons were made based on AIC (Thapa et al., 2019). The predictive map of the whole study area was then created from the most optimal model combination to represent the spatial and temporal pattern of occupancy state.

3. RESULTS AND DISCUSSION

Asian elephant occurrence was recorded within 608 grid cells (16.34% of the total sanctuary area) during 2012-2019. The majority of these occupied cells were located in the southern portion of TYW. The parameters of the selected model determined the three components: the probability of initial occupancy (Ψ), colonization (γ), extinction (ε), and detection probability (ρ). The best-supported models were those with the lowest AIC values. Final model candidates were identified with eight site covariates (Table 1). The coefficients of the best-supported model for ρ were composed of patrol frequency (P_{freq}), annual total rainfall (R_{avr}), terrain ruggedness index (TRI), and distance to nearest the ranger station (RGS); with AIC weight of 0.65 (Table 2). For the initial occupancy Ψ, the model included four coefficients consist of elevation (ELV), distance to the nearest secondary stream (SST), normalized difference vegetation index (NDVI), and distance to the neatest population source (PPS) (Figure 5 and Table 3). For colonization-extinction processes, according to the best-supported model, the average probability of colonization across the study area was -4.83. The positive coefficients in the colonization model were composed of NDVI and ELV. In contrast, PPS showed a negative effect on γ (Figure 6 and Table 3). The best-supported model for extinction probability, ε, estimated an average of -7.095 across the study area. The PPS and VLG coefficients were positively associated with ε while THTyear and NDVI were negatively associated with ε. However, the effect of SLP on ε was negative but not significant (Figure 7 and Table 3). The predictive maps of initial occupancy, colonization probability, and extinction probability across the study landscape are shown in Figure 8.

Table 2. Results of top-five dynamic occupancy model selected based on AIC. The model composed of 4 submodels includes detection probability (ρ), occupancy probability of initial stage (Ψ), colonization probability (γ), and extinction probability (ε).

Dynamic occupancy model	Model AIC	ΔAIC	AIC weight	Model likelihood	#Par
Detection probability (ρ)					
ρ (P_{freq}, R_{avr}, TRI, RGS)	10,340.59	0.00	0.65	0.65	8
ρ (P_{freq}, R_{avr}, RGS)	10,342.45	0.68	0.26	0.91	7
ρ (R_{avr}, RGS)	10,345.58	4.99	0.05	0.96	6
ρ (R_{avr}, TRI, RGS)	10,347.40	6.81	0.02	0.99	7
ρ (P_{freq}, R_{avr})	10,350.04	9.45	0.01	0.99	6
Occupancy probability of initial stage (Ψ)					
Ψ (SST, NDVI, ELV, PPS)	9,676.45	0.00	0.14	0.14	12
Ψ (NDVI, ELV, PPS)	9,677.39	0.94	0.09	0.24	11
Ψ (SST, NDVI, ELV, PPS, THT12)	9,677.82	1.37	0.07	0.31	13
Ψ (VLG, SST, NDVI, ELV, PPS)	9,677.98	1.53	0.06	0.38	13
Ψ (MST, SST, NDVI, ELV, PPS)	9,678.31	1.86	0.05	0.43	13
Colonization probability (γ)					
γ (NDVI, ELV, PPS)	9,638.19	0.00	0.61	0.61	15
γ (VLG, SST, NDVI, ELV)	9,640.51	2.31	0.19	0.80	16
γ (VLG, SST, NDVI, ELV, THTyear)	9,642.43	4.24	0.07	0.87	17
γ (MST, NDVI, ELV, THTyear)	9,642.91	4.72	0.06	0.93	16
γ (VLG, MST, NDVI, ELV, SLP)	9,644.25	6.06	0.03	0.96	17
Extinction probability (ε)					
ε (VLG, SST, NDVI, SLP, PPS, THTyear)	9,639.91	0.00	0.58	0.58	18
ε (VLG, MST, SST, NDVI, SLP, PPS, THTyear)	9,642.36	2.45	0.17	0.75	19
ε (VLG, SST, NDVI, PPS, THTyear)	9,644.60	4.69	0.06	0.81	17
ε (VLG, MST, SST, NDVI, PPS, THTyear)	9,646.02	6.11	0.03	0.84	18
ε (VLG, MST, NDVI, ELV, PPS, THTyear)	9,647.11	7.20	0.02	0.85	18

Table 3. Summaries of estimated coefficients based on the best-supported model of dynamic occupancy parameters composed of Initial (Ψ), Colonization (γ), and Extinction (ε)

Model	β_{PPS} (SE)	β_{ELV} (SE)	B_{NDVI} (SE)	B_{SST} (SE)	B_{VLG} (SE)	β_{SLP} (SE)	$\beta_{THTyear}$ (SE)
Occupancy of initial state (Ψ)	-0.52(0.09)*	0.32(0.09)*	-0.26(0.08)*	0.16(0.09)			
Colonization (γ)	-1.3(0.51)*	1.37(0.39)*	1.13(0.31)*				
Extinction (ε)	1.88(0.54)*		-0.80(0.30)*	-8.03(19.85)	0.80(0.38)*	-0.33(0.26)	-5.17(1.89)*

*Significant associate with β coefficients for each covariates.

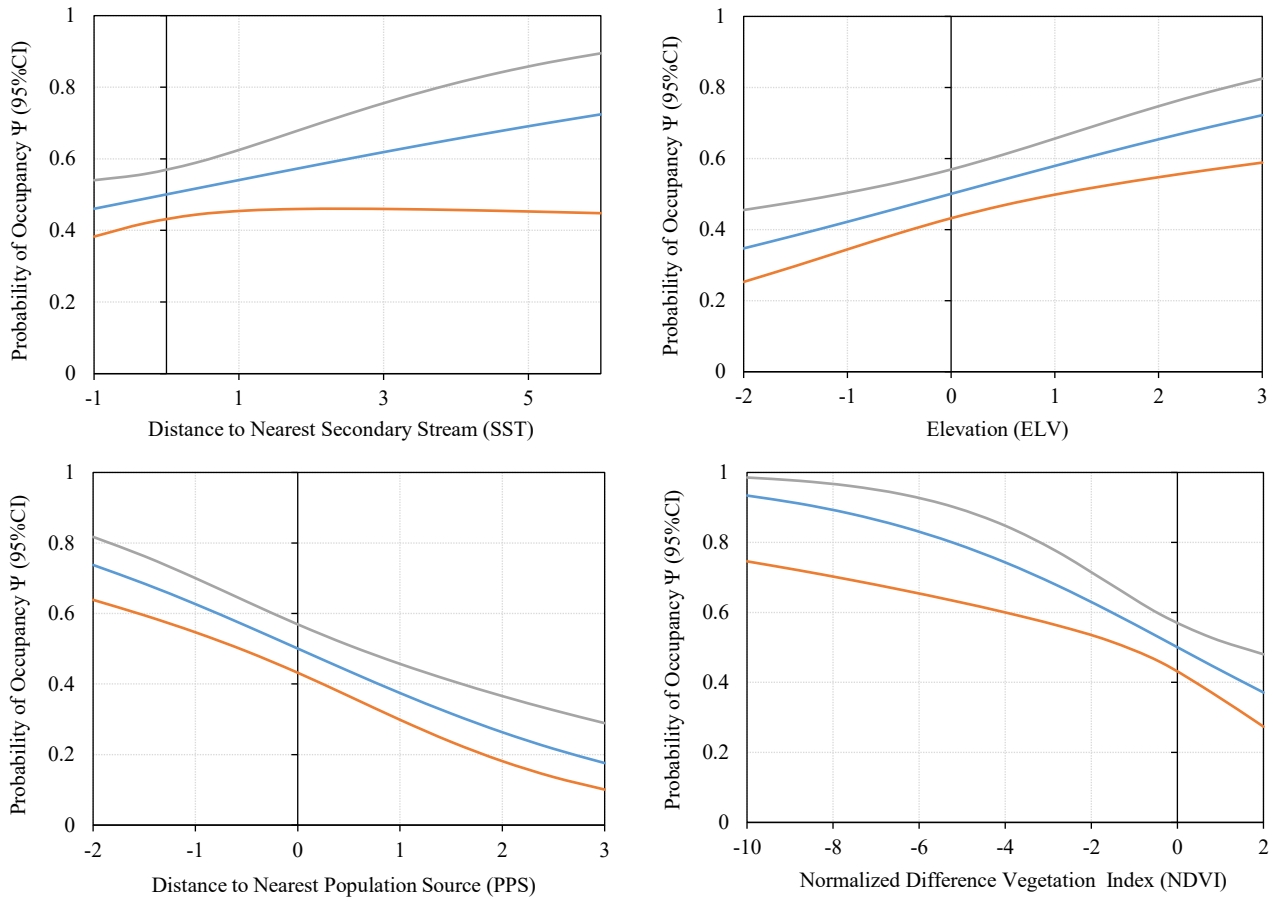

Figure 5. Relationship between influential covariates and estimated Ψ (95% CI) based on best-supported model

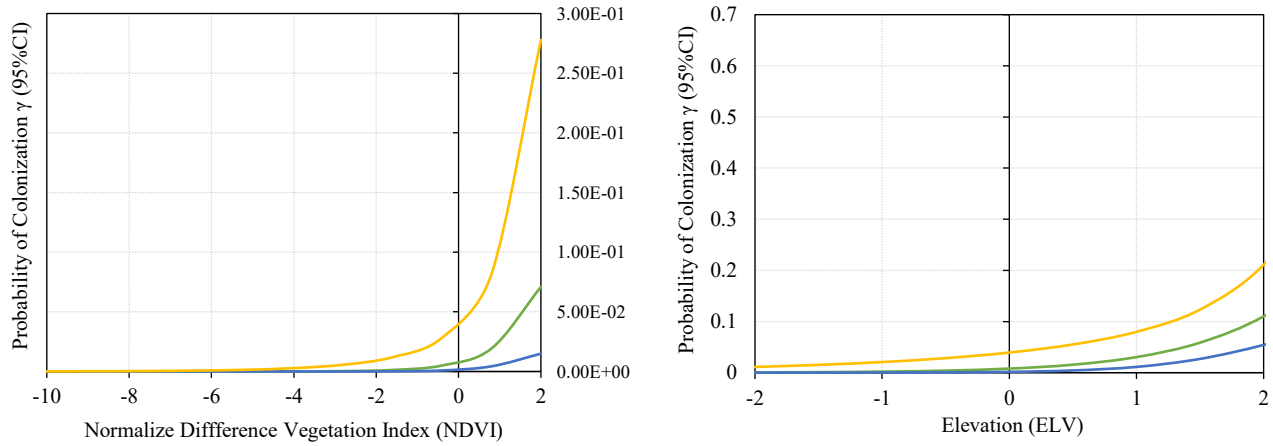

Figure 6. Relationship between influential covariates and estimated γ (95% CI) based on best-supported model

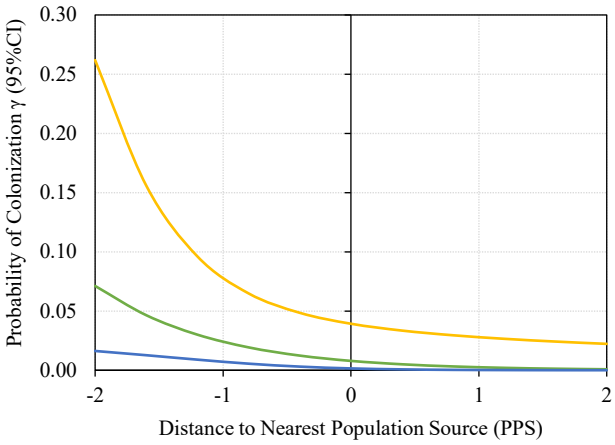

Figure 6. Relationship between influential covariates and estimated γ (95% CI) based on best-supported model (cont.)

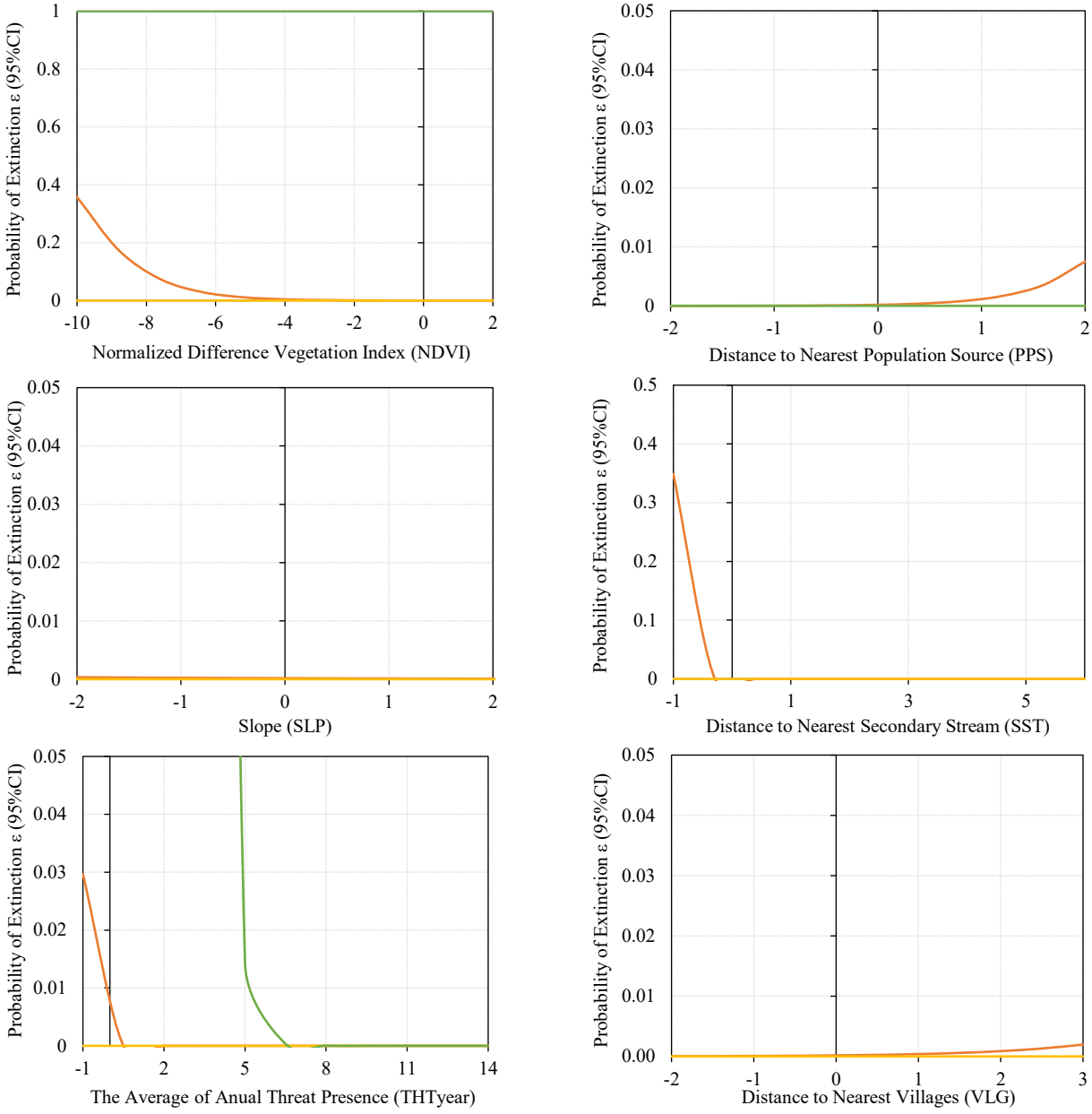

Figure 7. Relationship between influential covariates and estimated ϵ (95% CI) based on best-supported model

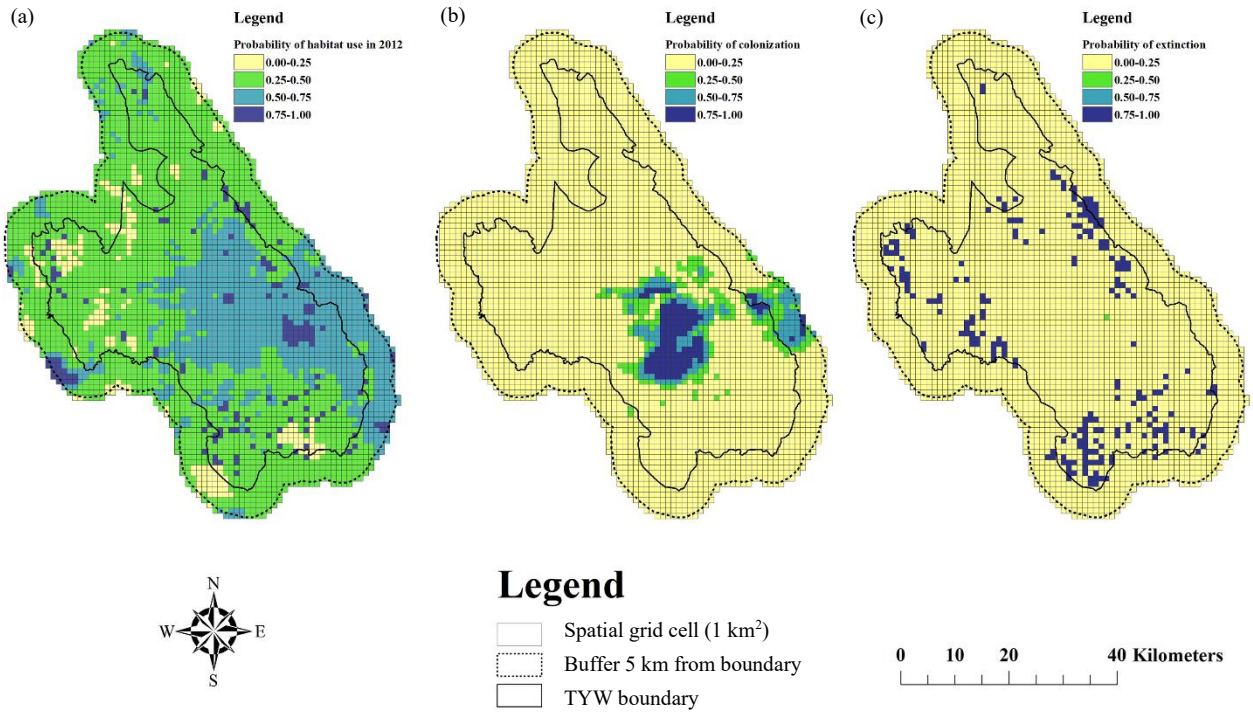

Figure 8. Map of spatially estimated dynamic occupancy parameters across the study area. (a) initial occupancy probability (Ψ), (b) colonization probability (γ), and (c) local extinction probability (ε)

Conservation and management of Asian elephant require robust assessments of populations and patterns of occupancy at the landscape scale. Analyzing occupancy across both spatial and temporal scales may provide helpful information about the influence of environmental conditions, human activity, and management on habitat use and dispersal across the landscape (DNP, 2013; Vinitpornsawan, 2013). Anthropogenic factors may significantly influence many wildlife species, especially keystone species like Asian elephant, and could subsequently affect others (Simberloff, 1998). Intensive human activities historically occurred in the TYW, especially exploration and site preparation for Nam Joan Dam between 1981 and 1988 and mineral extraction suspended in 1990. However, human activity in TYW still exists from nearby settlements in the easily accessible northern part of the conservation area that may affect wildlife habitat, behavior, and population (Duengkae, 2009; Steinmetz et al., 2006). The SMART patrol system has been in use in TYW since 2008, and has provided long-term data on natural resources and threats (Trisurat, 2004). A long-term database of patrol records has further revealed the restricted recolonization of Asian elephants in TYW between 2008 and 2018 (ca. 28.6%). The expansion of the Asian elephant population was thought to be attributable to effective law enforcement.

Dynamic prediction of Asian elephant occupancy patterns has indicated a high probability in TYW southern areas connected to the Huai Kha Kaeng Wildlife Sanctuary and Khuean Srinagarindra National Park, which is the source of the Asian elephant population in WEFCOM (DNP, 2017; IUCN, 2017; Sukmasuang, 2009). Habitat use of Asian elephant could have depended on the availability of resources and impeding factors in and to the destination site (Suksavate et al., 2019). The transboundary distribution extends across the Mae Klong River to the mountain range with ELV of 800-1,800 m and high canopy cover. Higher ELV and NDVI values impact the habitat occupancy of Asian elephants; however, Asian elephants are capable of moving to a wide variety of elevations, and Asian elephants were recorded from sea level to montane (Rood et al., 2010). The NDVI is related to plant community structure and land use that negatively affects primary productivity and reflects the availability of food sources in habitat patches (IUCN, 2020; Jathanna et al., 2015). Natural water sources also play an essential role in the seasonal distribution of elephants (Thouless, 1995). The temporal availability and spatial distribution of food and water are critical to elucidating the local habitat occupancy of the Asian elephant (Kumar et al., 2010; Thapa et al., 2019). According to the SMART database, nearly all

signs of Asia elephants have been found in dry evergreen forests compared to tropical rain forests, while Sukumar (2003) suggested that Asian elephants use a variety of habitats, ranging from dry to wet evergreen forests and attain high densities in deciduous forests with substantial grass and bamboo forage. We found weak evidence that the TRI affects occupancy, as nearly all Asian elephant tracks and other signs observed by rangers in mountainous areas were in the vicinity of ridges and flats. Goswami et al. (2014) reported that Asian elephant intensively used sites with high ruggedness. Thapa et al. (2019) reported that a higher TRI, along with forage and water resources, may drive occupancy patterns in areas of high ruggedness.

Our results indicate that human activity in the vicinity of villages within protected areas is a crucial variable impacting occupancy of Asian elephant. Buji et al. (2007) reported that human activity appears to drive Asian elephant distribution in areas where human impacts were thought to be a limiting factor, while Vinitpornsawan (2013) suggested that while the impacts of activities by local people are complex, poaching appears to be the critical factor influencing wildlife abundance and habitat use. Our model indicated dissociation between occupancy and proximity to human settlement and activities, overcoming threat occurrence that had a relatively negative effect on extinction probability. The SMART database indicated that the range of Asian elephants overlaps with the distribution of threats in the southern part of the TYW, which are associated with human settlements connected to other protected areas. The increasing patrol intensity in risky areas such as settlements (Duangchantrasiri et al., 2016; Jornburom et al., 2020) by controlling edge effects (Balme et al., 2010) could reduce the threat to the local wildlife population. Sampson et al. (2018) reported that poachers killed more than 40 Asian elephants in south-central Myanmar for their skin and ivory. However, we have not detected Asian elephant poaching in the TYW, the tiny Asian elephant population in the Myanmar transboundary area, which still lacks information of threat and status on Asian elephants, was found to be dispersed to the area with dense human population in the northern part of TYW.

In our study, the SMART database is highly biased information compared to the research survey, but it had a much larger capacity with continuous collection due to the extensive data recording across space and time. The data could be enhanced to increase the usefulness of studying and monitoring natural resources in the protected areas across the country by implementing bias alleviating methods, for example, dealing with auto-correlation sampling biases in developing occupancy models (Jornburom et al., 2020). Moreover, more detail in temporally ecological covariates could be necessary to accurately determine the occupancy dynamics by including the effect of season, resource availability, and microclimate (Thapa et al., 2019).

4. CONCLUSION

We evaluated and predicted the dynamic occupancy patterns of Asian elephants in the TYW using SMART data collected during 2012-2019 using the monitoring database collected during patrol. The most optimal dynamic occupancy model clarified the re-occupation pattern of the Asian elephant population within TYW and transboundary areas connecting to adjacent protected areas. The results showed that the distance to the initial population sources and vegetation pattern was influential to both the colonization and extinction processes. In contrast, the anthropogenic factors, distance to the nearest village, and poaching were essential to the local extinction process. The spatial prediction from a long-term sustained database could help managers gain insight into the dynamics of the Asian elephant occupation processes across the conservation landscape. The predicted map could provide valuable information in management approaches such as threat prevention to allow dispersal and availability of Asian elephant population and alleviate human-elephant conflict across the protected area and agricultural interface.

ACKNOWLEDGEMENTS

We sincerely thank Thailand's Department of National Park, Plant and wildlife Conservation (DNP), especially Thung Yai Naresuan West Wildlife Sanctuary (TYW) and SMART patrol monitoring center for permission to conduct this research. We also thank Wildlife Conservation Society (WCS) Thailand program for providing financial support. We special thank Mr. Manoon Pliosungnoen, Mr. Chatee Ariyapitak, Ms. Apinya Sisamorn, Mr. Krittaphat Lueachang and all of our colleagues in WCS for their assisstance.

REFERENCES

Allbrook DL, Quinn JL. The effectiveness of regulatory signs in controlling human behaviour and Northern gannet (*Morus*

bassanus) disturbance during breeding: An experimental test. Journal for Nature Conservation 2020;58:Article No. 125915.

Balme GA, Slotow R, Hunter LTB. Edge effects and the impact of non-protected areas in carnivore conservation: Leopards in the Phinda-Mkhuze Complex, South Africa. Animal Conservation 2010;13(3):315-23.

Broms KM, Hooten MB, Johnson DS, Altwegg R, Conquest LL. Dynamic occupancy models for explicit colonization processes. Ecology 2016;97(1):194-204.

Buji R, McShea WJ, Campbell P, Lee ME, Dallmeier F, Guimondou S, et al. Patch-occupancy models indicate human activity as major determinant of forest elephant *Loxodonta cyclotis* seasonal distribution in an industrial corridor in Gabon. Biological Conservation 2007;135:189-201.

Cardillo M, Mace GM, Jones KE, Bielby J, Bininda-Emonds ORP, Sechrest W, et al. Multiple causes of high extinction risk in large mammal species. Science 2005;309(5738):1239-41.

Davis M, Faurby S, Svenning J-C. Mammal diversity will take millions of years to recover from the current biodiversity crisis. Proceedings of the National Academy of Sciences 2018;115(44):11262-7.

Department of National Parks Plant and Willdife Conservation (DNP). Recovery of Tigers and Other Threatened Wildlife in the Western Forest Complex 2005-2013. DNP; 2013.

Department of National Parks Plant and Wildlife Conservation (DNP). Status of Large Mammals in Thailand. DNP; 2017. (in Thai).

Duangchantrasiri S, Umponjan M, Simcharoen S, Pattanavibool A, Chaiwattana S, Maneerat S, et al. Dynamics of a low-density tiger population in Southeast Asia in the context of improved law enforcement. Conservation Biology 2016; 30(3):639-48.

Duangchatrasiri S, Jornburom P, Jinamoy S, Pattanvibool A, Hines JE, Arnold TW, et al. Impact of prey occupancy and other ecological and anthropogenic factors on tiger distribution in Thailand's western forest complex. Ecology and Evolution 2019;9(5):2449-58.

Duengkae P. Change in Bird Species Assemblages Following Successional Stages in Abandoned Settlement Areas in Thung Yai Naresuan Wildlife Sanctuary [dissertation]. Thailand, Kasetsart University; 2009. (in Thai).

Fiske I, Chandler R. Unmarked: An R package for fitting Hierarchical model of wildlife occurrence and abundance. Journal of Statistical Software 2011;43(10):1-23.

Goswami VR, Sridhara S, Medhi K, Williams AC, Chellam R, Nichols JD, et al. Community-managed forests and wildlife-friendly agriculture play a subsidiary but not substitutive role to protected areas for the endangered Asian elephant. Biological Conservation 2014;177:74-81.

Hötte M, Kolodin I, Bereznuk S, Slaght J, Kerley L, Soutyrina S, et al. Indicators of success for smart Law enforcement in protected areas: A case study for Russian Amur Tiger (*Panthera tigris altaica*) reserves. Integrative Zoology 2015;11(1):2-15.

International Union for Conservation of Nature (IUCN). *Elephas maximus*. The IUCN red list of threatened species 2020 [internet]. 2020 [cited 2022 Mar 25]. Available from: https://www.iucnredlist.org/species/7140/45818198.

International Union for Conservation of Nature (IUCN). Updating 2017 Thailand Mapping of Wild Elephant Presence Sites, Population, and HEC Presence Sites. Bangkok, Thailand: IUCN; 2017.

Jathanna D, Karanth KU, Kumar NS, Karanth KK, Goswami VR. Patterns and determinants of habitat occupancy by the Asian elephant in the Western Ghats of Karnataka, India. PLoS ONE 2015;10(7):e0133233.

Jornburom P, Duangchantrasiri S, Jinamoy S, Pattanavibool A, Hines JE, Arnold TW, et al. Habitat use by tiger prey in Thailand's Western Forest Complex: What will it take to fill a half- full tiger landscape? Journal for Nature Conservation 2020;58:Article No. 125896.

Kanchanasaka B. Ecology of otters in the upper Khwae Yai River Thung Yai Naresuan Wildlife Sanctuary Thailand. Natural History Bulletin of the Siam Society 1997;45:79-92.

Krishnan V, Kumar MA, Raghunathan G, Vijayakrishnan S. Distribution and habitat use by Asian elephants (*Elephas maximus*) in a coffee-dominated landscape of Southern India. Tropical Conservation Science 2019;12:1-12.

Kumar MA, Mudappa D, Raman TRS. Asian elephant elephas maximus habitat use and ranging in fragmented rainforest and plantations in the Anamalai Hills, India. Tropical Conservation Science 2010;3(2):143-58.

Leimgruber P, Gagnon JB, Wemmer C, Kelly DS, Songer MA, Selig ER. Fragmentation of Asia's remaining wildlands: Implications for Asian elephant conservation. Animal Conservation 2003;6(4):347-59.

MacKenzie DI, Nichols JD, Hines JE, Knutson MG, Franklin AB. Estimating site occupancy, colonization, and local extinction when a species is detected imperfectly. Ecology 2003; 84(8):2200-7.

Marescot L, Lyet A, Singh R, Carter N, Gimenez O. Inferring wildlife poaching in southeast Asia with multispecies dynamic occupancy models. Ecography 2019;43(2):239-50.

McClenachan L, Andrew BC, Nicholas KD. Rethinking trade-driven extinction risk in marine and terrestrial megafauna. Current Biology 2016;26(12):1640-6.

Nekaris KA-I, Arnell AP, Svensson MS. Selecting a conservation surrogate species for small fragmented habitats using ecological Niche modelling. Animals (Basel) 2015;5(1):27-40.

Pettorelli N, Ryan S, Mueller T, Bunnefeld N, Jedrzejewska B, Lima M, et al. The normalized difference vegetation index (NDVI): Unforeseen successes in animal ecology. Climate Research 2011;46(1):15-27.

Rood E, Ganie AA, Nijman V. Using presence-only modelling to predict Asian elephant habitat use in a tropical forest landscape: Implications for conservation. Diversity and Distributions 2010;16(6):975-84.

Sampson C, McEvoy J, Oo ZM, Chit AM, Chan AN, Tonkyn D, et al. New elephant crisis in Asia-Early warning signs from Myanmar. PLoS ONE 2018;13(3):e0194113.

Scott JM, Heglund P, Morrison ML, Wall WA, Haufler J. Predicting Species Occurrences: Issues of Accuracy and Scale, Washington DC, USA: Island Press; 2002.

Simberloff D. Flagships, umbrellas, and keystones: Is single-species management passé in the landscape era? Biological Conservation 1998;83(3):247-57.

Simcharoen S, Pakpiean S, Arunprabharat W. Relationship between leopard and environmental factors in Huai Kha Khaeng Wildlife Sanctuary, Uthai Thani Province. Journal of Wildlife in Thailand 2007;14(1):65-79. (in Thai).

Steinmetz R, Chutipong W, Seuaturien N. Collaborating to conserve large mammals in Southeast Asia. Conservation Biology 2006;20(5):1391-401.

Stokes EJ. Improving effectiveness of protection efforts in tiger source sites: Developing a framework for law enforcement monitoring using MIST. Integrative Zoology 2010;5(4):363-77.

Sukmasuang R. Population density of Asian elephants in Huai Kha Khaeng Wildlife Sanctuary. Thai Journal of Forestry 2009; 28(1):40-50.

Suksavate W, Duengkae P, Chaiyes A. Quantifying landscape connectivity for wild Asian elephant populations among fragmented habitats in Thailand. Global Ecology and Conservation 2019;19:e00685.

Sukumar R. A brief review of the status, distribution and biology of wild Asian elephants *Elephas maximus*. International Zoo Yearbook 2006;40(1):1-8.

Sukumar R. The Living Elephants: Evolutionary Ecology, Behaviour, and Conservation. 1st ed. Oxford University Press; 2003.

Thapa K, Kelly MJ, Pradhan NMB. Elephant (*Elephas maximus*) temporal activity, distribution, and habitat use patterns on the tiger's forgotten trails across the seasonally dry, subtropical, hilly Churia forests of Nepal. PLoS ONE 2019;14(5): e0216504.

Thouless CR. Long distance movements of elephants in northern Kenya. African Journal of Ecology 1995;33(4):321-34.

Vasudev D, Goswami VR, Oli MK. Detecting dispersal: A spatial dynamic occupancy model to reliably quantify connectivity across heterogeneous conservation landscapes. Biological Conservation 2021;253:Article No. 108874.

Vinitpornsawan S. Population and Spatial Ecology of Tigers and Leopards Relative to Prey Availability and Human Activity in Thung Yai Naresuan (East) Wildlife Sanctuary, Thailand [dissertation]. Amherst, University of Massachusetts; 2013.

Trisurat Y. GIS Database and Its Applications for Ecosystem Management. Bangkok, Thailand: Department of National Parks, Wildlife and Plant Conservation (DNP) and The Western Forest Complex, Ecosystem Management Project (WEFCOM); 2004.

Synthesis of Hydroxyapatite/Zinc Oxide Nanoparticles from Fish Scales for the Removal of Hydrogen Sulfide

Dan-Thuy Van-Pham[1], Vien Vinh Phat[1], Nguyen Huu Chiem[2], Tran Thi Bich Quyen[1], Ngo Truong Ngoc Mai[1], Dang Huynh Giao[1], Ta Ngoc Don[3], and Doan Van Hong Thien[1*]

[1]Department of Chemical Engineering, Can Tho University, 3/2 Street, Ninh Kieu District, Can Tho City, Vietnam
[2]Department of Environmental Sciences, Can Tho University, 3/2 Street, Ninh Kieu District, Can Tho City, Vietnam
[3]Ministry of Education and Training, No 35, Dai Co Viet, Hanoi, Vietnam

ARTICLE INFO

Received: 21 Nov 2021
Received in revised: 28 Feb 2022
Accepted: 4 Mar 2022
Published online: 1 Apr 2022
DOI: 10.32526/ennrj/20/202100228

Keywords:
Hydrogen sulfide/ Hydroxyapatite/ Room temperature/ Zinc oxide

*** Corresponding author:**
E-mail: dvhthien@ctu.edu.vn

ABSTRACT

The presence of hydrogen sulfide (H_2S) is an issue for industrial processing, such as gasoline, natural gas, and biogas. In this study, hydroxyapatite (HA) nanoparticles with high purity were successfully extracted from red tilapia fish scales and used as supporting materials for zinc oxide (ZnO) to remove H_2S. Various amounts of ZnO decorated on HA nanoparticles were prepared from a zinc nitrate hexahydrate precursor. Powder X-ray diffraction (XRD) and Fourier transform infrared spectroscopy (FTIR) of the ZnO/HA samples demonstrated the successful synthesis of ZnO/HA with high purity. The scanning electron microscope (SEM) image analysis confirmed the uniform deposition of ZnO on HA nanoparticles which were smaller than 245 nm. The ZnO/HA samples with different ZnO loadings (i.e., 5, 10, and 15 wt%) were used to remove H_2S at room temperature. The specific surface area of HA and ZnO/HA determined by the Brunauer-Emmett-Teller (BET) method was 37.022 (m^2/g) and 111.609 (m^2/g), respectively. The experimental results demonstrated the highest breakthrough sulfur capacity of 26.3 mg S/g with the sorbent ZnO (15 wt%)/HA nanoparticles. This H_2S adsorption capacity was the highest capacity ever achieved for ZnO/HA.Therefore, there are great possibilities for effective removal of H_2S at the ambient conditions using the ZnO (15 wt%)/HA nanoparticles, where HA nanoparticles could be sustainably extracted from the abundant organic source of red tilapia fish scales.

1. INTRODUCTION

Hydrogen sulfide (H_2S) is one of the most difficult issues for energy industries such as natural gas, biogas, liquefied gas, and gasoline since it causes the corrosion of pipes and equipment, and poisons catalysts even at low concentrations (de Falco et al., 2018; Gupta et al., 2021; Han et al., 2020; Liu et al., 2012; Qiu et al., 2021). H_2S is usually treated by biological, physical and chemical methods (Gupta et al., 2021; Qiu et al., 2021; Wang et al., 2021). Among them, the chemical treatment method, particularly chemical adsorption, has the highest removal efficiency (Ali et al., 2020a; Ali et al., 2020b; Ali and Saleh, 2020; de Falco et al., 2018; Gupta et al., 2021; Qiu et al., 2021; Quan et al., 2021; Saleh, 2020; Saleh, 2021b; Singh et al., 2019). Metal oxides are often used as chemical adsorbents for high performance. For example, zinc oxide (ZnO) is a well-known photocatalyst for the degradation of several environmental contaminants due to being a non-toxic and inexpensive material with a high capacity to adsorb H_2S (Buazar et al., 2015). Moreover, it has been known to have a high equilibrium constant for H_2S removal at the ambient temperature ranging from 5.9 mg S/adsorbent to nearly 96.5 mg S/adsorbent (Al-Hammadi et al., 2018; Al-Jamimi and Saleh, 2019; de Falco et al., 2018; Geng et al., 2019; Gupta et al., 2021; Saleh et al., 2019; Saleh et al., 2020).

There are various ways to synthesize ZnO NPs (Buazar et al., 2016a; Buazar et al., 2016b). However, there are some difficulties in using ZnO directly as an adsorbent. The main drawback reported by previous

Citation: Van-Pham D-T, PhatVV, Chiem NH, Quyen TTB, Mai NTN, Giao DH, Don TN, Thien DVH. Synthesis of hydroxyapatite/zinc oxide nanoparticles from fish scales for the removal of hydrogen sulfide. Environ. Nat. Resour. J. 2022;20(3):323-329. (https://doi.org/10.32526/ennrj/20/202100228)

studies is that the higher the temperatures of the adsorption process are used, the lower the mechanical stability of chemical interaction between the support and the active site (Singh et al., 2019). Recently, ZnO on various base supports (e.g., activated carbon, zeolite, silicon dioxide, multiwall carbon nanotubes, and reduced graphite oxide) to remove H_2S at room temperature have been reported (de Falco et al., 2018; Geng et al., 2019; Singh et al., 2019). Hernández et al. (2011) used zinc oxide on activated carbon to remove H_2S (Hernández et al., 2011). Liu et al. (2012) implemented ZnO/SiO_2 gel composites to remove H_2S and the highest H_2S adsorption capacity was 96.4 mg/g (Liu et al., 2012). Song et al. (2013) removed hydrogen sulfide by zinc oxide/reduced graphite oxide composite (Song et al., 2013). Abdullah et al. (2018) reported the removal of hydrogen sulfide from biogas by using zinc oxide-impregnated zeolite with the maximum capacity of H_2S adsorption of 15.75 mg/g (Abdullah et al., 2018). Singh et al. (2019) used ZnO-decorated multiwall carbon nanotubes for efficient H_2S removal (Singh et al., 2019). Most recently, Geng and coworkers used a zinc oxide nanoparticle/ molecular sieve to remove hydrogen sulfide with the highest capacity of 54.9 mg/g (Geng et al., 2019).

Hydroxyapatite (HA) $Ca_{10}(PO_4)_6(OH)_2$ is the main component of bone and hard tissue of animals (Thien et al., 2015; Thien et al., 2021). HA nanoparticles are capable of binding to metal ions such as Zn^{2+}, Cd^{2+}, and Cu^{2+} (Ibrahim et al., 2020). HA nanomaterials have been synthesized by various methods including sol-gel, precipitation, hydrothermal, and microwave-assisted synthesis (Ibrahim et al., 2020; Thien et al., 2021). Significant advantages of the precipitation method for synthesizing HA are that it is simple, cost-effective, and highly repeatable. Moreover, this method can be used to extract HA from bio-wastes such as eggshell, cow bone, coral, shells, and especially fish scales, major wastes in aquatic product processing (Kongsri et al., 2013; Thien et al., 2021).

In this study, HA was extracted from the scales of red tilapia (*Oreochromis* sp.), the most popular freshwater fish in the Mekong Delta, Vietnam. Next, HA was combined with a precursor of zinc nitrate under appropriate conditions to prepare ZnO/HA materials available for the removal of H_2S. Finally, ZnO/HA materials were applied to remove H_2S at ambient conditions.

2. METHODOLOGY

2.1 Materials

Hydrochloric acid (HCl), sodium hydroxide (NaOH), ammonium hydroxide (NH_4OH) (28-30%), and zinc nitrate hexahydrate ($Zn(NO_3)_2 \cdot 6H_2O$) (99%) were purchased from Merck. Distilled water was used for all experiments. Hydrogen sulfide and nitrogen were supplied by a local company in Vietnam.

2.2 Methods

2.2.1 Preparation of hydroxyapatite nano-powders from fish scales

The scales of red tilapia (*Oreochromis* sp.) were collected from a local market in Ninh Kieu District, Can Tho City, Vietnam. They were soaked and rinsed in distilled water several times to remove salts and dirty substances. To deprotein, the scales were soaked and stirred in 0.1 M HCl solution for 15 min at room temperature and washed several times with distilled water. The residue of HCl was neutralized by 5% (w/v) NaOH solution. The remaining proteins of fish scales were treated with 50% (w/v) NaOH, heated and stirred at 100°C for 80 min. The precipitated (nanopowder) particles were filtered and washed with distilled water before being dried at 60°C (Kongsri et al., 2013; Zainol et al., 2019).

2.2.2 Preparation of ZnO/hydroxyapatite nano-powders

ZnO/hydroxyapatite nanopowders were prepared via a two-step in-situ deposition of $Zn(NO_3)_2$ on HA nanoparticles by a reaction with NH_4OH. Briefly, HA (1 g) was added to 50 mL of $Zn(NO_3)_2$ solution with the weight percent ZnO: HA ratios of 5/95, 15/85, and 30/70. Then, NH_4OH (25%) was added slowly to the solution until pH reached 10 under continuous stirring of 200 rpm for 24 h at room temperature. The precipitate was washed with distilled water several times. Finally, the precipitate was calcined at 500°C for 3 h.

2.2.3 Characterization of hydroxyapatite nano-powders and ZnO/hydroxyapatite nanopowders

Phase structures of HA and ZnO/HA materials were analyzed by X-ray diffraction (XRD, D8 Advance Brucker, Germany). XRD results were obtained for samples of HA and ZnO/HA at 2 theta in the range of 10°-70°.

The functional groups of HA and the interaction between ZnO and HA were characterized by Fourier transform infrared spectroscopy (FTIR, Nicolet 6700, Thermo Scientific).

Surface morphology of the hydroxyapatite and ZnO/HA nanopowders were observed by a scanning electron microscopy (SEM, JSM-6390LV, JEOL, Japan) at an accelerating voltage of 10 kV after gold coating.

2.2.4 Removal of H_2S

The adsorption experiments are described in Figure 1. The system consists of three main components: two gas cylinders for supplying a mixture of H_2S and nitrogen, a reactor (U-shaped Pyrex glass tube with an internal diameter of 8 mm and length of 30 cm), and a H_2S sensor (Alphasense company, England). To study H_2S adsorption ability, ZnO/HA samples (0.5 g) with ZnO/HA mass ratios of 5%, 10%, and 15% were fixed in the reactor. Experiments were carried out with an inlet H_2S concentration of 1,450 ppmv at ambient conditions (30°C, 1 atm). The sulfur adsorption capacity (SC) at the breakthrough point of the materials was determined by the following equation (Abdullah et al., 2018):

$$SC\left(\frac{g-sulfur}{100\ g-sorbent}\right) = WHSV \times \frac{M_S}{V_{mol}} \times \int_0^t (C_{in} - C_{out}) \times 10^{-4} dt \quad (1)$$

Where; WHSV is the weight hourly space velocity fixed at 0.176 (L/(min·g); M_S is the standard atomic weight of sulfur (32 g/mol); C_{in} is the inlet concentration of H_2S (1,450 ppmv); C_{out} is the outlet concentration of H_2S at the breakthrough point (ppmv); V_{mol} is the molar volume (24.5 L/mol) at standard condition (298 K and 1 atm); t is time of the adsorption until H_2S concentration in the output gases is higher than the breakthrough time (min).

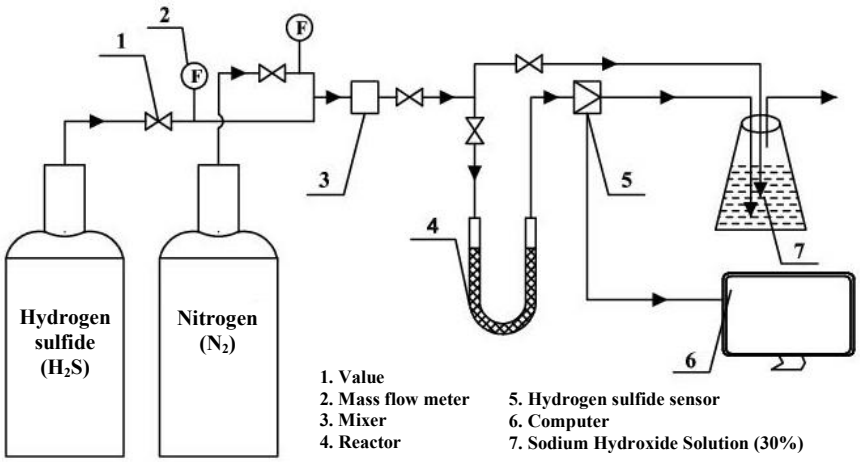

Figure 1. The experimental system for removing hydrogen sulfide

3. RESULTS AND DISCUSSION

3.1 Structural characterization of hydroxyapatite nanopowders and hydroxyapatite/ZnO nanopowders

Figure 2 shows XRD patterns of HA and HA/ZnO hydroxyapatite nanopowders with mass ratios of 5%, 15%, and 30%. From the XRD patterns, the intensities of the characteristic peaks of ZnO increased with the increase in concentrations of ZnO. The diffraction peaks at the 2θ of 25.9°, 31.78°, 32.15°, 32.83°, 34.04°, 39.70°, 46.68°, 49.39°, and 53.10° corresponding to the lattice planes of (002), (211), (112), (300), (202), (310), (222), (213), and (004), respectively could be exactly assigned to the HA phase (JCPDS No: 00-009-0432). The crystalline phase of ZnO can be observed at the 2θ of 31.7°, 34.4°, 36.3°, 47.5°, 56.6°, 62.9°, 66.4°, 67.9°, and 69.1° corresponding to the lattice planes of (100), (002), (101), (102), (110), (103), (200), (112), and (201) (JCPDS No: 36-1451). Thus, loaded ZnO based on HA materials were successfully prepared. To further understand the interactions between ZnO and HA as well as their morphologies, HA and ZnO/HA materials were characterized using FTIR and SEM methods.

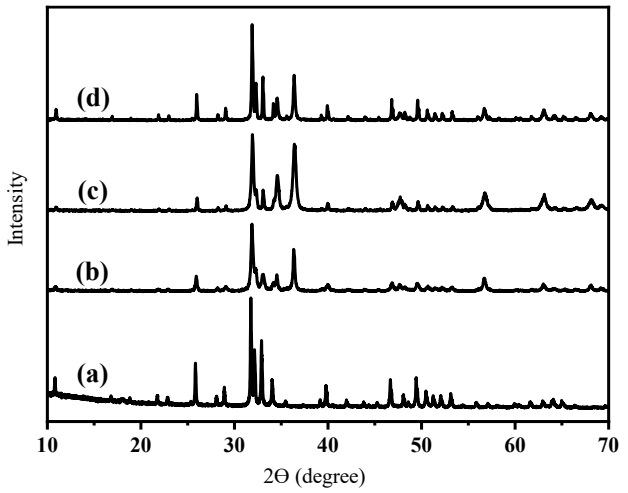

Figure 2. XRD patterns of HA and HA/ZnO nanopowders: (a) HA, (b) ZnO (5 wt%)/HA, (c) ZnO (15 wt%)/HA, and (d) ZnO (30 wt%)/HA

Figure 3 shows the FTIR spectra of HA and ZnO/HA particles. The functional groups OH^- and PO_4^{3-} of HA were characterized by oscillations at wavelengths 3,570 and 3,439 cm^{-1}. The characteristic P-O absorbances of PO_4^{3-} groups are at wavelengths 568, 603, 633, 1,035, 1,995 cm^{-1}. In the spectra, there are also typical fluctuations of CO_3^{2-} groups detected at the wavelength of 1,456 cm^{-1}, which indicates the presence of type B-HA, i.e., PO_4^{3-} functional groups are replaced by CO_3^{2-} functional groups. This result is completely consistent with that of Kongsri et al. (2013). In addition, no other strange vibrations were found in FTIR suggesting that HA material prepared from fish scales by the alkali heat method did not show the presence of other impurities. The FT-IR diagram of ZnO/HA in Figure 3(b) shows the functional groups are similar to those in Figure 3(a). This means that in the process of loading ZnO on HA, the functional groups of HA material were not changed (Saleh, 2011; Saleh, 2015a; Saleh, 2015b). However, from the FT-IR spectrum of ZnO/HA materials, the intensity of the oscillations of the PO_4^{3-} groups increases compared to that of HA material due to the connection between zinc and PO_4^{3-} groups (Zhou et al., 2008).

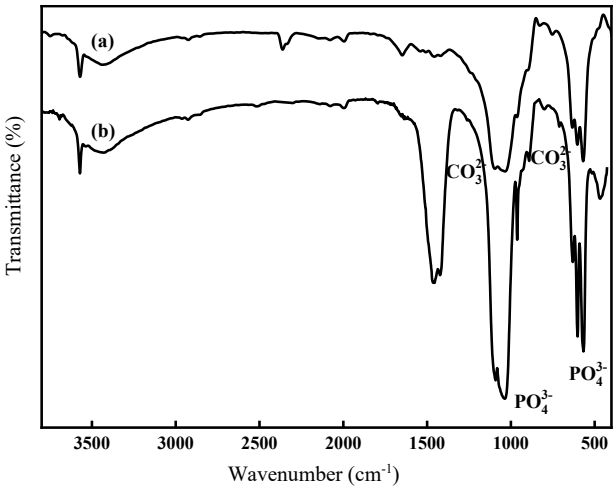

Figure 3. FTIR spectra: (a) HA and (b) ZnO (15 wt%)/HA

Figure 4 shows SEM images of synthesized HA and ZnO/HA. The morphology of HA and ZnO based on HA materials was the same. However, in Figure 4(b), the ZnO nanoparticles were uniformly deposited on the surface of the HA. The results were consistent with previous reports (Kongsri et al., 2013; Saleh, 2016; Saleh, 2018). Also, the specific surface area of HA was 37.022 m^2/g and ZnO/HA was 110.609 m^2/g. Thus, the H_2S adsorption capacity of ZnO/HA could be improved due to the enhanced surface area to volume ratio of the material.

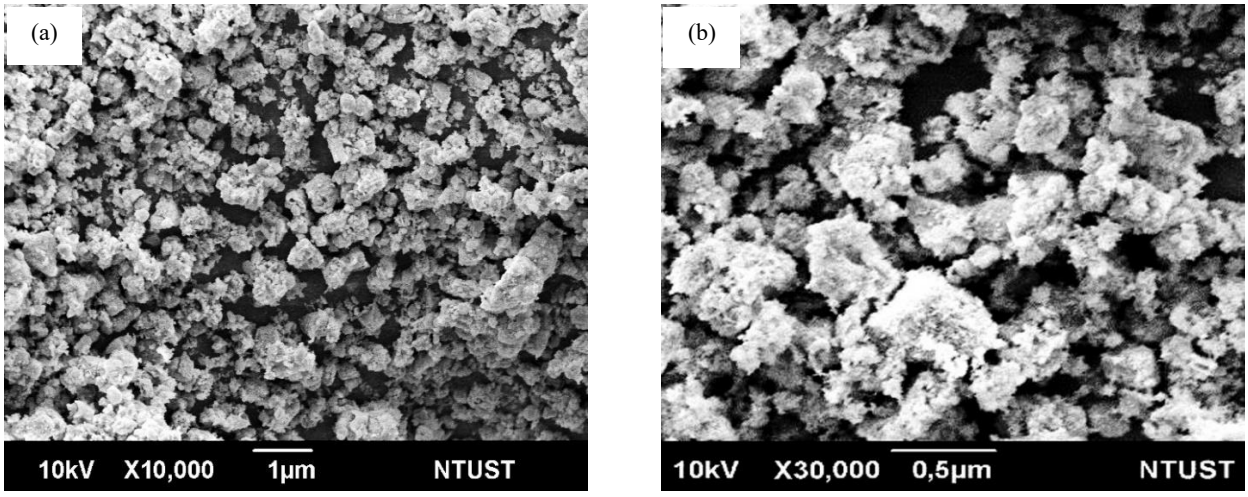

Figure 4. SEM images of (a) HA and (b) ZnO (15 wt%)/HA

3.2 Hydrogen sulfide adsorption capacity

The breakthrough curves of hydrogen sulfide for various samples of ZnO (5, 15, 30 wt%)/HA are shown in Figure 5(a). From the breakthrough curves of hydrogen sulfide, the corresponding adsorption capacities were determined according to Equation 1 and shown in Figure 5(b). At low loading ZnO, the adsorption capacity is low. When increasing ZnO content, the adsorption capacity increases and reaches a maximum value of 26.3 mg S/g sorbent for sample ZnO (15 wt%)/HA, then decreases with increasing ZnO content. Due to chemical affinity of ZnO to H_2S, the adsorption capacity increases when more ZnO is added. However, at the high content of ZnO loading, the excess of ZnO might agglomerate and collapse the active centers for desulphurization. Also, with 3 replicates in each sample, the difference is not significant. The results are in good agreement with previous studies (Abdullah et al., 2018; Geng et al., 2019; Liu et al., 2012; Saleh, 2021a; Saleh and Al-Hammadi, 2021; Wang et al., 2008). Therefore, 15 wt% of ZnO loaded on HA is the optimum content for the effective removal of H_2S.

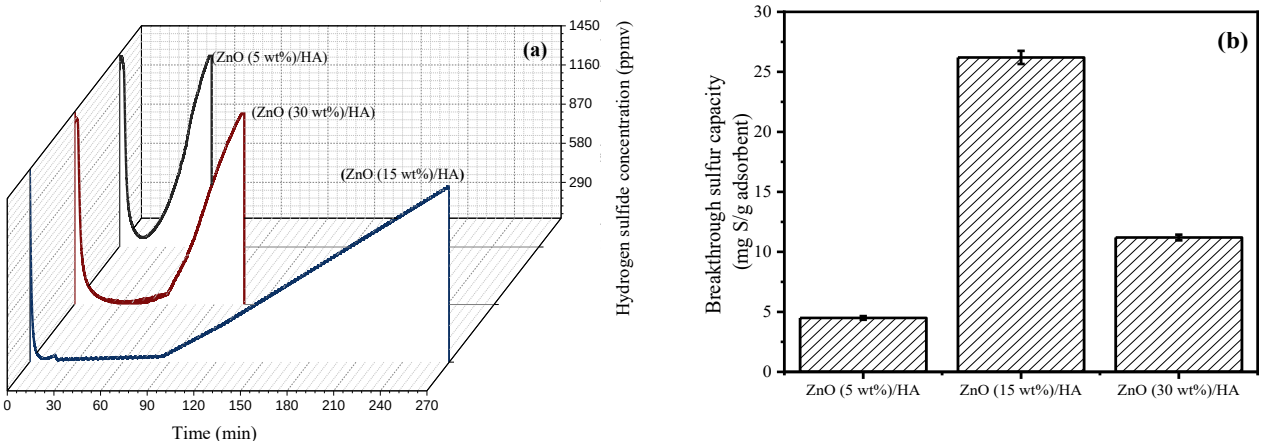

Figure 5. (a) The breakthrough curves of hydrogen sulfide with different ZnO loading (5, 15, 30 wt%) on HA nanoparticles; (b) The sulfur adsorption capacities of the different ZnO loading (5, 15, 30 wt%) on HA nanoparticles with 3 replicates (all experiments were carried out with an inlet H_2S concentration of 1,450 ppmv at 30°C, 1 atm)

Table 1 shows the adsorption capacity and the breakthrough time of (ZnO 15 wt%)/HA nanoparticles at the breakthrough point as well as ZnO based on some other carriers such as MCM-41, BSA-15, SiO_2, activated carbon, zeolite Na-A, and Zn-MOF reported in several studies for comparison. The adsorption capacity of ZnO based on HA is higher than that of ZnO based on MCM-41, BSA-15, activated carbon, and zeolite Na-A and lower than that of ZnO based on SiO_2 or activated carbon. It may be explained by the interactions between ZnO and carriers and by different morphologies and sizes of the sorbents. Thus, ZnO (15 wt%)/HA nanoparticles would be a promising material for the removal of H_2S.

Table 1. Sulfur capacities of sorbents based on ZnO at room temperature

Adsorbent	Sulfur adsorption capacity (mg S/g adsorbent)	Temperature (°C)	Breakthrough time (min)	References
ZnO (15 wt%)/MCM-41	5.9	25	~70	Hussain et al. (2012)
ZnO (15 wt%)/SBA-15-S	18.5	25	~200	Hussain et al. (2012)
ZnO (15 wt%)/SBA-15-F	15.6	25	~180	Hussain et al. (2012)
ZnO (15 wt%)/SiO_2	32.0	-	19	Dhage et al. (2010)
ZnO (20 wt%)/Activated carbons	17.1	30	2	de Falco et al. (2018)
ZnO (20 wt%)/Zeolite Na-A	24.0	28	60	Abdullah et al. (2018)
ZnO/Activated carbons	66.4	30	150	Yang et al. (2019)
ZnO-MgO (20 wt%)/Activated carbon	96.5	30	124	Yang et al. (2020)
Zn-MOF/ZnO nanocomposites	14.2	Ambient conditions	~11	Gupta et al. (2021)
ZnO (15 wt%)/HA	26.3	30	85	This work

4. CONCLUSION

High purity HA nanoparticles were successfully extracted from red tilapia scales, an abundant organic waste in the Mekong delta. From the obtained HA nanoparticles, ZnO/HA nanoparticles were also successfully prepared with a uniform ZnO loading of 5, 15, and 30 wt%. The uniform distribution of ZnO on HA, confirmed by SEM image analysis, facilitated the H_2S adsorption in a gas mixture. The adsorption processes at ambient conditions (30°C, 1 atm) were very useful in practical applications. Based on the adsorption capacity experiment results with different ZnO loadings, the 15 wt% ZnO/HA sample was found optimal with the maximum adsorption capacity for H_2S at the breakthrough point of 26.5 mg S/g adsorbent. This breakthrough sulfur capacity was the highest capacity ever reported for ZnO using HA as an effective carrier. Thus, ZnO/HA nanoparticles showed great potential in H_2S removal and the sustainable use of the enormous source of red tilapia scales.

ACKNOWLEDGEMENTS

This work was financially supported by the "Can Tho University Improvement Project VN14-P6, supported by a Japanese ODA loan", under grant number E7.

CONFLICT OF INTEREST

The authors declare that there is no conflict of interest.

REFERENCES

Abdullah AH, Mat R, Somderam S, Abd Aziz AS, Mohamed A. Hydrogen sulfide adsorption by zinc oxide-impregnated zeolite (synthesized from Malaysian kaolin) for biogas desulfurization. Journal of Industrial and Engineering Chemistry 2018;65:334-42.

Ali I, Al-Arfaj AA, Saleh TA. Carbon nanofiber-doped zeolite as support for molybdenum based catalysts for enhanced hydrodesulfurization of dibenzothiophene. Journal of Molecular Liquids 2020a;304:Article No. 112376.

Ali I, Al-Shafei EN, Al-Arfaj AA, Saleh TA. Influence of titanium oxide on the performance of molybdenum catalysts loaded on zeolite toward hydrodesulfurization reactions. Microporous and Mesoporous Materials 2020b;303:Article No. 110188.

Ali I, Saleh TA. Zeolite-graphene composite as support for molybdenum-based catalysts and their hydrodesulfurization performance. Applied Catalysis A: General 2020;598:Article No. 117542.

Al-Hammadi SA, Al-Amer AM, Saleh TA. Alumina-carbon nanofiber composite as a support for MoCo catalysts in hydrodesulfurization reactions. Chemical Engineering Journal 2018;345:242-51.

Al-Jamimi HA, Saleh TA. Transparent predictive modelling of catalytic hydrodesulfurization using an interval type-2 fuzzy logic. Journal of Cleaner Production 2019;231:1079-88.

Buazar F, Alipouryan S, Kroushawi F, Hossieni SA. Photo-degradation of odorous 2-mercaptobenzoxazole through zinc oxide/hydroxyapatite nanocomposite. Applied Nanoscience 2015;5(6):719-29.

Buazar F, Baghlani-Nejazd MH, Badri M, Kashisaz M, Khaledi-Nasab A, Kroushawi F. Facile one-pot phytosynthesis of magnetic nanoparticles using potato extract and their catalytic activity. Starch-Stärke 2016a;68(7-8):796-804.

Buazar F, Bavi M, Kroushawi F, Halvani M, Khaledi-Nasab A, Hossieni SA. Potato extract as reducing agent and stabiliser in a facile green one-step synthesis of ZnO nanoparticles. Journal of Experimental Nanoscience 2016b;11(3):175-84.

de Falco G, Montagnaro F, Balsamo M, Erto A, Deorsola FA, Lisi L, et al. Synergic effect of Zn and Cu oxides dispersed on activated carbon during reactive adsorption of H_2S at room temperature. Microporous and Mesoporous Materials 2018; 257:135-46.

Dhage P, Samokhvalov A, Repala D, Duin EC, Bowman M, Tatarchuk BJ. Copper-promoted ZnO/SiO_2 regenerable sorbents for the room temperature removal of H_2S from reformate gas streams. Industrial and Engineering Chemistry Research 2010;49(18):8388-96.

Geng Q, Wang LJ, Yang C, Zhang HY, Zhao YR, Fan HL, et al. Room-temperature hydrogen sulfide removal with zinc oxide nanoparticle/molecular sieve prepared by melt infiltration. Fuel Processing Technology 2019;185:26-37.

Gupta NK, Bae J, Kim S, Kim KS. Fabrication of Zn-MOF/ZnO nanocomposites for room temperature H_2S removal: Adsorption, regeneration, and mechanism. Chemosphere 2021;274:Article No. 129789.

Han X, Chen H, Liu Y, Pan J. Study on removal of gaseous hydrogen sulfide based on macroalgae biochars. Journal of Natural Gas Science and Engineering 2020;73:Article No. 103068.

Hernández SP, Chiappero M, Russo N, Fino D. A novel ZnO-based adsorbent for biogas purification in H_2 production systems. Chemical Engineering Journal 2011;176-177:272-9.

Hussain M, Abbas N, Fino D, Russo N. Novel mesoporous silica supported ZnO adsorbents for the desulphurization of biogas at low temperatures. Chemical Engineering Journal 2012;188:222-32.

Ibrahim M, Labaki M, Giraudon JM, Lamonier JF. Hydroxyapatite, a multifunctional material for air, water and soil pollution control: A review. Journal of Hazardous Materials 2020;383:Article No. 121139.

Kongsri S, Janpradit K, Buapa K, Techawongstien S, Chanthai S. Nanocrystalline hydroxyapatite from fish scale waste: Preparation, characterization and application for selenium adsorption in aqueous solution. Chemical Engineering Journal 2013;215:522-32.

Liu G, Huang Z-H, Kang F. Preparation of ZnO/SiO_2 gel composites and their performance of H_2S removal at room temperature. Journal of Hazardous Materials 2012;215-216:166-72.

Qiu B, Tao X, Wang H, Li W, Ding X, Chu H. Biochar as a low-cost adsorbent for aqueous heavy metal removal: A review. Journal of Analytical and Applied Pyrolysis 2021;155:Article No. 105081.

Quan W, Jiang X, Wang X, Song C. Hydrogen sulfide removal from biogas on ZIF-derived nitrogen-doped carbons. Catalysis Today 2021;371:221-30.

Saleh TA. Carbon nanotube-incorporated alumina as a support for MoNi catalysts for the efficient hydrodesulfurization of thiophenes. Chemical Engineering Journal 2021a;404:Article No. 126987.

Saleh TA. Isotherm, kinetic, and thermodynamic studies on Hg(II) adsorption from aqueous solution by silica-multiwall carbon nanotubes. Environmental Science and Pollution Research 2015a;22(21):16721-31.

Saleh TA. Nanocomposite of carbon nanotubes/silica nanoparticles and their use for adsorption of Pb(II): From surface properties to sorption mechanism. Desalination and Water Treatment 2016;57(23):10730-44.

Saleh TA. Nanomaterials: Classification, properties, and environmental toxicities. Environmental Technology and Innovation 2020;20:Article No. 101067.

Saleh TA. Protocols for synthesis of nanomaterials, polymers, and green materials as adsorbents for water treatment technologies. Environmental Technology and Innovation 2021b;24:Article No. 101821.

Saleh TA. Mercury sorption by silica/carbon nanotubes and silica/activated carbon: A comparison study. Journal of Water Supply: Research and Technology-Aqua 2015b;64(8):892-903.

Saleh TA. Simultaneous adsorptive desulfurization of diesel fuel over bimetallic nanoparticles loaded on activated carbon. Journal of Cleaner Production 2018;172:2123-32.

Saleh T. The influence of treatment temperature on the acidity of MWCNT oxidized by HNO_3 or a mixture of HNO_3/H_2SO_4. Applied Surface Science 2011;257:7746-51.

Saleh TA, Al-Hammadi SA. A novel catalyst of nickel-loaded graphene decorated on molybdenum-alumina for the HDS of liquid fuels. Chemical Engineering Journal 2021;406:Article No. 125167.

Saleh TA, Al-Hammadi SA, Al-Amer AM. Effect of boron on the efficiency of MoCo catalysts supported on alumina for the hydrodesulfurization of liquid fuels. Process Safety and Environmental Protection 2019;121:165-74.

Saleh TA, Sulaiman KO, Al-Hammadi SA. Effect of carbon on the hydrodesulfurization activity of MoCo catalysts supported on zeolite/active carbon hybrid supports. Applied Catalysis B: Environmental 2020;263:Article No. 117661.

Singh A, Pandey V, Bagai R, Kumar M, Christopher J, Kapur GS. ZnO-decorated MWCNTs as solvent free nano-scrubber for efficient H_2S removal. Materials Letters 2019;234:172-4.

Song HS, Park MG, Kwon SJ, Yi KB, Croiset E, Chen Z, et al. Hydrogen sulfide adsorption on nano-sized zinc oxide/reduced graphite oxide composite at ambient condition. Applied Surface Science 2013;276:646-52.

Thien DVH, Ho MH, Hsiao SW, Li CH. Wet chemical process to enhance osteoconductivity of electrospun chitosan nanofibers. Journal of Materials Science 2015;50(4):1575-85.

Thien DVH, Thuyen NTB, Quyen TTB, Chiem NH, Thuy VPD, Viet PH. Microwave-assisted synthesis of nanorod hydroxyapatite from eggshells. Vietnam Journal of Science, Technology and Engineering 2021;63(1):3-6.

Wang X, Sun T, Yang J, Zhao L, Jia J. Low-temperature H_2S removal from gas streams with SBA-15 supported ZnO nanoparticles. Chemical Engineering Journal 2008;142(1): 48-55.

Wang Y-C, Han M-F, Jia T-P, Hu X-R, Zhu H-Q, Tong Z, et al. Emissions, measurement, and control of odor in livestock farms: A review. Science of the Total Environment 2021; 776:Article No. 145735.

Yang C, Yang S, Fan H, Wang Y, Shangguan J. Tuning the ZnO-activated carbon interaction through nitrogen modification for enhancing the H_2S removal capacity. Journal of Colloid and Interface Science 2019;555:548-57.

Yang C, Wang Y, Fan H, de Falco G, Yang S, Shangguan J, et al. Bifunctional ZnO-MgO/activated carbon adsorbents boost H_2S room temperature adsorption and catalytic oxidation. Applied Catalysis B: Environmental 2020;266:Article No.118674.

Zainol I, Adenan NH, Rahim NA, Jaafar CNA. Extraction of natural hydroxyapatite from tilapia fish scales using alkaline treatment. Materials Today: Proceedings 2019;16:1942-8.

Zhou G, Li Y, Xiao W, Zhang L, Zuo Y, Xue J, et al. Synthesis, characterization, and antibacterial activities of a novel nano-hydroxyapatite/zinc oxide complex. Journal of Biomedical Materials Research Part A 2008;85(4):929-37.

Evaluation of Spontaneous DNA Damage Using the Alkaline Comet Assay in Lymphocyte Cells of Humans Living in the High Level Natural Radiation Area of Mamuju, Indonesia

Darlina, Teja Kisnanto, Devita Tetriana, Sofiati Purnami, Harry Nugroho Eko Surniyantoro, and Mukh Syaifudin*

Center for Research and Technology of Radiation Safety and Metrology, Research Organization of Nuclear Energy, National Agency for Research and Innovation, Jl. Lebak Bulus Raya No. 49 Jakarta, Indonesia

ARTICLE INFO

Received: 22 Dec 2021
Received in revised: 6 Mar 2022
Accepted: 11 Mar 2022
Published online: 1 Apr 2022
DOI: 10.32526/ennrj/20/202100253

Keywords:
DNA damage/ Comet assay/ Natural radiation exposure/ Mamuju

*** Corresponding author:**
E-mail:
mukh_syaifudin@batan.go.id

ABSTRACT

To evaluate the biological impacts of high background radiation exposures that are represented by spontaneous deoxyribonucleic acid (DNA) damage, an evaluation on lymphocyte cells from residents of Mamuju, West Sulawesi, Indonesia was tested. The mean annual dose received by individuals in this area is about 10.40 mSv. Of the 177 adult subjects studied, 102 were from high-level natural radiation areas of Mamuju and 75 subjects were from a nearby normal-level natural radiation area. Both areas are similar in living situations. DNA strand breaks and other parameters of study and control group were determined using a standardized comet assay. Our results showed that chronic low-level natural radiation had resulted in significantly higher ($p<0.001$) DNA damage based on the three parameters of the assay (tail length, tail DNA, and tail moment) compared to those of control. There was a positive correlation between the level of DNA damage and age, where people aged 40 years and older had a higher level of DNA damage than those under 40 year. The level of DNA damage was also found to be higher in females compared to that of males. It was concluded that chronic exposure to natural radiation in Mamuju had induced spontaneous DNA damage in human cells after long-term exposure which was dependent on age and sex.

1. INTRODUCTION

Natural radiation has participated to shaping the present form of human life and is still the largest contributor to the average dose received by the general population. The global mean annual dose from natural sources as background is 2.4 mSv, of which a part of that dose is an external exposure from terrestrial sources such as natural deposits of uranium, potassium, and thorium in soil, water, and vegetation (UNSCEAR, 2000). As in some other countries, Mamuju in the West Sulawesi Province of Indonesia has high level natural radiation areas (HLNRA) with a potential public annual effective dose higher than normal. HLNRA are areas that have radiation doses greater than the worldwide average background dose for a human being, whereas normal level natural radiation areas (NLNRA) have radiation doses at similar levels with the worldwide average background dose (Hosoda et al., 2021). The existence of davidite, thorianite, gummite, and autonite in alkaline volcanic rock in the Mamuju area have produced high natural radioactivity (Syaeful et al., 2014). In a recent survey, an average radioactivity of 32 mSv per year, which is about 13 times higher than the global mean, was detected (Nugraha et al., 2021). Therefore, deep radiobiological assessments are needed in this unique location.

A multi-dimension study with quite complete data allowing better evaluation of health effects related to chronically low-dose-rate radiation exposure has been conducted, and it can be used as the main input in future epidemiology studies (Nugraha et al., 2021; Hosoda et al., 2021). However, the previous study did not cover the natural radiation effects at the

Citation: Darlina, Kisnanto T, Tetriana D, Purnami S, Surniyantoro HNE, Syaifudin M. Evaluation of spontaneous DNA damage using the alkaline comet assay in lymphocyte cells of humans living in the high level natural radiation area of Mamuju, Indonesia. Environ. Nat. Resour. J. 2022;20(3):330-339. (https://doi.org/10.32526/ennrj/20/202100253)

molecular level, which needs to be examined in more detail. Preliminary research also revealed an insignificant difference in DNA damage between studied inhabitants and control samples based on the observation of all comet parameters (Rahardjo et al., 2017). These results should be validated in a larger study using a higher number of samples. Here we attempted to evaluate natural radiation doses that may induce molecular or genetic changes in the living bodies of local community members. Moreover, the basic mechanisms that trigger the cellular responses to low doses of ionizing radiation remain unclear.

Human organisms are highly sensitive to ionizing radiation, of which this physical insult has a genotoxic effect on the DNA molecule (Santivasi and Xia, 2014). The generation of this DNA damage or its inadequate repair seems to be an important initial event in carcinogenesis and other non-communicable diseases (Milic et al., 2021). The health effects of low doses or low dose-rates of ionizing radiation are not so clear. Much evidence shows that long-term exposure to elevated doses of natural radiation may cause a wide variety of DNA damage, including single strand and double strand breaks, base damage and destruction of sugars (Belli and Indovina, 2020), oxidative stress related DNA damage and interstrand crosslinks (Walczak et al., 2020), chromosomal instability (Elbakrawy et al., 2019), and chromatin modification (Kumar et al., 2013). One study showed that the level of DNA damage intensity found to be higher in subjects exposed to ionizing radiation doses compared to controls (Mavragani et al., 2017). DNA damage rate appears to increase with age, indicating a decline of its repair efficiency with age which is a multi-factorial process as revealed in some studies (Piperakis et al., 2009; Harris et al., 1986). A small variation of DNA damage by age was reported in some datasets (Milic et al., 2021). Although studies by Milic et al. (2021) revealed no effects of sex on DNA alteration, the relationship between the occurrence of DNA damage and sex as a biological variable needs to be clarified to expand our understanding of its importance.

There are several methods that can be utilized to search for the molecular basis of genotoxic agent effects, including exposure to radiation (Møller et al., 2021). One of them is the alkaline comet test, that can be used to measure DNA damage microscopically and is an important tool in *in vivo* and *in vitro* studies on the population due to radiation mutagen exposure. Several studies have used the comet technique to evaluate DNA damage in human (Møller et al., 2021; Kumar et al., 2015; Kumar et al., 2011), root cells of *Allium cepa* seeds (Saghirzadeh et al., 2008) or adult male albino rats (El-Marakby et al., 2021) exposed to high natural radiation. The assay was also used to measure the DNA damage in residents exposed to high concentrations of radon (Walczak et al., 2020); and DNA damage and its repair after a dose challenge (Dicu et al., 2022). This technique is relatively simple, visual, and sensitive for detecting DNA instability, even in early damage, without the requirement for cell culture (Møller et al., 2021; Gonzalez and Plasencia, 2017; Gradzka and Iwanenko, 2005; Olive et al., 1990). While some molecular studies conducted in high background radiation areas (HBRA) have shown significantly increased frequencies of DNA damage Geetha and Sreedharan (2016), other investigations failed to find a significant difference.

A previous study revealed that DNA damage observed in the blood obtained from residents living in Botteng Village with a comet assay demonstrated a difference, but not significant, between the study and the control group. This is predicted due to the limited number of subjects involved. The objective of the present work was to determine potential effects induced by exposure to high naturally occurring radiation doses on the population of inhabitants of Mamuju, in West Sulawesi, Indonesia, with a higher number of participants and a wider area than in the previous study. It was demonstrated that exposures in these areas cause genotoxicity as measured with a standard technique.

2. METHODOLOGY

2.1 Study site

Mamuju as a study area is located at 1º38′110″-2º54′552″ South Latitude and 11º54′47″-13º5′35″ East Longitude and is the largest district in West Sulawesi Province with an area of 5,056.19 km^2, consisting of 11 sub-districts with 99 villages. The concentration of radon, a naturally occurring radioactive gas, that was measured in this area was between 184 and 380 Bq/m^3 (Syaifudin et al., 2018), which may cause external and internal radiological hazards to the local population.

The study was conducted in four villages of Mamuju, located in an area with a reddish yellow color shown in Figure 1, which shows a highly natural radiation area based on the radioactivity measurement using a portable gamma spectrometer of Exploranium GR-135 Plus (Iskandar et al., 2010). The results of an initial survey conducted in several villages in Mamuju show that the range level of gamma radiation in this

area is 700-1,000 nSv/h with a mean annual exposure of 6.15±0.81 mSv, whereas in the control area it is 2.02±0.03. However, a follow-up survey conducted with a more precise and sophisticated measurement tool in 2020 revealed that annual exposure in that study area was 32 mSv (Nugraha et al., 2021). One near-by village served as a control, shown in yellow in Figure 1.

2.2 Subjects

One hundred and two volunteers, with ages from 14 to 85 years old, who were residents of one of four studied villages (Botteng, Botteng Utara, Binanga, and Tampa Padang Villages) with high background radiation (exposed group, HLNRA) and 75 volunteers from one village (Topoyo) with normal or lower background radiation (control group, NLNRA), took part in the study. In more detail, the study group consisted of 32 people from Botteng, 20 from Binanga, 26 from Botteng Utara, and 24 from Tampa Padang. All subjects were explained the purpose of the study, signed a consent form, and answered a questionnaire before blood sampling. The interview contained some questions about their diet and the history of any illness they may had. The study's ethics approval was granted by the Indonesian Ministry of Health with the number LB.02.01/02/KE.070/2019 (date of March 14, 2019). The study group area had a similar living situation to the control group.

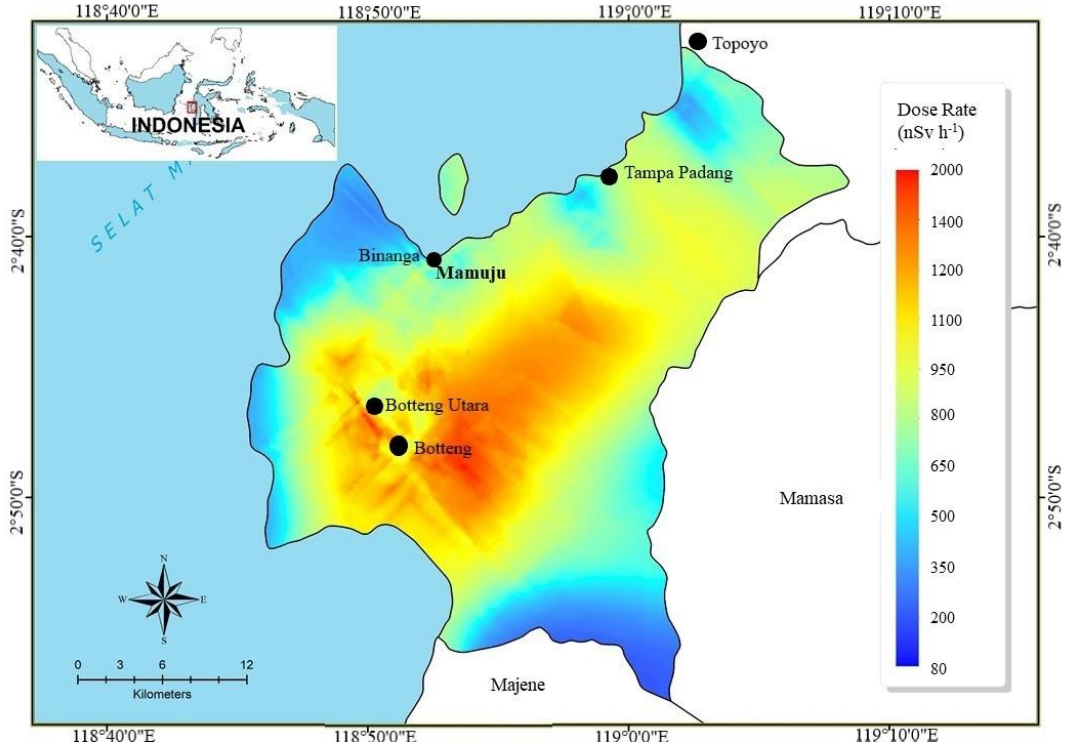

Figure 1. Study area of Mamuju, West Sulawesi Province (Botteng Utara, Botteng, Tampa Padang, and Binanga) and control area (Topoyo). The map of Indonesia, Sulawesi Island, with boxed area and scaled radioactivity level is shown.

2.3 Blood collection

Blood samples were collected from the antecubital vein (~5 mL) of all healthy adult subjects of the study and control areas via venipuncture using a 21-gauge needle and syringe and immediately transferred into heparinized vacutainer tubes (BD Vacutainer systems). After that, the samples were sent to the laboratory in Jakarta as quickly as possible by placing them in proper storage to minimize deterioration. Blood was then processed for the isolation of lymphocytes for the comet assay.

2.4 Isolation of lymphocytes

The isolation of lymphocytes procedure was done according to Bonassi et al. (2021). Briefly, 2 mL of blood samples were mixed with 2 mL of freshly prepared phosphate buffer saline (PBS) solution. Three milliliters of this mixed solution were added very slowly and layered on into a tube containing 3 mL of Histopaque (Sigma), and then the tube was centrifuged at 1,500 rpm for 30 min, after which four layers were formed (PBS, plasma, buffy coat, and blood cells). After transferring buffy coat containing lymphocyte cells to new tube, 5 mL of PBS was added

and shaken until homogeneous, then the tube was centrifuged at 1,000 rpm for 15 min. After supernatant was discarded, the pellet was resuspended by adding 75 µL RPMI and then stored in the freezer.

2.5 The comet assay

The procedure was carried out according to Lu et al. (2017). Briefly, preparation of the slide/preparate was carried out by making 3 layers of gel as a sandwich. The base layer was made of 1% normal melting point (NMP) agarose. The second layer was made of 10 µL of isolated cells (40×10^3 cells/mL) suspended in 90 µl of 0.5% low melting point (LMP) agarose. The third layer was made by dripping 75 µL 0.5% LMP agarose just above the second gel layer, and covering the sandwich with a cover glass.

Cell lysis was carried out by inserting the slide into a staining jar, then the lysis solution was poured into it until the slide was completely submerged. After that, the slide that was submerged in the jar was stored in the refrigerator at 4ºC for 1 h. Alkaline electrophoresis was carried out by placing the slide into an electrophoresis tank, about 1.2 L of DNA unwinding solution was poured slowly until the slide was completely submerged. After that, the electrophoresis voltage was adjusted at a voltage of 25 volts and 300 A and stored in a refrigerator at 4ºC for 40 min. Duplicate slides were prepared and run together for every sample and about 10 cells were observed for every sample. The neutralization process was carried out by immersing the slide in a Tris-base solution containing pH 7.5 at room temperature for 5 min (washing was carried out 3 times). After that, the slide was fixed by immersing it in a 100% ethanol solution for 3 sec. After being fixed the slide was placed in a desiccator for overnight. To observe DNA damage, staining was done by dripping 75 µL of ethidium bromide (EtBr) dye on the slide, then covering it with cover glass. Observations were made in a dark room using a fluorescent microscope at a wavelength of 510-560 nm at a magnification of 400X. All steps of the comet assay were conducted in the dark room. An example of a microscopic view of comet assay results with different levels of DNA damage shown as the length of the tail is presented in Figure 2.

2.6 Statistical analysis

The statistical analysis was performed basically as described in the previous article by Rahardjo et al. (2017). Data analysis was done using SPSS 22.0. Statistical significance of the difference between normal and high background radiation group means was performed by t-test with $p<0.001$ considered to have a statistically significant difference. For all potential confounding factors (age group and sex as presented in Table 1) which have been reported to influence the parameters investigated, the same statistical program was applied.

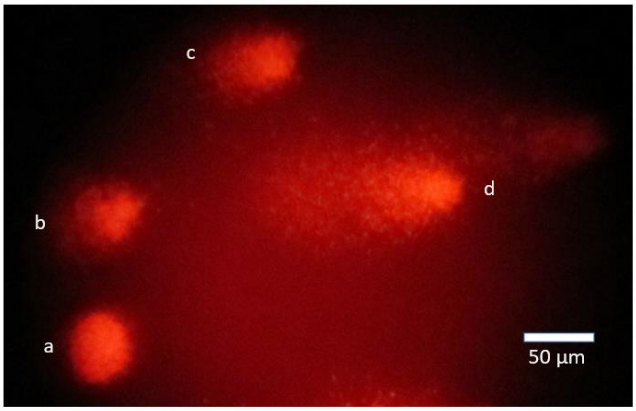

Figure 2. Microscopic view of comet assay results with four types of intact (a), slightly damaged (b), moderately damaged (c), and highly damaged (d) cells 1,000 times magnification

3. RESULTS AND DISCUSSION

3.1 Annual dose of radioactivity

Annual mean radioactivity in HLNRA of the entire Mamuju was reported between 17 and 115 mSv/year, with an average of 32 mSv/year, whereas in NLNRA it was reported at 2.46 mSv/year, indicating that HLNRA has radioactivity 13 times higher (Nugraha et al., 2021). Recently, a paper reported that the results of measurements on ambient dose equivalent rates in the HLNRA for residential houses indoors was 551 nSv/h (4.83 mSv/year); whereas the rates for outdoors were 613 nSv/h (5.37 mSv/year). The measurement result of ambient dose equivalent rates in NLNRA or the control area for indoors was 81 nSv/h (0.71 mSv/year) and the rates outdoors had a geometric mean of 71 nSv/h (0.62 mSv/year) (Hosoda et al., 2021). Previous research found that the annual effective dose received by Botteng Utara residents from terrestrial gamma rays was lower (10.40-18.62 mSv/year) (Nurokhim et al., 2020).

3.2 Alkaline comet assay

Results for all parameters (TL, TDNA, and TM) of the alkaline comet assay in the present study are presented in Table 1. These results showed that the spontaneous level of DNA damage in the inhabitants of HBRA was higher than that of the inhabitants of NBRA. It is also known that there is a statistically

significant increase in the mean values for all three parameters of the standard comet assay ($p<0.001$) in the sample of the study area in contrast to the control sample (Figure 3). The mean values of TL, TDNA, and TM in the HLNRA were 36.60 µm, 9.51%, and 4.81 µm, respectively, whereas in the NLNRA samples they were 21.71 µm, 7.57%, and 2.66 µm, respectively.

Table 1. The characteristics of subjects, its age and sex groups, and parameters of DNA damage (Tail length (TL), TDNA, and tail moment) were measured with the comet assay in people of the studied area (HLNRA) and its matched control (NLNRA).

Characteristics	NLNRA mean±SD (range)	HLNRA mean±SD (range)
Subjects		
Number of samples	75	102
Age (years)	40.37±13.14 (20-79)	41.61±13.06 (19-79)
Age and sex groups		
<40 year	40	58
≥40 year	35	44
Male	36	51
Female	39	51
Comet parameters		
TL (µm)	21.71±11.03 (7.76-68.68)	36.60±10.50 (18.32-58.71)
TDNA (%)	7.57±3.04 (3.89-19.65)	9.50±3.40 (3.92-18.81)
TM (µm)	2.66±2.12 (0.75-13.75)	4.81±2.64 (1.45-11.94)

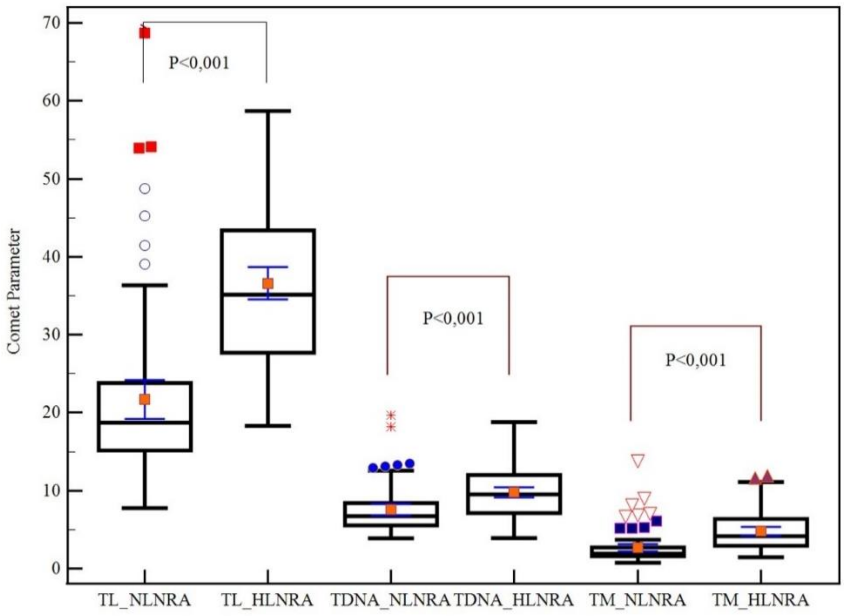

Figure 3. Graph of parameters of DNA damage (tail length (TL) (2 left graphs), tail DNA (TDNA) (2 graphs in the middle) and tail moment (TM) (2 right graphs)) measured with a comet assay on samples of NLNRA and HLNRA of Mamuju. A significant difference was shown between NLNRA and HLNRA ($p<0.001$).

Of the four HLNRA villages, Binanga had the lowest comet test value of all the parameters observed, and the comet test results in this village were not significantly different from NLNRA. It is contradicted by the fact that the reported effective dose of environmental radioactivity in Binanga village was 5.22 (2.71-6.01 mSv/year), almost similar with other villages of HLNRA. Low DNA damage in this village is probably related to the high level of nutrition status of the respondents. The highest comet test value was found in Tampa Padang Village and was higher than NLNRA. The TL values of comet measurements in three HLNRA areas (Botteng, Botteng Utara, Tampa Padang) were significantly higher than NLNRA (39.7 vs 21.71) ($p<0.05$), as were the values of TM and TDNA parameters. Among the villages in the exposed area under study, Tampa Padang village has the highest values of all comet parameters except for TM, where Botteng Utara is the highest value (Figure 4).

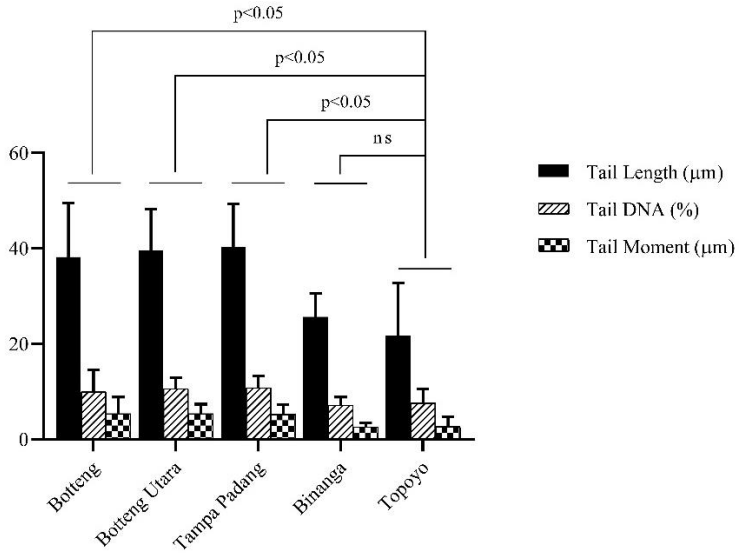

Figure 4. Measurement of all comet assay parameters (TL, TDNA, and TM) among a study group of 4 villages in HLNRA (Botteng, Botteng Utara, Tampa Padang, and Binanga) compared to a control group of 1 village in NLNRA (Topoyo). Ns denotes a non-significant difference.

From the tables and graphs, it is shown that all parameters of the Comet assay in the NLNRA sample have a wider range of values compared to HNLRA (for example 7.76-68.68 µm vs. 18.32-58.71 µm in TL). It means there is a larger variety of subjects in NLNRA. This suggests that many factors contribute to DNA damage in humans other than radiation. Endogenous and exogenous factors can cause changes in DNA structure. Endogenous factors come from inside the cell, such as reactive oxygen species (ROS) produced by mitochondria (Madamanchi and Runge, 2007). Under normal circumstances, low ROS production can be neutralized by antioxidants (Ozougwu, 2016). Exogenous factors come from outside the cell, namely cytotoxic and genotoxic inducing agents such as ionizing radiation, ultraviolet (UV) rays, and harmful chemical compounds (Desouky et al., 2015). In addition, the other factor is each individual's response to different cytotoxic-inducing agents.

Previous research by Rahardjo et al. (2017) showed that there were insignificant differences in comet tail length (TL) and tail moment (TM) between Takandeang inhabitants, an adjacent village of Botteng, and control samples (p=0.578). Regression analysis revealed that DNA damage increased with age in control samples, even though the correlation was not significant (p>0.05). In contrast, a significant negative correlation (p=0.02) was observed in the studied inhabitants. Therefore, results found in this research should be validated in a larger study using more samples from Mamuju. However, unlike in a previous study where the TL, %T, and TM values from HLNRA samples were lower compared to the normal background radiation area as control (Rahardjo et al., 2017), which is also found in the research by Kumar et al. (2015), where the results are inconsistent or conflicting. This fact indicates that there are inconsistent or controversial outputs or results among different research projects at the same study area, which are influenced by several factors such as sample size collected and preservation, as well as the entire process from collection to analysis, technique and condition used, parameters and cell types tested, sampling location that related to effective dose of radiation, individual's response and adaptation, and so on.

3.3 Relationship between DNA damage and age

As seen in Figure 5, DNA damage represented by TL in the people of both NLNRA and HLNRA showed that people aged 40 years and over had higher damage than those under 40 years, but statistically, there was no significant difference found (p>0.001) between both age groups. However, it is very clear trend that mean value of DNA damage in the HLNRA group was higher than that of the NLNRA group. We suspect that natural radiation has an effect on increasing DNA damage in HLNRA. This assumption is strengthened by references which state that the slightest exposure to natural radiation received by the population will result in DNA changes and carry a risk of cancer (Mortazavi and Mozdarani, 2013). Meanwhile, because each individual had the ability to carry out an adaptive response systemically expressed after radiation exposure, the value of DNA damage

that was not statistically significant different between both groups was suspected (Shimura and Kojima, 2018). Here TL is considered as a sign and information of how high the DNA damage level are where they migrate away from the undamaged DNA-containing nucleoid body, resembling the structure of a comet. Thus, the percentage of DNA in the tail is directly proportional to the percentage of DNA damage that has occurred in a particular cell (Møller et al., 2014).

It was also reported in some datasets, suggesting a higher number of DNA damage events in the oldest age-classes. The increase in DNA damage with age may be caused by a decrease in DNA repair capacity that results in its accumulation (Singh et al., 1990; Piperakis et al., 2009) and is characterized by reducing physiological integration and function (Fischer and Riddle, 2018). Garm et al. (2013) stated that the improvement of single strand breaks can still be maintained in individuals aged 40-70 years, but experienced a decrease in the improvement of double strand breaks. Li et al. (2016) stated that there is a decrease in the expression of proteins and factors in old age that help improve DSB in each of these pathways. It means that DSB repair decreases in old age.

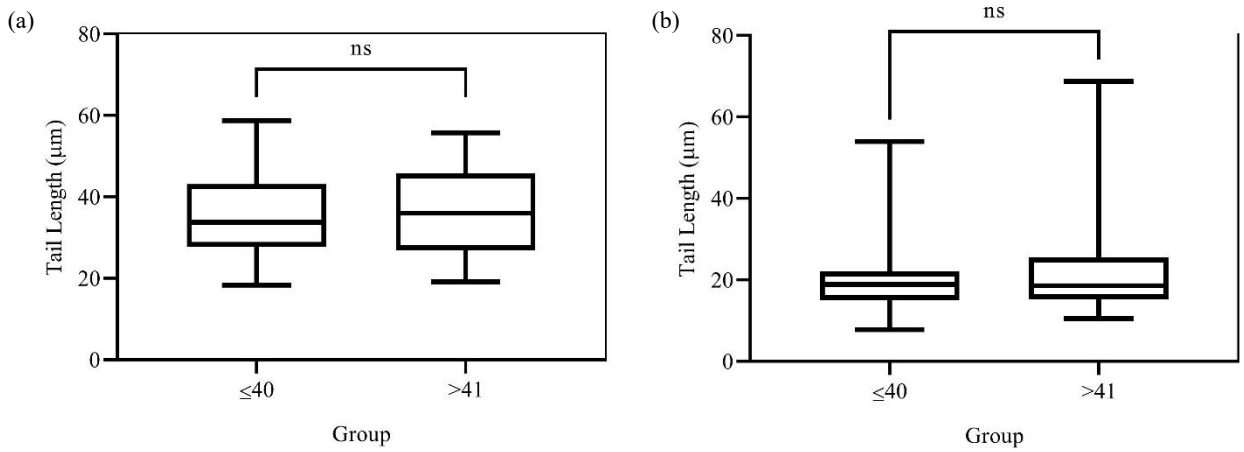

Figure 5. Comparison of DNA damage represented by tail length (TL in µm) of residents according to age group (≤40 and >40) from study area (A, HLNRA) and from control area (B, NLNRA) of Mamuju, West Sulawesi. Ns denotes a non-significant difference.

3.4 Relationship between DNA damage and sex

The relationship between gender (sex) and DNA damage represented by TL in HLNRA residents showed that DNA damage in in females was higher than in that of males, but statistical analysis revealed no significant difference ($p>0.001$). The result is presented in Figure 6. The finding is in contrast with previous study by Ishikawa et al. (2003) which stated that the DNA damage in a male is higher than in a female, which is caused by the characteristics of the Y chromosome in a male which is more fragile than the X chromosome in a female. Another DNA damage biomarker, micronuclei, showed that females had 2.48-fold higher micronuclei values than males (Surniyantoro et al., 2018). This shows that females are more sensitive to radiation exposure than males (Babayan et al., 2018). Different results were shown in the study by Garm et al. (2013), who conducted a study on 200 residents in Denmark, where this study shows that there is no influence of gender on DNA damage. A higher incidence of DNA damage in males compared to females was found by Fischer and Riddle (2018). Besides that, there is another factor such as smoking and drinking habits that should be considered mainly in the male group (Bonassi et al., 2021).

In contrast with our finding, a previous paper by Rahardjo et al. (2017) reported that DNA damage in males was higher compared to that of females, which was in good agreement with another study by Kopjar et al. (2006) and Ishikawa et al. (2003). A higher level of DNA damage is predicted to be caused by smoking habits that generate free radicals.

Human and other organism cells are constantly exposed to stress caused by external genotoxic agents and a verity of environmental factors such as high levels of natural radiation that cause cellular components damage (Li and Sancar, 2020). Many methods are available to detect this damage. Single cell gel electrophoresis or comet assay, immunological and PCR-based methods of monitoring DNA damage and its repair at the sub-gene and single nucleotide level are among these methods. Due to its technical simplicity and sensitivity, it is possible that the comet assay is the most useful method

in biomonitoring of the human population suffering from this environmental mutagen (Sykora et al., 2018), including its new Cometchip platform. Here, the potential use of this molecular technique to monitor the effects of natural radiation in the environment has been tried and exploited as conducted by others (Valverde and Rojas, 2009; Rahardjo et al., 2017; Syaifudin et al., 2018; Sykora et al., 2018). It is shown that the comet assay used for evaluation of spontaneous DNA damage induction is a relatively simple and cost-effective test at the single cell level when applied to low level radiation genotoxicity studies. In wider application, induction of endogenous strand breaks, oxidized bases and resistance to H_2O_2-induced damage as well as its mechanisms of action of this genotoxic chemical in cells can also be measured by the comet assay (Martini et al., 2021).

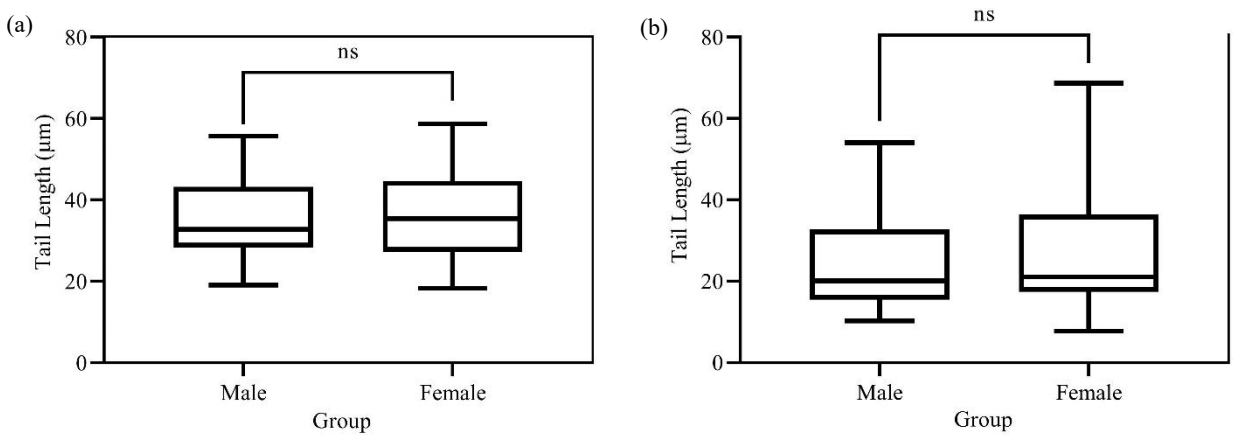

Figure 6. Comparison of DNA damage represented by tail length (TL in µm) of residents according to sex (male and female) from study area (A, HLNRA) and from control area (B, NLNRA) of Mamuju, West Sulawesi. Ns denotes a non-significant difference.

DNA damage, recognized as an important biomarker of cell tumorigenesis, may result in several mechanisms such as unrepaired chromosome telomere damage, causing the activation of signaling events, through which altered cells are predicted to be a more potent driver of aging and disease (Russo et al., 2020; Yousefzadeh et al., 2021). Moreover, another important factor is the presence of an adaptive response of the cell through expression of protective stress response proteins (Nishad et al., 2021) and the process of virtually removal (reduction) of DNA damage, as proposed for the comet assay results, that could not be excluded in the study of DNA damage. Other than environmental situation, some factors that affect DNA damage such as nutrition, lifestyle and occupation must also be considered. To all these individuals, the systemic adaptive responses that may have been prominently expressed at high effective doses of natural radiation also need to be explored.

4. CONCLUSION

Is conclusion, it was revealed that chronical exposure to high natural radiation in Mamuju significantly ($p<0.001$) induced higher DNA damage in local human cells compared to control. This was detected with a validated comet assay where DNA damage was evaluated by three parameters of the assay. The level of DNA damage was influenced by age as well as sex. Humans at age of 40 years and older have a higher level of DNA damage than younger ones; and females have higher DNA damage compared to males. Some confounding factors exist in the inconsistency of these results with others.

ACKNOWLEDGEMENTS

The authors profusely thank all the volunteers who have participated in the study. We are thankful to the Center, which supported this research through an Annual Research Project from the Nuclear Energy Research Organization, National Agency for Research and Innovation with contract no. 080.01.06 3447.008 004.012.A524111A. We acknowledge Dr. Eka Djatnika Nugraha and Dwi Ramadhani, M. Si. Med. for useful discussions. Darlina, Teja Kisnanto, and Mukh Syaifudin are the main contributors to the manuscript.

CONFLICT OF INTERREST

We declare no conflicts of interest associated with this publication.

REFERENCES

Babayan N, Grigoryan B, Hovhannisyan G, Tadevosyan G, Khondkaryan L, Grigoryan RM, et al. Gender differences in DNA damage/repair after laser-generated ultrafast electron beam irradiation. International Journal of Radiology and Radiation Therapy 2018;5:85-6.

Belli M, Indovina L. The response of living organisms to low radiation environment and its implications in radiation protection. Frontiers in Public Health 2020;8:Article No. 601711.

Bonassi S, Ceppi M, Moller P, Azqueta A, Milić M, Neri M, et al. DNA damage in circulating leukocytes measured with the comet assay may predict the risk of death. Scientific Reports 2021;11:1-11.

Desouky O, Ding N, Zhou G. Targeted and non-targeted effects of ionizing radiation. Journal of Radiation Research and Applied Sciences 2015;8:247-54.

Dicu T, Virag P, Brie I, Perde-Schrepler M, Fischer-Fodor E, Victor B, et al. A comparative study of genotoxicity endpoints for women exposed to different levels of indoor radon concentrations. International Journal of Radiation Biology 2022;98(1):18-29.

Elbakrawy EM, Hill MA, Kadhim MA. Radiation-induced chromosome instability: The role of dose and dose rate. Genome Integrity 2019;10:Article No. 3.

El-Marakby RM, Abdelgawad MH, Awad MM, Eraba KM, Desouky OS. DNA damage detection after chronic exposure and radio-adaptive response of naturally occurring radioactive materials (NORM). Arab Journal of Nuclear Sciences and Applications 2021;54(3):34-45.

Fischer KE, Riddle NC. Sex differences in aging: Genomic instability. Journals of Gerontology Series A Biological Sciences and Medical Sciences 2018;73(2):166-74.

Garm C, Moreno-Villanueva M, Burkle A, Petersen I, Bohr VA, Christensen K, et al. Age and gender effects on DNA strand break repair in peripheral blood mononuclear cells. Aging Cell 2013;12:58-66.

Gonzalez GF, Plasencia CP. Strategies for the evaluation of DNA damage and repair mechanisms in cancer: Review. Oncology Letters 2017;13(6):3982-8.

Gradzka W, Iwanenko T. A non-radioactive, PFGE-based assay for low levels of DNA double-strand breaks in mammalian cells. DNA Repair 2005;4:1129-39.

Geetha AC, Sreedharan H. Review on studies in high background radiation areas (HBRAs) of various parts of the world. International Journal of Advanced Research in Biological Sciences 2016;3(8):163-9.

Harris G, Holmes A, Sabovijev SA, Cramp WA, Hedges H, Hornsey S, et al. Sensitivity to X-irradiation of peripheral blood lymphocytes from ageing donors. International Journal of Radiation Biology 1986;50:685-94.

Hosoda M, Nugraha ED, Akata N, Yamada R, Tamakuma Y, Sasaki M, et al. A unique high natural background radiation area-Dose assessment and perspectives. Science of the Total Environment 2021;750:1-11.

Ishikawa H, Rattigan A, Fundele R, Burgoyne PS. Effects of sex chromosome dosage on placental size in mice. Biology of Reproduction 2003;69(2):483-8.

Iskandar D, Bunawas, Syarbaini. Mapping radiation and radioactivity in Sulawesi Island, Proceedings of The Third Asian and Oceanic Congress on Radiation Protection (AOCRP-3). 2010 May 24-28; Tokyo, Japan; 2010.

Kopjar N, ŽeljeŽić D, Garaj-vrhovac V. Evaluation of DNA damage in white blood cells of healthy human volunteers using the alkaline comet assay and the chromosome aberration test. Acta Biochimica Polonica 2006;53(2):321-36.

Kumar PRV, Cheriyan VD, Seshadri M. Evaluation of spontaneous DNA damage in lymphocytes of healthy adult individuals from high-level natural radiation areas of Kerala in India. Radiation Research 2011;177:643-50.

Kumar PRV, Seshadri M, Jaikrishan G, Das B. Effect of chronic low dose natural radiation in human peripheral blood mononuclear cells: Evaluation of DNA damage and repair using the alkaline comet assay. Mutation Research 2015; 775:59-65.

Kumar R, Horikoshi N, Singh M, Gupta A, Misra HS, Albuquerque K, et al. Chromatin modifications and the DNA damage response to ionizing radiation. Frontiers in Oncology 2013;2:1-9.

Li W, Sancar A. Methodologies for detecting environmentally induced DNA damage and repair. Environmental and Molecular Mutagenesis 2020;61:664-79.

Li Z, Zhang W, Chen Y, Guo W, Zhang J, Tang H, et al. Impaired DNA double-strand break repair contributes to the age-associated rise of genomic instability in humans. Cell Death and Differentiation 2016;23:1765-77.

Lu Y, Liu Y, Yang C. Evaluating in vitro DNA damage using comet assay. Journal of Visualized Experiments 2017;128:2-7.

Madamanchi NR, Runge MS. Mitochondrial dysfunction in atherosclerosis. Circulation Research 2007;100:460-73.

Martini D, Domínguez-Perles R, Rosi A, Tassotti M, Angelino D, Medina S, et al. Effect of coffee and cocoa-based confectionery containing coffee on markers of DNA damage and lipid peroxidation products: Results from a human intervention study. Nutrients 2021;13(7):Article No. 2399.

Mavragani IV, Nikitaki Z, Souli MP, Aziz A, Nowsheen S, Aziz K, et al. Complex DNA damage: A route to radiation-induced genomic instability and carcinogenesis. Cancers 2017;9: Article No. 91.

Milic M, Ceppi M, Bruzzone M, Azqueta A, Brunborg G, Godschalk R, et al. The hCOMET project: International database comparison of results with the comet assay in human biomonitoring [Baseline frequency of DNA damage and effect of main confounders]. Mutation Research/Reviews in Mutation Research 2021;787:1-13.

Møller P, Bankoglu EE, Stopper H, Giovannelli LC, Ladeira C, Coppen D, et al. Collection and storage of human white blood cells for analysis of DNA damage and repair activity using the comet assay in molecular epidemiology studies. Mutagenesis 2021;36:193-211.

Møller P, Loft S, Ersson C, Koppen G, Dusinska M, Collins A. On the search for an intelligible comet assay descriptor. Frontiers in Genetics 2014;5:Article No. 217.

Mortazavi SMJ, Mozdarani H. Non-linear phenomena in biological findings of the residents of high background radiation areas of Ramsar. International Journal of Radiation Research 2013;11:1-9.

Nishad S, Chauhan PK, Sowdhamini R, Ghosh A. Chronic exposure of humans to high level natural background radiation leads to robust expression of protective stress response proteins. Scientific Reports 2021;11:1-14.

Nugraha ED, Hosoda M, Kusdiana, Untara, Mellawati J, Nurokhim, et al. Comprehensive exposure assessments from the viewpoint of health in a unique high natural background

radiation area, Mamuju, Indonesia. Scientifc Reports 2021; 11:1-16.

Nurokhim, Kusdiana, Pudjadi E. Assessment of natural radioactivity levels in soil sample from Botteng Utara Village, Mamuju Regency Indonesia. IOP Conference Series: Journal of Physics 2020;1436:Article No. 012139.

Olive PL, Banath JP, Durand RE. Heterogeneity in radiation-induced DNA damage and repair in tumor and normal cells measured using the "comet" assay. Radiation Research 1990; 122:86-94.

Ozougwu JC. The role of reactive oxygen species and antioxidants in oxidative stress. International Journal of Research in Pharmacy and Biosciences 2016;3:1-8.

Piperakis SM, Kontogianni K, Karanastasi G, Iakovidou-Kritsi Z, Piperakis MM. The use of comet assay in measuring DNA damageand repair efficiency in child, adult, and old age populations. Cell Biology and Toxicology 2009;25:65-71.

Rahardjo T, Mailana W, Kisnanto T, Darlina, Nurhayati S, Tetriana D, et al. Assessment of DNA damage in lymphocytes of Mamuju (a high background radiation area) inhabitants using alkaline single cell gel electrophoresis. International Journal of Low Radiation 2017;10:314-23.

Russo C, Acito M, Fatigoni C, Villarini M, Moretti M. B-comet assay (comet assay on buccal cells) for the evaluation of primary DNA damage in human biomonitoring studies. International Journal of Environmental Research and Public Health 2020;17(9234):2-14.

Saghirzadeh M, Gharaati MR, Mohammadi Sh, Ghiassi-Nejad M. Evaluation of DNA damage in the root cells of *Allium cepa* seeds growing in soil of high background radiation areas of Ramsar - Iran. Journal of Environmental Radioactivity 2008;99:1698-702

Santivasi WL, Xia F. Ionizing radiation-induced DNA damage, response, and repair. Antioxidants and Redox Signaling 2014;21:251-9.

Shimura N, Kojima S. The lowest radiation dose having molecular changes in the living body. Dose-Response 2018;16:1-17.

Singh NP, Danner DB, Tice RR, Brant L, Schneider EL. DNA damage and repair with age in individual human lymphocytes. Mutation Research 1990;237:123-30.

Surniyantoro HNE, Lusiyanti Y, Rahardjo T, Tetriana D, Nurhayati S, Date H. Polymorphism of XRCC1 gene exon 6 (Arg194Trp) in relation to micronucleus frequencies in hospital radiation workers. Atom Indonesia 2018;44:105-11.

Syaeful H, Sukadana IG, Sumaryanto A. Radiometric mapping for naturally occurring radioactive materials (NORM) assessment in Mamuju, West Sulawesi. Atom Indonesia 2014;40(1):33-9.

Syaifudin M, Purnami S, Rahardjo T, Kurnia I, Rahajeng N, Darlina, et al. Cytogenetic and molecular damages in blood lymphocytes of inhabitants living in high level natural radiation area (HLNRA) Botteng Village, Mamuju, West Sulawesi. Radiation Environment Medicine 2018;7(2):65-76.

Sykora P, Witt KL, Revanna P, Smith-Roe SL, Dismukes J, Lloyd DG, et al. Next generation high throughput DNA damage detection platform for genotoxic compound screening. Scientific Reports 2018;8:1-20.

United Nations Scientific Committee on the Effects of Atomic Radiations (UNSCEAR). Report I: Sources and Effects of Ionizing Radiation Annex B Exposures from Natural Radiation Sources. New York: United Nations; 2000. p. 27-78.

Valverde M, Rojas E. Environmental and occupational biomonitoring using the Comet assay. Mutation Research 2009;681:93-109.

Walczak K, Olszewski J, Politański P, Domeradzka-Gajda K, Kowalczyk K, Zmyślony M, et al. Residential exposure to radon and levels of histone γH2AX and DNA damage in peripheral blood lymphocytes of residents of Kowary City Regions (Poland). Chemosphere 2020;247:Article No. 125748.

Yousefzadeh M, Henpita C, Vyas R, Soto-Palma C, Robbins P, Niedernhofer L. DNA damage-how and why we age? eLife 2021;10:e62852.

INSTRUCTION FOR AUTHORS

Publication and Peer-reviewing processes of Environment and Natural Resources Journal

Environment and Natural Resources Journal is a peer reviewed and open access journal that is published twice a year (January-June and July-December). Manuscripts should be submitted online at https://ph02.tci-thaijo.org/index.php/ennrj/about/submissions by registering and logging into this website. Submitted manuscripts should not have been published previously, nor be under consideration for publication elsewhere (except conference proceedings papers). A guide for authors and relevant information for the submission of manuscripts are provided in this section and also online at: https://ph02.tci-thaijo.org/index.php/ennrj/author. All manuscripts are refereed through a **double-blind peer-review** process.

Submitted manuscripts are reviewed by outside experts or editorial board members of **Environment and Natural Resources Journal**. This journal uses double-blind review, which means that both the reviewer and author identities are concealed from the reviewers, and vice versa, throughout the review process. Steps in the process are as follows:

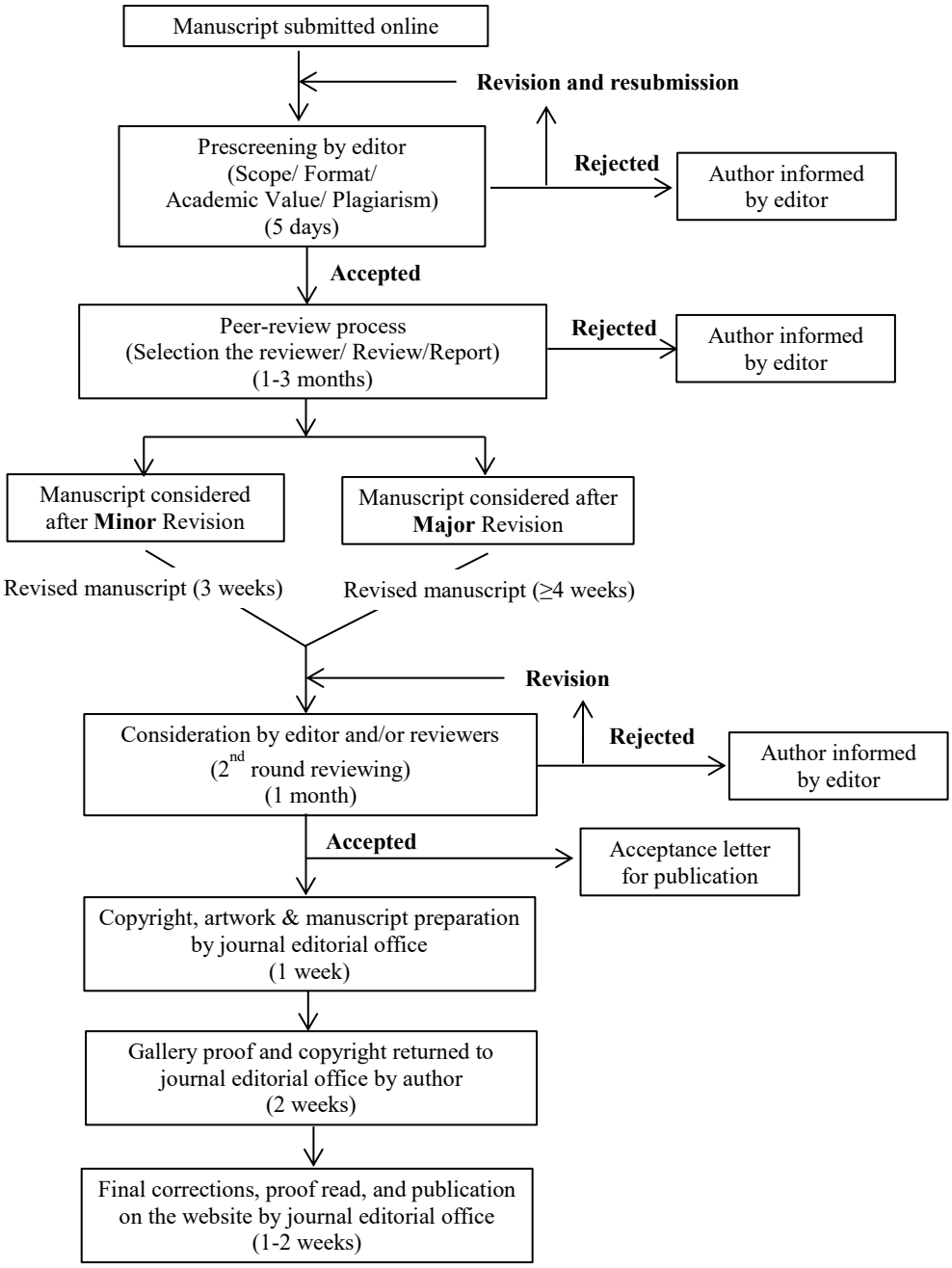

The Environment and Natural Resources Journal (EnNRJ) accepts 2 types of articles for consideration of publication as follows:

- *Original Research Article:* Manuscripts should not exceed 3,500 words (excluding references).
- *Review Article (by invitation):* This type of article focuses on the in-depth critical review of a special aspect in the environment and also provides a synthesis and critical evaluation of the state of the knowledge of the subject. Manuscripts should not exceed 6,000 words (excluding references).

Submission of Manuscript

Cover letter: Key points to include:

- Statement that your paper has not been previously published and is not currently under consideration by another journal
- Brief description of the research you are reporting in your paper, why it is important, and why you think the readers of the journal would be interested in it
- Contact information for you and any co-authors
- Confirmation that you have no competing interests to disclose

Manuscript-full: Manuscript (A4) must be submitted in Microsoft Word Files (.doc or .docx). Please make any identifying information of name(s) of the author(s), affiliation(s) of the author(s). Each affiliation should be indicated with superscripted Arabic numerals immediately after an author's name and before the appropriate address. Specify the Department/School/Faculty, University, Province/State, and Country of each affiliation.

Manuscript-anonymized: Manuscript (A4) must be submitted in Microsoft Word Files (.doc or .docx). Please remove any identifying information, such as authors' names or affiliations, from your manuscript before submission and give all information about authors at title page section.

Reviewers suggestion *(mandatory)*: Please provide the names of 3 potential reviewers with the information about their affiliations and email addresses. *The recommended reviewers should not have any conflict of interest with the authors. Each of the reviewers must come from a different affiliation and must not have the same nationality as the authors.* Please note that the editorial board retains the sole right to decide whether or not the recommended potential reviewers will be selected.

Preparation of Manuscript

Manuscript should be prepared strictly as per guidelines given below. The manuscript (A4 size page) must be submitted in Microsoft Word (.doc or .docx) with Times New Roman 12 point font and a line spacing of 1.5. *The manuscript that is not in the correct format will be returned and the corresponding author may have to resubmit*. The submitted manuscript must have the following parts:

Title should be concise and no longer than necessary. Capitalize first letters of all important words, in Times New Roman 12 point bold.

Author(s) name and affiliation must be given, especially the first and last names of all authors, in Times New Roman 11 point bold.

Affiliation of all author(s) must be given in Times New Roman 11 point italic.

Abstract should indicate the significant findings with data. A good abstract should have only one paragraph and be limited to 250 words. Do not include a table, figure or reference.

Keywords should adequately index the subject matter and up to six keywords are allowed.

Text body normally includes the following sections: 1. Introduction 2. Methodology 3. Results and Discussion 4. Conclusions 5. Acknowledgements 6. References

Reference style must be given in Vancouver style. Please follow the format of the sample references and citations as shown in this Guide below.

Unit: The use of abbreviation must be in accordance with the SI Unit.

Format and Style

Paper Margins must be 2.54 cm on the left and the right. The bottom and the top margin of each page must be 1.9 cm.

Introduction is critically important. It should include precisely the aims of the study. It should be as concise as possible with no sub headings. The significance of problem and the essential background should be given.

Methodology should be sufficiently detailed to enable the experiments to be reproduced. The techniques and methodology adopted should be supported with standard references.

Headings in Methodology section and Results and Discussion section, no more than three levels of headings should be used. Main headings should be typed (in bold letters) and secondary headings (in bold and italic letters). Third level headings should be typed in normal and no bold, for example;

2. Methodology
2.1 Sub-heading
2.1.1 Sub-sub-heading

Results and Discussion can be either combined or separated. This section is simply to present the key points of your findings in figures and tables, and explain additional findings in the text; no interpretation of findings is required. The results section is purely descriptive.
Tables Tables look best if all the cells are not bordered; place horizontal borders only under the legend, the column headings and the bottom.
Figures should be submitted in color; make sure that they are clear and understandable. Please adjust the font size to 9-10, no bold letters needed, and the border width of the graphs must be 0.75 pt. *(Do not directly cut and paste them from MS Excel.)* Regardless of the application used, when your electronic artwork is finalized, please 'save as' or convert the images to TIFF (or JPG) and separately send them to EnNRJ. The images require a resolution of at least 300 dpi (dots per inch). If a label needed in a figure, its font must be "Times New Roman" and its size needs to be adjusted to fit the figure without borderlines.

All Figure(s) and Table(s) should be embedded in the text file.

Conclusions should include the summary of the key findings, and key take-home message. This should not be too long or repetitive, but is worth having so that your argument is not left unfinished. Importantly, don't start any new thoughts in your conclusion.

Acknowledgements should include the names of those who contributed substantially to the work described in the manuscript but do not fulfill the requirements for authorship. It should also include any sponsor or funding agency that supported the work.

References should be cited in the text by the surname of the author(s), and the year. This journal uses the author-date method of citation: the last name of the author and date of publication are inserted in the text in the appropriate place. If there are more than two authors, "et al." after the first author' name must be added. Examples: (Frits, 1976; Pandey and Shukla, 2003; Kungsuwas et al., 1996). If the author's name is part of the sentence, only the date is placed in parentheses: "Frits (1976) argued that . . ."

Please be ensured that every reference cited in the text is also present in the reference list (and vice versa).

In the list of references at the end of the manuscript, full and complete references must be given in the following style and punctuation, arranged alphabetically by first author's surname. Examples of references as listed in the References section are given below.

Book
Tyree MT, Zimmermann MH. Xylem Structure and the Ascent of Sap. Heidelberg, Germany: Springer; 2002.

Chapter in a book
Kungsuwan A, Ittipong B, Chandrkrachang S. Preservative effect of chitosan on fish products. In: Steven WF, Rao MS, Chandrkachang S, editors. Chitin and Chitosan: Environmental and Friendly and Versatile Biomaterials. Bangkok: Asian Institute of Technology; 1996. p. 193-9.

Journal article
Muenmee S, Chiemchaisri W, Chiemchaisri C. Microbial consortium involving biological methane oxidation in relation to the biodegradation of waste plastics in a solid waste disposal open dump site. International Biodeterioration and Biodegradation 2015;102:172-81.

Published in conference proceedings
Wiwattanakantang P, To-im J. Tourist satisfaction on sustainable tourism development, amphawa floating marketSamut songkhram, Thailand. Proceedings of the 1st Environment and Natural Resources International Conference; 2014 Nov 6-7; The Sukosol hotel, Bangkok: Thailand; 2014.

Ph.D./Master thesis

Shrestha MK. Relative Ungulate Abundance in a Fragmented Landscape: Implications for Tiger Conservation [dissertation]. Saint Paul, University of Minnesota; 2004.

Website

Orzel C. Wind and temperature: why doesn't windy equal hot? [Internet]. 2010 [cited 2016 Jun 20]. Available from: http://scienceblogs.com/principles/2010/08/17/wind-and-temperature-why-doesn/.

Report organization:

Intergovernmental Panel on Climate Change (IPCC). IPCC Guidelines for National Greenhouse Gas Inventories: Volume 1-5. Hayama, Japan: Institute for Global Environmental Strategies; 2006.

Remark

** Please be note that manuscripts should usually contain at least 15 references and some of them must be up-to-date research articles.*

** Please strictly check all references cited in text, they should be added in the list of references. Our Journal does not publish papers with incomplete citations*.

Copyright transfer

The copyright to the published article is transferred to Environment and Natural Resources Journal (EnNRJ) which is organized by Faculty of Environment and Resource Studies, Mahidol University. The accepted article cannot be published until the Journal Editorial Officer has received the appropriate signed copyright transfer.

Online First Articles

The article will be published online after receipt of the corrected proofs. This is the official first publication citable with the Digital Object Identifier (DOI). After release of the printed version, the paper can also be cited by issue and page numbers. DOI may be used to cite and link to electronic documents. The DOI consists of a unique alpha-numeric character string which is assigned to a document by the publisher upon the initial electronic publication. The assigned DOI never changes.

Mahidol University

Wisdom of the Land

Research and Academic Service Section, Faculty of Environment and Resource Studies, Mahidol University
999 Phutthamonthon 4 Rd, Salaya, Nakhon Pathom 73170, Phone +662 441-5000 ext. 2108 Fax. +662 441 9509-10
E-mail: ennrjournal@gmail.com Website: https://www.tci-thaijo.org/index.php/ennrj